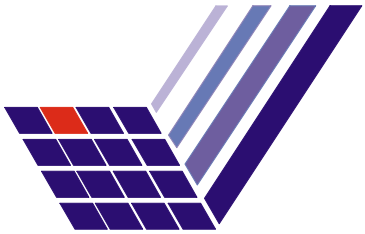

Fachbereich Chemie, Universität Dortmund, Germany

Metal Coordination to Nucleobases and its Consequences: Group Acidifications, Migration Processes and Multiple Metalation

Marta Garijo Añorbe

Ph.D. Thesis submitted to the
Fachbereich Chemie der Universität Dortmund, Germany
for obtaining the degree of a
Doktor der Naturwissenschaften

Ph.D. Advisor:	Prof. Dr. Bernhard Lippert
Referee:	PD Dr. Andrea Erxleben

This work was carried out between August 2002 and January 2006
under the supervision of Prof. Dr. B. Lippert
at the Chair of Bioinorganic Chemistry,
Fachbereich Chemie, Universität Dortmund, Germany.

My special thanks go to my Ph. D. Supervisor

Prof. Dr. Bernhard Lippert

for the opportunity to carry out research in his group, the interesting topic, the chemistry that I learnt from him, the kindness with which he has always treated me and for all his help.

I would also like to thank

Dr. Jens Müller and Dr. Gabi Trötscher-Kaus for carefully reading my thesis and correcting my English; Fabian (“El Genio”) for helping me to translate my English summary into German; Dr. Andrea Erxleben for kindly acting as referee;

my colleagues in the laboratory and the office, Patrick Lax, Dr. Michael Roitzsch, Dr. Michael Willermann, Dr. Ralf Nowak, Marta Morell, Dr. Pablo Sanz, Dr. Deepali Gupta, Dr. Kathrin Schmidt, Dr. Clodagh Mulcahy, Dr. David Amantia, Pilar Brandi and especially to Myriam Gil and Weizheng Shen for the good atmosphere in the office and the great time we spent together;

Marta Morell, Dr. Thorsten Oldag, Dr. Pablo Sanz and Dr. Uwe Zachwieja for their help with the X-ray structures and for teaching me all I know about crystallography; Dr. Jens Müller and Marta Morell for measuring my NMR samples after working hours; Dr. Pablo Sanz for recording ^{195}Pt NMR spectra. Patrick Lax for the DFT calculations; Thorsten Grund for his help with technical support;

Prof. Dr. Burkhard Costisella and Annette Danzmann for the innumerable NMR spectra that they carried out (too many pD dependences!), for the nice conversations and for the good work atmosphere;

Markus Hüffner for the exact determinations of the elemental analysis and Wilga Buß for recording the Raman spectra;

Michaela Market (and Lara), Dr. Dinah Dux, Dr. Andrea Erxleben, Dr. Jola Hermann, Dr. Irene Szymanski, Barbara Müller, Lars Holland, Fabian Polonius, Dominik Böhme, Oliver Gerbersmann, Simone Goritz, Dr. Elisa Barea, Christine Klimek, Sultan Cosar and Mahdi Hadjizadeh-Ziabari for the the nice atmosphere at work; Dr. Bülent Ceyhan for being there when I needed to talk to someone about chemistry and life; Javier Cuesta for his chemical advices.

Prof. Dr. Helmut Sigel and his group for their cooperation with some of the pD dependences;

Simon Albracht and Olga Karsten, my “Auszubildende”, for their help in preparing compounds; Lucia Staude for her contribution to the section 2.10;

Birgit Thormann for her help from the beginning until the end and Burkhard Wellnitz for his “lustige” jokes;

Prof. Dr. Luis Oro and Prof. Dr. Fernando Lahoz for the Erasmus Stipendium and the possibility of coming to Dortmund;

Dr. Miguel Sanz, Pilar Flores, Inés López, Myriam Gil and Dr. Joaquín Gomis for their friendship and for being always there when I needed them; also for the good time we spent together in Dortmund;

Magnus Nigmann for his patience with me and for helping me in a number of ways, especially with my German;

Anastasia Bouziani and Rebecca Friese for supporting me during these years in our “WG” and for their friendship;

the team from Limericks (Irish pub), where I had great times, especially to Sherie, Steve, Stan, Cherry Q. and Yusuf, for improving my English;

all my Spanish friends, that they were always waiting for me in Spain. Do not worry, I will come back soon!

my family, Ángel, Maribel, Beatriz, Angelines, Pepe, Raúl, Pilar, Jesús for their encouragement and support. I would like to thank in particular my parents for their help and support during these years. I dedicate this thesis to them.

Dedicado a mis padres.

1 INTRODUCTION

The heterocyclic rings of nucleobases are generally not involved in acid-base equilibria, since pK_a values (pK_a < 4 or pK_a > 9) are outside the physiological pH range.[1]

This picture is changed if nucleobases are modified, e. g. following alkylation or metal binding. For example, the N1H group in 7,9-dimethylguaninium has a pK_a value of 7.22 ± 0.01,[2] compared to a value of 9.56 for 9-methylguanine,[3] and metal binding to N7 generally lowers the pK_a value of this proton by one to two log units, depending on the metal, net charge, etc.[2-4] Another example, Pt^{II} bonded to N7 of a guanine model base reduces the pK_a from 10.1 to ca. 8.8 (Figure 1).[2]

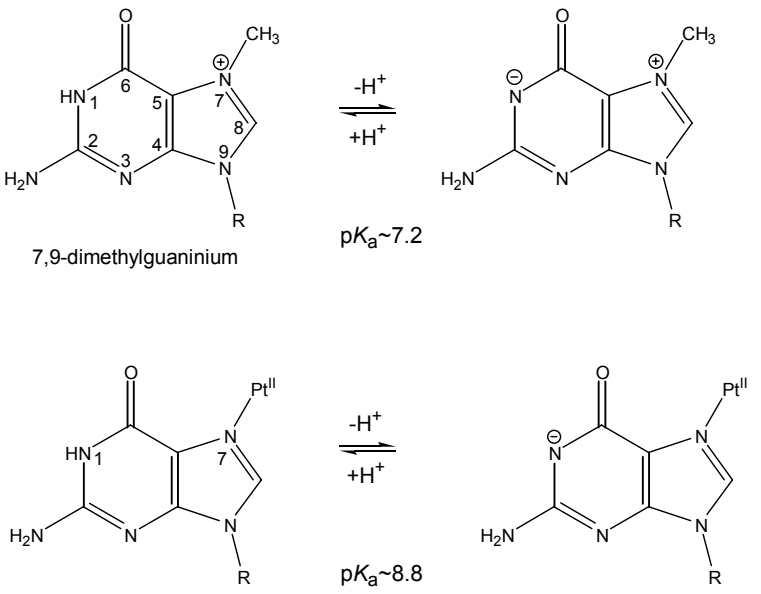

Figure 1: *Examples of modification of pK_a values through alkylation or metal binding.*

It is known that in biological macromolecules the environment of an acidic proton can likewise modify its pK_a value, in either direction. In special nucleic acid structures, for example, the “i motif” of hemiprotonated cytosine or DNA

triplex structures containing cytosine·guanine·cytosinium triplets, this phenomenon is well established.[5] Shifts of the pK_a values of nucleobase protons into the physiological pH range are currently of great interest in that they potentially permit acid-base catalysis.[6] In principle, systems with pK_a values reasonably close to 7 could act as acid/base catalysts in biological reactions. It has been reported that an adenine residue in ribosomal RNA with the highly unusual pK_a value of 7.6 ± 0.2 acts as a catalyst in the ribosomal peptidyl transferase center,[7] and nucleobase functions with near-neutral pK_a values have been associated with ribozyme catalysis of the Hepatitis Delta Virus (HDV).[8] This ribozyme was the first RNA enzyme proposed to use a proton-transfer mechanism for catalysis (Figure 2). There is a possibility of hydrogen bonding between the oxygens of the phosphate and this contributes significantly to the ground-state stabilization of the protonated C75 (cytosine 75). The cis-cleavage reaction may be initiated by specific base deprotonation of the 2´-OH group of the first nucleobase (NB), followed by nucleophilic attack at the phosphate. A charge redistribution in the transition state involving a proton transfer from the N3 of protonated C75 to the 5´-oxyanion leaving group drives the reaction equilibrium in favour of the cleavage products. A scheme of the different bases which can attack the 2´-OH group and the different acids is shown in Figure 2.

Similarly, an unusual pK_a value of 6.5 for an adenine base close to the active site of a Pb-dependent ribozyme (“leadzyme”) has been described.[9]

Other authors[10-12] and ourselves[3,4,13,14] have demonstrated in numerous instances that metal binding to a nucleobase acidifies protons of NH groups and, conversely, causes an apparent increase in nucleobase basicity upon metal coordination to a deprotonated, and hence anionic, nucleobase.[15,16] This is because the proton has a stronger polarizing effect than (most) divalent metal ions.[13a] The effect depends on a combination of factors such as the charge of the metal(s), the number of metal ions, the coligands, the distance between the metal center and the proton, and hence the site(s) of metal binding.[10c]

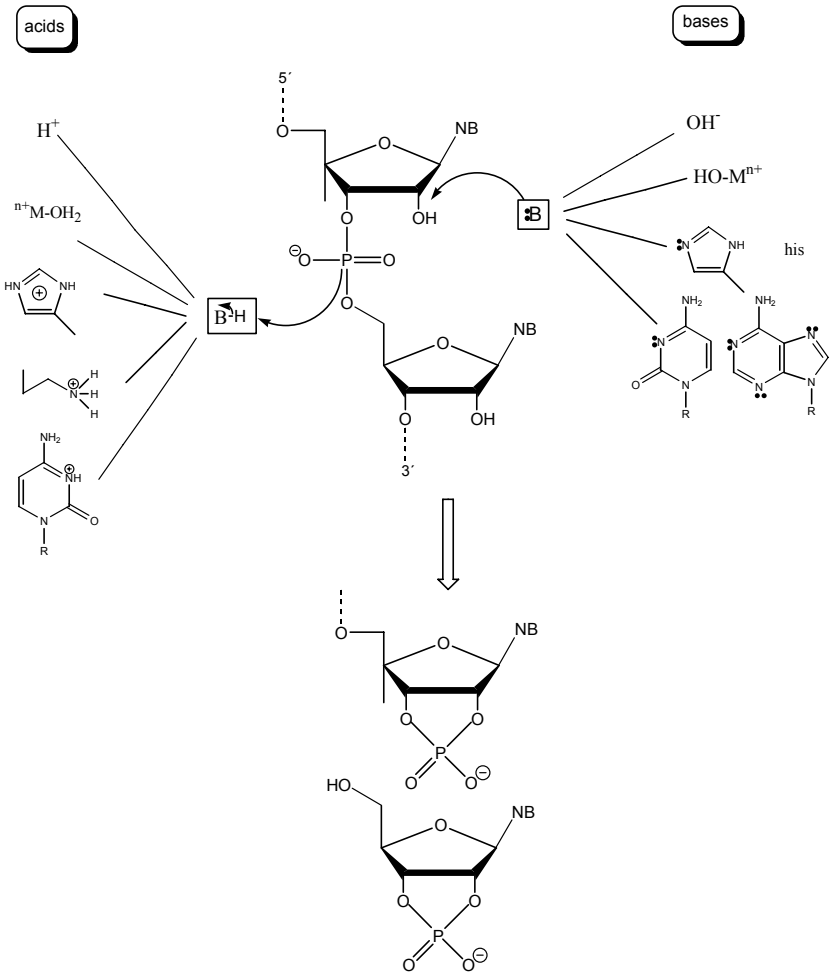

Figure 2: *Present views of catalysis in the ribozymes using different bases and acids. In the HDV ribozime, Cytosine 75 with a shifted pK_a value is essential for catalysis.*

In this work, one of the most interesting parts is the effect of twofold Pt^{II} binding to N1 and N7 of adenine model nucleobases. Specifically, the acidification of the exocyclic amino group at the 6-position was of interest. As has recently been demonstrated by Lüth et al.,[17] the acidity of this amino group is not only affected by electronic effects of coordinated metal ions (here: Pt^{II} at N1 and N7), but in addition by steric effects, viz. an efficient stabilization of the deprotonated amino group (Figure 3). For example, it has been found that while the acidity of this amino group (pK_a ca. 16.7[18] of free base) is increased by 4 - 6 log units upon Pt^{II} binding at N1 and N7 (pK_a ca. 10.8-12.6), it is further

increased (to pK_a~7.9) in the complex *trans*, *trans*, *trans*-[$(NH_3)_2$Pt(*N7*-9-MeA-*N1*)$_2${$(CH_3NH_2)_2$Pt(1-MeU-*N3*)}$_2$]$(ClO_4)_4$. The drop in this pK_a value was attributed to a synergy of electronic effects (Lewis acidification by two metal ions) and favourable geometrical conditions, that is, an efficient stabilization of the deprotonated adenine by intramolecular H-bond formation with the neutral adenine ligand (Figure 4).

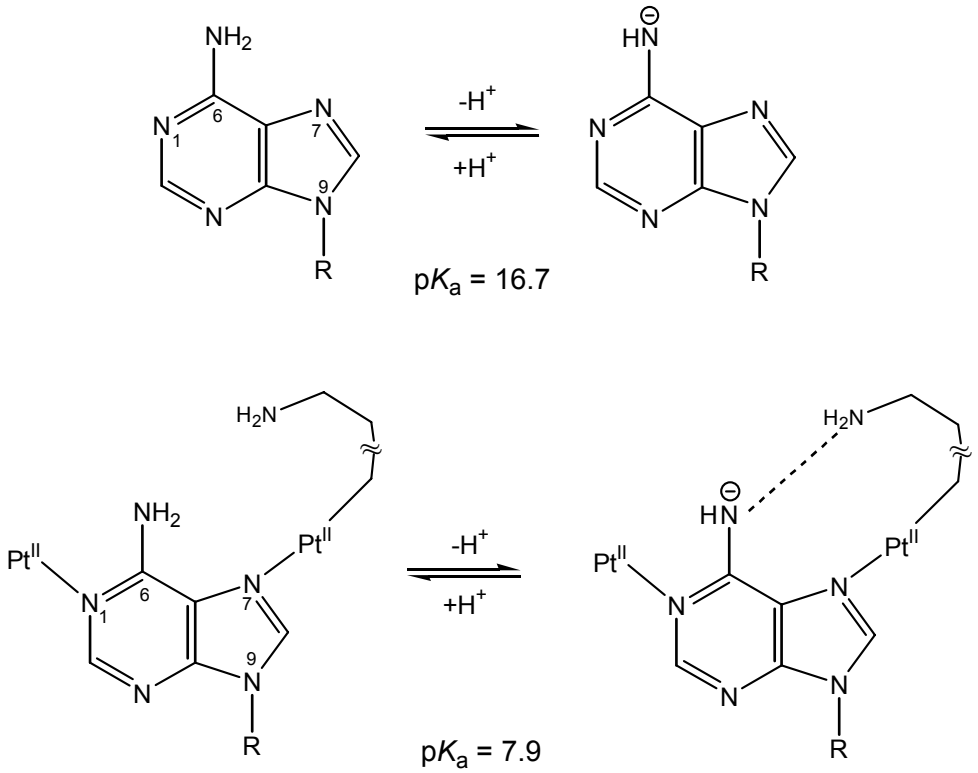

Figure 3: *Acid-base equilibria of N9-blocked adenine involving neutral and anionic species: the free nucleobase (top) and the N1,N7-diplatinated complex with a record-low pK_a value (bottom).*

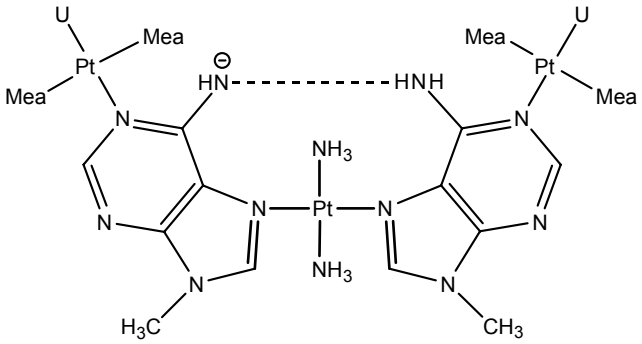

Figure 4: Intramolecular H-bond formation between the deprotonated adenine and the neutral adenine ligand.[17]

In a sense, the situation is reminiscent of that found in dinuclear complexes of Pt^{IV} containing the amido-ammine bridging ligands $H_5N_2^-$.[19]

One of the scopes of this thesis is to examine in more detail the effects of metal coordination on the pK_a values of a nucleobase, hence on its acidity and basicity, respectively, and consequences arising from perturbations. These physicochemical properties are of enormous significance not only for the charge of the nucleobase, but also for its tautomeric structure, and its ability to engage in hydrogen bonding and base recognition.[20]

Another scope of this thesis is to study the migration of the platinum entity in Pt-complexes. The isomerization reactions of Pt–nucleobase adducts are expected to be rare owing to the inertness and thermodynamic stability of the Pt–N bond.[21] Unfortunately, data on thermodynamic stability constants for Pt–N complexes is very limited because of the inertness of the Pt-compounds. Considering the greater basicity of the N1 site over the N7 site in purine bases, the N7→N1 migration of Pt may be anticipated. In fact, this type of isomerization has been observed in (dien)Pt^{II} complexes of inosine[22] and adenosine[23]. Both isomerization reactions have been proposed to follow a similar mechanism, i.e. the change of Pt^{II} binding mode proceeds via N1,N7-diplatinated species.

Although findings[22,23] suggest greater thermodynamic strength for the N1 platinated complexes over the N7 bound species, migration of Pt also seems to be possible in the opposite direction. In the case of (dien)Pt^{II}, this process only occurs in acidic solution. Under neutral and basic conditions no isomerization was observed. In addition, the N1,N7-diplatinated complex is perfectly stable at pH 2.8. Therefore, it was concluded that protonation of the unplatinated N7 site is necessary for the migration reaction. Very interestingly, this N1→N7 migration was found to occur intramolecularly, since addition of excess of Cl^- (a good inactivator for Pt^{II}) caused no significant difference in the overall process.[24] It was suggested that Pt^{II} remains hydrogen bonded to the C(6)–N group during migration which could explain the rapid and efficient conversion to the N7 bound species, since after breaking the Pt–N1 bond very fast deprotonation (N7) and protonation (N1) take place.

Platinum migration from endocyclic to exocyclic nitrogen has also been observed.[25] Migration of Pt^{II} from the N1 site to the exocyclic C(6) – NH_2 group, proceeds in strongly basic solution without any detectable redox reaction. Two mechanistic explanations may be given for the adenine N1→N6 isomerization, both of which require deprotonation of the exocyclic amino group. First, migration of Pt may be analogous to the Dimroth rearrangement, in which an alkyl group formally migrates from heterocyclic nitrogen to an *α*-amino or *α*-imino group.[26] Some examples of this reaction will be explained in Section 2.6.3.

2 RESULTS AND DISCUSSION

2.1 ^{1}H NMR Method for Determination of pK_a

There are numerous ways to determine pK_a values of chemical compounds experimentally.[27] Potentiometric titration and ultraviolet (UV) spectroscopy are classical methods, for example. These techniques have been applied for nucleobases and also for metal-nucleobase complexes. For the determination of nucleobase pK_a values, which are in the pH range of aqueous solutions (pH 0─14), NMR methods are widely used today.

Acidity constants have been determined in this work by measuring the pD dependence of the chemical shifts in ^{1}H NMR experiments in D_2O. In case of D_2O as solvent, 0.4 log units are added to the pH-meter readings (pH*) in D_2O to give the corresponding pD values.[28,29] The pD was adjusted with DNO_3 and NaOD solutions of different concentrations.

The change of the chemical shift of one or several C-H protons in dependence on the pD values was evaluated by a Newton-Gauss non-linear least-squares curve-fitting procedure. Frequently the methyl resonances of the ligands proved to be more suitable for pK_a determination than the aromatic protons because they do not undergo isotopic exchange with time. If the molecule has two deprotonation sites –and thus also two pK_a values– the relationship between the observed chemical shift (δ_{obs}) and the varying pD value is described by equation (1), which was taken from the literature[30] and reformulated for the present situation:

$$\delta_{obs.} = \frac{\delta_B + \delta_{BH^+} \cdot 10^{(pK_{BH^+} - pD)} + \delta_{BH_2^{2+}} \cdot 10^{(pK_{BH_2^{2+}} + pK_{BH^+} - 2 \cdot pD)}}{1 + 10^{(pK_{BH^+} - pD)} + 10^{(pK_{BH_2^{2+}} + pK_{BH^+} - 2 \cdot pD)}} \quad (1)$$

Equation (1) can be easily adjusted to the situation where only one deprotonation site is present, thus giving equation (2):

$$\delta_{\text{obs..}} = \frac{\delta_{\text{B}} + \delta_{\text{BH}^+} \cdot 10^{(\text{p}K_{\text{BH}^+} - \text{pD})}}{1 + 10^{(\text{p}K_{\text{BH}^+} - \text{pD})}} \qquad (2)$$

In equations (1) and (2), δ_B, δ_{BH^+} and $\delta_{BH_2^{2+}}$ represent the chemical shifts of nucleobase species and complexes, which are not protonated (δ_B), protonated (δ_{BH^+}) once or twice ($\delta_{BH_2^{2+}}$). The values pK_{BH^+} and p$K_{\text{BH}_2^{2+}}$are the negative logarithms of the acidity constants of BH^+ and BH_2^{2+} respectively. These acidity constants, which describe the situation in D_2O can be transformed to aqueous solution (H_2O) by application of equation (3).[31]

$$\text{p}K^{\text{H}_2\text{O}} = \frac{\text{p}K^{\text{D}_2\text{O}} - 0.45}{1.015} \qquad (3)$$

Error limits given correspond to one time the standard deviation (1σ).

2.2 The pK_a Values of Nucleobases

The pK_a values of the heterocyclic moieties of the five nucleobases of nucleic acids – guanine (G), adenine (A), cytosine (C), thymine (T), uracil (U) – are well outside the physiological pH range. At physiological pH, the heterocycles are therefore neutral (Fig. 5 and Fig.6).

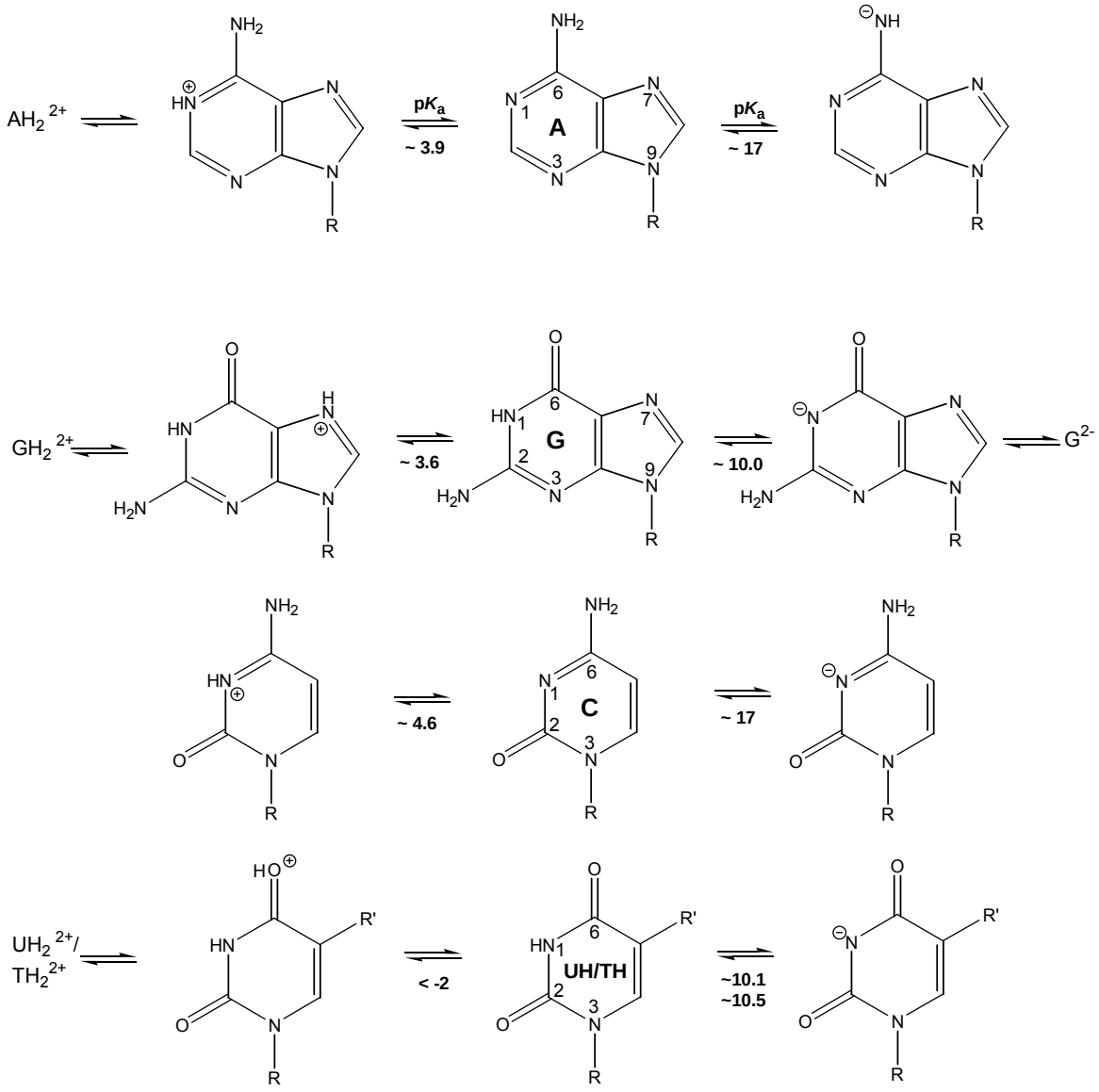

Figure 5: *Lewis formulas of nucleobases A, G, C, U(T) in different protonation states. Only single mesomeric and preferred tautomeric forms are given. Additionally, protonated forms of A, G, U(T) and twofold deprotonated forms of G are not shown. R = CH_3, alkyl,....R' =CH_3*

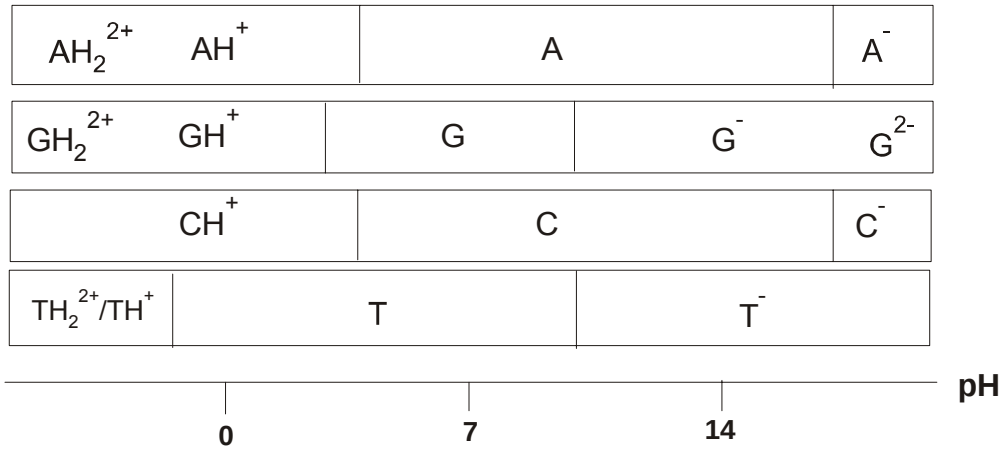

Figure 6: *Distribution of protonated states of nucleobases in dependence of pH.*

The pK_a values of the nucleobases can be modified through alkylation or metal coordination. In this work, both modifications have been studied.

2.3 Electrostatic Effects and H bonds

The understanding of alterations on pK_a values and base pairing properties of nucleobases following metal coordination begins with an in-depth understanding of the forces determining the binding strength of metal-nucleobase interactions. Among others, *ab initio* quantum mechanical calculations have greatly contributed to achieve this goal. Our present understanding of metal-nucleobase bond formation may be summarized as follows.

i) The electrostatic interaction between a metal ion and the nucleobase dipole appears to be the major contribution.[32] In the gas phase, this attraction is dominant, but in solution and in the solid state it can be minimized or even canceled as a consequence of countereffects of a polar solvent (e.g., water, and by anions). The large dipole moment of guanine (7.5 D) and its favorable orientation have been proposed to rationalize, at least in the case of the isolated base, the general high affinity of metal ions for the N7 position. In double-helical DNA, unlike in single-stranded DNA, the situation is more complex in that the affinity of metal ions for G-N7 is strongly modulated by the nature of the base on

the 5´-side, hence depends on the molecular electrostatic potential and also on the accesibility of N7.[33] In contrast, the absolute values of the dipole moment of adenine (2.9 D) and its orientation renders it less favorable for N7 metal binding. The steric hindrance of the exocyclic amino group undoubtedly adds to this situation.

ii) Hydrogen bonds between coligands of the metal (e.g., aqua or ammonia ligands) and the nucleobase add to complex stability.[34-36] An unexpected and surprising result of the computations was the finding that the exocyclic amino group of adenine in its N7 metal complexes can become substantially pyramidalized and can act as a weak hydrogen-bond acceptor for aqua ligands of the metal.[36] So the “neighbour group effects” on individual pK_a values is very important. This term refers to the significance of favorable or unfavorable hydrogen-bonding interactions in stabilizing or destabilizing protonated or deprotonated nucleobase sites. If more than a single nucleobase is attached to the metal, the possibilities for stabilization or destabilization of protonated or deprotonated sites increases.

In the system with N1,N7 diplatinated 9-MeA nucleobases, this aspect has been studied in more detail.[37] Depending on the nature of coligands, pK_a values for deprotonation of the exocyclic amino group of 9-MeA have been found to vary between a high of ~ 12 and a minimum of 7.9. There are at least two possible interpretations for these findings: (1) Assuming that values of ~ 12 essentially reflect the acidifying effects of the two metal ions, then the two Pt^{II} ions were cause of an ~ 10^5-fold acidification of the exocyclic amino group, and the minimum value of 7.9 means an additional 10^4-fold acidification due to favorable neighbour group effects. The minimum pK_a value observed in a trinuclear complex of *trans*-a_2Pt^{II} containing a central (9-MeA-*N7*)Pt(*N7*-9-MeA) cross-link and two Pt(1-MeC-*N3*) units coordinated to the N1 positions of the two 9-MeA ligands,[17] has been attributed to the hydrogen-bond donor properties of the amino group of the neutral 9-MeA, which stabilizes the ─NH^- group of the second adenine base. The role of the amino group of the neutral 9-MeA is thus similat to that of amino groups in certain metalhydroxo species where it likewise

stabilizes the anion and adds to the acidity of the metal aqua complex.[38] A survey of pK_a values of a class of related complexes of *cis*- and *trans*-a_2Pt^{II} as well as a_3Pt^{II} with 9-methyladenine and 9-ethyladenine ligands and other nucleobases[37] seem to be in aggrement with this hypothesis. (2) An alternative interpretation would be to assume a priori additive effects of two metal entities at N1 and N7 in acidifying the exocyclic group, which are reduced by an insufficient stabilization of the deprotonated group due to unfavorable intramolecular hydrogen-bonding interactions. For example, the individual acidifications of the N(6)H_2 group of 9-MeA in complexes of dienPt^{II} with N1 coordination (≤ 6 log units) and with N7 coordination (≤ 4 log units) do not add up, as the pK_a of the diplatinated complex (pK_a ~ 11)[11] displays an acidification of only ~ 6 units. This situation is in contrast to the roughly additive effects of N1 methylation and N7 Pt^{II} coordination in *trans*-[$(NH_3)_2$Pt(1,9-DimeAH-*N7*)$_2$]$^{4+}$.

It is obvious that details of fine tuning of pK_a values still need to be settled. However, presently available pK_a data in any case support the general view that an appropriately located hydrogen bond donor such as an exocyclic amino group of a nucleobase causes a lowering of the pK_a value of N(6)H_2 of adenine complexes, whereas a hydrogen bond acceptor such as an exocyclic carbonyl group of another nucleobase, increases the pK_a (Figure 7). Considering the fact that in all these compounds am(m)ine coligands of the Pt(II) are present, one might argue that hydrogen bonding among these ligands and the deprotonated adenine site could have provided the stabilization required to reduce the pK_a. In fact, DFT calculations are supportive of such a scenario (see Chapter 2.5).

At the same time, they reveal an alternative to a direct ─NH$^-$···H_2N interaction, namely, via a solvent molecule.[37] We do not wish to exclude such a possibility, even though it does not readily rationalize the spread in pK_a values experimentally observed in Pt am(m)ine complexes. If true (for all compounds) pK_a values should display only slight variations.

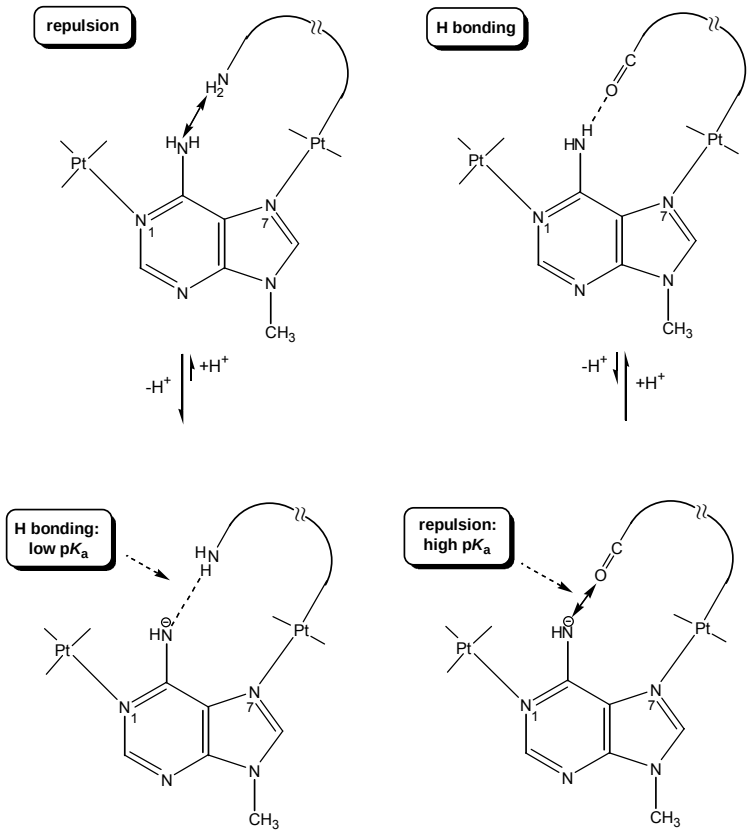

Figure 7: *Effects of neighbour groups on N(6)H_2 acidity of N1,N7 diplatinated adenine: Low pK_a by efficient hydrogen bonding between ─NH_2 donor and ─NH^- versus high pK_a due to repulsion between ─NH^- and O acceptor.*

iii) In addition to electrostatics and hydrogen-bond formation, polarization, and charge-transfer effects, also termed nonelectrostatic effects, are active.[39] These refer to changes associated with a redistribution of electrons in the bonds within the nucleobase of the metal complex. They are less influenced by solvent and counterions. Not unexpectedly, substitution of nucleobase protons (e.g., of N─H) by metal ions increases this contribution as compared to binding of the metal to an available lone pair of an endocyclic nitrogen or an exocyclic oxygen atom. The influence of the solvent will be discussed in chapter 2.8.

2.4 Altered pK_a Values of Nucleobases in Metal Complexes

Metal binding to exocyclic oxygen atoms of nucleobases such as O2 or O4 of T(U), O6 of G, and O2 of C [40, 41, 42-45] is expected to acidify endocyclic NH and exocyclic NH_2 protons and reduce the basicity of endocyclic N as well as that of other carbonyl groups (T, U). The effect of metal coordination to any of the endocyclic N atoms can be also expressed in terms of a loss in basicity of the remaining endocyclic N atoms, hence in a reduced tendency to accept a proton and to become a metalated cation.

Nucleid acids are composed of nucleosides which are joined through phosphodiester linkages. Nucleosides are composed of a nucleobase to a ribose ring. Nucleosides can be phosphorylated by specific kinases in the cell, producing nucleotides, which are the molecular building blocks of DNA and RNA. Each nucleotide consists of a cyclic sugar (ß-D-ribose in RNAs, ß-D-2´ deoxyribose in DNA), which is phosphorylated in the 5´position of the sugar and carries a heterocyclic ring at the C1´ position (ß-glycosyl C1´-N bond). The heterocycles are, in general, the purine bases guanine, adenine and the pyrimidine bases cytosine as well as thymine (DNA) or uracil (RNA).

There are many more reports on pK_a changes of nucleobase funcionalities in which neutral nucleobases provide endocyclic N atoms as bonding sites. These have been studied in this thesis. First of all, we are going to discuss the case of adenine.

2.5 9-MeA System

The ligand 9-methyladenine (Figure 8) is used as a model compound for adenosine. The structural difference between adenosine and 9-MeA is the replacement of the sugar moiety by a methyl group in the latter. Adenine was methylated at N9 according to Krüger.[46]

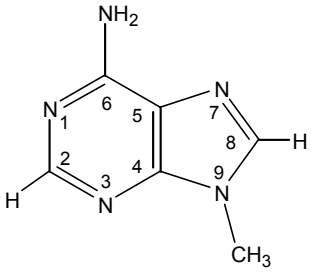

Figure 8: *Amino form of 9-methyladenine.*

N-9 substituted adenines can exist theoretically in four tautomeric forms, with the first one, the amino form (I), being the preferred tautomer (Figure 9). pK_a values of 9-MeA and its cationic forms are listed in Table 1.

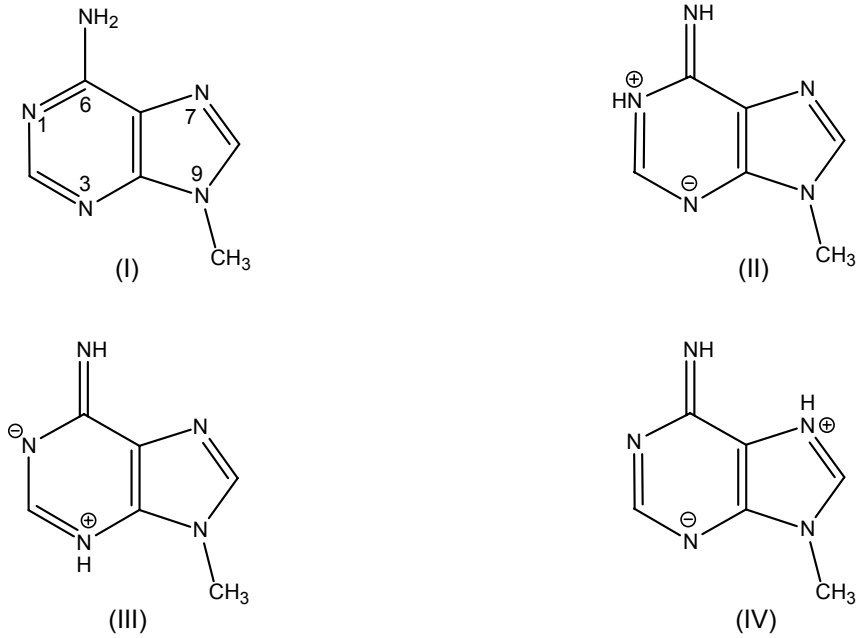

Figure 9: *The four possible tautomeric forms of 9-methyladenine: (I): amino tautomer, (II), (III) and (IV): imino tautomers.*

Table 1: *pK_a values of 9-methyladenine determined potentiometrically and with UV-spectroscopy [for 9-MeA].*

Position	pK_a values [47]
N7 (at 9-MeAH$^+$-*N1*)	-0.37 ± 0.06
N1 (at 9-MeAH$^+$-*N7*)	1.30 ± 0.31
N7 (at 9-MeA)	2.43 ± 0.30
N1 (at 9-MeA)	4.10 ± 0.01
Exocyclic amino group NH_2	16.7

Adenine provides three unprotonated endocyclic nitrogen atoms (N1, N3, N7) at physiological pH, all of which are potential metal binding sites. The basicity order (affinity for H^+) is N1>N7>N3.[48] The N9-substituted purine nucleobase adenine exhibits several potential binding sites for metal ions. These include the ring nitrogens N1, N3 and N7, and the exocyclic amino group. In native DNA, however, various Pt compounds seem to prefer the N7 site [22]. The N7 site of purine nucleobases is the major target for anticancer Pt drugs and related compounds in DNA. Because of the general inertness of Pt(II)/Pt(IV) and the high thermodynamic stability of the Pt-N bond, substitution of the nucleobases in the relevant Pt adducts is expected to be very difficult. In this respect, findings on relatively easy rearrangements of various Pt(II) bisadducts at the oligonucleotide level are of great interest, though the mechanism of the rearrangement is not known yet.[25]

We have extended our studies of Pt^{II}-adenine complexes to compounds with different amine ligands (*cis*-[a_2Pt^{II}], [a_3Pt^{II}], *trans*-[ma_2Pt^{II}], and [dienPt^{II}], where a=NH_3 and ma=NH_2CH_3). In addition, we have employed other nucleobases as coligands (Figure 10). We have been particularly interested in the effect of cytosine since this nucleobase also contains a suitably located exocyclic amino group for stabilization of an NH group of adenine.

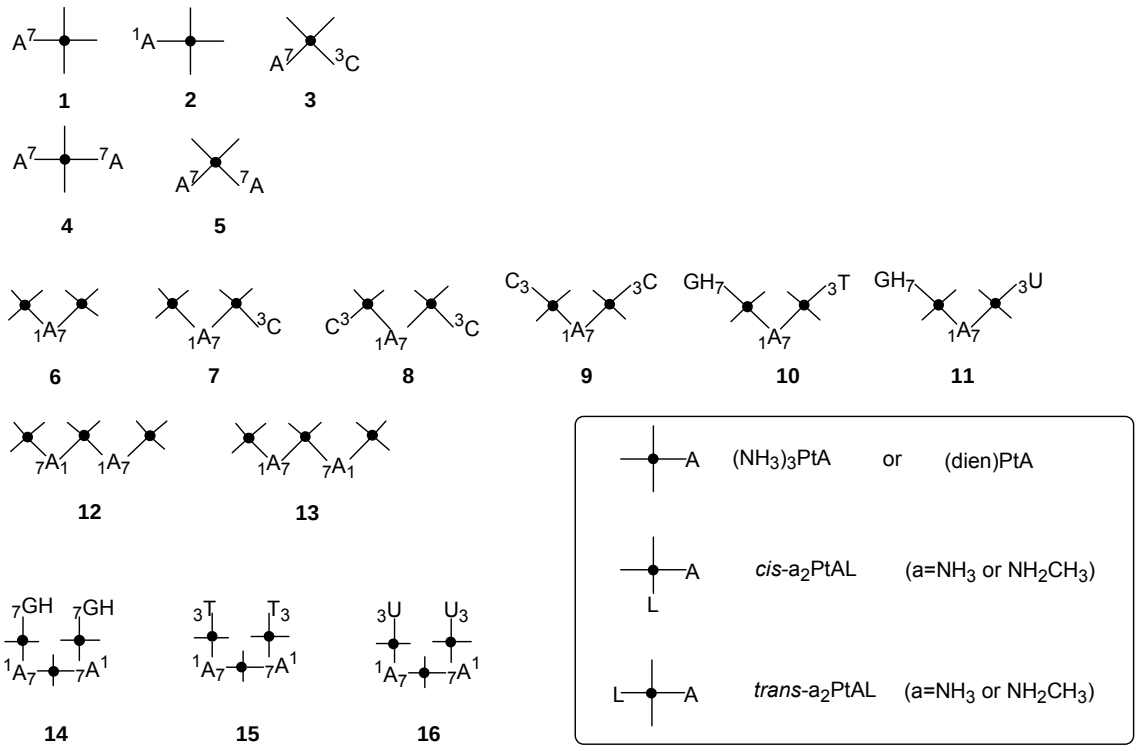

Figure 10: *Schematic representation of Pt^{II} complexes studied in this work. Coordination sites are indicated.*

2.5.1 $N6H_2$ Acidification of Adenine by a Single Pt^{II}

The acidification of adenine nucleobases by a coordinated metal ion can be expressed in terms of a loss in basicity for accepting a proton at one of the three available endocyclic nitrogen atoms, N1 (preferably), N7, or N3. Pt^{II} binding to N7 of a N9-substituted adenine, for example, 9-methyladenine, makes protonation of the preferred N1 position more difficult by approximately 2 log units, that is, the pK_a value of N1H drops from 4.10 in free 9-methyladeninium (9-MeAH^+) to approximately 2 in its Pt^{II} complexes.[13] If Pt^{II} is bonded to N1, protonation occurs at N7 with a pK_a value of approximately 1.2,[49] and if the N3 site is carrying a Pt^{II} entity, the overall basicity of the adenine ring drops by 4 log units, with N7 then being more basic than N1.[13a,50]

Table 2: *pK_a values of the $N6H_2$ group in 9-alkyladenine complexes of Pt^{II}.[39] For simplification, the N1 and N9 alkylnucleobases were named with the general symbols of the nucleobases (A, G, C, T, U). [a] Determinated by potentiometry. The remaining values were determinated by ^1H NMR spectroscopy (n.d. = not determined). The compounds with numbers were studied in this thesis.*

Compound	Cation Composition	pK_{a1}	pK_{a2}
A	[(dien)Pt(A-*N7*)]$^{2+}$	> 13[11]	-
1	[(dien)Pt(A-*N1*)]$^{2+}$	> 11	-
B	[{(dien)Pt}$_2$(A-*N1*,*N7*)]$^{4+}$	ca. 11[11]	-
2	*cis*-[a$_2$Pt(A-*N7*)(C-*N3*)]$^{2+}$	> 12.6	-
3	*trans*-[a$_2$Pt(A-*N7*)$_2$]$^{2+}$	> 12.8	n. d.
4	*cis*-[a$_2$Pt(A-*N7*)$_2$]$^{2+}$	> 13	n. d.
5	*cis*-[a$_2$Pt(C-*N3*)(*N7*-A-*N1*)Pt(dien)]$^{4+}$	10.79	
6	*cis*-[{a$_2$Pt(C-*N3*)}$_2$(A-*N1*,*N7*)]$^{4+}$	11.03	-
7	*trans*-[{a$_2$Pt(C-*N3*)}$_2$(A-*N1*,*N7*)]$^{4+}$	10.00	-
C	*trans*,*trans*-[(ma)$_2$Pt(C-*N3*)(*N1*-A-*N7*)Pta$_2$(GH-*N7*)]$^{4+}$	10.66[37]	-
D	*trans*,*trans*-[(ma)$_2$Pt(A-*N7*)(*N1*-A-*N7*)Pta$_2$(GH-*N7*)]$^{4+}$	10.08[37]	-
E	*trans*,*trans*-[a$_2$Pt(T-*N3*)(*N7*-A-*N1*)Pt(ma)$_2$(GH-*N7*)]$^{3+}$	12.06[51]	-
F	*trans*,*trans*-[a$_2$Pt(U-*N3*)(*N7*-A-*N1*)Pt(ma)$_2$(GH-*N7*)]$^{3+}$	12.62[51]	-
11	*cis*-[a$_2$Pt{(*N1*-A-*N7*)Pta$_3$}$_2$]$^{6+}$	8.7, 9.10[a]	10.7, 10.9[a]
12	*cis*-[a$_2$Pt{(*N7*-A-*N1*)Pt(dien)}$_2$]$^{6+}$	9.23[a]	10.56[a]
G1	*trans*,*trans*,*trans*-[a$_2$Pt(*N7*-A-*N1*)$_2${a$_2$Pt(GH-*N7*)}$_2$]$^{6+}$	8.67[a]	10.96[a]
G2	*trans*,*trans*,*trans*-[a$_2$Pt(*N7*-A-*N1*)$_2${(ma)$_2$Pt(GH-*N7*)}$_2$]$^{6+}$	8.57[a]	10.61[a]
H	*trans*,*trans*,*trans*-[a$_2$Pt(*N7*-A-*N1*)$_2${a$_2$Pt(T-*N3*)}$_2$]$^{4+}$	8.61[a]	11.31[a]
I	*trans*,*trans*,*trans*-[a$_2$Pt(*N7*-A-*N1*)$_2${(ma)$_2$Pt(U-*N3*)}$_2$]$^{4+}$	7.94[17]	11.66[17]

The acidifying effect of metal coordination on any of the ring nitrogen atoms is also reflected by a drop in the pK_a value of the exocyclic amino group (Table 2). Of course, this is numerically different from the ΔpK_a values measured for the protonated endocyclic nitrogen atoms but it also depends on the site of metal binding. It appears that N1Pt^{II} binding to adenine nucleobases causes a larger acidification of the $N6H_2$ group than N7 Pt^{II} binding: In the N1(dien)Pt^{II} complex of 9-MeA (**1**) deprotonation starts above pH* 11,[11] and with [$(NH_3)_3$Pt(adenosine-*N1*)]$^{2+}$ a pK_a value of 12.4 has been reported.[12] Our own

findings with *cis*-[$(NH_3)_2$Pt(9-MeA-*N7*)(1-MeC-*N3*)]$(ClO_4)_2 \cdot H_2O$ (**2**) and with compounds *trans*-[$(NH_3)_2$Pt(9-MeA-*N7*)$_2$]$(ClO_4)_2 \cdot 2H_2O$ and *cis*-[$(NH_3)_2$Pt(9-MeA-*N7*)$_2$]$(NO_3)_2 \cdot 2H_2O$ (**3** and **4**, respectively) are also consistent with a relatively moderate effect of the metal ion at N7 (pK_a values > 12.6), although it might be argued that the charge effect of the metal is reduced in the bis(nucleobase) complex relative to that in a mono(nucleobase) complex. Anyway, there is more stabilization of deprotonated adenine in case of the *trans*-isomer. In the ^{1}H NMR spectra, the two deprotonation steps of the *trans*-[$(NH_3)_2$Pt(9-MeA-*N7*)$_2$]$^{2+}$ are well separated. For the *cis* complex, however, the second one occurs at high pD (Figure 11).

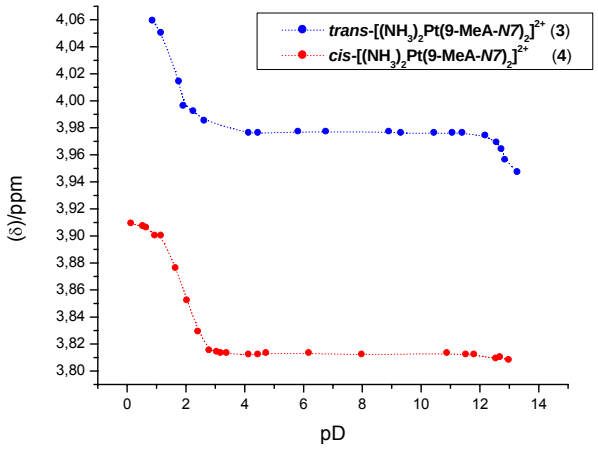

Figure 11: *pD dependence of the N(9) CH_3 resonance of (**3**) and (**4**) in the ^{1}H NMR spectra. The first pK_a corresponds to the protonation at N1 and the values are 1.00 ± 0.06 and 1.84 ± 0.04 respectively.*

2.5.2 N6H$_2$ Acidification of Adenine by Twofold Pt^{II} Binding through N1 and N7

Coordination of a second Pt^{II} entity to an adenine nucleobase causes a more pronounced acidification of the exocyclic adenine amino group and permits ready detection in water. In early studies, pK_a values of 11.0 - 11.3 have been

determined for [{(dien)Pt}$_2$(9-MeA-*N1*,*N7*)]$^{4+}$(**B**),[11] and 10.8 was the value reported for [{(NH$_3$)$_3$Pt}$_2$(adenosine-*N1*,*N7*)]$^{4+}$.[12]

2.5.2.1 Mixed Adenine/Cytosine Complexes of *cis*- and *trans*-a$_2$Pt(II)

The dinuclear mixed adenine/cytosine complexes (**5**) – (**7**) studied in this thesis (Figure 10) essentially confirm that coordination of a second Pt^{II} entity to an adenine causes a more pronounced acidification of the NH$_2$ group. Still, there is an interesting detail to be noted: For the *trans*-[(NH$_3$)$_2$Pt^{II}] compound (**7**) a pK_a value of 10.0 ± 0.1 is observed, which is significantly lower than the corresponding pK_a value of 11.1 ± 0.1 for the *cis* isomer (**6**) (Table 2, pag. 18). In two previously described nucleobase triplets containing a central Pt(*N1*-adenine-*N7*)Pt unit,[28] *trans*,*trans*-[(NH$_3$)$_2$Pt(1-MeT-*N3*)(*N7*-9-MeA-*N1*)Pt(NH$_2$CH$_3$)$_2$(9-EtGH-*N7*)](ClO$_4$)$_3$·5.2H$_2$O (**E**) and *trans*,*trans*-[(NH$_3$)$_2$Pt(1-MeU-*N3*)(*N7*-9-EtA-*N1*)Pt(NH$_2$CH$_3$)$_2$(9-EtGH-*N7*)]$^{3+}$ (**F**), the pK_a values for deprotonation of the exocyclic amino group of the adenine nucleobase in water were found to be substantially higher, around 12.1 and 12.6 in both cases. This difference of two log units from the value for (**7**) clearly suggests a substantial internucleobase effect (Figure 12).

Although a charge influence is also likely to play a role, ((**7**) has a charge of +4; (**E**) and (**F**) have charges of +2 once the guanine ligands have undergone deprotonation), it is probably not dominant. For example, (**D**) has almost the same pK_a value (10.08 ± 0.22) as (**7**), although it has a charge of only +3 once the guanine ligand is deprotonated. An internucleobase effect on the pK_a value of adenine is further suggested by a comparison of (**C**) and (**D**): Both compounds have identical charges (and identical pK_a values of the guanine ligands), yet the pK_a values of the bridging adenine ligand are different (10.66 ± 0.03 and 10.08 ± 0.22, respectively).

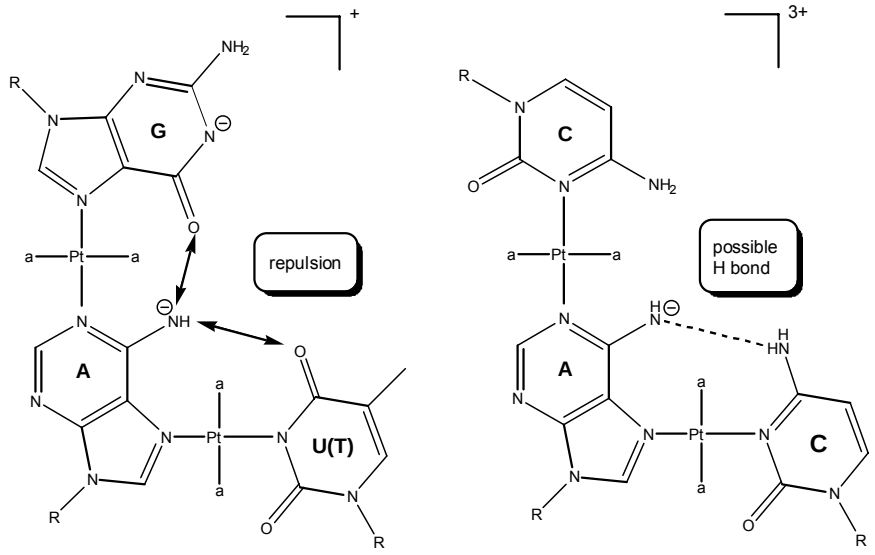

E,F **7**

Figure 12: *Internucleobase effects on deprotonated adenine group N6H⁻ in (**E**) and (**F**) (left) and (**7**) (right).*

2.5.2.2 *trans*-[$(NH_3)_2$ClPt(*N7*-9-MeA-*N1*)(dienPt)]$(ClO_4)_3$ (8) as Starting Compound

In order to study the acidification of $N6H_2$ in a trinuclear bis(adenine-*N1*,*N7*), this compound was synthesized. The starting compound *trans*-[$(NH_3)_2$ClPt(*N7*-9-MeA-*N1*)(dienPt)]$(ClO_4)_3$ (**8**) (with dien = diethylenetriamine) was prepared by reaction of [(dienPt)(9-MeA-*N1*)]$^{2+}$ and *trans*-DDP. As counterion perchlorate was applied.

2.5.2.2.1 Crystal Structure of *trans*-[$(NH_3)_2$ClPt(*N7*-9-MeA-*N1*)(dienPt)]$(ClO_4)_3$ (8)

Crystals of *trans*-[$(NH_3)_2$ClPt(*N7*-9-MeA-*N1*)(dienPt)]$(ClO_4)_3$ (**8**) were isolated from an aqueous solution and characterized by X-ray crystallography.

The complex (**8**) crystallizes in the triclinic space system. In the refinement process of the X-ray data, all non-hydrogen atoms of the crystal were refined anisotropically. The hydrogen atoms were placed at geometrical idealized positions and refined isotropically. Crystal data, data collection and refinement parameters for (**8**) are summarized in Table A-1 (see Appendix).

The solid state structure of (**8**) consists of an adenine nucleobase coordinated to two platinum atoms, which are binding to N1 and N7 of the 9-methyladenine as well as three perchlorate counter ions. The platinum binding through N1 (Pt1), is coordinated to the three nitrogen atoms of the dien ligand and the other one (Pt2), through N7, is in addition coordinated to a chloride and two ammonia ligands in *trans*-position. A view of the cation *trans*-[$(NH_3)_2$ClPt(*N7*-9-MeA-*N1*)(dienPt)]$(ClO_4)_3$ (**11**) with the labeling scheme is shown in Figure 13.

The geometry of the (dien)Pt1 moiety is normal and compares well with published data.[52] Thus, the N1E-Pt1-N3E angle deviates markedly from 180° (167.5(4)°), unlike the N2E-Pt1-N1B angle, which is 177.9(4)°. The dien ring displays the characteristic sting ray structure, with C2E and C3E out of the Pt coordination plane by 0.69(2) and 0.44(2) Å, respectively. The other C atoms (C1E and C4E) are by 0.08(2) and -0.18(2) Å out of the platinum coordination plane. Pt-N distances about the Pt1 center range from 1.992(9) to 2.056(9) Å. A list of selected distances and angles between atoms of *trans*-[$(NH_3)_2$ClPt(*N7*-9-MeA-*N1*)(dienPt)]$(ClO_4)_3$ is given in Table 3.

The two Pt1-N-C angles are clearly different; in the case of the CH group, the Pt1-N1B-C2B angle is 118.5(8)° and on the side containing the exocyclic amino group, the Pt1-N1B-C6B angle is larger, 121.2(7)°

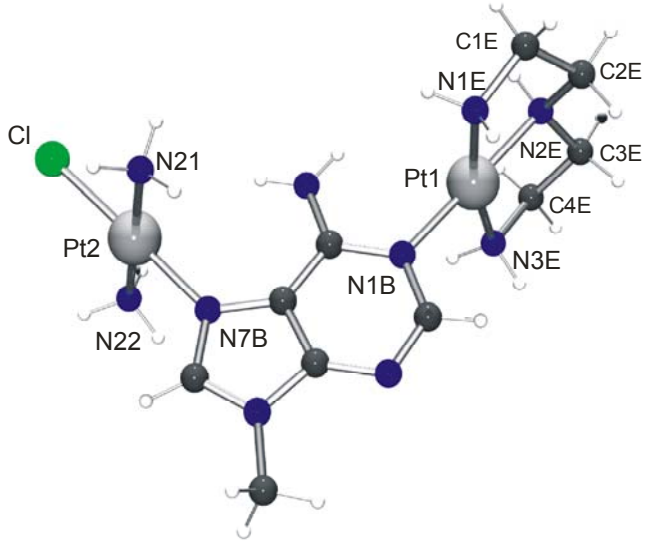

Figure 13: *View of the cation trans-[$(NH_3)_2$ClPt(N7-9-MeA-N1)(dienPt)]$^{3+}$ of (**8**).*

Table 3: *Selected distances (Å) and angles (º) for non-hydrogen atoms in **8**.*

Pt1-N2E	1.992(9)	N2E-Pt1-N1B	177.9(4)
Pt1-N1B	2.008(9)	N2E-Pt1-N1E	85.3(4)
Pt1-N1E	2.044(9)	N1B-Pt1-N1E	92.5(4)
Pt1-N3E	2.056(9)	N2E-Pt1-N3E	84.3(4)
Pt2-N7B	2.007(9)	N1B-Pt1-N3E	97.8(4)
Pt2-N22	2.034(9)	N1E-Pt1-N3E	167.5(4)
Pt2-N21	2.041(9)	C2B-N1B-C6B	120.7(10)
Pt2-Cl	2.294(3)	N7B-Pt2-N22	92.0(4)
		N7B-Pt2-N21	89.0(4)
		N22-Pt2-N21	179.0(4)
		N7B-Pt2-Cl	179.1(3)
		N22-Pt2-Cl	88.0(3)
		N21-Pt2-Cl	91.1(3)

The *trans*-$(NH_3)_2ClPt^{II}$ entity presents normal distances and angles between atoms.

The atoms of the 9-methyladenine base are coplanar, with a r.m.s. deviation of 0.014. The dihedral angle between the adenine ring and the platinum(1) coordination plane is 85.8(3)°. However, the dihedral angle with the other platinum(2) coordination plane is lower, 78.4(2)°. The atoms of this plane have a r.m.s deviation of 0.011. Pt-N1 and Pt-N7 vectors are approximately perpendicular to each other [87.7(2)°].

The unit cell of complex (**8**) has two molecules, which are identical by a center-inversion symmetry operation. For the discussion of the hydrogen bonding pattern, the different hydrogen bonds of both molecules are going to be explained separately.

There are not intramolecular hydrogen bonds, because the distance between the exocyclic amino group of the adenine nucleobase and one of the nitrogen of the dien ligand is too long: N6B···N1E, 3.77(1) Å. There are no intermolecular hydrogen bonds interactions between ligands of neighbouring cations. The perchlorates are involved in intermolecular hydrogen bonds. The O14 of the perchlorate anion forms a hydrogen bond to the proton of the dien ligand (H3E), O14···N3E(H3E), 2.98(1)Å and N2E(H2E) of the same dien ligand, forms a hydrogen bond with a O41(a) of another perchlorate anion, O41(a) (-x+1, -y, -z+1)···N2E(H2E), 2.90(1) Å. One of the ammine ligands is also involved in hydrogen bonds with two different perchlorate anions: N21··· O31, 3.09(1) Å and N21···O41, 3.09(1) Å (Figure 14).

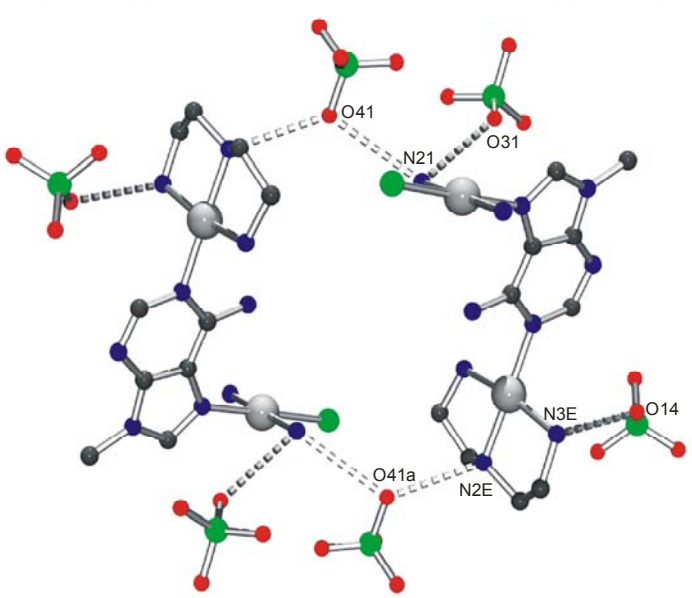

Figure 14: *View of intermolecular H bonding between symmetry-related pairs of trans-[$(NH_3)_2$ClPt(N7-9-MeA-N1)(dienPt)]$(ClO_4)_3$ (**8**).*

In the other orientation there are also hydrogen bonds between the cations and the perchlorate anions. The distances are the following: O53···N31, 3.11(1) Å; O51···N31, 3.26(1) Å; N31···O21, 3.05(1); O23···N6b(H6b) (-1+x, y, z), 3.089(4) Å and O61···N3D(H3D), 2.94(1) Å (Figure 15).

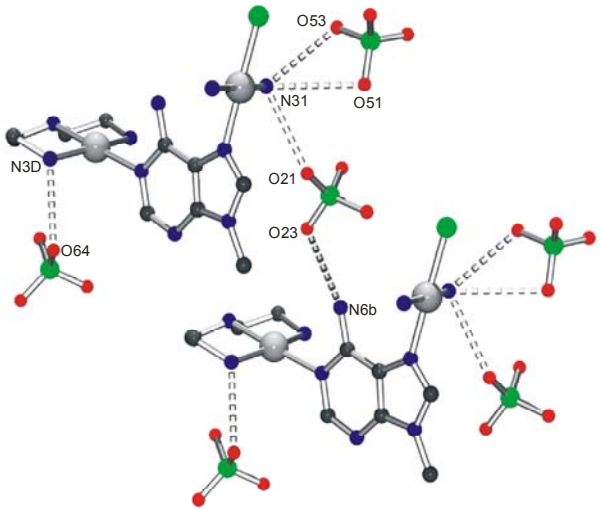

Figure 15: *View of intermolecular H bonding between another symmetry-related pairs of trans-[$(NH_3)_2$ClPt(N7-9-MeA-N1)(dienPt)]$(ClO_4)_3$ (**8**).*

The arrangement of the *trans*-[$(NH_3)_2$ClPt(*N7*-9-MeA-*N1*)(dienPt)]$^{3+}$ cations is shown in Figure 16. Perchlorate anions are located between the layers acting as connection. No π-stacking interactions are observed between aromatic nucleobases.

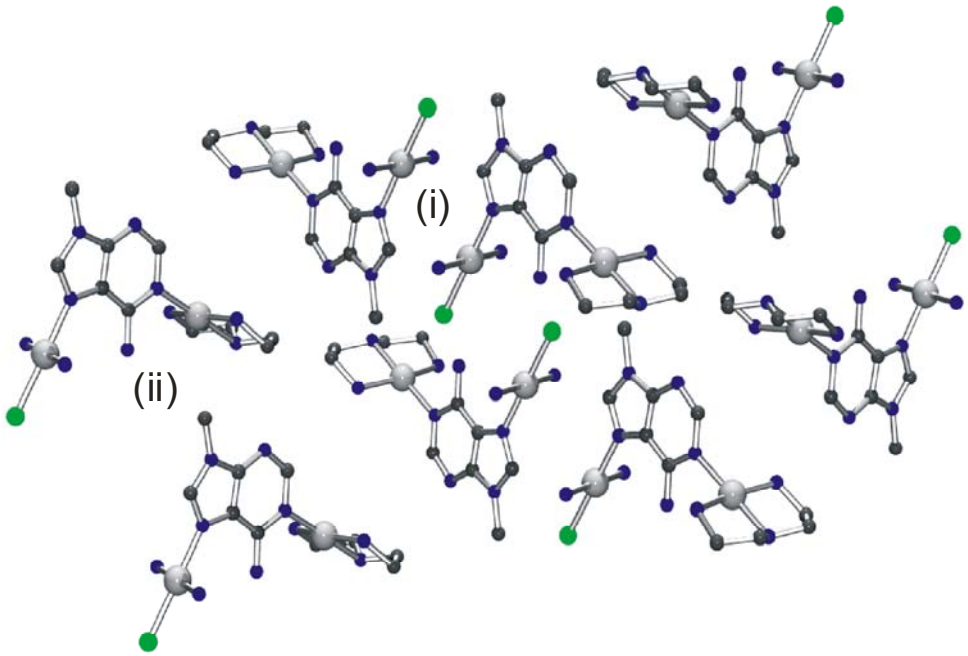

Figure 16: *View of the crystal packing of the cations of (**8**).Symmetry operations: (i) –x+1, -y, -z+1; (ii) -1+x, y, z.*

2.5.2.2.2 NMR Spectroscopy of *trans*-[$(NH_3)_2$ClPt(*N7*-9-MeA-*N1*)(dienPt)]$(ClO_4)_3$ (8)

The first characterization of (**8**) prepared in situ was done by means of NMR spectroscopy. The ^{1}H NMR spectrum of a solution containing the cationic *trans*-[$(NH_3)_2$ClPt(*N7*-9-MeA-*N1*)(dienPt)]$^{3+}$ entity displays two signals in the aromatic region. One of them is a sharp singlet, while the other one is a broad signal, corresponding to the H2 and H8 protons of the 9-methyladenine base. In addition, a sharp singlet (s) of the methyl group of 9-MeA and the CH_2 resonances of the dien ligand are observed. When the solution is in the neutral pH, the signal corresponding to H8 as well as the CH_3 singlet of 9-MeA have

chemical shifts of δ = 8.86 and 3.95 ppm, respectively; signals associated with the dien ligand range from 2.7 to 3.3 ppm (Figure 17). The assigment of H8 of 9-MeA was established by an NOE experiment.

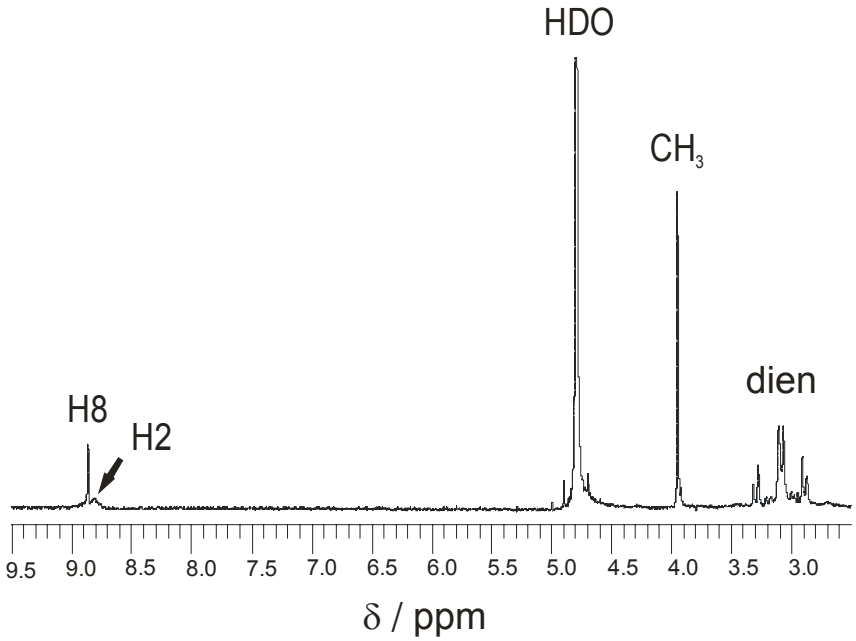

Figure 17: *^{1}H NMR spectrum in D_2O of the trans-[$(NH_3)_2$ClPt(N7-9-MeA-N1)(dienPt)]$^{3+}$ at room temperature (pD = 4.9).*

2.5.2.2.3 pH Dependence of *trans*-[$(NH_3)_2$ClPt(*N7*-9-MeA-*N1*)(dienPt)]$(ClO_4)_3$ (8)

The acidity constant of *trans*-[$(NH_3)_2$ClPt(*N7*-9-MeA-*N1*)(dienPt)]$^{3+}$ has been determined by pD dependent ^{1}H NMR measurements. In the course of this study, a complication of the spectra at high pH was observed. At pD > 8, two signals occured for the methyl group of the 9-MeA, which is a consequence of a migration of Pt, leading to the formation of one new compound. This will be explained in Chapter 2.5.4.

2.5.2.3 *trans*-[$(NH_3)_2$Pt(*N7*-9-MeA)(*N7*-9-MeA-*N1*)(dienPt)]$^{4+}$ (9)

In order to compare the pK_a value of compound (**8**) with that of a similar one, in which an additional adenine is binding to one of the platinum atoms, *trans*-[$(NH_3)_2$Pt(*N7*-9-MeA)(*N7*-9-MeA-*N1*)$_2$(dienPt)]$^{4+}$ was synthesized (**9**). The difference between compound (**8**) and (**9**) is a substitution of the chloro ligand by a 9-MeA. Two different ways for the synthesis of the complex with two adenine nucleobases have been worked out. The first one consists of the treatment of (**8**) with one equivalent of silver nitrate. After removal of AgCl, one equivalent of 9-MeA was added. The subsequent substitution reaction was carried out in 24 hours at 40 °C. The resulting ^{1}H NMR spectra were very complicated because of the formation of other species, which could not be identified. Therefore, a different strategy was needed. The compound *trans*-[$(NH_3)_2$Pt(*N7*-9-MeA)(*N7*-9-MeA-*N1*)(dienPt)]$^{4+}$ was prepared by reaction of *trans*-[$(NH_3)_2$Pt(9-MeA-*N7*)$_2$]$^{2+}$ (**3**) with [(dienPt)$(H_2O)_2$]$^{2+}$. The resulting ^{1}H NMR spectra recorded at different pD values are shown in Figure 18.

The resonances **A**, B1, B2 and C correspond to three different compounds. The structure and the formulas of these complexes are summerized in Table 4. The resonance **A** corresponds to the methyl group of the starting material [*trans*-[$(NH_3)_2$Pt(9-MeA-*N7*)$_2$]$^{2+}$ (**3**)]. The resonance B1 corresponds to the methyl group of the adenine containing the dienPt^{II} entity at N1 in the desired product *trans*-[$(NH_3)_2$Pt(*N7*-9-MeA-*N1*)$_2$(dienPt)]$^{4+}$ (**9**). The resonance B2 corresponds to the methyl group of the adenine with the N1 position free in *trans*-[$(NH_3)_2$Pt(*N7*-9-MeA-*N1*)$_2$(dienPt)]$^{4+}$ (**9**). Finally, the resonance C corresponds to the methyl group of the compound *trans*-[$(NH_3)_2$Pt(*N7*-9-MeA-*N1*)$_2$(dienPt)$_2$]$^{6+}$ (**10**).

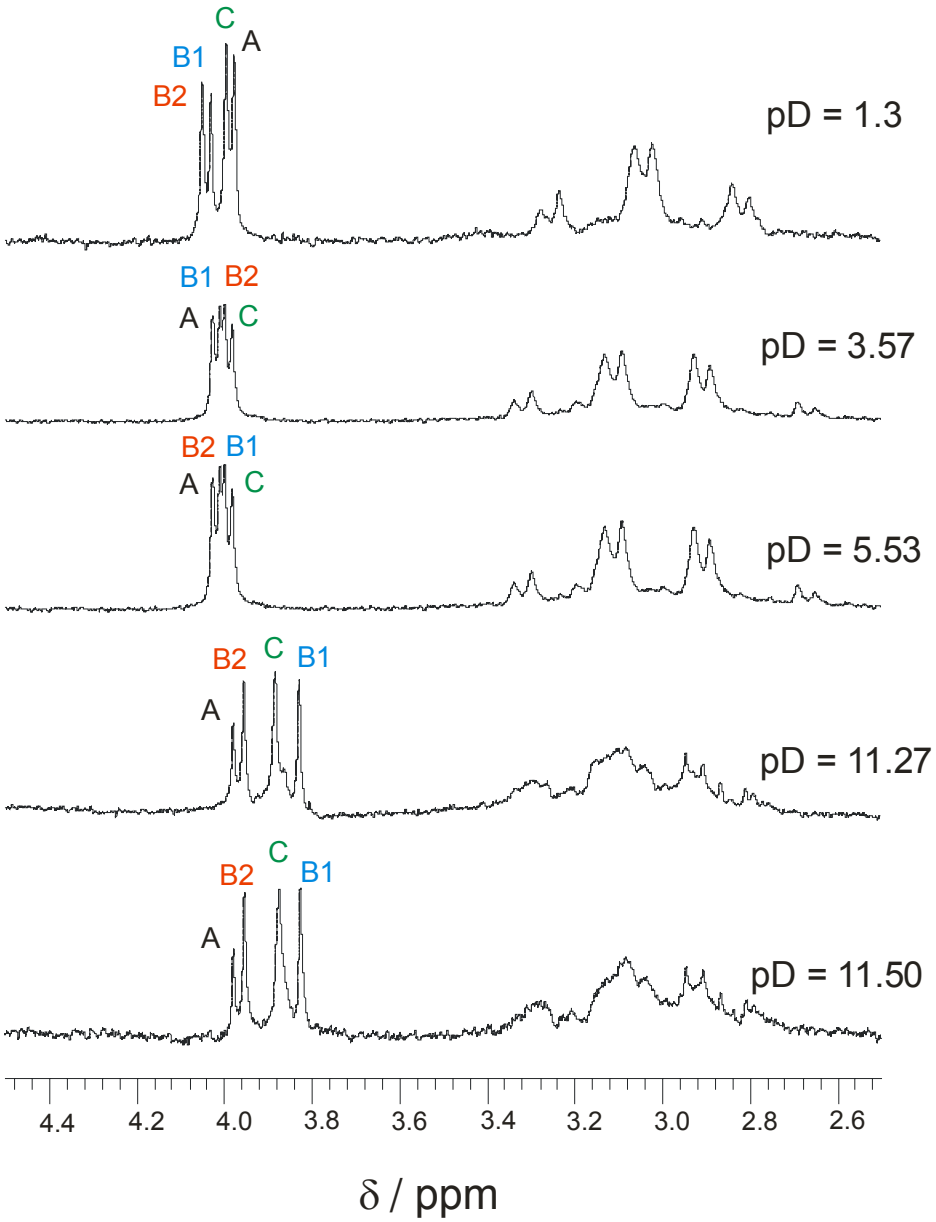

Figure 18: *Stackplot of the aliphatic region of ^{1}H NMR spectra at different pD values (from top to bottom: pD = 1.3, 3.57, 5.53, 11.27, 11.50) of the mixture of three compounds. The chemical shifts of B1 are strongly affected by basic pD.*

It can be well seen that it is easy to distinguish the different species coexisting in the solution. If we consider the methyl groups, we can observe four signals, which correspond to three different compounds. There is one singlet, which corresponds to the starting compound *trans*-[$(NH_3)_2$Pt(9-MeA-*N7*)$_2$]$^{2+}$(**3**). This complex has been studied before (see part 2.5.1; its behavior in solution

with different pD´s has been followed). There are two singlets, which can be assigned to both methyl groups of the 9-MeA nucleobases of the desired dinuclear compound *trans*-[$(NH_3)_2$Pt(*N7*-9-MeA)(*N7*-9-MeA-*N1*)(dienPt)]$^{4+}$ (**9**). And finally, the last signal corresponds to the trinuclear complex *trans*-[$(NH_3)_2$Pt(*N7*-9-MeA-*N1*)$_2$(dienPt)$_2$]$^{6+}$ (**10**). This will be discussed further in the next chapter.

The pD dependence of compound (**9**) was easy to follow, because the determination of the pK_a value of (**3**) has previously been shown (Figure 11) and the pD dependence of the compound (**10**) will be shown later.

Table 4: *Summary of the three different compounds observed in the reaction of trans-[$(NH_3)_2$Pt(9-MeA-N7)$_2$]$^{2+}$ (**3**) with [(dienPt)$(H_2O)_2$]$^{2+}$. The resonance **A** corresponds to the complex (**3**); the resonances B1 and B2 to (**9**) and the resonance C to (**10**).*

Compound	Formula	CH_3-Res.
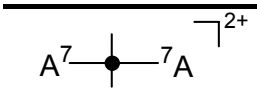	*trans*-[$(NH_3)_2$Pt(9-MeA-*N7*)$_2$]$^{2+}$ (**3**) {starting material}	**A**
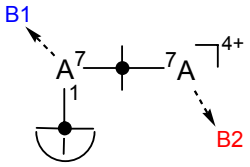	*trans*-[$(NH_3)_2$Pt(*N7*-9-MeA-*N1*)$_2$(dienPt)]$^{4+}$ {desired product (**9**)}	B1 B2
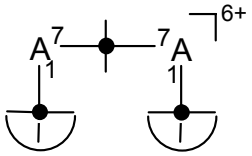	*trans*-[$(NH_3)_2$Pt(*N7*-9-MeA-*N1*)$_2$(dienPt)$_2$]$^{6+}$ (**10**)	C

It should be noted that resonance B1 is not very sensitive at acid conditions, whereas it is very sensitive at basic conditions. On the contrary, the resonance B2 is very sensitive at acid conditions. This is due to the presence of a dienPt^{II} entity at N1 in the 9-MeA, which contains B1. The N1 position in the other 9-methyladenine is free, so the methyl resonance corresponding to this

nucleobase B2, will be more affected at acidic conditions than the methyl resonance of the 9-MeA, which has a dienPt^{II} entity at N1 position B1.

The change in chemical shift of the adenine methyl groups B1 and B2 depending on pD is shown in Figure 19. Looking at the course of the two methyl groups over the pD range one can easily attribute the deprotonation of the exocyclic amino group. On one hand, in the pD range from 1 to 3 the methyl group B2 undergoes a strong upfield shift ($\Delta\delta > 0.1$ ppm), whereas the other CH_3 group B1 is not so much affected ($\Delta\delta \approx 0.04$ ppm). The first pK_a value corresponds to the protonation at N1 position and its value is estimated to be < 2. On the other hand, in the pD range from 8 to 10 the CH_3 group B1 of the adenine ligand undergoes a strong upfield shift ($\Delta\delta \approx 0.15$ ppm), whereas the other adenine resonance is hardly affected (slight upfield shift of $\Delta\delta \approx 0.04$ ppm). This indicates, that deprotonation of the exocyclic amino group occurs first at the adenine moiety, carrying a dienPt^{II} entity coordinated to N1. The second pK_a value corresponding to this inflection point is 9.75 ± 0.1. This value is markedly decreased in comparison with the pK_a value (~ 16.7)[18] of the free nucleobase. Thus, the presence of two platinum atoms coordinated to N1 and N7 positions influences the acid-base properties of the exocyclic amino group. In addition to this effect, there is an intramolecular stabilization by a H-bond donor (Figure 20).

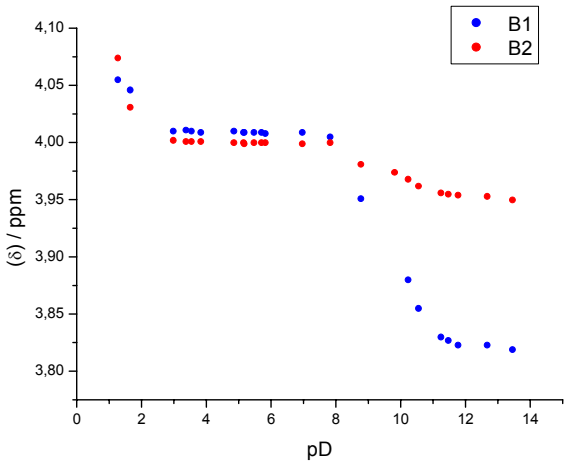

Figure 19: *pD dependence of the CH_3 proton chemical shifts of trans-$[(NH_3)_2Pt(N7\text{-}9\text{-}MeA\text{-}N1)_2(dienPt)]^{4+}$ (**9**).*

The deprotonation of the second N6H$_2$ group could not be determined. The estimated pK_{a3} value is >13.

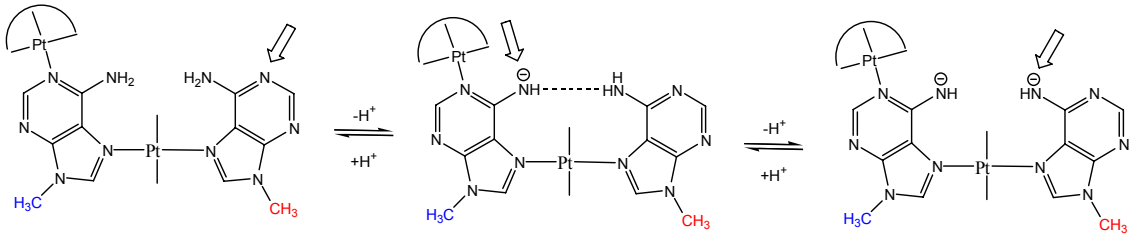

Figure 20: *Assignment of the three deprotonation steps. First, deprotonation at N1 (not shown); second at NH$_2$ of adenine with (dien)Pt^{II} at N1 and third, at NH$_2$ of the other adenine.*

2.5.2.4 Comparison of *trans*-[(NH$_3$)$_2$Pt(*N7*-9-MeA-*N1*)$_2$(dienPt)]$^{4+}$ (9) with *trans*-[(NH$_3$)$_2$Pt(*N7*-9-MeA-*N1*)$_2$(dienPt)$_2$]$^{6+}$ (10)

Treatment of *trans*-[(NH$_3$)$_2$Pt(*N7*-9-MeA-*N1*)$_2$]$^{2+}$ with two equivalents of *trans*-[(dienPt)(H$_2$O)]$^{2+}$ at 40°C during three days leads to the formation of (**10**). The NMR spectroscopic study of the deprotonation of the exocyclic group of both adenine nucleobases reveals that the first pK_a value in water has a value of 8.3 ± 0.1 (corresponding to the deprotonation of NH$_2$ of one adenine) and the pK_a value corresponding to the deprotonation of the second adenine in water is 10.1 ± 0.1 (Figure 21). If we compare these values with the values obtained for (**9**), the pK_a values of (**10**) are lower, because *trans*-[(NH$_3$)$_2$Pt(*N7*-9-MeA-*N1*)$_2$(dienPt)$_2$]$^{6+}$ (**10**) has one platinum entity more than (**9**).

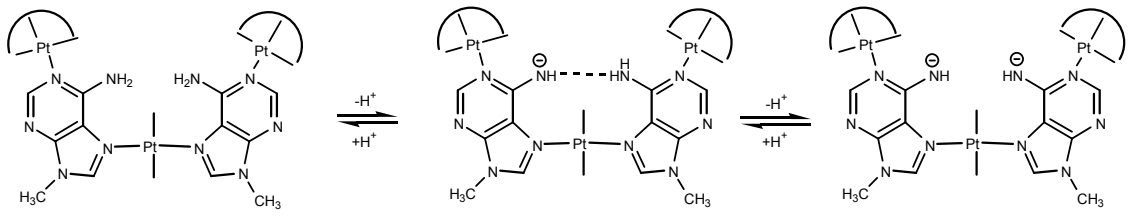

Figure 21: *Deprotonation of the exocyclic amino groups in (**10**).*

2.5.3 Acidification of $N6H_2$ in Trinuclear Bis(Adenine-*N1*,*N7*) Complexes with *cis*- and *trans*- Geometries

We have prepared several complexes of general composition Pt_3A_2 (A = 9-MeA or 9-EtA), with formally 1.5 Pt entities per adenine base and either a *cis*- or a *trans*-[a_2Pt^{II}] or [ma_2Pt^{II}] entity cross-linking two central adenine bases. Surprisingly, pK_a values in the compounds studied are substantially lower than in the cases with two Pt entities per adenine (compare with the results in Table 2, pag. 18). This rules against the charges of the metal entities being the major determinants of ligand acidity.

Several examples of trinuclear Pt^{II} complexes containing a single *cis*-[a_2Pt^{II}] as well as two monofunctional a_3Pt^{II} units have been studied. In *cis*-[$(NH_3)_2Pt\{(N1\text{-9-MeA-}N7)Pt(NH_3)_3\}_2](NO_3)_6\cdot 2H_2O$ (**11**), the X-ray crystal structure of which has been reported before,[53] pD-dependent ^1H NMR spectra in D_2O and potentiometric titrations in H_2O gave pK_{a1} values of approximately 8.7 (^1H NMR spectroscopy, calculated for H_2O) and 9.10 ± 0.03 (potentiometry, calculated for H_2O) for deprotonation of the exocyclic amino group of the first adenine base and pK_{a2} values of approximately 10.7 (^1H NMR spectroscopy) and 10.99 ± 0.10 (potentiometry) for deprotonation of the second adenine. In the NMR spectra, the two deprotonation steps of (**11**) are particularly well separated for the adenine H2 resonance (Figure 22). It is noted that above pD 7.5 and at ambient temperature only single sets of H2 and H8 resonances are observed; this is unlike the situation at lower pH values, where resonance doubling (with an intensity ratio of about 1:3) is observed due to slow nucleobase rotation.

While the pK_{a2} value is in the range expected for a Pt_2(9-MeA-*N1*,*N7*) species (see above), pK_{a1} is significantly shifted to lower values. We propose that the first proton loss from the exocyclic amino group is facilitated by an efficient stabilization of the deprotonated species involving donation of a proton from the $N6H_2$ group of the second 9-MeA in a hydrogen bond (Figure 23).

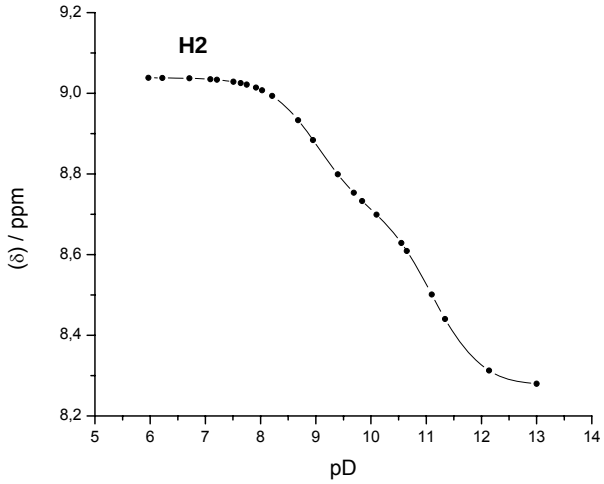

Figure 22: *pD dependence of the H2 resonance of (**11**) in the ^{1}H NMR spectra. Two distinct deprotonation processes for the two adenine ligands are indicated, with pK_a values of 8.7 and 10.7 (converted to H_2O).*

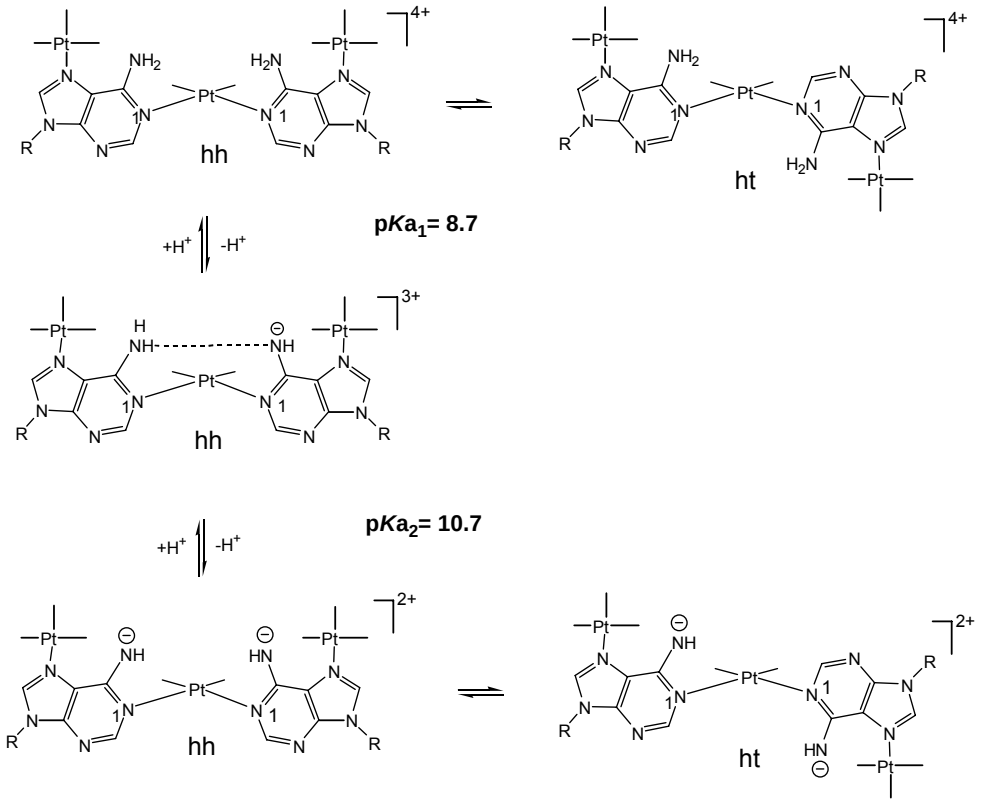

Figure 23: *Proposed rotamer distribution of (**11**) depending on the pH of the solution. hh = head-head, ht = head-tail.*

This scenario is supported by structural arguments: In the solid-state structure of (**11**)[53] the two adenine bases are in a head-head arrangement with the two exocyclic amino groups 3.35 Å apart (N6A···N6A') and essentially perpendicular to each other. Following removal of a single proton only a slight tilting of the two bases would be required to lower the separation of the two exocyclic nitrogen atoms to well below 3 Å and to permit stabilization of the deprotonated species by H-bond formation. Removal of a second proton (from the other adenine base) is expected to lead to mutual repulsion of the NH groups, to a larger separation of these groups, and probably, as a consequence, to base rotation into a head-tail orientation. With no extra stabilization of the deprotonated species possible, the pK_{a2} value is again in the "normal" range for diplatinated adenines, namely close to 11.

When the positions of the *cis*-[a_2Pt^{II}] and the [a_3Pt^{II}] entities on the adenine bases are interchanged, that is, in *cis*-[$(NH_3)_2$Pt{(*N7*-9-MeA-*N1*)Pt(dien)}$_2$]$(NO_3)_6$ (**12**), differences between the pK_{a1} and pK_{a2} values are somewhat lower than in (**11**), but the values are still significantly apart (9.23 ± 0.08 and 10.56 ± 0.17, respectively; measured by potentiometry). The low pK_a value of the first deprotonation step calls for a similar interpretation as in the case of (**11**). Although X-ray crystal structures are not available for (**12**) or for the *cis*-[$(NH_3)_2$Pt(9-MeA-*N7*)$_2$]$^{2+}$ fragment (**4**) with a head-head arrangement of the two bases, comparison with the positions of the O6 atoms in *cis*-[$(NH_3)_2$Pt(9-EtGH-*N7*)$_2$]$^{2+}$ (two guanines in the head-head orientation)[54] leaves no doubt that hydrogen bonding between the NH^- and NH_2 groups in (**12**) is feasible on steric grounds.

Altogether, four compounds containing a central *trans*-[a_2Pt^{II}] unit bridging two adenine nucleobases through their N7 positions were studied: *trans*,*trans*,*trans*-[$(NH_3)_2$Pt(*N7*-9-MeA-*N1*)$_2${$(NH_3)_2$Pt(9-EtGH-*N7*)}$_2$]$(ClO_4)_6\cdot 6H_2O$ (**G1**), *trans*,*trans*,*trans*-[$(NH_3)_2$Pt(*N7*-9-EtA-*N1*)$_2$ {$(CH_3NH_2)_2$Pt(9-MeGH-*N7*}$_2$] $(ClO_4)_6$ (**G2**), *trans*,*trans*,*trans*-[$(NH_3)_2$Pt(*N7*-9-EtA-*N1*)$_2$ {$(NH_3)_2$Pt(1-MeT-*N3*)}$_2$] $(ClO_4)_4\cdot 11H_2O$ (**H**), and *trans*,*trans*,*trans*- [$(NH_3)_2$Pt(*N7*-9-EtA-*N1*)$_2$ {$(CH_3NH_2)_2$Pt(1-MeU-*N3*)}$_2$] $(ClO_4)_4\cdot 4H_2O$ (**I**). As can be seen from Table 2

(Page 18), there is a further drop in the pK_{a1} value of 9-MeA for these compounds compared to the examples containing a central *cis*-[a_2Pt^{II}] unit, with a minimum of 7.9 ± 0.3 (^{1}H NMR spectroscopy) reached in the case of (**I**).

With the mixed guanine/adenine complexes (**G1**) and (**G2**) deprotonation takes place at the two guanine ligands (N1 positions) prior to deprotonation at the bridging adenine ligands ($N6H_2$). The pK_a values for the guanine bases in (**G1**) and (**G2**) are between 7.1 and 7.6 and are thus also remarkably lower than in other cases of guanine model nucleobase complexes with Pt^{II}.[3,28] Interestingly, hemideprotonation and stabilization of the guanine anion through three hydrogen bonds with a neutral guanine ligand[55] could again be the reason for the observed low pK_a values of the two bases, although the scenario of anion stabilization is radically different from that seen in the case of adenine bases. In principle, the argument of guaninate stabilization should hold up for any Pt^{II} complex containing guanine ligands. However, as an inspection of a model of deprotonated (**G**) reveals, there is the possibility of formation of a loop structure with intermolecular stacking of H-bonded guanines, which would make hemideprotonated (**G**) different from all mononuclear Pt complexes previously studied by us. Additional work is required to verify or disprove such a scenario.

2.5.3.1 Extent of Formation of H-Bonded Species

If one accepts the idea that intramolecular hydrogen bonding, either directly or indirectly (through an H_2O molecule, see below), is responsible for stabilization of the $N6H^-$ species and for the extra lowering of the pK_a value, it is possible to estimate the degree of formation of the H-bonded structure. According to such an analysis[56] an extra acidification of 2 log units, say from 11 to 9 (the effect of two metals only, modified by charge considerations), corresponds to a degree of formation of the H-bonded species of more than 99%, and a ΔpK_a value of 1.6 still requires a degree of formation of 97%.

2.5.3.2 Protonation of *cis*-[$(NH_3)_2Pt\{(N1\text{-}9\text{-}MeA\text{-}N7)Pt(NH_3)_3\}_2$] $(NO_3)_6 \cdot 2H_2O$ (11) and *cis*-[$(NH_3)_2Pt\{(N7\text{-}9\text{-}MeA\text{-}N1)Pt(dien)\}_2](NO_3)_6$ (12)

The relative ease of deprotonating the exocyclic amino group of the two 9-MeA nucleobases in (**11**) and (**12**) is contrasted by the superacidic conditions required to accomplish protonation of the 9-MeA ligands. According to results obtained from UV spectroscopy, protonation of (**11**) and (**12**) occurs with pK_a values of –4.4 ± 0.3 and –4.3 ± 0.3, respectively (H_o scale). It is assumed that protonation takes place at the N3 position of 9-MeA. These values are somewhat lower than that of threefold protonated adenine, which also loses its first proton from N3.[2]

2.5.3.3 Quantum-mechanical Calculations of *cis*-[$(NH_3)_2Pt\{(N1\text{-}9\text{-}MeA\text{-}N7)Pt(NH_3)_3\}_2](NO_3)_6 \cdot 2H_2O$ (11)

Geometry-optimized structures for the cation *cis*-[$(NH_3)_2Pt\{(N1$-9-MeA-$N7)Pt(NH_3)_3\}_2]^{6+}$ of (**11**) were calculated by Patrick Lax with the Gaussian 98 suite of programs.[57] The calculated structures are, however, different from the solid-state structure of (**11**) (nitrate salt, dihydrate)[53] in that one of the two adenine bases is strongly tilted with respect to the central *cis*-[$(NH_3)_2Pt^{II}$] plane. Optimizations converged toward geometries in which the $N6H^-$ group is stabilized by hydrogen bonding with an NH_3 group, either from the $(NH_3)_3Pt^{II}$ unit at N7 or from the *cis*-[$(NH_3)_2Pt^{II}$] unit at N1.

This picture changed dramatically when a water molecule was inserted between the two N6 positions: Then, the two exocyclic amino groups were interconnected through hydrogen bonds extending from the water molecule (Figure 24). An additional hydrogen bond is formed between the exocyclic N6 amide group and the *cis*-oriented NH_3 ligand (N_{am}).

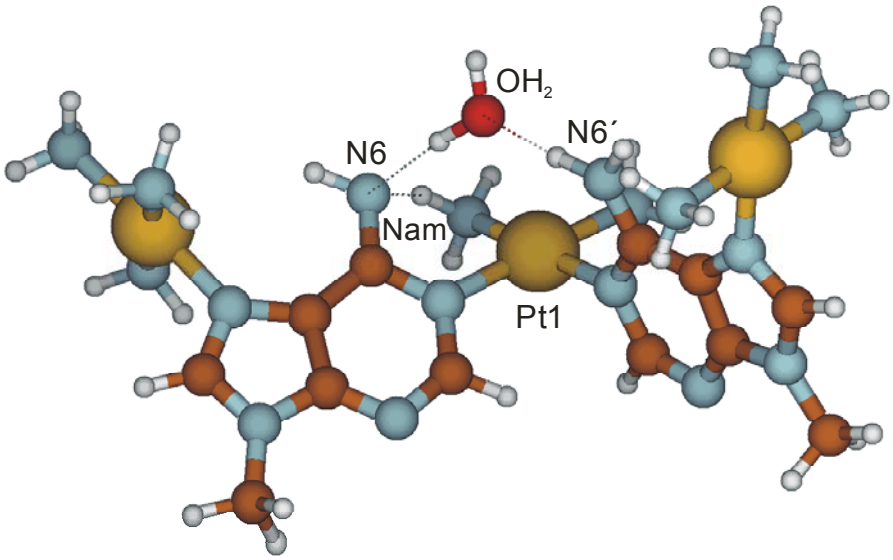

Figure 24: *Geometry-optimized gas-phase structure of the cation of (**11**) with the H-bonding pattern involving N6H⁻, N6´H₂, the water molecule, and one of the central NH₃ ligands (N_am).*

2.5.3.4 Mixed Adenine/Guanine Complexes of *cis*- and *trans*-a₂Pt(II)

The simple concept of replacement of a weakly acidic proton of a hydrogen bond between nucleobases by a metal entity of suitable geometry yields “metal-modified base pairs” or larger aggregates (Figure 25).[58,59] The metal complexes obtained in this way may be considered models of temporary or permanent interstrand cross-links of metal ions with nucleic acids.[60] If extended to metalated oligonucleotides, targeting single-stranded or double-stranded nucleic acids is relevant to antisense and antigene approaches for gene silencing.[61] Finally, regular metal cross-linking of duplex DNA (*M* – DNA) can lead to a situation in which DNA behaves as a molecular wire.[62]

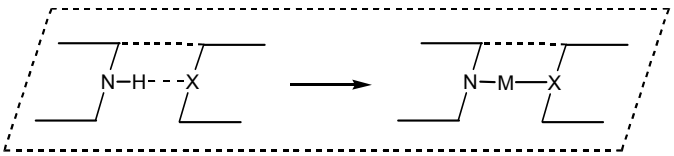

Figure 25: *Concept of generating metal-modified base pairs.*

In the course of studies on metal-modified nucleobase quartets[63] an example of an extreme acidification (10^9) of the 6-amino group of adenine in the complex *trans,trans,trans*-{$(NH_3)_2$Pt(*N7*-9-EtA-*N1*)$_2$[$(MeNH_2)_2$Pt(1-MeU-*N3*)]$_2$}$^{4+}$ has been demonstrated.[17] In this chapter, there will be discussed a similar complex, with three platinum atoms, but only three nucleobases.

2.5.3.4.1 *trans,trans,trans*-[$(NH_3)_2$Pt(*N7*-9-MeA-*N1*)(dienPt)(*N7*-9-EtA-*N1*){$(NH_3)_2$Pt(9-MeGH-*N7*)}]$(ClO_4)_3(NO_3)_3$ (13)

Colourless crystals of *trans,trans,trans*-[$(NH_3)_2$Pt(*N7*-9-MeA-*N1*)(dienPt)(*N7*-9-EtA-*N1*){$(NH_3)_2$Pt(9-MeGH-*N7*)}]$(ClO_4)_3(NO_3)_3$ (**13**) were obtained from a solution of *trans*-[$(NH_3)_2(H_2O)$Pt(*N7*-9-MeA-*N1*)(dienPt)]$^{4+}$ (aqua species of the cation (**8**)) and *trans*-[$(NH_3)_2$Pt(9-EtA-*N1*)(9-MeGH-*N7*)]$^{2+}$ after several days at room temperature. Compound (**13**) crystallizes in the monoclinic C2/c space group. Unfortunately, these crystals were very small, and the observed reflections were not sufficiently strong to permit anisotropical refinement of all the atoms; for this reason in the refinement process of the X-ray data, only the platinum atoms were refined anisotropically. Not all the anions were properly refined.

Complex (**13**) consists of two adenine nucleobases (9-MeA and 9-EtA), a 9-methylguanine model nucleobase, a (dien)Pt^{II} unit and two *trans*-a$_2$Pt^{II} entities. *trans,trans,trans*-[$(NH_3)_2$Pt(*N7*-9-MeA-*N1*)(dienPt)(*N7*-9-EtA-*N1*){$(NH_3)_2$Pt(9-MeGH-*N7*)}]$(ClO_4)_3(NO_3)_3$ (**13**) crystallizes in a characteristic Z-shape with the three bases and the (dien)Pt^{II} being nearly coplanar (Figure 26). As in related compounds,[63] Pt–N1 and Pt–N7 vectors are approximately perpendicular to each other [85.7(7)°].

Geometries of the square-planar coordination spheres of the three Pt atoms have normal values of angles and distances, taking into account the low quality of the crystal (Table 5).

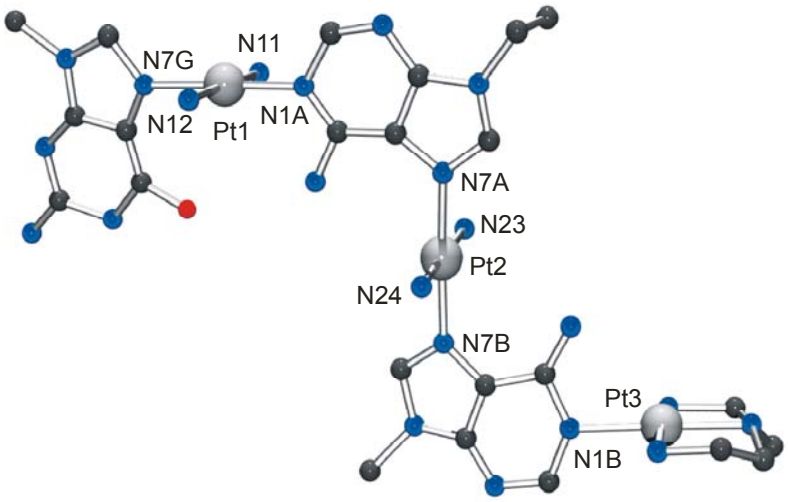

Figure 26: *View of the cation trans,trans,trans-[$(NH_3)_2$Pt(N7-9-MeA-N1)(dienPt)(N7-9-EtA-N1){$(NH_3)_2$Pt(9-MeGH-N7)}]$^{6+}$ (**13**).*

Table 5: *Selected distances (Å) and angles (°) for non-hydrogen atoms in **13**.*

Pt1-N1A	1.98(2)	N1A-Pt1-N7G	176(1)
Pt1-N7G	2.07(2)	N1A-Pt1-N12	94(1)
Pt1-N12	2.12(2)	N1A-Pt1-N11	84(1)
Pt1-N11	2.17(3)	N12-Pt1-N7G	89(1)
		N11-Pt1-N7G	93(1)
		N11-Pt1-N12	177(1)
Pt2-N7A	2.02(3)	N7A-Pt2-N7B	178(1)
Pt2-N7B	2.04(3)	N7A-Pt2-N24	90(1)
Pt2-N24	2.04(4)	N7A-Pt2-N23	87(1)
Pt2-N23	2.06(3)	N7B-Pt2-N24	92(1)
		N7B-Pt2-N23	91(1)
		N23-Pt2-N24	174(1)
Pt3-N1B	2.14(3)	N31-Pt3-N32	173(1)
Pt3-N31	2.06(3)	N31-Pt3-N33	86(1)
Pt3-N32	2.05(4)	N31-Pt3-N1B	93(1)

Pt3-N33	2.12(4)	N32-Pt3-N33	88(1)
		N32-Pt3-N1B	93(1)
		N1B-Pt3-N33	176(1)

The dihedral angles formed by the coordination planes of the platinum atoms and the different nucleobases are as follows: 77.4(6)° (Pt1-G), 81.3(6)°(Pt1-A), 89.9(7)° (Pt2-A), 87.4(7)° (Pt2-B) and 87.0(7)° (Pt3-B). This means, that with the exception of the first angle, all others are close to 90° and hence the vectors are close to perpendicular.

A weak intramolecular contact was found between the exocyclic amino group of the guanine base and the exocyclic amino group of the 9-ethyladenine base: O6G···N6A, 3.37(4) Å.

The formation of compound (**13**) was also studied by ^{1}H NMR spectroscopy. The spectrum shown in Figure 27 was recorded after one week of reaction. As can be observed in this spectrum, resonances due to the starting compound have almost disappeared, while the new signals of (**13**) have appeared. The signals are easily assigned.

The existence of different rotameric forms in D_2O at ambient temperature is not observed. The corresponding H(A) signals show no doubling. Therefore, a rotation with a different activation energy about the central A-*N7*-Pt(2)-*N7*-A bonds is assumed, with the repulsive interaction of the two exocyclic A-NH_2 groups favouring the Z-form, as found in the solid state (Figure 26).

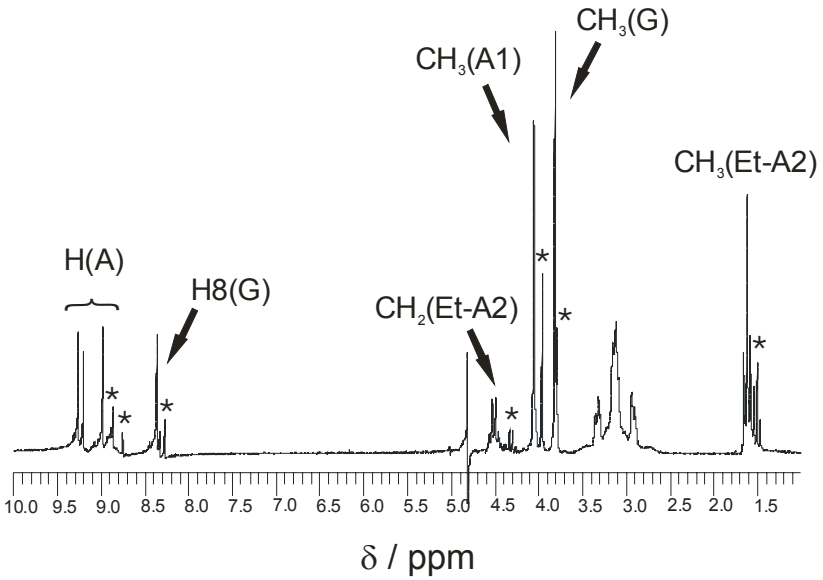

Figure 27: *Resonances of the aromatic protons and the methyl groups in the ^{1}H NRM spectrum of (**13**).The signals (*) correspond to the starting compound trans-*$[(NH_3)_2Pt(9\text{-EtA-}N1)(9\text{-MeGH-}N7)]^{2+}$.

pD-dependent ^{1}H NMR spectra (2 < pD < 14) reveal two deprotonation steps ocurring with pK_{a1} = 7.14 ± 0.07 and pK_{a2} = 8.32 ± 0.01 (calculated for H_2O). The deprotonation of the second adenine occurs at pD > 10 (pK_{a3}). The first pK_a value is assigned to a single deprotonation step of NH_2 group of adenine and the second one to the deprotonation of N1 of guanine. Comparison with literature data show that the amino group acidity (pK_a ~ 16.7 in the free base[18]) increases upon Pt^{II} coordination to N7 or N1 by 2─3 log units and even more so if both positions are simultaneously platinated (pK_a ~ 10.8─12.6[63,11,12]). The unusually low pK_{a1} of 7.14 can only be rationalized if in addition to the polarizing effect of the two metal ions a fundamental conformational change is taken into account. Here it is proposed that the transition of the Z-shaped cation to a U-shaped one takes place, which stabilizes the first deprotonated species $\{\mathbf{13}\text{-}H^{+}\}^{5+}$ (Figure 28). On the basis of structural models as well as X-ray data of (**13**) it is obvious that (i) the three nucleobases and the dien entity can addopt a perfectly planar arrangement, and (ii) the exocyclic amino groups of the head-head arranged adenine bases are 3 Å or less apart. In fact, any reduction of the N7-Pt-N7 angle from 180° further reduces this separation. This short distance

permits an efficient stabilization of the NH^- group by the NH_2 group of the second adenine through intramolecular H bond formation (Figure 28, bottom). The situation is reminiscent of that occurring in the $N_2H_5^-$ ligand of the dinuclear Pt^{IV} complex $[(NH_3)_3Pt(NH_2)_2(N_2H_5)Pt(NH_3)_3]^{5+}$.[19] This conclusion concerning the conformational change during the first deprotonation of (**13**) is in agreement with observations for linkage isomers, *viz*. complexes containing a central N1-Pt-N1 bond and additional Pt^{II} entities at the N7 positions.[63,64] There, mainly the electronic effects of the two metal ions are operative, hence pK_a values are higher and close to the normal range (10–11). As the pH is raised further, the cation is expected to adopt again the *Z*-shape to avoid the mutual repulsion of the two amide groups.

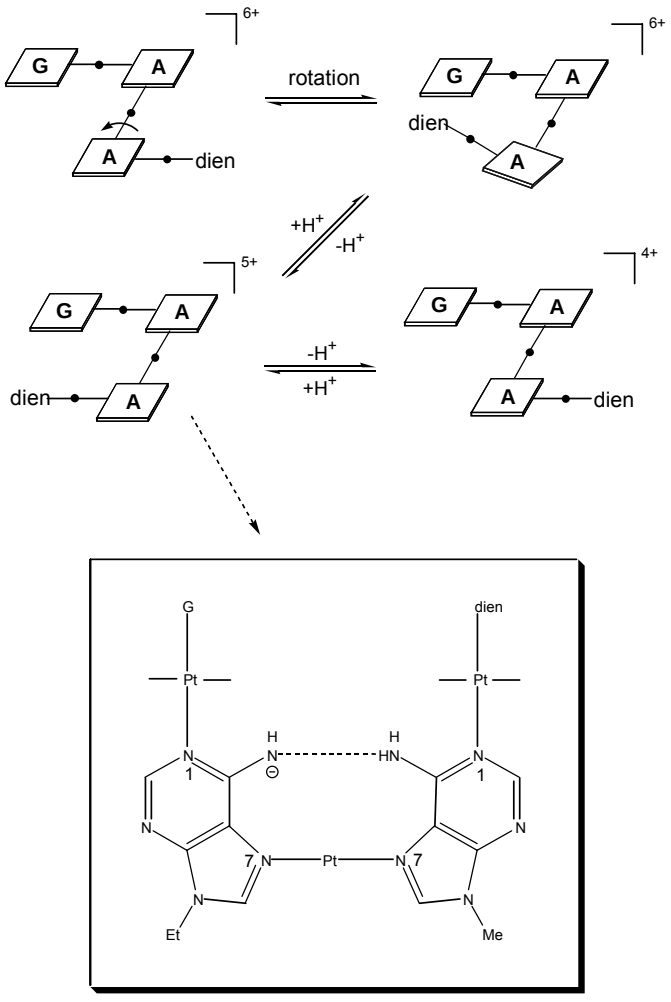

Figure 28: *Schematic presentation of the conformational pH switch (**13**).*

The compound described here behaves as a pH switch,[16b] and hence changes its conformation from Z to U upon removal of a single proton and again from U to Z if a second proton is removed. The mutual orientation of the two adenine nucleobases and the close distance of the exocyclic amino groups make the compound a system with the potential of acting as an acid and a base in a reversible manner at physiological pH. The only requirement to achieve such a function would be to have the system confined in space to a situation in which the cation adopts a structure halfway between the two extremes (Figure 28, top). As a consequence of slight mechanical oscillations of the two halves a proton might be ejected or picked up from the environment.

There is another interesting aspect of the cationic {**13**-H^+}$^{5+}$ in its U-shape, which refers to its possible interaction with (anionic) telomere sequences of DNA. The enzyme telomerase is a key player in the development of cancer and has been found to be inhibited by conjugated π-systems capable of stabilizing guanine quartet structures of the telomeres.[65]

2.5.3.4.2 Comparison of (13) with *trans*,*trans*,*trans*-{$(NH_3)_2$Pt(*N7*-9-MeA-*N1*)$_2$[$(NH_3)_2$Pt(9-EtGH-*N7*)]$_2$}$^{6+}$ (14)

In order to compare the above mentioned compound (**13**) with a similar one, *trans*,*trans*,*trans*-{$(NH_3)_2$Pt(*N7*-9-MeA-*N1*)$_2$[$(NH_3)_2$Pt(9-EtGH-*N7*)]$_2$}$^{6+}$ (**14**), synthetized by M. Lüth, was studied.[47] Four pK_a values are expected, two corresponding to the deprotonation of the NH_2 of adenine nucleobases and the other two corresponding to the deprotonation of N1 of the guanine nucleobases. The acidity constants were determined by potentiometry[47] and by ^{1}H NMR spectroscopy. The values are summerized in Table 6.

Table 6: *Different pK_a values for (**14**) obtained with potentiometry.*

Position	Potentiometry[47]	pK_a
9-MeA-NH_2	7.13 ± 0.02	**pK_{a1}**
	11.0 ± 0.1	pK_{a4}
9-EtGH-N1	7.59 ± 0.02	pK_{a2}
	8.67 ± 0.03	pK_{a3}

The first deprotonation of the NH_2 of one adenine presents a low value (7.13 ± 0.02). This phenomenon was also found before.[17] When this happens, an intramolecular hydrogen bond between the NH^- and the NH_2 is possible (Figure 29).

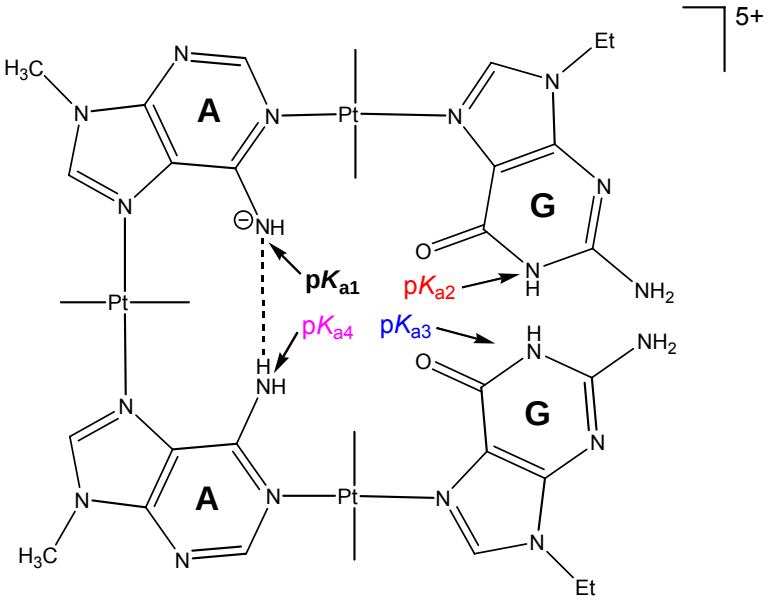

Figure 29: *One of the possible arrangemenst of trans,trans,trans-{$(NH_3)_2$Pt(N7-9-MeA-N1)$_2$[$(NH_3)_2$Pt(9-EtGH-N7)]$_2$}$^{5+}$ (**14**). In this U conformation, there is a stabilization of the NH^- group by the NH_2 of the second adenine through an intramolecular H bond.*

Similar values were found applying ^{1}H NMR spectroscopy. The ^{1}H NMR studies reveal that the adenine deprotonates first, then two guanines and

eventually the second adenine. The signals are more affected in the case of the adenine (Figure 30). From pD 6.6 to pD 7.6, the H8 and H2 resonances become broad, however 9-EtGH resonances remain sharp. A tautomer equilibrium is feasible, given the relatively slight differences between pK_{a1} and pK_{a2}.

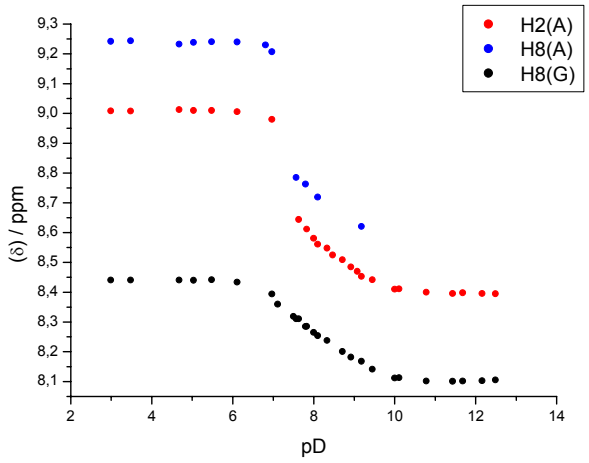

Figure 30: *pD dependence of the resonances corresponding to the protons of adenine (H2 and H8) and the proton of guanine (H8).*

2.5.4 Pt^{II} Migration from N1 to N6 in 9-Methyladenine

In the course of our ^{1}H NMR studies with platinated adenine nucleobases we noticed in many instances a complication in the spectra of samples kept at high pH conditions (pH*>10). We considered two scenarios, both of which are precedented in nucleobase chemistry, namely deamination of adenine and conversion into a hypoxanthine ligand, and/or migration of Pt^{II} from N1 or N7 to N6. The latter aspect has been studied in detail by Arpalahti and co-workers.[25,66,67]

2.5.4.1 Migration in *trans*-$[(NH_3)_2ClPt(N7\text{-}9\text{-}MeA\text{-}N1)(dienPt)](ClO_4)_3$ (8)

In the course of the study of the pD dependence of complex (**8**), new

resonances were observed. During the determination of the acidity constant of (**8**), a new signal of a methyl group was observed at pD ~ 9. With time, the signal due to the starting compound disappeared and only the new singlet remained. The solution was brought to pD ~ 2.5 and the spectrum was compared with the spectrum of a solution of (**8**) at identical pD (Figure 31). There is a very strong difference in the chemical shifts of the resonances (particularly pronounced in the case of the heteroaromatic proton resonance). The resonances corresponding to the CH_2 of the dien are also different in both spectra. The spectrum on the top in Figure 31 belongs to a solution of (**8**) in D_2O at pD ~ 2.5. The spectrum on the bottom corresponds to a solution of (**8**), which was during one week at pD ~ 9 and then brought to pD ~ 2.5 with DNO_3. Due to this difference, the spectrum on the bottom corresponds to another compound. It could be possible that the dienPt entity has migrated from N1 to N6. This could explain the doubling of the CH_3-resonances after two days, probably due to the existence of rotamers (Figure 32).

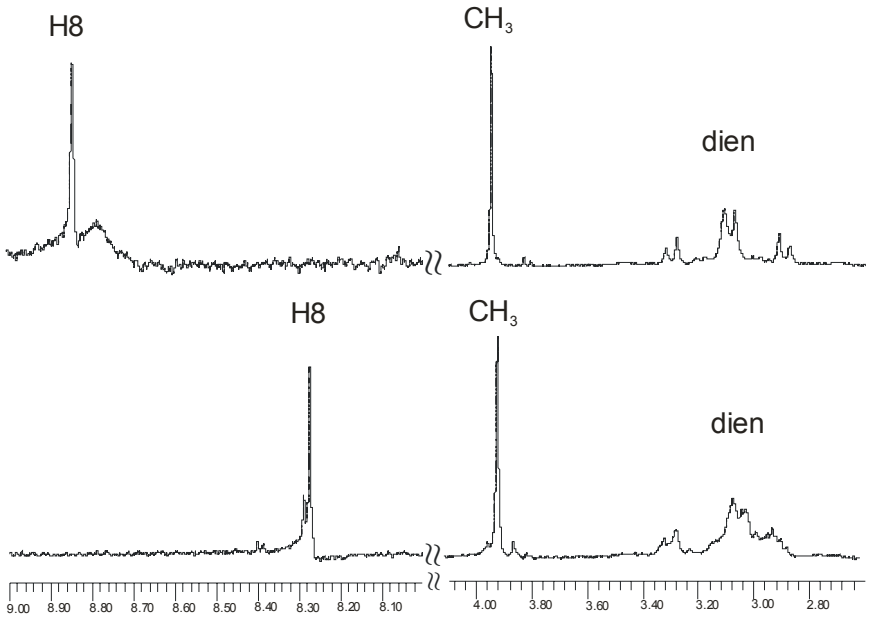

Figure 31: *Possibility of migration in (**8**). Complex (**8**) in D_2O at pD ~ 2.5 (top) and spectrum of (**8**) after being treated with NaOD and brought to pD ~ 2.5 (bottom)*

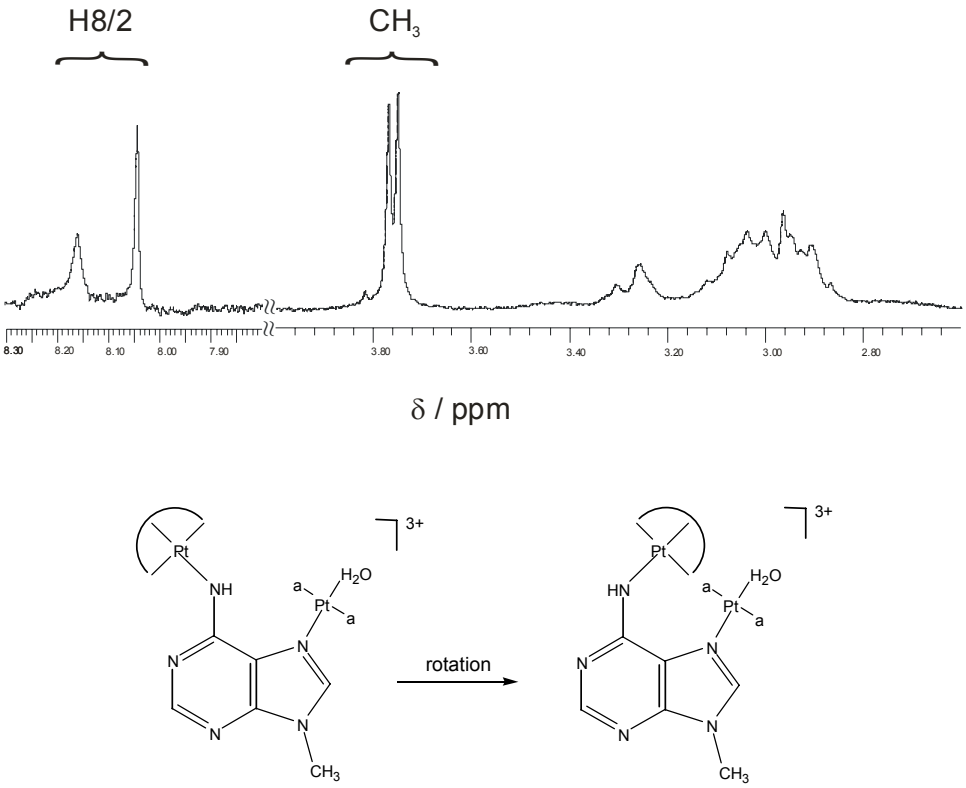

Figure 32: *Rotamers in trans-[$(NH_3)_2(H_2O)$Pt(N7-9-MeA-N1)(dienPt)]$^{3+}$ (**8**). ^{1}H NMR Spectrum with two signals corresponding to the CH_3 goups of both rotamers (D_2O, pD ~ 9).*

In order to prove the existence of another species, *trans*-[$(NH_3)_2$ClPt(*N7*-9-MeA-*N1*)(dienPt)]$(ClO_4)_3$ (**8**) was dissolved in DMSO-*d6* and the ^{1}H NMR signals were followed with time (Figure 33). After ten minutes, a new signal B can be observed. This signal increases with time, while the signal corresponding to (**8**) **A**, decreases. After two hours, the starting compound (**8**) is gone, and only *trans*-[$(NH_3)_2$(DMSO)Pt(*N7*-9-MeA-*N1*)(dienPt)]$^{3+}$ is present, in which the chloro atom is exchanged for one molecule of the deuterated solvent, DMSO (Figure 34). After one week, a new signal C appears. This signal was thought to correspond to [(dienPt)(9-MeA-*N1*)]$^{2+}$ (**1**), but it was found that C does not agree with this assumption, since the chemical shifts of (**1**) in DMSO are not the same as the resonances of C. Therefore, we assume that C corresponds to the product of a migration of dienPt^{II} entity from N1 to N6.

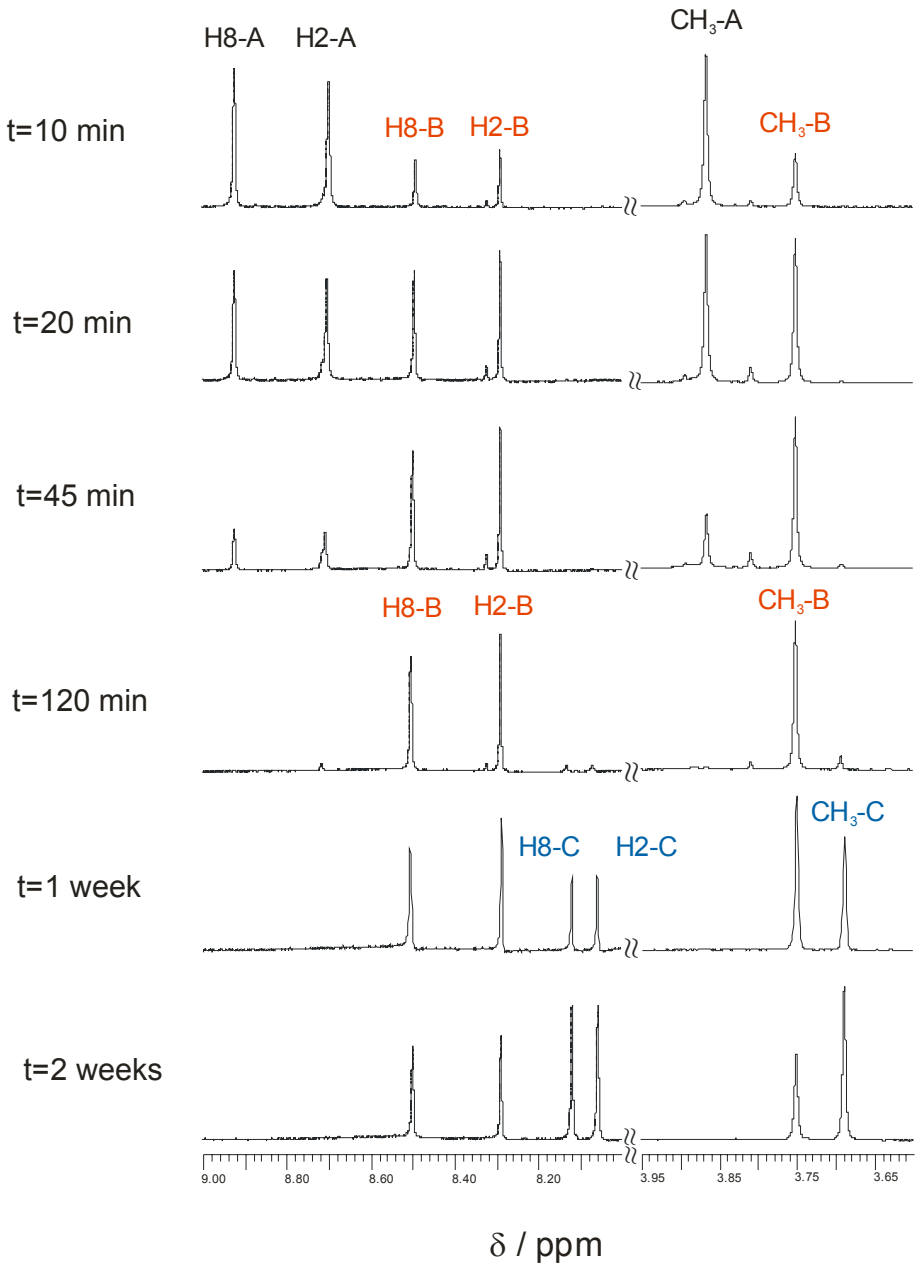

Figure 33: *^{1}H NMR spectra of (**8**) and related compounds in DMSO-d6 after different periods of time.*

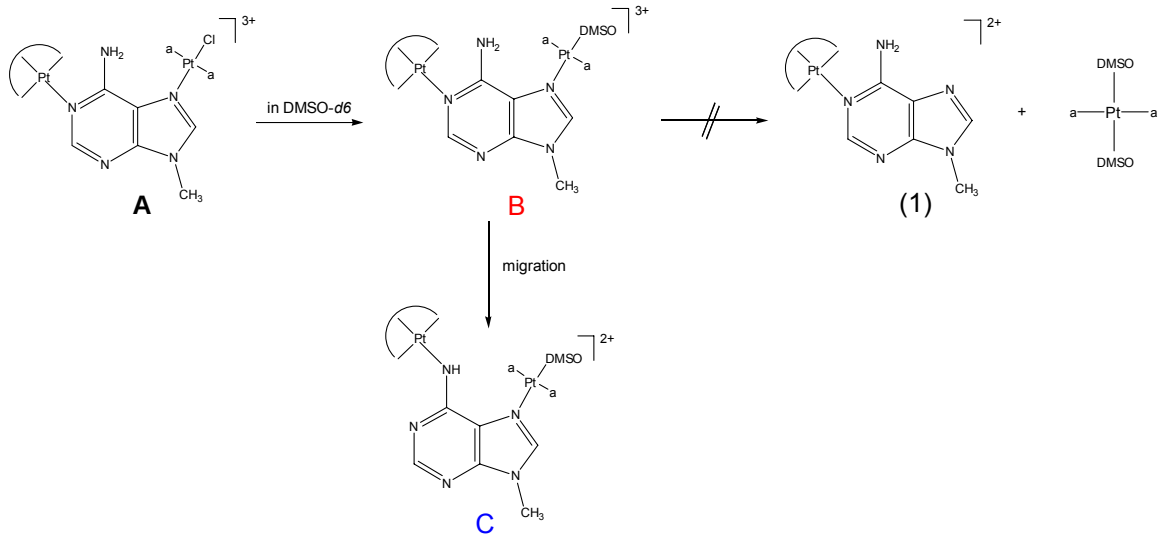

Figure 34: *Different species starting from trans-[$(NH_3)_2(H_2O)$Pt(N7-9-MeA-N1)(dienPt)]$^{3+}$ (**8**) with the course of time in DMSO-d_6.*

2.5.4.2 *trans*-[{$(NH_3)_2$Pt(1-MeC-*N3*)}$_2$(9-MeA-*N7*,*N6*)]$(ClO_4)_3 \cdot 3.5H_2O$ (15)

We were successful in isolating a reaction product. By applying compound *trans*-[{$(NH_3)_2$Pt(1-MeC-*N3*)}$_2$(9-MeA-*N1,N7)*]$(ClO_4)_4$ (**7**) and titrating it with NaOH to pH 11.1, we aimed to obtain crystals of the deprotonated form (**7'**). The isolated crystals (**15**) proved, however, to be a linkage isomer of (**7'**) (Figure 35) in which the Pt entity, which originally resided at N1, had moved to N6. (**15**) can be reprotonated to give (**15'**), which is formally the twofold-platinated rare imino tautomer of adenine.[13b,25,68,69]

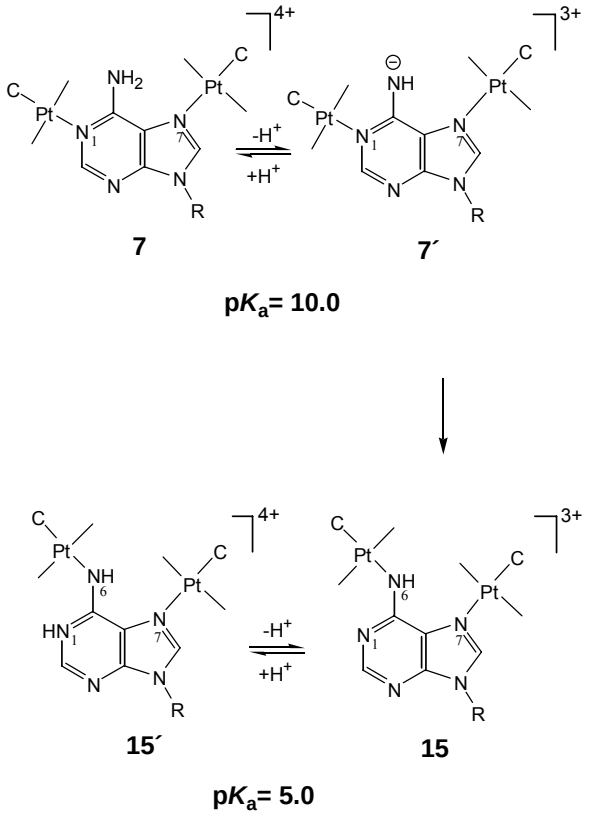

Figure 35: *Linkage isomerization of (**7**) to (**15´**) and relevant pK_a values of the protonated forms, (**7´**) and (**15**). Note the large difference of 5 log units.*

The crystals were characterized by X-ray crystallography. Complex (**15**) crystallizes in the monoclinic space group. During the refinement of the structure, all non-hydrogen atoms in the strucuture were refined anisotropically and all hydrogen atoms were included in geometrically calculated positions. Details concerning the crystal, X-ray measurement, and the refinement of data are listed in Table A-2 (see Appendix).

The angles between the platinum atom (Pt1) and (Pt2) and the four coordination sites are approaching 180°: N3B-Pt1-N7A, 174.6(3)° and N3C-Pt2-N6A, 174.7(2)°. Pt-N distances about the Pt center range from 1.988(6) to 2.046(5) Å. Selected distances and angles are provided in Table 7.

The cation *trans*-[{$(NH_3)_2$Pt(1-MeC-*N3*)}$_2$(9-MeA-*N7*,*N6*)]$^{3+}$ of (**15**) and the atom numering scheme are depicted in Figure 36.

Table 7: *Selected distances (Å) and angles (°) for non-hydrogen atoms in* ***15****.*

Pt1-N3B	2.018(7)	N3B-Pt1-N7A	174.6(3)
Pt1-N7A	1.988(6)		
Pt1-N1L	2.043(6)		
Pt1-N2L	2.034(7)		
Pt2-N3C	2.046(5)	N3C-Pt2-N6A	174.7(2)
Pt2-N6A	1.993(6)		
Pt2-N3L	2.025(6)		
Pt2-N4L	2.033(6)		
N6A-C6A	1.316(9)	C2A-N1A-C6A	119.1(6)
O2B···N4L	2.944(9)	C2A-N3A-C4A	109.2(7)
O2B···N6A	3.126(9)		
N3L···N1A	3.064(9)		

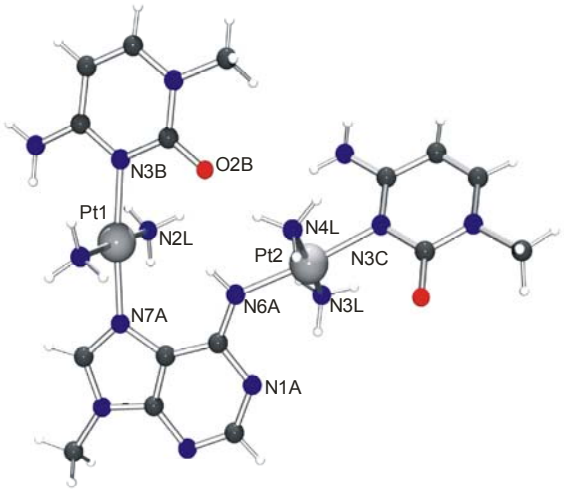

Figure 36: *X-ray structure of the cation of trans-[{$(NH_3)_2$Pt(1-MeC-N3)}$_2$(9-MeA-N7,N6)]$(ClO_4)_3 \cdot 3.5H_2O$ (**15**).*

As can be seen, the *trans*-$[(NH_3)_2Pt(1\text{-}MeC\text{-}N3)]^{2+}$ residue has migrated from N1 to N6 and adopts a *syn* conformation with respect to N1 of the adenine nucleobase. While the cytosine ring opposite to N7 of the adenine ring is close

to coplanar with adenine (dihedral angle of 12.3°) and is involved in weak H-bond formation (O2B···N6A 3.13(1) Å; O2B···N4L 2.944(9) Å; numbering as given in Figure 36), the cytosine opposite to N6 is at a substantial angle (45.5°) with the adenine plane. The N1 position of adenine is deprotonated in (**15**) (internal ring angle of 119.1(6)°, very similar to the value of 118.8(1)° in neutral 9-MeA[70]) but is involved in weak H-bond formation (3.06(1) Å) with the NH_3 ligand of Pt2 (N3L in Figure 36).

Pairs of cations of (**15**) are arranged in such a way as to permit stacking of the adenine ring with the cytosine ring B of an adjacent cation (3.5–3.7 Å). Additional contacts between cations of (**15**) are mediated by numerous hydrogen bonding interactions, which involve ClO_4^- anions, NH_3 groups, and water molecules. None of these contacts is unusually short. With a single exception, direct contacts between bases of adjacent cations are not seen. The exception is a short contact between the oxygen atom of the cytosine ring coordinated to the N6-bonded Pt and the H8 atom of an adjacent adenine (2.53 Å; symmetry operation –x, –1/2 + y, –1/2–z).

The *syn* orientation of the N6-bonded Pt (Pt2) is also seen in [(dien)Pt(9-MeA-*N6*)]$^{2+}$, in which the 9-MeA ligand is neutral and carries a proton at N1.[25] From modeling studies, it appears that an anti orientation of Pt2 in (**15**) is unfavourable because of the presence of the co-ligands of Pt1 at N7. Of course, in the absence of a metal at N7, *anti* orientations of N6-bonded metal ions are possible,[66,69] sometimes in equilibrium between both forms,[71] and an *anti* orientation is realized if dinuclear, metal–metal bonded units (Rh_2,[72] Mo_2[73]) are attached to N7 and N6 simultaneously.

A study of the hydrogen bonding pattern reveals the existence of a water oligomer. There are two types of hydrogen bonds involving water molecules: the first one, between water molecules interacting only with water molecules (formation of water polymer); and the second one, between water molecules interacting with the ones which form the water cluster and at the same time with the N3 position of the adenine (O4w and its symmetric one) or with the ammine

ligand of the Pt2, N2L. Each cation of (**15**) and its corresponding water molecules of crystallization forms intermolecular hydrogen bonds between the water molecules with the cation at 1-x, 1/2+y, 1/2-z, thus leading to a pair of related cations (Figure 37).

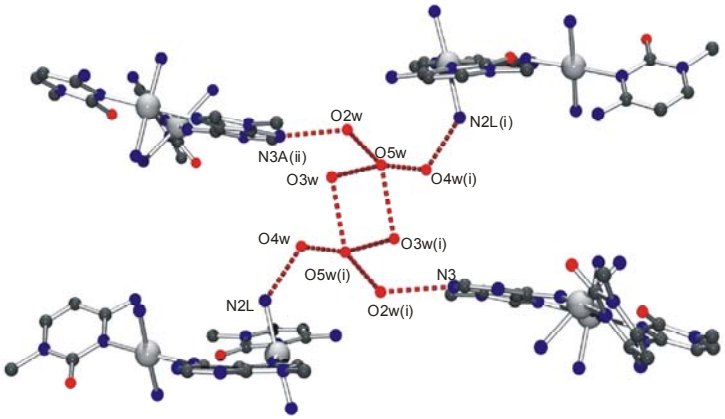

Figure 37: *View of the water cluster of (**15**).*

The symmetry operator for the description of hydrogen bonds is (i) 1-x, 1/2+y, 1/2-z. Oxygen atoms of the water molecules that are involved in hydrogen bond formation exclusively between water molecules are : O5w···O3w, 2.730 Å; O5w···O3w(i), 2.857 Å. Oxygen atoms of the water cluster with other water molecules: O5w···O2w, 2.903 Å and O5w···O4w(i), 2.011 Å. The latter distance is artificially short because O5w and O4w have occupancy factors of 0.5 only. O3w is also only partially (50%) occupied. Oxygen atoms of the water which do not form the cluster, also join the nucleobase oligomer: O2w···N3A(ii) (x, 1/2–y,1/2+z), 2.811 Å; O4w···N2L, 2.746 Å.

The principal motif of the water polymer is a cyclic water tetramer, in which the atoms O5w, O3w and its symmetric ones are joined via hydrogen bonds. The internal angles of the tetramer are 96.8° (O3w-O5w-O3w(i)) and 91.8° (O5w-O3w-O5w(i)). Figure 38 shows in detail the distances between atoms of the cyclic tetramer.

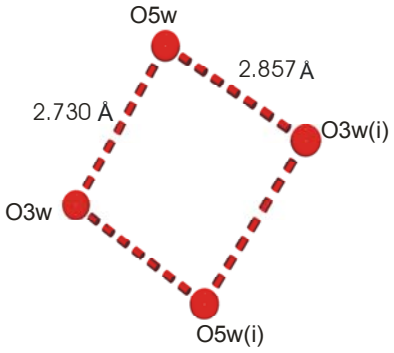

Figure 38: *View of the cyclic water tetramer present in (**15**).*

The ^{1}H NMR spectrum of a freshly dissolved sample of (**15**) in D_2O (pD 7.8, ambient temperature) indicates the presence of two different rotamer forms, but given the various possibilities (rotation about the Pt1–N7A bond, the Pt2–N6A bond, or the C6A–N6A bond; numbering as given in Figure 36), a straightforward interpretation is difficult. Aromatic adenine proton resonances are observed at δ = 8.36, 8.14, and 8.07 ppm with relative intensities of approximately 0.2:1:0.2, and two methyl resonances of 9-MeA$^-$ occur at δ = 3.86 and 3.81 ppm (ca. 3:0.6). As to cytosine resonances, two H6 and two H5 doublets (ca. 1:1) are clearly discernable (H6: δ = 7.69 and 7.65 ppm; H5: δ = 6.10 and 6.09 ppm), as are two CH_3 singlets at δ = 3.51 and 3.47 ppm (ca. 1:1). There are indications for two additional weak doublets at approximately δ = 7.63 and 6.12 ppm, which are, however, superimposed with the other doublets. Partial isotopic exchange appears to be responsible for the weak intensities of two of the three aromatic protons of 9-MeA$^-$. On the basis of a 2D NOESY spectrum we can assign the intense singlet at δ = 8.14 ppm to the H2 proton of 9-MeA$^-$, as it does not exhibit a cross-peak with the methyl group at N9. This finding tentatively suggests that there is hindered rotation about the Pt1–N7A bond.

2.5.4.3 pK_a Value of *N7*,*N6*-diplatinated 9-MeA in (15)

The acidity of the proton at N1 of (**15´**) was determined by ^{1}H NMR spectroscopy (pD dependence of CH_3 of adenine and H2 of adenine) and found to be 5.0 ± 0.1(calculated for H_2O). This value is lower by 2.6 log units than that of [(dien)Pt(9-MeA-*N6*)]$^{2+}$, which is 7.65 ± 0.05,[25] and is a consequence of the second Pt^{II} at N7. The difference is reasonably close to the ΔpK_a values for N1-protonated residues carrying a Pt^{II} at N7 (2.2 ± 0.1).[13] This suggests that the acidifying effect of multiple metal ion binding is roughly additive.

Comparison with other metal ions reveals that the acidification brought about by Pt^{II} at N6 is moderate: For an RHg^{II} complex the pK_a value for N1H has been found to be 4.5,[69] for an Ru^{II} chelate (*N7*,*N6*) the value was 6.5,[74] and for [$(NH_3)_5Ru^{III}$] values of 2.5 and 4.9 have been estimated,[10a,c] depending on the rotamer state (metal *syn* or *anti* with respect to N1H).[75]

2.5.4.4 Pt^{II} Migration in Bis(9-MeA) Complexes

Due to the general inertness of Pt^{II} and Pt^{IV} and the high thermodynamic stability of Pt–N bonds, the factors affecting the initial binding step of Pt to DNA are considered crucial for understanding the biological activity of anticarcinogenic Pt drugs.[48,76,77] In this respect, findings on relatively facile Pt–N bond rearrangements at the oligonucleotide level are of prime interest[78,79] since they may occur as soon as the platinated oligonucleotides are hybridised with their complementary ribo- or deoxyribonucleotide strands.[78] But the exact mechanism for this type of rearrangement is unknown, rendering model studies in this field highly desirable. In some cases, Pt–N bond rearrangements have been reported in simple complexes within the nucleobase moiety[25,66] or within the auxiliary ligand.[80] A clear picture though, is not apparent regarding the factors controlling these migrations and they may even require the cooperation of other nucleophiles[79a] or involve Pt^{IV} as an intermediate.[81,82]

It has been shown that in isomeric bis(9-methyladenine) complexes under basic conditions, coordinated Pt^{II} undergoes an intramolecular N1→N6 or N7→N6 migration upon displacement of a NH_2 proton.[83] Subsequently, the product, *cis*-[$(NH_3)_2$Pt(9-MeA-*N6*)(9-MeA-*N7*)]$^{n+}$, undergoes a slow deamination reaction of the N7-bound 9-MeA to provide the corresponding hypoxanthine complex instead of a second migration step.

Herein, we discuss an intramolecular migration of coordinated platinum(II) from the N1 site to the exocyclic amino group in 9-MeA. Although the exact migration mechanism has not yet been unequivocally determined, the platinum N1→N6 migration in adenine proceeds without any detectable redox reaction, thus differentiating it from the Pt migration from the ring nitrogen to the exocyclic amino group in platinated pyrimidine complexes, which involve Pt^{IV} as an intermediate.[81,82,84]

2.5.4.4.1 [(9-MeA-*N7*)Pt$(NH_3)_3$]Cl_2·2H_2O as Starting Compound (16)

In order to study platinum migration in the complex *cis*-[$(NH_3)_2$Pt(*N1*-9-MeA-*N7*)$_2${Pt$(NH_3)_3$}$_2$]$(NO_3)_6$ (**11**), compound [(9-MeA-*N7*){Pt$(NH_3)_3$}]Cl_2·2H_2O (**16**) was prepared by reaction of [(9-MeA-*N7*)$PtCl_3$] with NH_3. After keeping the reaction in the refrigerator for a while, colourless crystals were obtained. These crystals were isolated and charaterized by X-ray crystallography. Complex (**16**) crystallizes in the monoclinic space system. In the refinement process of the X-ray data, all non-hydrogen atoms of the crystal were refined anisotropically. All the hydrogen atoms were found in the difference Fourier map and refined without restraints. A summary of crystallographic data, data collection parameters and refinement parameters of (**16**) data is given in Table A-3 (see Appendix). Figure 39 gives an illustration of [(9-MeA-*N7*){Pt$(NH_3)_3$}]$^{2+}$ with the atom numbering scheme.

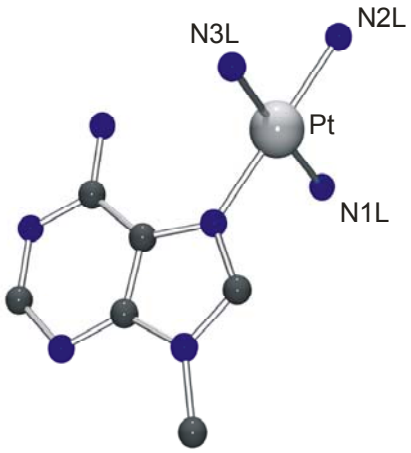

Figure 39: *View of [(9-MeA-N7){Pt(NH$_3$)$_3$}]$^{2+}$(**16**) with the atom numbering scheme.*

The geometry of the 9-methyladenine ligand does not differ very much from other reported adenine nucleobases coordinated via N7 to a platinum.[85] The most important effect is due to the coordination of the N7 site of the ring, which leads to a significant enlargement of 3° of the C5-N7-C8 angle. Significant differences of the bond distances compared with the 9-MeA[70] are a lengthening of the N7-C5 bond (Δ = 0.02 Å) and C4-C5 (Δ = 0.02 Å), and shortenings of the N9-C8 (Δ = -0.01 Å) bonds.

Protons bonded to the corresponding atoms have normal bond distances, ranging from 0.74(7) to 1.13(8) Å. The atoms in the adenine nucleobase are almost coplanar, within a maximum deviation from the least-squares plane of less than 0.007 Å. However, the square-planar coordination of the platinum atoms presents a r.m.s. deviation of 0.041. The N1L and N3L atoms are situated below (-0.047(2) and -0.049(2) Å, respectively) the platinum coordination plane. The dihedral angle between the adenine ring and the platinum coordination plane is 80.6(1)°. The bond distances and angles of [(9-MeA-*N7*){Pt(NH$_3$)$_3$}]$^{2+}$ cation are compiled in Table 8.

Table 8: *Selected distances (Å) and angles (°) for non-hydrogen atoms in* ***16****.*

Pt-N7	2.015(3)	N7-Pt-N2L	177.02(16)
Pt-N2L	2.039(4)	N7-Pt-N1L	90.93(15)
Pt-N1L	2.043(4)	N2L-Pt-N1L	91.34(19)
Pt-N3L	2.048(4)	N7-Pt-N3L	89.28(16)
N1-C2	1.340(5)	N2L-Pt-N3L	88.6(2)
N1-C6	1.350(5)	N1L-Pt-N3L	176.82(16)
N3-C2	1.329(6)	C2-N1-C6	119.1(3)
N3-C4	1.344(5)	C2-N3-C4	111.0(3)
N6-C6	1.335(5)	C8-N7-C5	106.0(3)
N7-C8	1.315(6)	C8-N7-Pt	125.3(3)
N7-C5	1.391(5)	C5-N7-Pt	128.2(3)
N9-C8	1.342(6)		
N9-C4	1.369(5)		
N9-C9	1.464(5)		
C4-C5	1.390(5)		
C5-C6	1.411(5)		

The hydrogen pattern is relatively uncomplicated; it is defined by interactions between the water molecules and the Cl2 anion. Water molecule O2w interacts with the ammonia ligand (N1L) and with the N3 position of the adenine nucleobase of another molecule: O2w···N1L, 2.907(6) Å and O2w···N3a(-x+2, -y-1, -z+1), 2.947(5) Å. The chloride ion (Cl2) interacts with a water molecule and with the ammino ligand (N2L) of two different neighbour molecules: Cl2···O1wa(-x+2, y-1, -z+3/2), 3.226(4) Å and Cl2···N2La(x+1/2, -y-3/2, z+1/2), 3.224(5) Å (Figure 40).

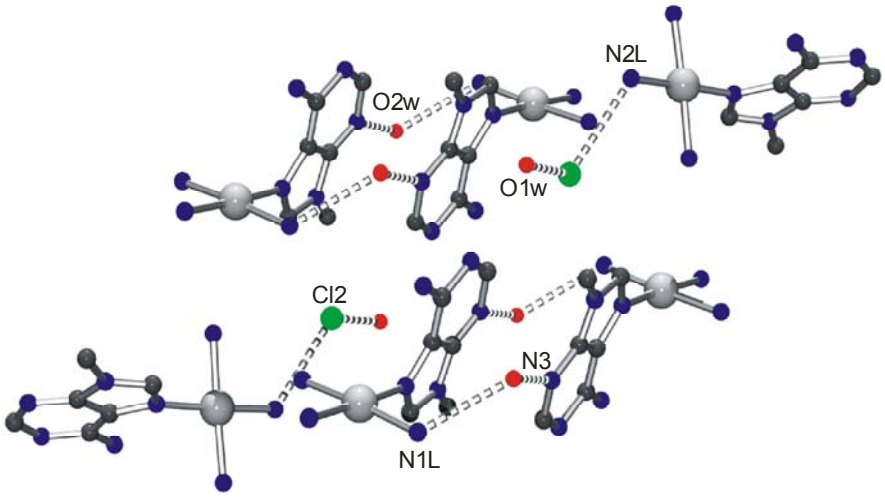

Figure 40: *View of the hydrogen bond pattern of (**16**).*

Figure 41 gives a view of the arrangement of the cations in the layers of the crystal, in which the unit motifs are repeated in all directions, but the cations in every line are rotated 180° respect to the other one. The separation distance between two consecutives layers is 3.33 Å. This distance means the π-stacking of the aromatic rings of the nucleobases is present, but only between pairs.

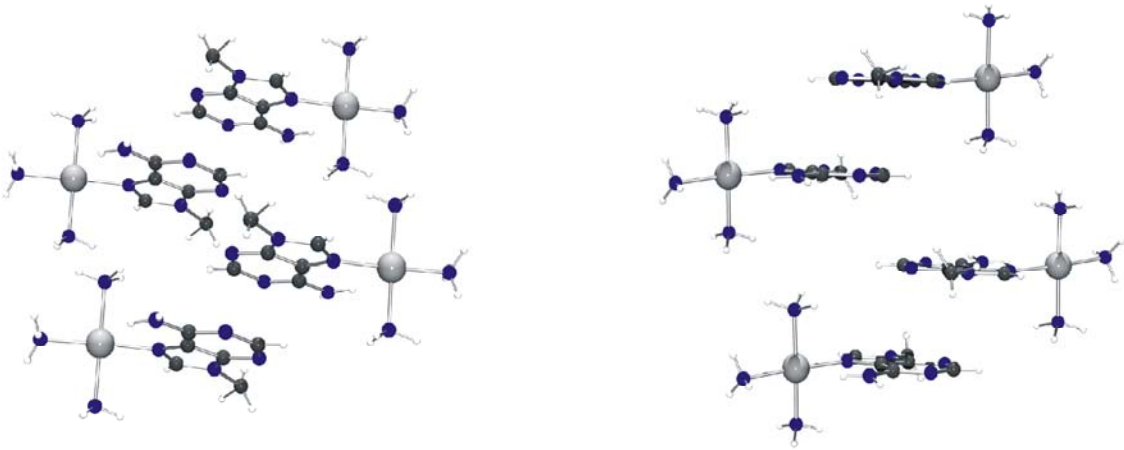

Figure 41: *Details of the packing of (**16**).*

The second step to obtain the complex (**11**) is the reaction of [(9-MeA-*N7*){Pt(NH_3)$_3$}]$^{2+}$(**16**) with *cis*-(NH_3)$_2$Pt^{II} in a 2:1 ratio.

Treatment of *cis*-[$(NH_3)_2$Pt(*N1*-9-MeA-*N7*)$_2${Pt$(NH_3)_3$}$_2$]$(NO_3)_6$ (**11**) with base resulted in the migration of the coordinated Pt^{II} from the endocyclic N1 site to the exocyclic NH_2 group as shown by a crystal structure determination of the reaction product. So, in aqueous NaOH, the compound (**11**) first undergoes an intramolecular migration to give the N1,N6-bound species *cis*-[$(NH_3)_2$Pt(*N1*-9-MeA-*N7*)(*N6*-9-MeA-*N7)*${Pt$(NH_3)_3$}$_2$]$^{5+}$ (**17**), which can then be slowly transformed into the doubly-migrated species *cis*-[$(NH_3)_2$Pt(*N6*-9-MeA-*N7)*$_2${Pt$(NH_3)_3$}$_2$]$^{4+}$ (**18**).

2.5.4.5 Linkage Isomerization of *cis*-[$(NH_3)_2$Pt(*N1*-9-MeA-*N7*)$_2${Pt$(NH_3)_3$}$_2$]$(NO_3)_6$ (11)

Complex (**17**) was obtained by addition of 1M NaOH to a solution of *cis*-[$(NH_3)_2$Pt(*N1*-9-MeA-*N7*)$_2${Pt$(NH_3)_3$}$_2$]$(NO_3)_6$ (**11**). This compound exists in solution as a mixture of two rotamers (*head-head*; *head-tail*). After several days, it was observed that the H8 resonance splits (pD ~ 9.7, δ = 8.6 ppm) in two sets occurring at approximately 9.0 and 8.2 ppm. The intensity of these new resonaces increases with time. At the same time, two new A(N-CH_3) resonances in 1:1 ratio appear. It is suspected that there are two differently bonded 9-MeA ligands, presumably through linkage isomerization (Figure 42).

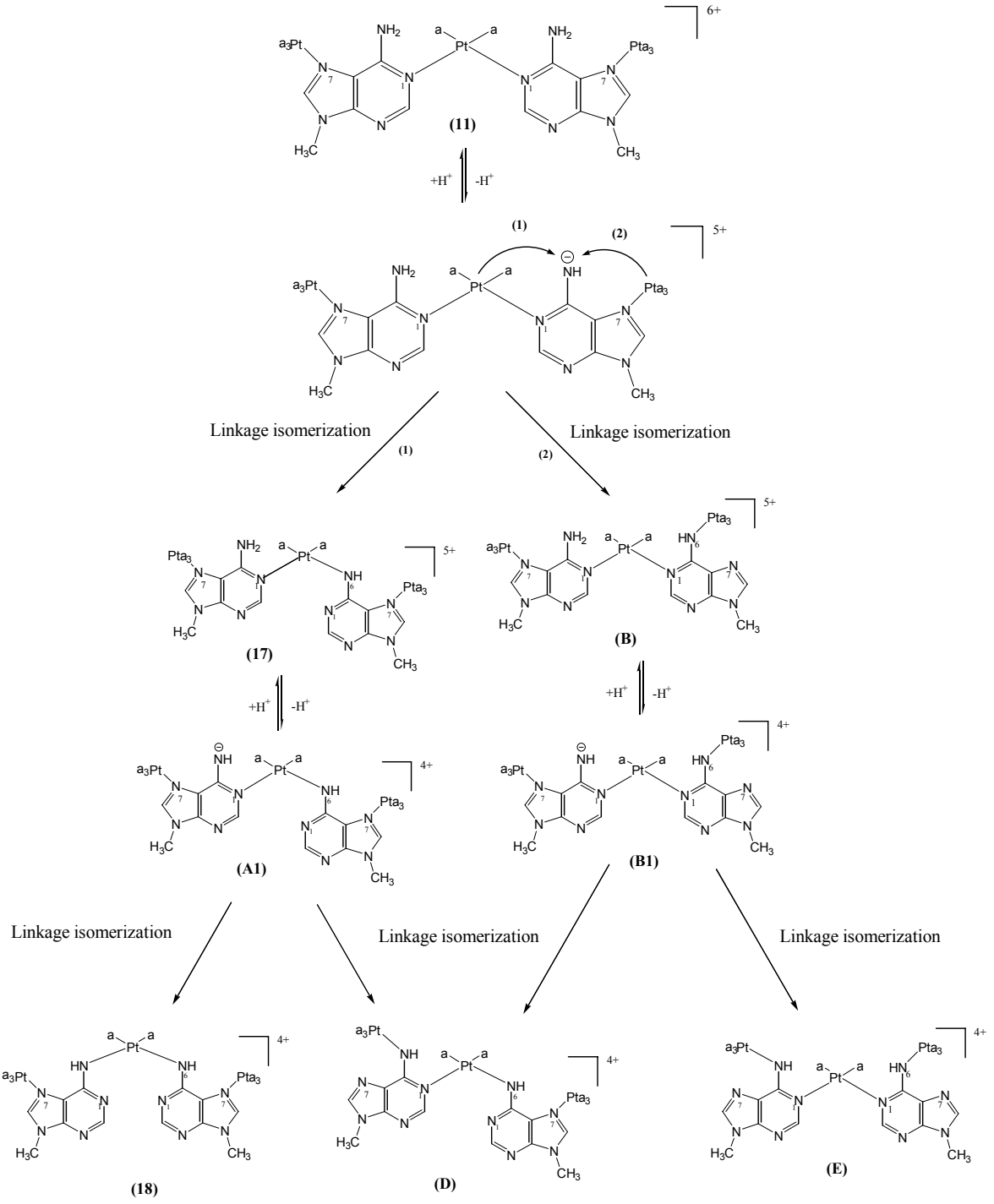

Figure 42: *Pt^{II} migration following $N(6)H_2$ deprotonation. Different pathways for the formation of the possible linkage isomers of cis-$[(NH_3)_2Pt(N1\text{-}9\text{-}MeA\text{-}N7)_2\{Pt(NH_3)_3\}_2]^{6+}$ (**11**).*

Under basic conditions, the exocyclic amino group of compound (**11**) loses a proton. This deprotonation of the N6 amino group facilitates Pt migration from N1 to N6 to give *cis*-[$(NH_3)_2$Pt(*N1*-9-MeA-*N7*)(*N6*-9-MeA-*N7)*{Pt$(NH_3)_3\}_2]^{5+}$ (**17**); or from N7 to N6 to obtain the compound *cis*-[$(NH_3)_2$Pt(*N1*-9-MeA-*N6*)Pt$(NH_3)_3$(*N1*-9-MeA-*N7)*{Pt$(NH_3)_3\}]^{5+}$ (**B**). In both cases, a second deprotonation is possible, so the compounds (**A1**) and (**B1**) would be obtained. Thus, a second migration step can take place, giving the compounds (**18**), (**D**) and (**E**), as shown in Figure 42.

In order to elucidate which routes of migration take place, we tried to obtain crystals of the compounds under alkaline conditions. In one case a compound was successfully isolated and it was shown by X-ray crystallography to be *cis*-[$(NH_3)_2$Pt(*N6*-9-MeA-*N7)*$_2${Pt$(NH_3)_3\}_2]^{4+}$ (**18**). Characterization of compound (**17**) was carried out by applying ^{1}H NMR spectroscopy. There is no indication for N7→N6 migration; consequently one has to conclude that the Pt migration takes place from N1 to N6.

2.5.4.6 *cis*-[$(NH_3)_2$Pt(*N1*-9-MeA-*N7*)(*N6*-9-MeA-*N7)*{Pt$(NH_3)_3\}_2]^{5+}$ (17)

Treatment of *cis*-[$(NH_3)_2$Pt(*N1*-9-MeA-*N7*$)_2${Pt$(NH_3)_3\}_2]^{6+}$ (**11**) with base produces (**17**), for which the ^{1}H NMR spectrum displays two pairs of interconverting sets of nucleobase signals in the ratio of 1:1 for each of the converting sets (Figure 43). The resonances of the other H8/2 cannot be seen, because these signals disappear very rapidly due to isotopic exchange of hydrogen for deuterium from the deuterated solvent.

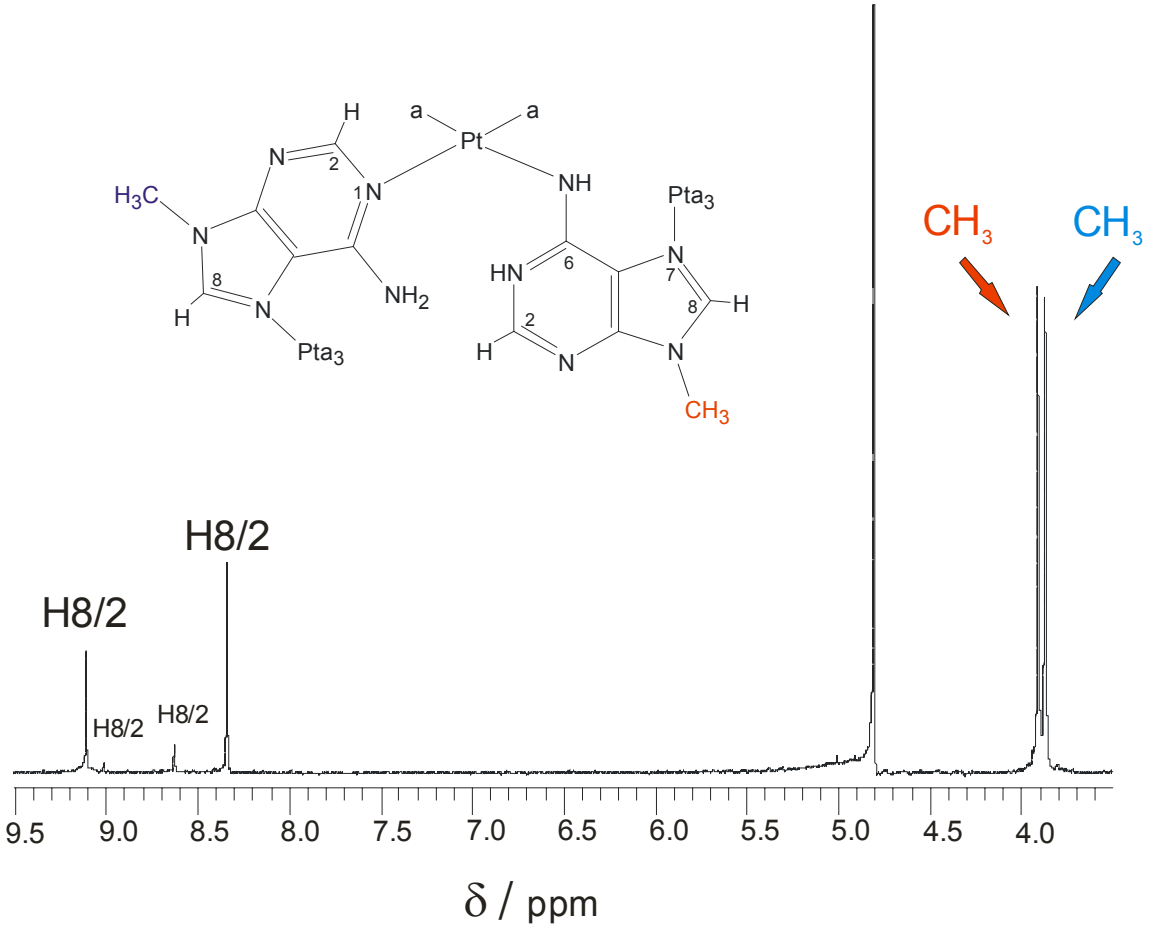

Figure 43: *^{1}H NMR spectrum of (**17**) in D_2O (pD ~9.5) of the compound cis-$[(NH_3)_2Pt(N1\text{-}9\text{-}MeA\text{-}N7)(N6\text{-}9\text{-}MeA\text{-}N7)\{Pt(NH_3)_3\}_2]^{5+}$ (**17**). The spectrum displays two sets of methyl resonances, one corresponding to the adenine nucleobase with cis-a_2Pt^{II} at N1 (CH_3) and the other one to cis-a_2Pt^{II} at N6 position (CH_3).*

The exchange processes likely to be in effect are the often encountered restricted rotation about the Pt-$N_{nucleob.}$ bonds due to internal hydrogen bonding involving the non-complexed nitrogens of the nucleobases (*e. g.* N1, N6, N7) and suitable donor sources (*e. g.* NH_3), and/or the *syn*/*anti* interconversion about the N_6–C_6 bond in the adenine moiety.[67,83] Therefore, either two different bases were present in (**17**), or a single base type was present but coordinated at different sites. But given the expectation based on previous observations[25,83] and the crystal obtained for a double metal migration product (see next chapter),

it was ascertained that the bis-complex, where one 9-MeA ligand is coordinated at the N1 site and the other at the N6 site, was formed. Unfortunately, attempts to crystallize this complex were not successful.

The experiment for the determination of the acidity constant of N1H and NH_2 of (**17**) was performed in relatively dilute solution (c = 2 mM). In Figure 44, the chemicals shifts of one methyl group and the adenine H8/2 hydrogen atoms are shown in dependence on pD.

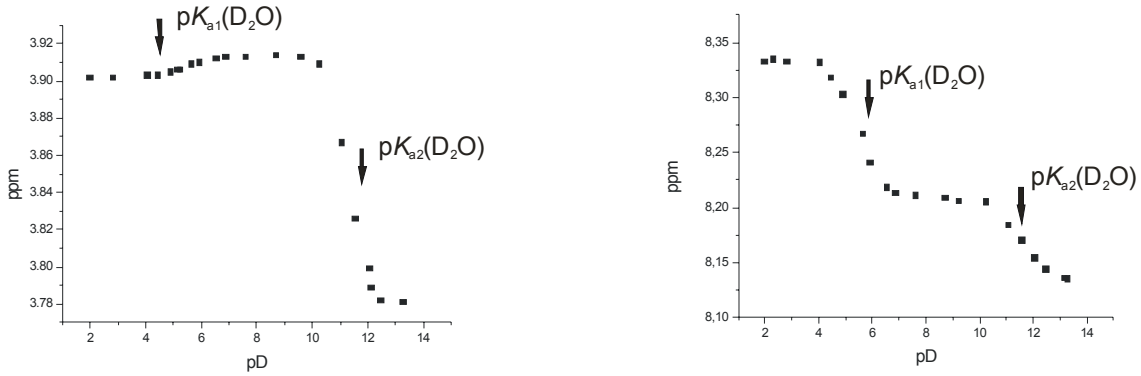

Figure 44: *^{1}H NMR pD-dependence (δ, ppm) of H8/2 and CH3 resonances in D_2O of the cation cis-[$(NH_3)_2$Pt(N1-9-MeA-N7)(N6-9-MeA-N7){Pt$(NH_3)_3$}$_2$]$^{5+}$ (**17**). The values for calculating the first pK_a value in the left diagramm correponds to the methyl group (CH_3) and the diagramm in the right to one of the H8I2.*

In both diagrams, the NMR data were evaluated by a curve-fitting procedure based on equation (3) (see Section 2.1) which considers two deprotonation steps. The final results for deprotonation of the N1 position and NH_2 were obtained by calculating the weighted mean of the pK_a* values, giving pK_{a1}(D_2O) = 5.46 ± 0.03 and pK_{a2}(D_2O) = 11.52 ± 0.07. Finally, the pK_a values determinated in D_2O were transformed to aqueous solution by applying equation (4) resulting in

$$pK_{a1}(H_2O) = 4.94 \pm 0.03$$
$$pK_{a2}(H_2O) = 10.91 \pm 0.07$$

In agreement with other N6-platinated compounds, the pK_a value corresponding to the deprotonation of the N1 position is the expected range.

2.5.4.7 *cis*-$[(NH_3)_2Pt(N6\text{-}9\text{-}MeA\text{-}N7)_2\{Pt(NH_3)_3\}_2](NO_3)_4 \cdot 6H_2O$ (18)

Compound (**11**) was dissolved in water and the pH value was raised from 5.5 to 11 by adding 1M NaOH. The solution was kept in a closed vial until crystals of (**18**) appeared after several weeks. The structure of (**18**) was determinated at room temperature by X-ray crystallographic analysis (Figure 45). Compound (**18**) crystallizes in the monoclinic space group C2/c. All the hydrogen atoms were found in the difference Fourier map and refined without restraints. A summary of crystallographic data, data collection parameters and refinement parameters of (**18**) is given in Table A-4 (see Appendix).

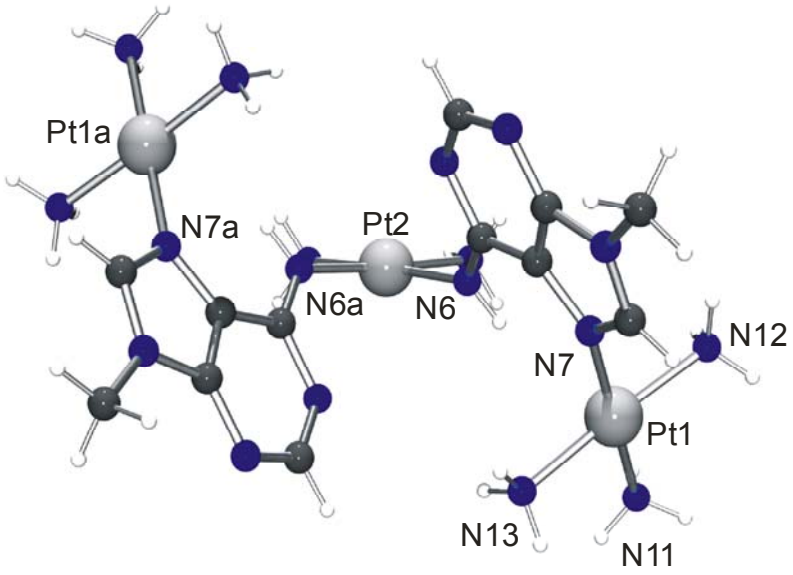

Figure 45: *View of the cation cis-$[(NH_3)_2Pt(N6\text{-}9\text{-}MeA\text{-}N7)_2\{Pt(NH_3)_3\}_2]^{4+}$ of (**18**). The anions and water molecules are omitted for clarity.*

The cation of (**18**) consists of two 9-MeA model nucleobases coordinated to a *cis*-$(NH_3)_2Pt^{II}$ entity via N6 and two $(NH_3)_3Pt^{II}$ entities bound at N7. The cation (**18**) is centrosymmetric, with Pt2 sitting in the inversion center.

The angles between the platinum atom (Pt1) and the four coordination sites are nearly 180°: N7-Pt-N11, 178.63(19)° and N13-Pt1-N12, 177.8(2)°. The Pt1, N11, N7 atoms are situated below (-0.007(2), -0.027(2), -0.027(2) Å, respectively) and the N12 and N13 above (0.030(2) and 0.030(2) Å, respectively) the platinum coordination plane, with a r.m.s. deviation of 0.026. Pt1-N distances about the Pt1 center range from 2.010(4) to 2.045(5) Å. Similar Pt-N bond lengths are observed for the platinum atom (Pt2). Bond distances and angles between atoms of *cis*-$[(NH_3)_2Pt(N6\text{-}9\text{-}MeA\text{-}N7)_2\{Pt(NH_3)_3\}_2]^{4+}$ (**18**) are listed in Table 9.

Non-hydrogen atoms of each 9-MeA are essentially planar, with a r.m.s. deviation of 0.02. Distances and angles between atoms of the 9-MeA bases are not unusual in comparison to other reported adenine compounds. The N1 position of adenine is deprotonated in (**18**) (internal ring angle of 119.7(4)°, very similar to the value of 118.8(1)° in neutral 9-MeA[70]).

Table 9: *Selected distances (Å) and angles (°) for non-hydrogen atoms in **18**.*

Pt1-N7	2.010(4)	N7-Pt1-N13	91.04(19)
Pt1-N11	2.045(5)	N7-Pt1-N12	89.59(18)
Pt1-N12	2.045(4)	N13-Pt1-N12	177.8(2)
Pt1-N13	2.029(4)	N7A-Pt1-N11	178.63(19)
		N13-Pt1-N11	89.8(2)
		N12-Pt1-N11	89.6(2)
Pt2-N6	2.017(4)	N6-Pt2-N21	87.84(17)
Pt2-N21	2.053(4)	N6-Pt2-N6a	92.16(15)
Pt2-N21a	2.053(4)	N6-Pt2-N21a	176.79(18)
Pt2-N6a	2.017(4)		
C6-N6	1.302(6)	C2-N1-C6	119.7(4)

The dihedral angle between the adenine ring and the platinum (Pt1) coordination plane is nearly perpendicular, 84.6(1)°. However, the angle between the adenine base and the other platinum atom (Pt2) is 63.4(1)°. The

dihedral angle formed between the adenine nucleobase and its symmetric one is 59.7(1)°.

No intramolecular or intermolecular hydrogen bonds are observed within the cationic entity. The arrangement of the *cis*-$[(NH_3)_2Pt(N6\text{-}9\text{-}MeA\text{-}N7)_2\{Pt(NH_3)_3\}_2]^{4+}$ cations in the solid state is shown in Figure 46.

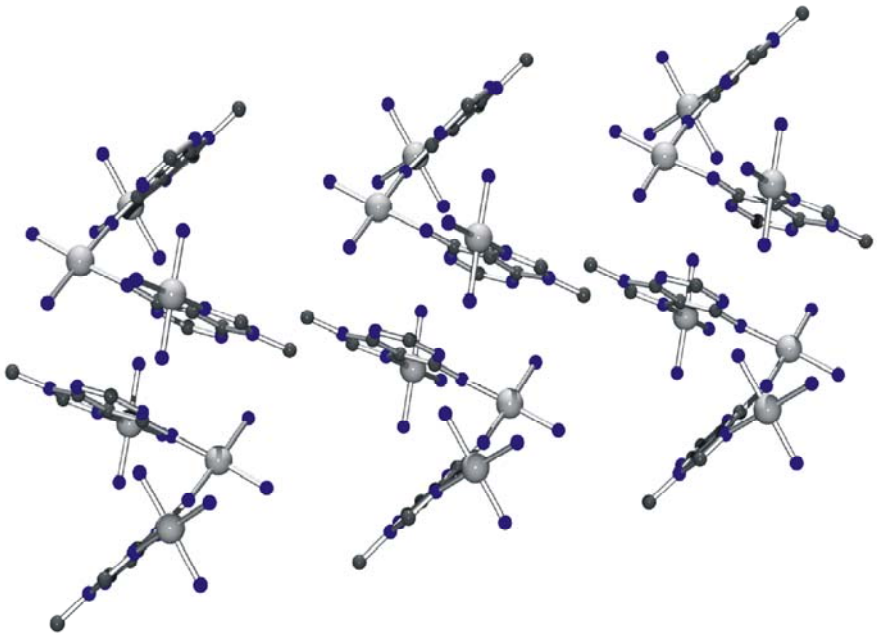

Figure 46: *View of the arrangement of the cis-$[(NH_3)_2Pt(N6\text{-}9\text{-}MeA\text{-}N7)_2\{Pt(NH_3)_3\}_2]^{4+}$ cations of (**18**).*

However, there are intermolecular hydrogen bond contacts between the cations of (**18**), the water molecules and the nitrate anions. The most important ones are: O1w···O23(nitrate), 2.82(2) Å,; O1w···N13a (–x+1, y, -z+1/2), 2.925(6) Å,; O2w···N21, 3.034(7) Å; O2w···N21a (–x+1, y, -z+1/2), 3.034(7) Å; O3w···N13, 2.933(7) Å; O11(nitrate)···N11, 3.072(8) Å; O11···N13, 2.933(7) Å; O13(nitrate)···N13, 2.933(7) Å; O22(nitrate)···N11a (–x+1, y, -z+1/2), 3.14(2) Å (Figure 47).

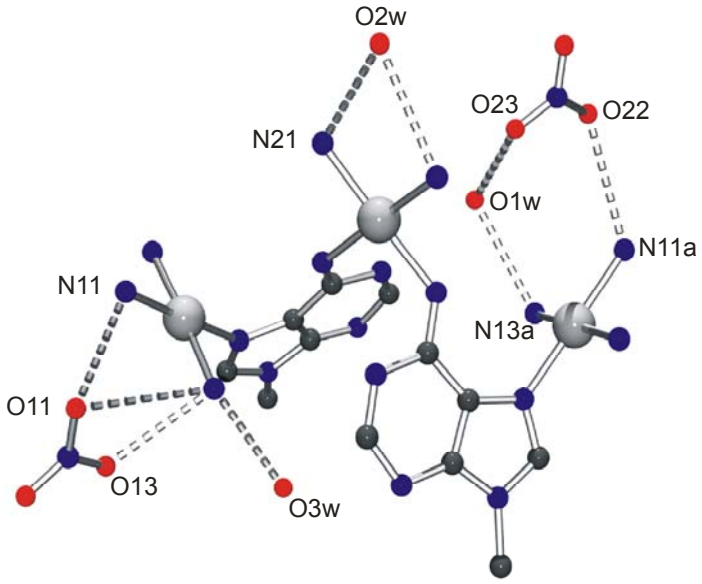

Figure 47: *Intermolecular hydrogen bonds in (**18**).*

Therefore, the crystal packing of (**18**) is based on interactions between *cis*-$[(NH_3)_2Pt(N6\text{-}9\text{-}MeA\text{-}N7)_2\{Pt(NH_3)_3\}_2]^{4+}$ cation, water molecules and nitrate counter anions. As shown in Figure 48, the arrangement of the cations, the water molecules and the nitrate anions in the crystal does not allow π-stacking between the aromatic rings of the adenines. The layers are separated by the nitrate counter anions.

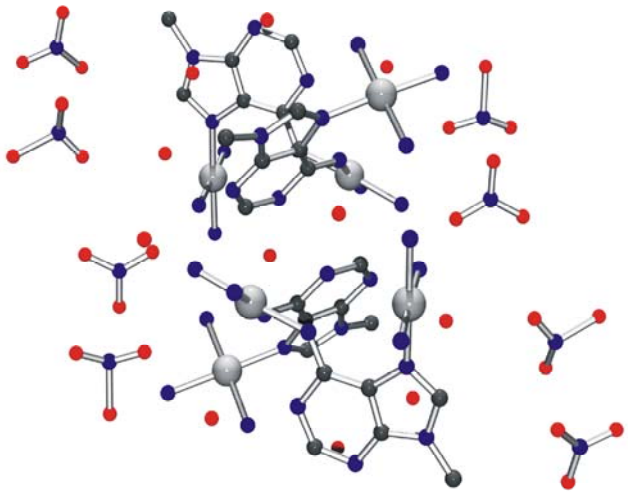

Figure 48: *Detail of packing of cis-$[(NH_3)_2Pt(N6\text{-}9\text{-}MeA\text{-}N7)_2\{Pt(NH_3)_3\}_2](NO_3)_4\cdot 6H_2O$ (**18**).*

In the ^{1}H NMR spectrum of (**18**) (Figure 49), only a single set of nucleobase signals is present, consistent with the fact that both 9-MeA bases are equivalent and hence have identical metal binding patterns. Due to the extreme conditions of the reaction (high pH values and long time), an isotopic exchange (H→D) is observed for one of the two aromatic protons of the adenine base.

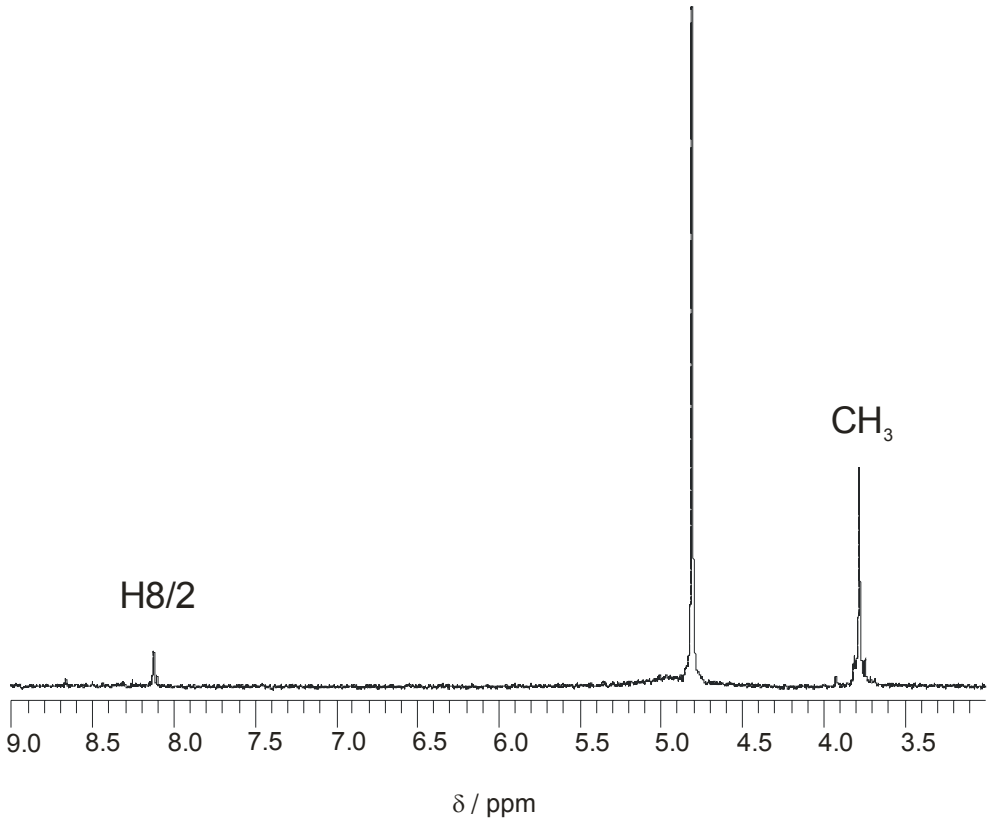

Figure 49: *^{1}H NMR spectrum in D_2O (pD ~ 7.80) of the compound cis-$[(NH_3)_2Pt(N6\text{-}9\text{-}MeA\text{-}N7)_2\{Pt(NH_3)_3\}_2]^{4+}$ (**18**). The spectrum displays one singlet for the CH_3 and another singlet in the aromatic region, which corresponds to H8 or H2. The other proton has disappeared due to isotopic exchange.*

The individual acidity constants pK_{a1} (for the deprotonation of N1H of one adenine) and pK_{a2} (for deprotonation of N1H of the other adenine), calculated with a non-linear least squares fit after Newton-Gauss with equation (3) for each

proton, are given in Table 10. The values for the situation in water were then calculated by applying equation (4).

Table 10: *Negative logarithms of the acidity constants (pK_a) of cis-[$(NH_3)_2$Pt(N6-9-MeA-N7)$_2${Pt$(NH_3)_3$}$_2$]$^{4+}$ (**18**) in D_2O and in H_2O. Values for pK_a of the proton H8/2 and the methyl group are given with one standard deviation (1σ).*

	D_2O		H_2O	
	pK_{a1}	pK_{a2}	pK_{a1}	pK_{a2}
A–H8/2	5.48 ± 0.14	7.11 ± 0.12	4.95 ± 0.14	6.56 ± 0.12
A–CH_3	5.34 ± 0.12	7.05 ± 0.11	4.82 ± 0.12	6.50 ± 0.11
Average	5.41 ± 0.13	7.08 ± 0.11	4.89 ± 0.13	6.53 ± 0.11

2.5.5 Multiple Metalation of 9-Methyladenine

Twofold metal binding, to N1 and N7 is likewise quite common. Here it has been discussed some examples. N1,N7 binding gives a rise to two mutually perpendicular M–N vectors which permit construction of molecular rectangles and meanders with 90°-angles.[86] Threefold metal binding to a neutral, 9-blocked adenine via N1, N3 and N7 has recently been observed in a polymeric, helical complex.[87]

Deprotonation of the exocyclic amino group prior to metal complexation does, however, not necessarily imply that the nucleobase becomes anionic. Rather, metal binding to this group can be accompanied by a shift of an amino proton to another site, e.g. N1, therefore generating a metalated form of a rare adenine tautomer.[25,69,88] As to the formation of N6 metalated species, initial metal coordination to N1 or N7 is likely to take place, followed by metal migration. This has been demonstrated in this work. In one case, the *cis*-$(NH_3)_2Pt^{II}$ migrates from N1 to N6 (see Section 2.5.4.5). Once the metal resides at N6, it may adopt two different orientations, either *syn* to N1 or *anti*. Examples

exists for both cases.[69,88a] As far as consequences for the H bonding ability of a N6 metalated adenine nucleobase are concerned, the relevance to metal mutagenicity is an obvious one.[89]

There are several reports on binding mode **A** (Figure 50) with simultaneous metal binding to N1, N6, N7,[90,91] leading to trinuclear, cyclic metal complexes with remarkable receptor properties. A record fourfold metalation of a 9-methyladenine dianion has been observed with M = (trpy)Pd^{II} (**B**) with metal entities simultaneously bound to N1, N6, N7, and C8 (Figure 50).[92]

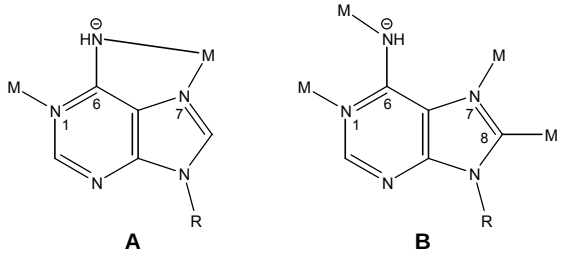

Figure 50: *Multiple metalation of 9-(R)adenine. Modes of metal binding.*

2.5.5.1 Palladium Binding to 9-Methyladenine

A threefold metalation of a 9-methyladenine has been observed with metal entities simultaneously bound to N1, N6 and N7 (Figure 51). In this case, the metal entity is (dien)Pd^{II}. Two equivalents of (dien)Pd^{II} were added to a solution containing 9-MeA and the mixture was brought to pH 5-6. The fast rate of the reaction allows instantaneous coordination of Pd either at the N1 site (**C**) of the free nucleobase, or at the N7 site of the 9-MeA (B) or both sites, N1 and N7 (A) (Figure 51). In order to deprotonate the exocyclic amino group, the pH was brought to 8-9 by addition of 1M NaOH. In this case, a metal migration can occur, from N1 to N6 (E) or from N7 to N6 (F). According to our studies, we suggest that the migration occurs from N1 to N6. The addition of a third (dien)Pd^{II} to this solution of the di-nuclear complex (E or F), leads to the formation of a tri-nuclear palladium complex of 9-methyladenine: {[(dien)Pd]$_3$(9-MeA-*N1*,*N7*,*N6*)}$^{5+}$ (**19** = D).

The reaction was followed by ^{1}H NMR spectroscopy. It was very difficult to assign the signals to the different complexes. In order to simplify this problem, different reactions were carried out.

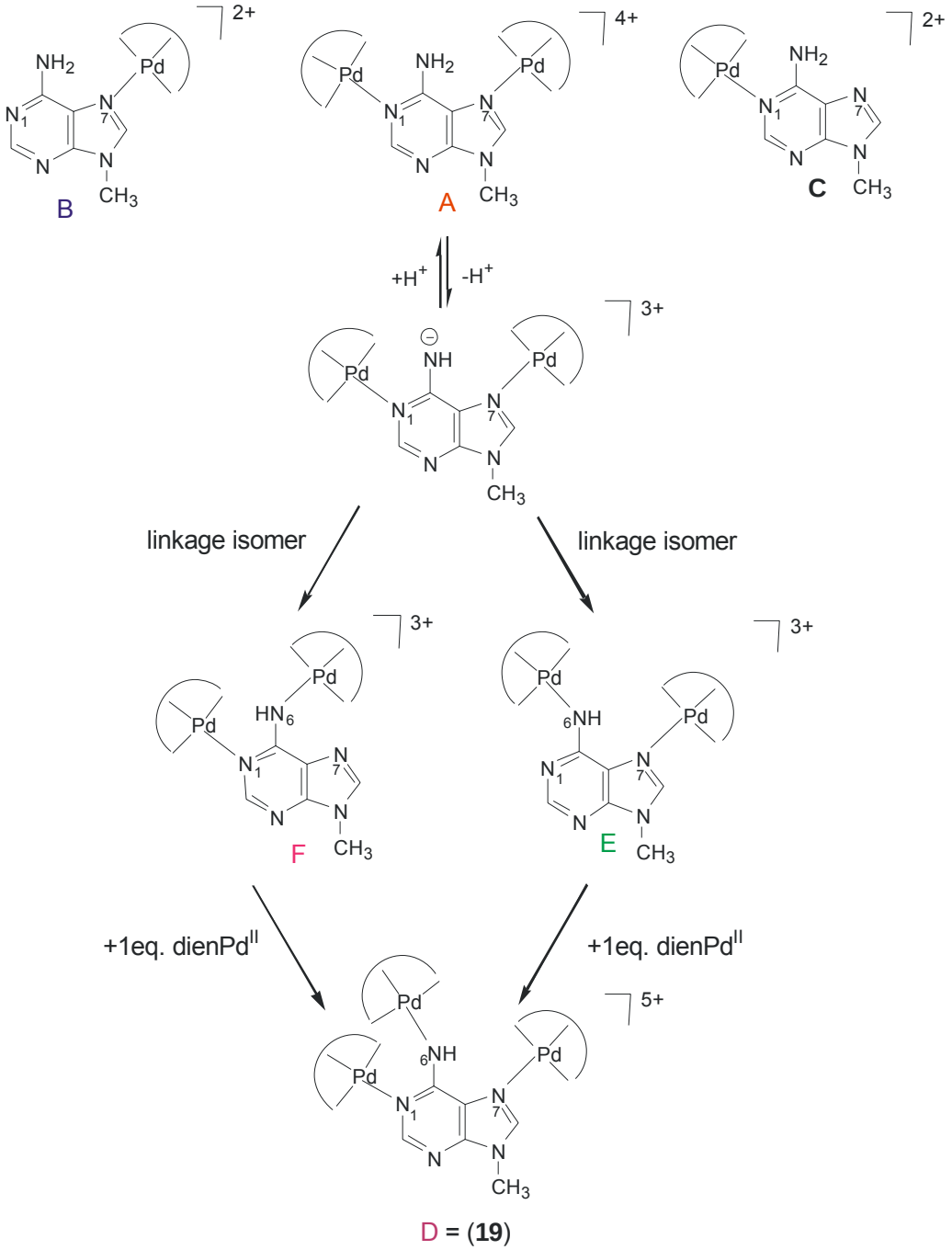

Figure 51: *Deprotonation of the N(6)H_2 of the adenine nucleobase in {[(dien)Pd]$_2$(9-MeA-N1,N7)}$^{3+}$ (A) and competing migration of Pt^{II} from N1 or N7 to N6. Formation of {[(dien)Pd]$_3$(9-MeA-N1,N7,N6)}$^{5+}$ (**19**).*

2.5.5.1.1 NMR Studies with dienPd^{II} and 9-MeA

When the yellow crystals {[(dien)Pd]$_3$(9-MeA-*N1,N7,N6*)}$^{5+}$ (**19**) are dissolved in D_2O (pD ~ 8.5), one can observe multiple sets of H2 and H8 resonances and three major ones (N-CH_3) (spectrum (i) in Figure 52). There are also several minor signals. This multiplicity apparently arises from a rapid equilibrium of different dienPd^{II} complexes. If an excess of dienPd^{II} is added to the solution of the crystals, spectrum (ii) is obtained (Figure 52). The pD was decreased to pD ~ 6.7 and only one majority signal can be observed. This signal corresponds to the dinuclear complex (A: {[(dien)Pd]$_2$(9-MeA-*N1*,*N7*)}$^{4+}$). We know that A is the dinuclear species, because a reaction of 9-MeA with three equivalents of [dienPd(H_2O)]$^{2+}$ at pD ~ 2.9 leads to a main signal, and this signal has the same chemical shifts at pD ~ 6.7. The chemical shifts of the resonances of A are the following: 3.88 ppm (s, CH_3), 8.75 ppm (s, H2) and 8.66 ppm (s, H8). If the reaction is carried out with 0.33 equivalents of dienPd^{II} and one equivalent of 9-MeA, no dinuclear complex is expected, only mononuclear complexes (A-*N1* and A-*N7*). This was observed at pD ~ 5.3.

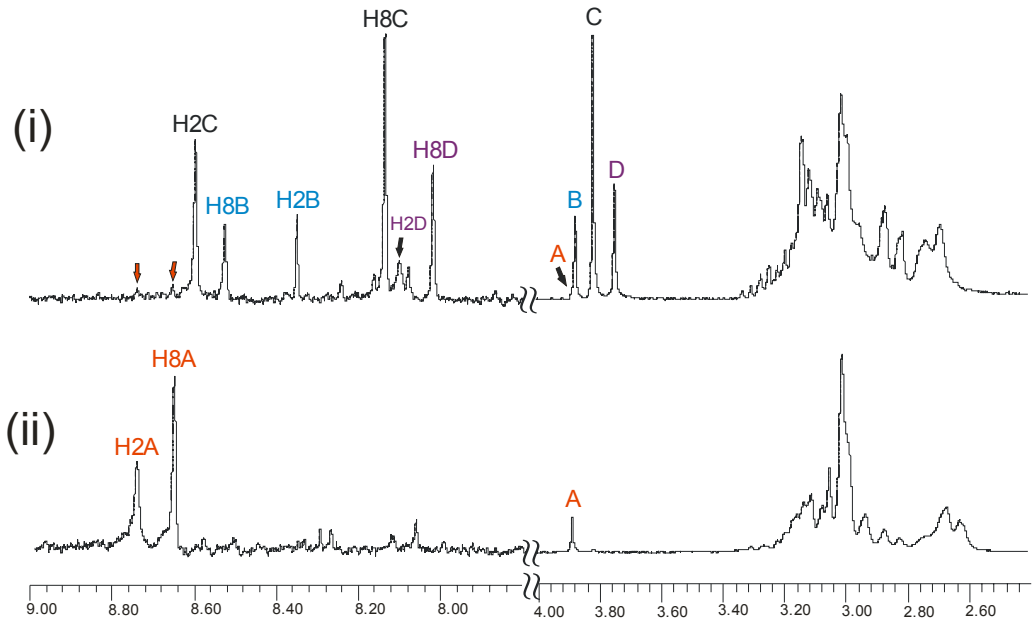

Figure 52: *^{1}H NMR spectrum of (**19**) at pD ~ 8.5 (i). Addition of an excess of [dienPd(H_2O)]$^{2+}$ leads to spectrum (ii) on the bottom (pD ~ 6.7).*

In order to find out which compounds correspond to the rest of the signals, the following experiment was carried out. Two equivalents of $[dienPd(H_2O)]^{2+}$ were added to a solution of 9-methyladenine at pD ~ 5.82. There is no signal of free adenine. But there are three principal sets of signals A, B and **C** (spectrum (iii) Figure 53). The chemical shifts at pD ~ 5.82 of the species B are 3.88 ppm (s, CH_3), 8.52 ppm (s, H8) and 8.35 ppm (s, H2). The resonances of **C** are at 3.82 ppm (s, CH_3), 8.60 ppm (s, H2) and 8.14 ppm (s, H8). The protons at lowest field correspond to the dinuclear complex A. The assignment of the proton resonances was made by performing the same reaction with deutered 9-methyladenine (9-MeA-*d8*) (spectrum (iv), Figure 53). Both reactions, with 9-MeA and with 9-MeA-*d8*, were brought to pD ~ 8.8 and to pD ~ 10.25.

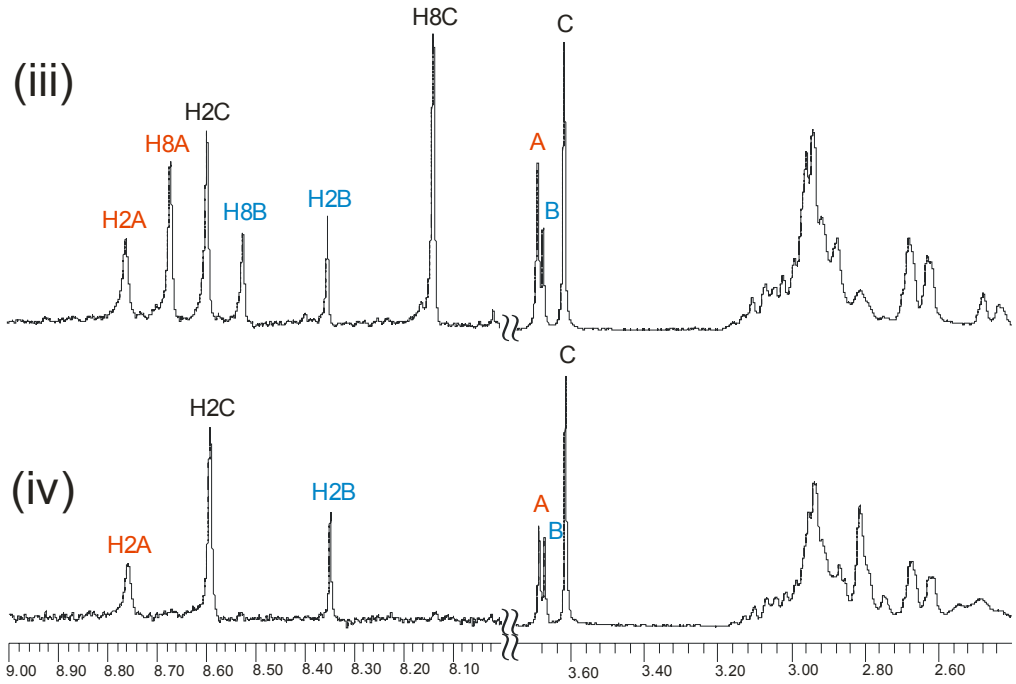

Figure 53: *Reaction of 2 dienPd^{II} with 9-MeA at pD ~ 5.82 (iii). Comparison with the same reaction using 9-MeA-d8 (iv).*

At pD ~ 8.8 there are two new signals (D and E), one of them, E, is of very intensity. Signal A decreases strongly. **C** is the main signal (Figure 54).

Spectrum (v) corresponds to the reaction with 9-MeA and spectrum (vi) to the reaction with 9-MeA-*d8*.

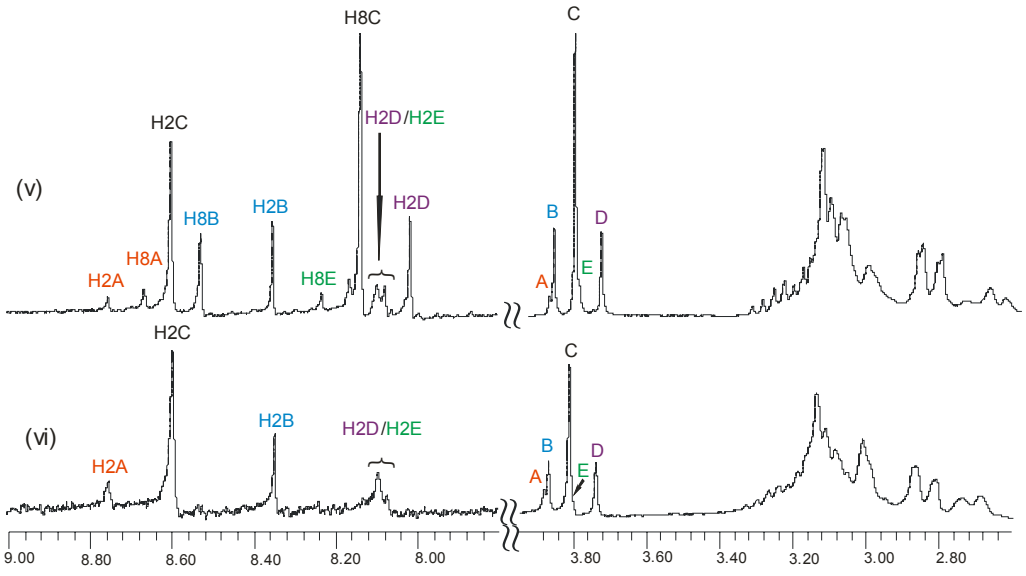

Figure 54: *^{1}H NMR spectrum of the reaction between 2 [dienPd(H_2O)]$^{2+}$ with 1 equivalent 9-MeA at pD ~ 8.8 (v) and with 9-MeA-d8 (vi).*

At pD ~ 10.25 the signal corresponding to A has disappeared and the resonance E has increased in intensity. The main signals are now D and E (see Figure 55). The chemicals shifts corresponding to the compound D are: 3.75 ppm (s, CH_3), 8.10 ppm (s, H2) and 8.01 ppm (s, H8) and the ones corresponding to E are: 3.80 ppm (s, CH_3), 8.07 ppm (s, H2) and 8.22 ppm (s, H8).

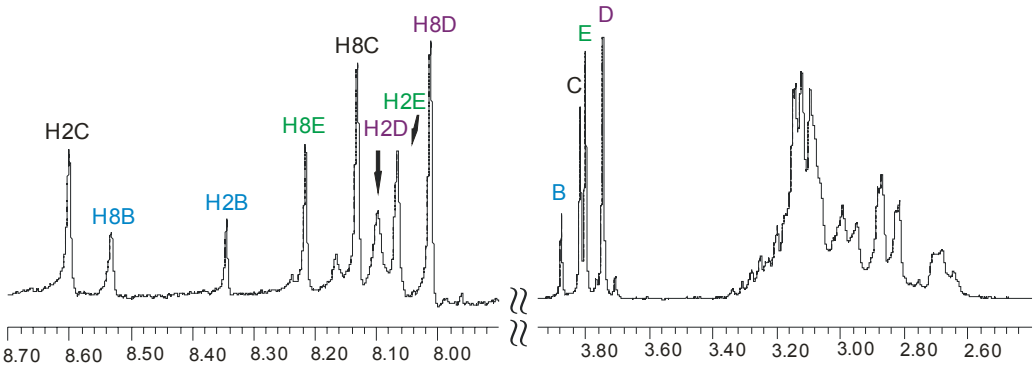

Figure 55: *^{1}H NMR spectrum of the reaction of 2 [dienPd(H_2O)]$^{2+}$ with 9-MeA at pD ~ 10.25.*

If another equivalent of $[dienPd(H_2O)]^{2+}$ is added to the reaction mixture at pD ~ 9, signal A reappears in low intensity and E decreases strongly. Now, the main signals are **C** and D (Figure 56).

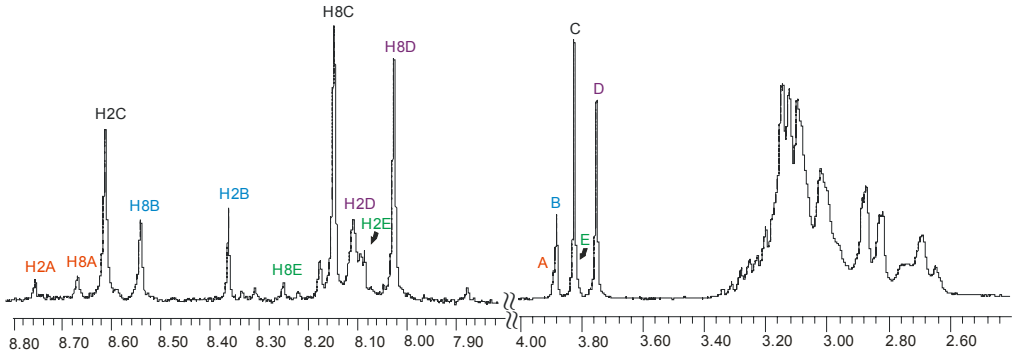

Figure 56: *^{1}H NMR spectrum of the reaction of 3 $[dienPd(H_2O)]^{2+}$ with 9-MeA at pD ~ 9.*

Instead of adding two equivalents of $[dienPd(H_2O)]^{2+}$, the reaction is carried out by adding one equivalent of $[dienPd(H_2O)]^{2+}$ to one equivalent of 9-MeA and keeping the mixture at pD ~ 5.3, 40°C for a day. There are three sets of signals, one of which is due to free 9-methyladenine (Figure 57). A pD dependence was measured, in order to find out which resonance corresponds to $\{[(dien)Pd](9\text{-MeA-}N1)\}^{2+}$ (**C**) and which one to $\{[(dien)Pd](9\text{-MeA-}N7)\}^{2+}$ (B).

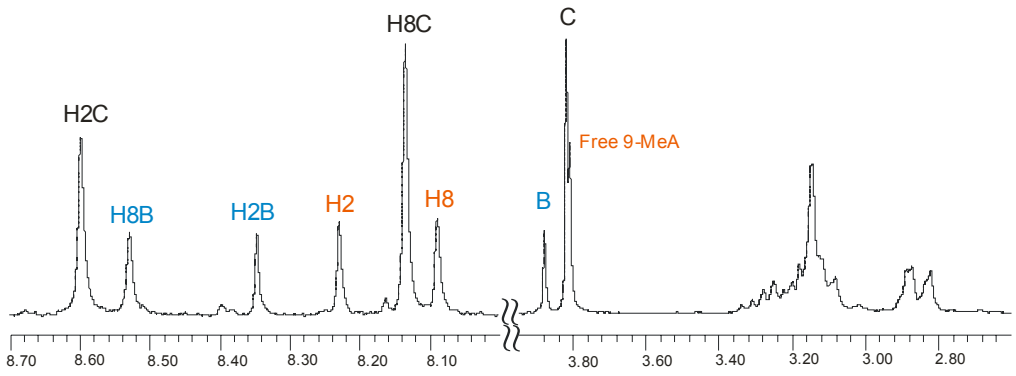

Figure 57: *^{1}H NMR spectrum of the reaction of one equivalent of dienPd^{II} and one equivalent of 9-MeA at pD ~ 5.30.*

It was observed, that the more acidic the solution is, the more free 9-methyladenine is present. Resonance **C** is always more intensive than signal B. Looking at the values of the chemical shifts of B and **C** summerized in Table 11, it can be noted that the resonances corresponding to the compound {[(dien)Pd](9-MeA-*N1*)}$^{2+}$ (**C**) are not very sensitive at acidic conditions, since the N1 position is metalated. However, the resonances of {[(dien)Pd](9-MeA-*N7*)}$^{2+}$ (B) are very sensitive at acidic conditions. In the pD range from 1.7 to 5.3 the H8 resonance of compound B undergoes a stronger upfield shift ($\Delta\delta$= 0.271) than the H8 resonance of **C** ($\Delta\delta$= 0.125). So in this pD range, the resonances of B are more affected than those corresponding to **C**. Based on this observation B is tentatively assigned to {[(dien)Pd](9-MeA-*N7*)}$^{2+}$ and **C** to {[(dien)Pd](9-MeA-*N1*)}$^{2+}$. However, these results are different in the case of Pt(II). The chemical shifts are also different from the values found by Jorma Arpalahti[93] for dienPt(Ado) isomers.

Table 11: *Values of the pD dependence from 1.7 to 5.3 of the1:1 reaction of dienPd^{II} and 9-MeA.*

pD	δ_{H2C}	δ_{H2B}	δ_{H8C}	δ_{H8B}	δ_{CH_3C}	δ_{CH_3B}
	ppm					
1.70	8.63	8.54	8.27	8.82	3.84	3.96
2.55	8.60		8.15		3.82	
3.33	8.60	8.37	8.14	8.55	3.82	3.89
4.10	8.60	8.36	8.14	8.54	3.82	3.88
5.30	8.60	8.35	8.13	8.53	3.82	3.88

After the assignment of the signals A, B and **C**, it is proposed that signal D corresponds to (**19**), in other words, to {[(dien)Pd]$_3$(9-MeA-*N1*,*N7*,*N6*)}$^{5+}$. E could be the intermediate {[(dien)Pd](9-MeA-*N7*,*N6*)}$^{4+}$. All the obtained results are summarized in Table 12.

Table 12: *Chemical shifts of the different compounds containing one, two or three entities of dienPd^{II} and one 9-methyladenine bonding through N1,N7 and N6.*

Signal	Compound	δ_{CH_3}	δ_{H2}	δ_{H8}
A	{[(dien)Pd]$_2$(9-MeA-*N1*,*N7*)}$^{4+}$	3.88	8.75	8.66
B	{[(dien)Pd](9-MeA-*N7*)}$^{2+}$	3.88	8.35	8.52
C	{[(dien)Pd](9-MeA-*N1*)}$^{2+}$	3.82	8.60	8.14
D	{[(dien)Pd]$_3$(9-MeA-*N1*,*N7*,*N6*)}$^{5+}$ (**19**)	3.75	8.10	8.01
E	{[(dien)Pd](9-MeA-*N7*,*N6*)}$^{4+}$	3.80	8.07	8.22

2.5.5.1.2 {[(dien)Pd]$_3$(9-MeA$^-$-*N1*,*N7*,*N6*)}Cl$_{3.5}$(PF$_6$)$_{1.5}$·3H$_2$O (19)

Yellow crystals of {[(dien)Pd]$_3$(9-MeA-*N1*,*N7*,*N6*)}Cl$_{3.5}$(PF$_6$)$_{1.5}$·3H$_2$O (**19**) were obtained from an alkaline solution containing 9-methyladenine, [(dien)Pd(H$_2$O)]$^{2+}$, NaCl and KPF$_6$. The yellow crystals are not stable at room temperature, so they were measured at low temperature. They crystallize in the monoclinic P2(1)/c space group. In the refinement process of the X-ray data, all non-hydrogen atoms of the crystal were refined anisotropically. Crystal data, data collection and refinement parameters for (**19**) are summarized in Table A-5 (see Appendix).

The solid state structure of (**19**) consists of three (dien)Pd^{II} entities bound to the N7, N1 and N6 positions of the anionic 9-methyladenine nucleobase. A view of the cation {[(dien)Pd]$_3$(9-MeA$^-$-*N1,N7,N6*)}$^{5+}$ with the labeling scheme is shown in Figure 58.

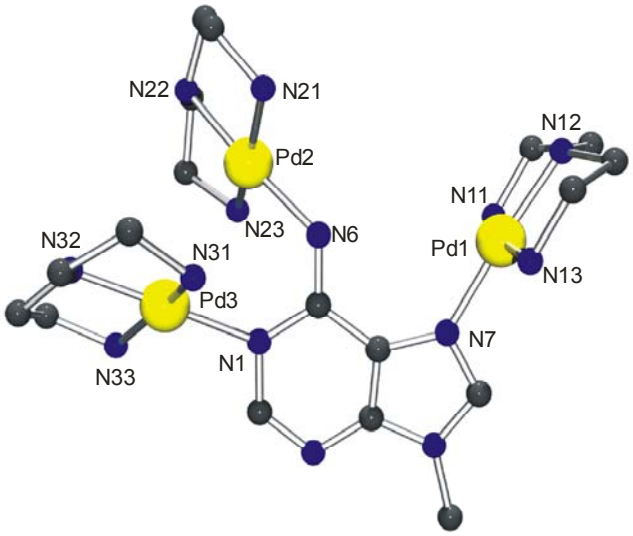

Figure 58: *View of the cation {[(dien)Pd]$_3$(9-MeA$^-$-N1,N7,N6)}Cl$_{3.5}$(PF$_6$)$_{1.5}$·3H$_2$O (**19**). The Cl$^-$ and PF$_6^-$ anions and the three water molecules are omitted for clarity.*

The (dien)Pd^{II} entities at N1 and N6 are mutually *syn* oriented, leading to a contact of 3.23 Å between Pd3 and Pd2. Consequently, Pd1 at N7 and Pd2 at N6 are *anti*, displaying a large separation of 5.24 Å. Pd-N distances to the nucleobase are between 2.031(3) (Pd1-N7) and 2.063(3) Å (Pd3-N1). It is to be noted that the Pd2-N6 distance, hence the bond distance to the deprotonated exocyclic amino group, is in between these extremes (2.041(3) Å), and not shorter, as might have been suspected.

Geometries of the dienPd^{II} entities are normal. In the case of dienPd1^{II} entity, the N13-Pd1-N11 angle deviates markedly from 180° (166.93(13)°), unlike the N12-Pd1-N7 angle, which is 175.61(13)°. The dien ring displays the characteristic sting ray structure, with C12 and C13 out of the Pd coordination plane by -0.707(5) and -0.568 (5) Å, respectively. The two central CH$_2$ groups (at either site of N12) are oriented toward the C8 of 9-MeA$^-$.

In the case of the palladium atom coordinated at N6 of the adenine (Pd2) a similar situation is observed. There is a deviation from linearity of the angle between Pd2 and the two coordinated sites of the dien ligand *cis* positioned to the adenine nucleobase: N23-Pd2-N21, 164.59(13)°. This contrasts with the almost linear orientation of N22-Pd2-N6, 175.92(13)°. The dien ring also displays the characteristic sting ray structure, with C22 and C23 out of the Pd coordination plane by -0.609(5) and -0.587(5) Å, respectively. In this case, the central CH_2 groups (at N22) are oriented toward the C5 of 9-MeA$^-$.

The largest deviation from an ideal square-planar coordination of the palladium atoms is present in Pd3, which is coordinated to the N1 position of the adenine nucleobase. The N33-Pd-N31 angle deviates markedly from 180° (162.88(12)°), unlike the angle N32-Pd3-N1, which is 178.65(13)°. The dien ring displays again the characteristic sting ray structure, with C32 and C33 out of the Pd coordination plane by -0.543(6) and -0.486 (5) Å, respectively. The central CH_2 groups (adjacent to N32) are pointing toward the C2 of 9-MeA$^-$.

Pd1-N, Pd2-N and Pd3-N distances about the Pd center range from 2.002(3) to 2.063(3) Å. A list of selected distances and angles involving the Pd atoms of (**19**) is given in Table 13.

Table 13: *Selected distances (Å) and angles (°) for non-hydrogen atoms in* ***19****.*

Pd1-N7	2.031(3)	N12-Pd1-N13	85.00(13)
Pd1-N11	20.46(3)	N12-Pd1-N7	175.61(139
Pd1-N12	2.005(3)	N13-Pd1-N7	95.65(129
Pd1-N13	2.020(3)	N12-Pd1-N11	84.25(13)
		N13-Pd1-N11	166.93(13)
		N7-Pd1-N11	94.51(12)
Pd2-N6	2.041(3)	N22-Pd2-N6	175.92(13)
Pd2-N21	2.046(3)	N22-Pd2-N23	83.63(13)
Pd2-N22	2.010(3)	N6-Pd2-N23	95.84(12)
Pd2-N23	2.043(3)	N22-Pd2-N21	84.52(13)
		N6-Pd2-N21	95.27(12)

		N23-Pd2-N21	164.59(13)
Pd3-N1	2.063(3)	N32-Pd3-N31	83.88(12)
Pd3-N31	2.036(3)	N32-Pd3-N33	83.45(12)
Pd3-N32	2.002(3)	N31-Pd3-N33	162.88(12)
Pd3-N33	2.055(3)	N32-Pd3-N1	178.65(13)
		N31-Pd3-N1	95.71(12)
		N33-Pd3-N1	96.69(12)
C6-N6	1.314(4)	C8-N7-C5	105.1(3)
C6-N1	1.391(4)	N1-C6-C5	113.9(3)
C2-N1	1.363(5)	C2-N1-C6	120.0(3)

The adenine ligand in (**19**) has normal distances and angles between atoms. But if we compare the distance C6-N6 between complex (**19**) and 9-MeA,[70] a slight shortening is observed for (**19**): 1.314(4) in (**19**) and 1.348(9) Å in 9-MeA. The atoms of the 9-methyladenine base are coplanar, with a r.m.s. deviation of 0.019.

The dihedral angle between the adenine ring and the PdN_4 coordination sphere of Pd1 is 84.43(8)°; hence the two planes are almost perpendicular. The dihedral angles between the adenine ring and the two other metal coordination planes are 54.12(9)° and 50.0(1)°, respectively for Pd2 and Pd3.

The crystal packing of (**19**) is dictated by interactions between the $\{[(dien)Pd]_3(9\text{-MeA-}\textit{N1,N7,N6})\}^{5+}$ cation, the chloro counter anions and the crystallization water molecules. Weak interactions between fluoro ligands of the hexafluorophosphate anions and the $N11H_2$ of the dienPd1 entity were found, and between PF_6^- and $C34H_2$ of the dienPd3 entity. As shown in Figure 59, the Cl2 anion in the crystal structure is shared by another cation, and forms hydrogen bonds with the protons of the dien ligand: Cl2···N13(H13), 3.253(3) Å, Cl2···N22b(H22b)(x-1, y, z), 3.155(3) Å and Cl2···N32b(H32b)(x-1, y , z), 3.126(4) Å (Figure 59).

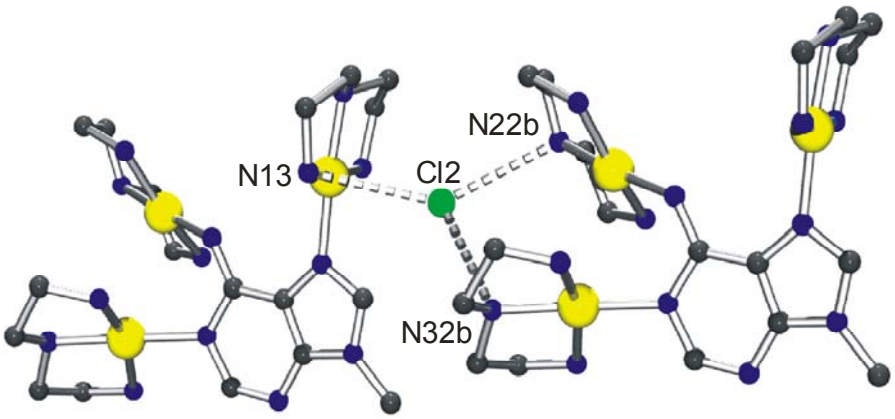

Figure 59: *View along the a axis of the packing of the cation of (**19**).*

A view along the b axis, shown in Figure 60, reveals that there are also intermolecular hydrogen bonds between Cl4 anions and the protons of the dien group. These hydrogen bond contacts are: Cl4···N23(H23), 3.225(3) Å, Cl4···N33a(H33a)(-x+2, -y+1, -z+1), 3.205(3) Å. Two consecutive cations are related by a center of symmetry. No intramolecular hydrogen bonds are present in the structure of (**19**).

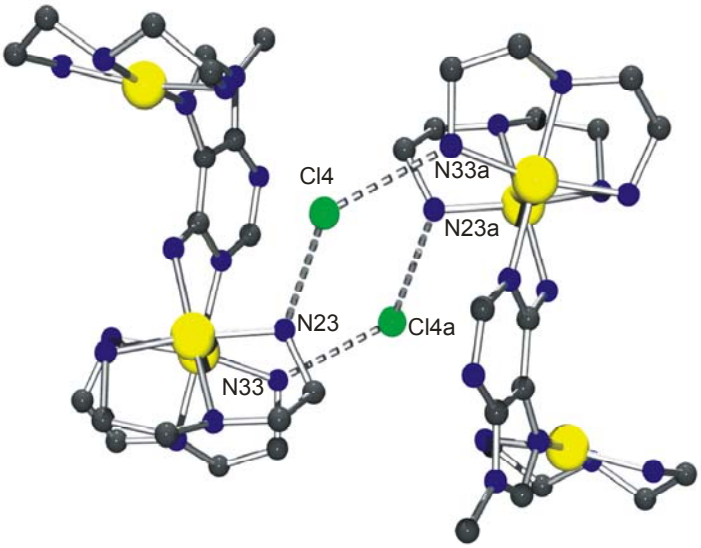

Figure 60: *View along the b axis of the packing of the cation of (**19**).*

Packing of (**19**) does not allow π-stacking interactions between aromatic rings. The Cl4 is also involved in another hydrogen bond with a water molecule: Cl4···O2w, 3.089(4) Å. Hexafluorophosphate anions are located between ribbons of cations of (**19**) (Figure 61).

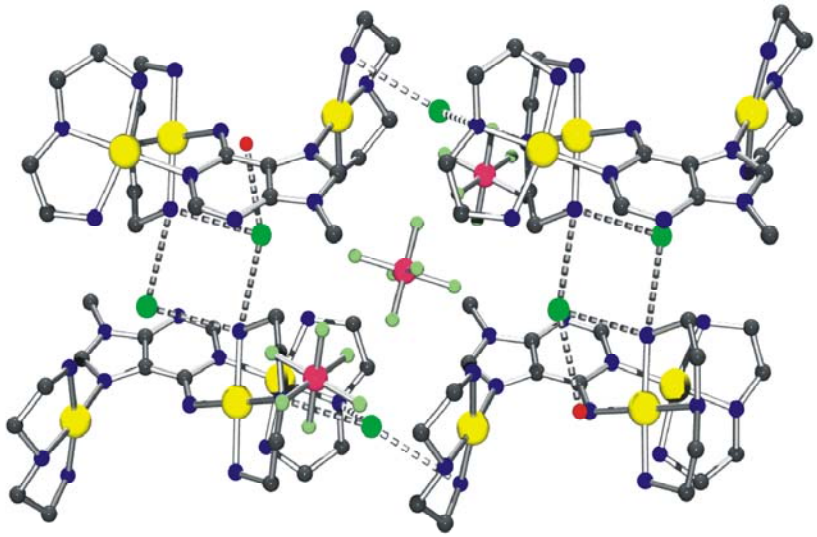

Figure 61: *Top view of a layer in the solid state structure of (**19**).*

2.5.6 Tris(cytosine) Complexes

2.5.6.1 PtC_3A

In order to study if there is a possibility of stabilization of the $N(6)H^-$ by the exocyclic amino group of a cytosine nucleobase, a tetrakis (nucleobase) complex with three cytosine ligand and one adenine ligand was studied. The starting compound $[Pt(1\text{-}MeC\text{-}N3)_3Cl]NO_3 \cdot 1.5H_2O$ was synthesized according to a published method.[94] The platinum is coordinated through the N3 positions of three cytosine nucleobases. Its respective aqua species $[Pt(1\text{-}MeC\text{-}N3)_3(H_2O)]^{2+}$ has been studied in solution by means of ^1H NMR spectroscopy.[95]

Reaction of $[Pt(1\text{-MeC-}N3)_3(H_2O)]^{2+}$ with 9-MeA in water (1:1 ratio, 40°C, pD ~ 4) gave two products together with some unreacted ligand (ca. 15% after 16 days).[95] According to a pD dependence of the ^{1}H NMR resonances, they are identified as $[Pt(1\text{-MeC-}N3)_3(9\text{-MeA-}N7)]^{2+}$ (ca. 70%) and $[Pt(1\text{-MeC-}N3)_3(9\text{-MeA-}N1)]^{2+}$ (ca. 15%). The N7 linkage isomer $[Pt(1\text{-MeC-}N3)_3(9\text{-MeA-}N7)]^{2+}$ (**20**) was isolated as NO_3^- salt in crystalline form, but the quality was not good enough for an X-ray crystal structure analysis. However, the X-ray structure of the ClO_4^- salt has been previously described[95] and is expected to be similar to the nitrate salt as far as the structure of the cation is concerned. Figure 62 shows the ^{1}H NMR spectrum of complex (**20**). Signals associated with the methyl groups of the 1-methylcytosine ligands appear in a 2:1 ratio at 3.43 ppm and 3.34 ppm, which suggests that the one at 3.43 ppm corresponds to the methyl group of the cytosine *trans* to the adenine nucleobase. The signals associated with H5 and H6 display two sets of doublets in a 2:1 ratio, which is also attributed to the different types of 1-methylcytosine ligands. Resonances due to the 9-MeA can readily be assigned: H8 (8.80 ppm,s); H2 (8.26 ppm, s) and CH_3 (3.85 ppm, s).

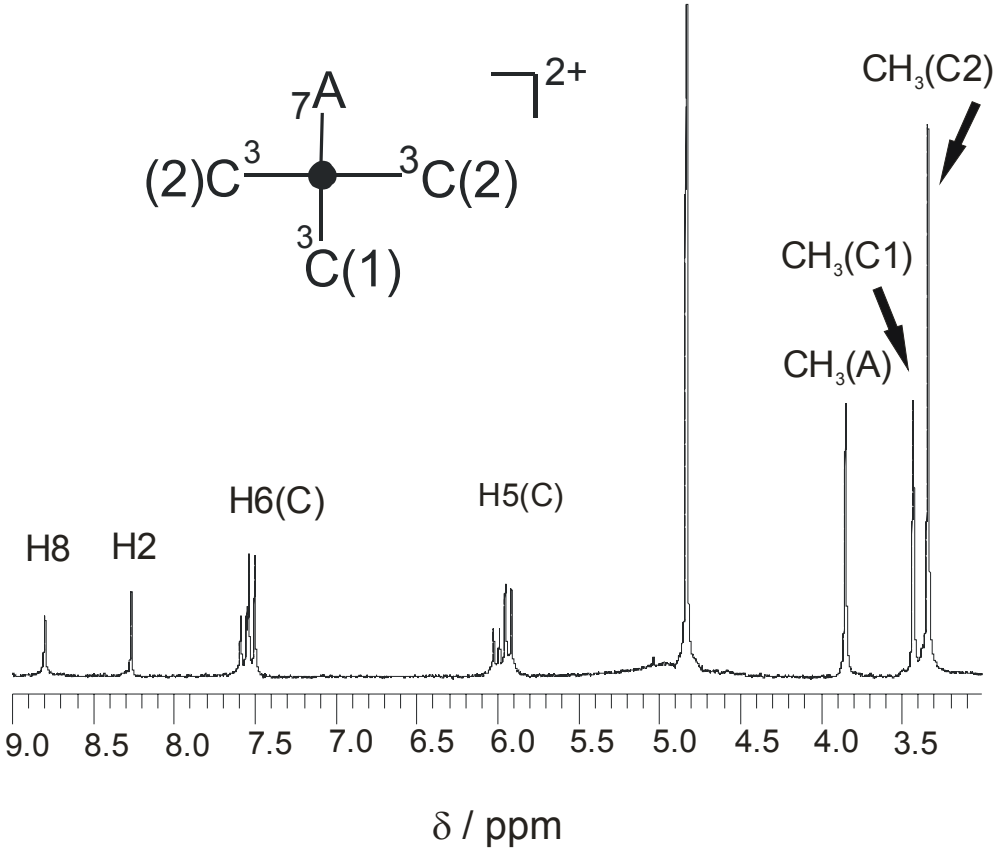

Figure 62: *^{1}H NMR spectrum of [Pt(1-MeC-N3)$_3$(9-MeA-N7)]$^{2+}$ (**20**) in D_2O (pD =7.54)*

The Pt atom is coordinated to the respective N3 sites of the three 1-methylcytosine ligands and the N7 position of a 9-methyladenine, and it adopts a square-planar PtN_4 coordination geometry. The orientation of the cytosine rings in the ClO_4^- salt[95] is *head-tail-head* (*h-t-h*), meaning that each *cis*-arranged 1-MeC ligand is oriented *head-tail* with respect to its neighbour. A resonable explanation for this orientation is the stabilization of the structure by intramolecular hydrogen bonds. Intramolecular hydrogen bonding between the exocyclic groups of pyrimidine bases requires a *cis* arragement of the respective ligands.[96] In the ClO_4^- salt of (**20**), four intramolecular hydrogen bonds between N4 and O2 of the cytosine ligands are found[95] and the adenine ligand is oriented in a way that permits H-bonding interactions with both the two cytosine ligands in *cis* position, one being significantly shorter than the other. The N7 coordinated complex undergoes protonation at the N1 position with a pK_a of 1.97 ± 0.03.[97] In order to check if this intramolecular interactions affect the pK_a

value of the exocyclic amino group of the adenine, a pD dependence of the complex [Pt(1-MeC-*N3*)$_3$(9-MeA-*N7*)]$^{2+}$ (**20**) was recorded (Figure 63). We observed that the 1-MeC resonances are more affected than the 9-MeA resonances. So the pK_a value obtained (pK_a(H_2O) = 12.63 ± 0.04) corresponds to the deprotonation of the NH_2 of the cytosine nucleobase. To conclude, there is no stabilization between the 9-methyladenine and the 1-MeC ligands. This value compares well with the pK_a value of *cis*- and *trans*-[Pt(1-MeC-*N3*)(9-MeA-*N7*)]$^{2+}$ (see Section 2.4.2.1).

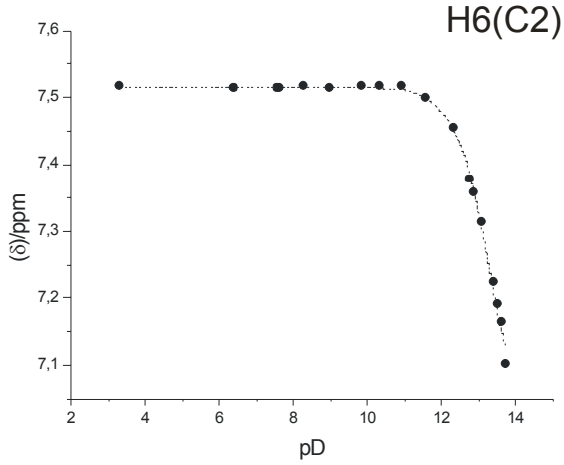

Figure 63: *pD dependence of [Pt(1-MeC-N3)$_3$(9-MeA-N7)]$^{2+}$ (**20**).*

2.5.6.2 Water Cluster: [Pt(1-MeC-*N3*)$_3$(OH)](ClO$_4$)$_{0.5}$(OH)$_{0.5}$·7H$_2$O (21)

In an attempt to isolate a deprotonated derivate of [Pt(1-MeC-*N3*)$_3$(9-MeA-*X*)]$^{2+}$ (*X* = *N1* or *N7*), the reaction mixture was brought to basic pH by addition of 1M NaOH. Eventually colourless crystals were isolated and charaterized by X-ray analysis. However, the crystals proved to be [Pt(1-MeC-*N3*)$_3$(OH)](ClO$_4$)$_{0.5}$(OH)$_{0.5}$·7H$_2$O (**21**), hence a deprotonated form of the starting compound [Pt(1-MeC-*N3*)$_3$(H_2O)]$^{2+}$, which had not reacted with 9-MeA.

Compound (**21**) crystallizes in the monoclinic system. In the refinement process, all the hydrogen atoms, including the ones of the seven water molecules, were found in the difference Fourier map and refined without

restraints. Crystallographic data, data collection parameters and refinement parameters of (**21**) data are listed in Table A-6 (see Appendix).

Complex (**21**) proved to be quite interesting in that it contained a well-structured mixed hydroxo, aqua oligomer. Discrete water clusters represent a topical research issue. Of particular interest are, among others, fundamental aspects such as the geometrie of water structure,[97] the mobility of protons in hydrogen bonds between water molecules,[98] structural changes of ice in confined space,[99] or the role of water stabilizing biopolymer aggregates.[100] The crystallographic characterization of clusters or chains of water molecules is usually aided by the presence of guest molecules (such as in water clathrates),[101] by supramolecular architectures,[102] or even by the presence of simple coordination compounds.[103] In the compound (**21**), the H bonding between the nucleobases display well-structured water cluster which also interact with the heterocyclic rings.

The relevance of water clusters in biological systems and chemical processes has been intensively studied in recent years.[97,104-109] The H bonded water molecules of the clusters can display different geometries. Some examples of tetramers,[110,111] pentamers,[112] hexamers,[113-116] octamers,[117,118] and decamers[119] have been reported. These water rings as basic units can be considered as building blocks for the formation of supramolecular entities. There are many examples of 1D,[120,121-123] 2D,[124-127] and 3D polymers.[103a]

The platinum atom is coordinated to the respective N3 sites of three 1-methylcytosine ligands and to a OH group, which is coordinated to four water molecules, forming a cyclic pentamer (Figure 64). The Pt atom adopts a square-planar PtN_3O coordination geometry. The metal is coplanar with the four donors with a deviation of ± 0.023 Å. Selected bond lengths and angles are given in Table 14.

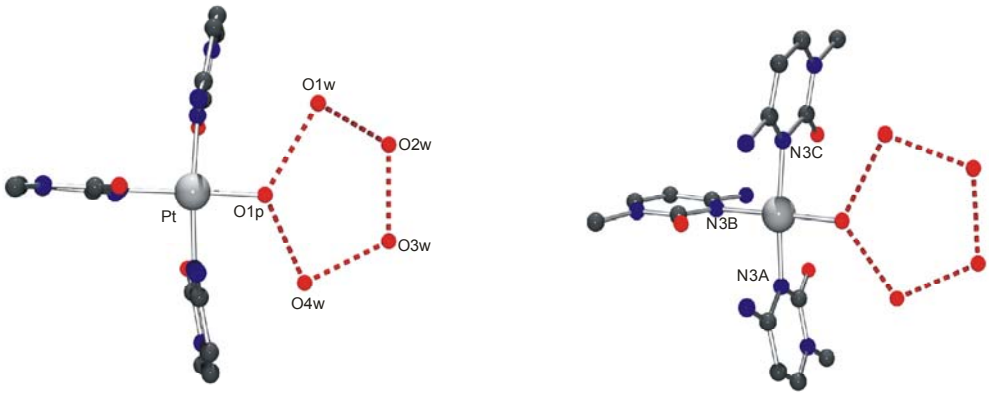

Figure 64: *Views of the water cluster of (**21**) linked to the platinum atom via the OH^- ligand.*

Table 14: *Selected distances (Å) and angles (°) for non-hydrogen atoms in **21**.*

Pt-N3A	2.030(6)	O1P-Pt-N3B	178.4(18)
Pt-N3B	2.022(6)	O1P-Pt-N3C	88.3(2)
Pt-N3C	2.027(6)	N3B-Pt-N3C	92.5(2)
Pt-O1P	2.001(5)	O1P-Pt-N3A	86.4(2)
N4A···O2B	2.951(9)	N3B-Pt-N3A	92.9(2)
N4C···O2B	3.009(8)	N3C-Pt-N3A	174.4(2)
N4B···O2A	2.954(9)		
N4B···O2C	3.036(8)		
O1P···O1w	2.821(8)		
O1w···O2w	2.706(9)		
O2w···O3w	2.63(1)		
O3w···O4w	2.69(1)		
O4w···O1P	2.879(9)		

There are no unusual bond distances or angles either in the Pt coordination sphere or in the heterocycles. The atoms of the heterocyclic rings are approximately coplanar within ±0.0251, ±0.0138 and ±0.0087 Å, respectively for 1-MeC_a, 1-MeC_b and 1-MeC_c. Their mean planes form dihedral angles with the Pt coordination plane which do not deviate significantly from a perpendicular

arrangement (89.9(2)° and 86.0(2)° for the cytosines *trans* to each other, 87.2(2)° for the cytosine *trans* to the OH group).

The orientation of the cytosine rings is head-tail-head (h-t-h), meaning that each cis-arranged 1-MeC ligand is oriented head-tail with respect to its neighbour, a feature also confirmed for $[Pt(1\text{-}MeC\text{-}N3)_3(9\text{-}EtGH\text{-}N7]^{2+}$, for the precursor compound of (**21**), $[Pt(1\text{-}MeC)_3Cl]^{+}$[94], as well as for other structurally characterized Pt(II)[128] and Pd(II) complexes[96] containing three cytosine ligands. A reasonable explanation for the preference of the h-t-h orientation is the stabilization of the structure by intramolecular hydrogen bonds. Intramolecular hydrogen bonding between the exocyclic groups of pyrimidine bases requires a *cis* arrangement of the respective ligands.[96] Therefore the h-t-h arrangement in tris(1-methylcytosine) compounds and the analogous h-t-h-t arrangement in a tetrakis(1-methylcytosine) Pt(II) complex,[94] which likewise has been confirmed by X-ray analysis, allow the formation of the maximum number of intramolecular hydrogen bonds. In (**21**), four intramolecular hydrogen bonds between N4 and O2 of the cytosine ligands are found, ranging from 2.951(9) to 3.036(8) Å (Figure 65).

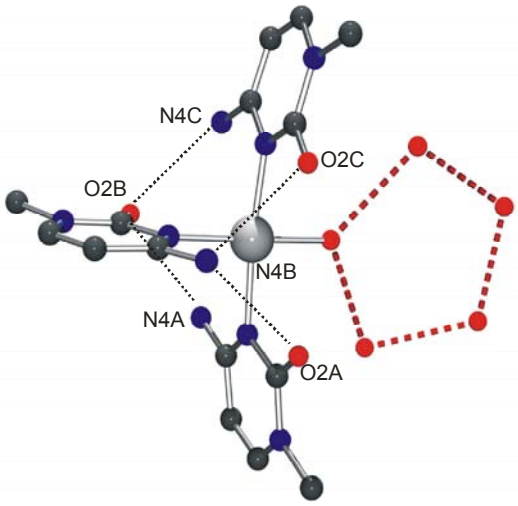

Figure 65: *Molecular cation of $[Pt(1\text{-}MeC\text{-}N3)_3(OH)]^{+}\cdot 4H_2O$ with intramolecular H bonds between cytosine ligands.*

The hydroxo ligand (O1P) is incorporated in a cyclic structure comprised of four additional water molecules, O1w, O2w, O3w and O4w. Other water

molecules (O5w and O6w) are joined to the cyclic pentamer (via O1w and O4w, respectively). The atoms of the cyclic pentamer are arranged in an envelope conformation, in which the O1P atom lies slightly (0.016(3) Å) above the plane defined by the remaining four atoms. Distances between oxygens atoms within the pentamer are: O1P···O1w, 2.821(8) Å; O1w···O2w, 2.706(9) Å; O2w···O3w, 2.63(1) Å; O3w···O4w, 2.69(1) Å; O4w···O1P, 2.879(9) Å. Internal angles of the pentamer range from 93.25(3)° (O1P···O1w···O2w) to 120.5(3)° (O4w···O1P···O1w). Figure 66 shows in detail the distances and angles between atoms of the cyclic pentamer.

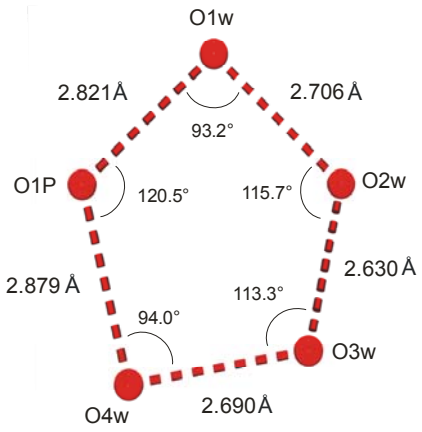

Figure 66: *View of the cyclic pentamer present in (**21**).*

A study of the hydrogen bonding pattern shows the formation of a dense water polymer. There are two types of hydrogen bonds involving water molecules: the first one, between water molecules interacting only with water molecules (formation of water polymer); and the second one, between water molecules of the water polymer interacting with the exocyclic oxygen atoms of the cytosine rings. Each cation of (**21**) and its corresponding water molecules of crystallization forms intermolecular hydrogen bonds between the water molecules with the cation at 1/2–x, 1/2–y, -z, thus leading to a pair of centrosymmetrically related cations (Figure 67). The hydrogen bonds and the water molecules in orange are closest to the viewer.

The symmetry operator (i) for the description of hydrogen interactions is 1/2–x, 1/2–y, -z. Oxygen atoms of the water molecules that are involved in

hydrogen bond formation exclusively between water molecules are: O5w (H-bonds with O1w and one symmetrical O6w), O6w (H-bonds with O4w, O8w, O7w and one symmetrical O5w). Oxygen atoms of the water molecules of the water polymer which also join the nucleobase polymer are: O2w (H bond with one symmetrical O2A), O3w (H bond with one symmetrical O2C). A detailed list of the interactions including the symmetry operator is given in Table 15.

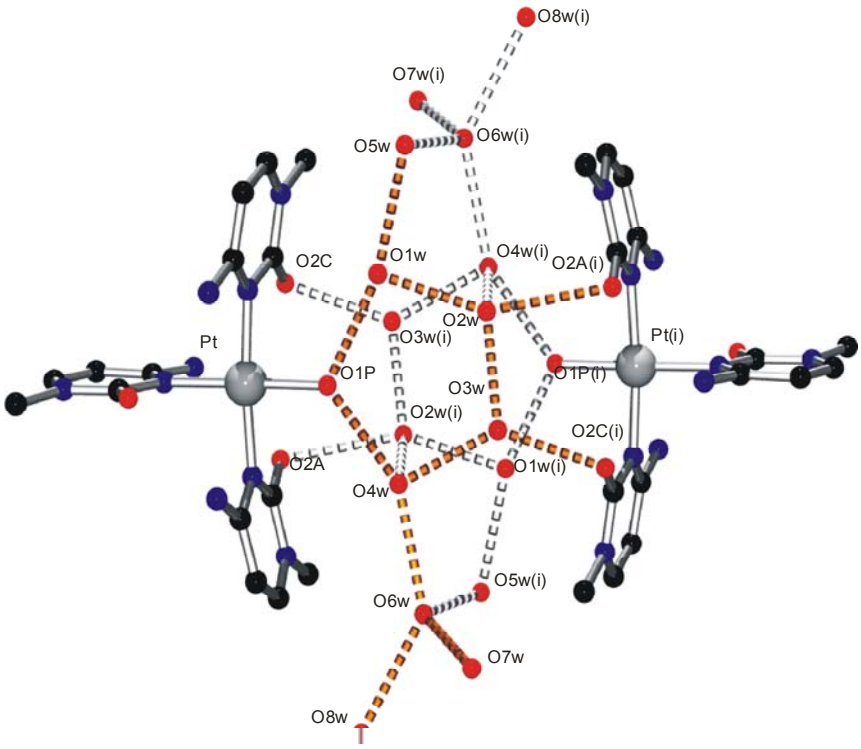

Figure 67: *View of the polymeric structure of crystallization water in (**21**).*

In the 3D building of the polymer, the side defined by the O4w···O2w atoms of two pentamers of adjacent unit cells approach each other very closely. As a consequence of this, a cyclic hexamer can be observed between two pentamers. The hexamer and the pentamer entities share the O4w and O2w oxygen atoms.

Table 15: *Hydrogen bond distances (Å) involving the water of crystallization in **21**.*

O2C···O3w(i)	2.750(1)	O6w···O8w	3.040(2)
O2A···O2w(i)	3.104(9)	O4w···O6w	2.890(1)

O1w···O5w	2.920(1)	O4w···O2w(i)	2.900(9)
O5w···O6w(i)	2.950(1)		
O6w···O7w	2.530(2)		

Atoms in the hexamer adopt a slight chair conformation. The value of the sum of the internal angles of the ring is 482.2°; this value is much closer to 360° (planar structure) than to 657° (perfect chair conformation). The atoms O4w and symmetrical related atom O4w(i) lie 1.76(1) Å out (below and above, respectively) of the plane defined by the other four water molecules (O2w, O3w, O2w(i), O3w(i)). The distances and angles in (**21**) are in agreement with reported examples that include this type of water cyclic architectures.[97,103,120] A perspective of two basic units of the water polymer is depicted in Figure 68.

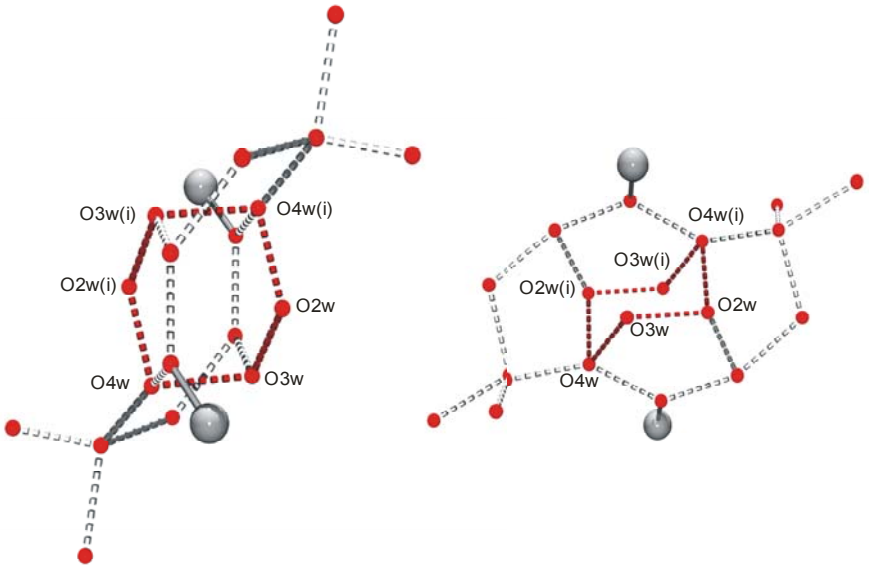

Figure 68: *Top view of the cyclic water hexamer structure in (**21**) (left). Side view of the cyclic water hexamer structure showing its chair conformation (right).*

Probably, one of these water molecules corresponds to the $(OH^-)_{0.5}$, but it is very difficult to distinguish between a water molecule and a hydroxyl group, because these molecules are continuously moving in the crystal structure. The

distance between O6w and O7w is very short. It could be possible, that one of these oxygen atoms in fact represents a hydroxide rather than a water molecule.

The ^{1}H NMR spectrum of [Pt(1-MeC-*N3*)$_3$(OH)]$^+$ (**21**) (Figure 69) bears no peculiarities. There are two sets of inequivalent cytosine ligands of 2:1 ratio. The chemical shifts of cytosine H6 and H5 doublets, in position *trans* to the hydroxo ligand, are 7.43 and 5.89 ppm. However, the chemical shifts of H6 and H5 of the cytosines *cis* to OH are 7.54 and 5.96 ppm respectively. Two different sets of methyl groups can be likewise observed, at 3.41 (for 1-MeC *cis* to OH group) and 3.35 ppm (for 1-MeC *trans* to OH group).

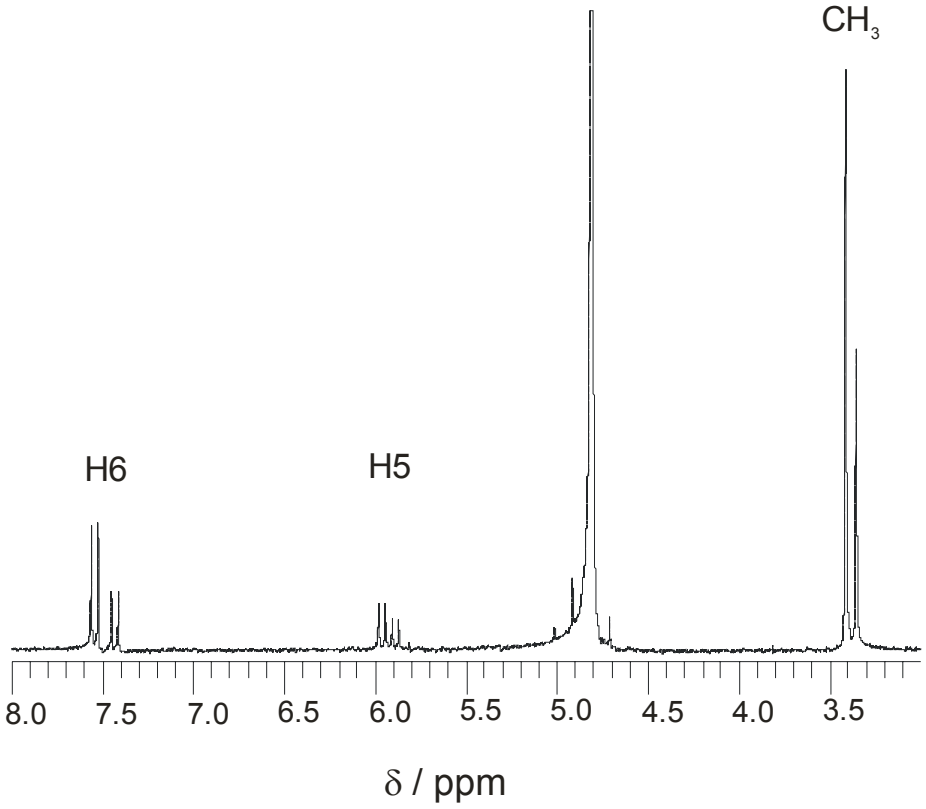

Figure 69: ^{1}H NMR spectrum of [Pt(1-MeC-*N3*)$_3$(OH)](ClO$_4$)$_{0.5}$(OH)$_{0.5}$·7H$_2$O (**21**) (D$_2$O, pD ~ 7.1)

The pH dependence of (**21**) was measured (Figure 70). The first pK_a value corresponds to the deprotonation of the aqua ligand and it was found to be in water pK_a = 5.72 ± 0.06. This value agrees with the one calculated for the acidity of the aqua ligand in the complex *cis*-[(NH$_3$)$_2$Pt(1-MeC-*N3*)(H$_2$O)]$^{2+}$

(Chapter 2.8). The second deprotonation step begins at pD 12 and corresponds to the loss of one proton of the NH_2 of the cytosine nucleobase.

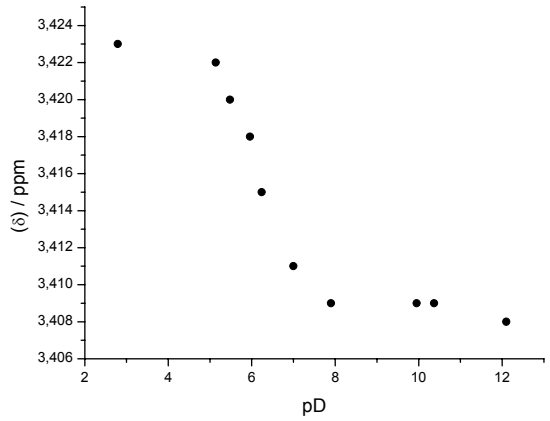

Figure 70: *Representation of the chemical shifts of H5 of the 1-methylcytosine in (**21**) in dependence of pD.*

2.6 1,9-DimeAH$^+$ System

Methylation of the N1 site of 9-methyladenine acidifies the protons of the exocyclic amino group considerably. Thus, the pK_a of the cationic 1,9-DimeAH$^+$ is 9.1[129] as compared to 16.7 for neutral 9-MeA[18] (Figure 71). As expected, metal coordination to N7 of 1,9-DimeAH$^+$ acidifies the N(6)H_2 group further. 1,9-DimeA is a model of the corresponding nucleoside, which occurs in its protonated form (1,9-DimeAH$^+$) as a rare base in tRNAs[130] and occasionally in rRNAs.[131] It is known that there is a difference between deprotonation of the cationic 1,9-dimethyladeninium cations in the here described complexes and deprotonation of the neutral ligand 9-methyladenine. However, this difference is a formal one only, as both the methyl group at N1 and the metal binding to this site are causing an acidification of the exocyclic NH_2 group. The effect is only larger in the case of methylation (ΔpK_a = 16.7 – 9.1 = 7.6) as compared to platination (ΔpK_a ~ 4[37]), thus leading to a shift of qualitatively identical processes from strongly alkaline medium (Pt(9-MeA-*N1*), pK_a = 12 – 13) to less alkaline medium (1,9-DimeAH$^+$, pK_a = 9.1). In both instances, binding of

(additional) Pt^{II} at N7 reduces these pK_a values further, by approximately identical 3 log units. Moreover, the steric situations (possibility of formation of an intramolecular hydrogen bond) in both cases are closely similar.

As previously shown[132], the two pK_a values of *trans*-[$(NH_3)_2$Pt(1,9-DimeAH-*N7*)$_2$]$^{4+}$ are 4.1 ± 0.2 and 6.4 ± 0.3.

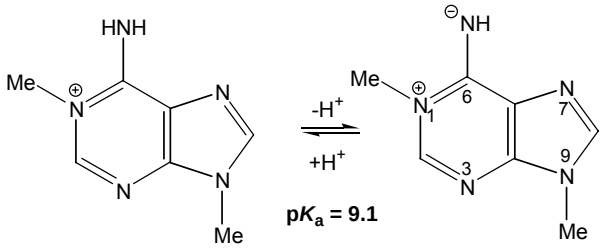

Figure 71: *pK_a value of 1,9-DimeAH$^+$.*

Two forms of the bis(1,9-DimeA) complex of *trans*-$(NH_3)_2Pt^{II}$ containing Pt^{II} bonded to N7 with different protonation states of the adenine ligands have been prepared and characterized by ^{1}H NMR spectroscopy: *trans*-[$(NH_3)_2$Pt(1,9-DimeAH-*N7*)(1-MeC-*N3*)]$(NO_3)_3$ (**22**) and *trans*-[$(NH_3)_2$Pt(1,9-DimeAH-*N7*)(9-MeGH-*N7*)]$(NO_3)_3$ (**23**).

2.6.1 pK_a values of *trans*-[$(NH_3)_2$Pt(1,9-DimeAH-*N7*)(1-MeC-*N3*)]$(NO_3)_3$ (22)

pK_a values of the mixed 1,9-dimethyladeninium, 1-methylcytosine complex (**22**) were determined by pD dependent ^{1}H NMR spectroscopy. There were several problems associated with this method, as in part previously reported.[132] First, due to 1,9-DimeA(H) rotation, all proton resonances of this ligand are considerably broadened, in particular at pD values where deprotonation of the 1,9-DimeAH$^+$ ligand takes place. Second, Pt^{II} migration was a serious problem even at pD ~ 5. Third, isotopic exchange of the

heteroaromatic protons took place, causing disappearance of the respective resonances. However, the presence of a second nucleobase (in this case 1-MeC) also proved advantageous, because (de)protonation reactions of 1,9-DimeA(H) were sensed by these ligands as well. $\Delta\delta$ values were considerably smaller though.

Compound (**22**) was studied in the pD range 1.5 – 12.5. Determination of the acidity of the 1,9-DimeAH$^+$ ligand was straightforward, giving an average value of 6.84 ± 0.05 (D_2O), corresponding to 6.29 ± 0.05 in H_2O for the four resonances of the 1,9-DimeA(H) ligand. An intramolecular hydrogen bonding between N(6)H_2 of 1,9-DimeAH and the exocyclic amino group of the cytosine should be possible (Figure 72). No deprotonation of the exocyclic amino group of the 1-MeC ligand was observed up to pD 10. However, a major rearrangement took place when a sample of (**22**) was kept at this pD for some time. This process will be discuss in the next chapter.

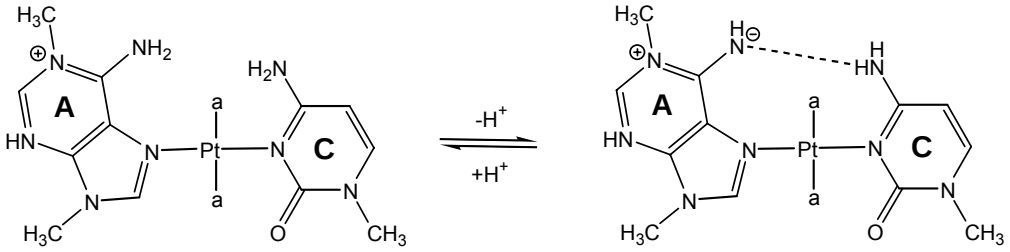

Figure 72: *Intramolecular hydrogen bond between NH$^-$ of 1,9-DimeA and the exocyclic amino group of 1-methylcytosine in the deprotonated form of (**22**).*

2.6.2 pK_a values of *trans*-[$(NH_3)_2$Pt(1,9-DimeAH-*N7*)(9-MeGH-*N7*)]$(NO_3)_3$ (23)

Compound (**23**) has been prepared on a small scale. pD dependent ^{1}H NMR spectra for the individual nucleobase resonances gave a pK_a value of 7.16 ± 0.06 in H_2O. This can be considered as an average of two

pK_a values. Here two pK_a values are expected, one of the exocyclic amino group of the adenine and the other one due to the deprotonation at N1 of the guanine ligand. Probably, the difference between both of them is so small, that more data points are needed to get individual pK_a values. Even then the possibility of a tautomer equilibrium must not be overlooked. Due to the appearance of new resonances the spectra become very complicated, however.

In comparison with the complex *trans*-[$(NH_3)_2$Pt(1,9-DimeAH-*N7*)(1-MeC-*N3*)]$(NO_3)_2$ (**22**), here no stabilization of the 1,9-DimeA ligand by hydrogen bonding is expected in the deprotonation form of (**23**) (Figure 73).

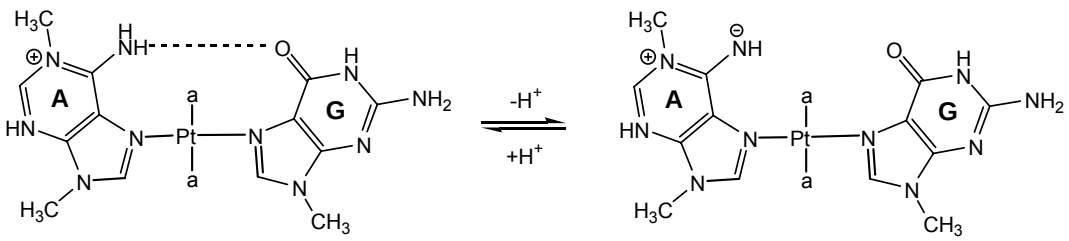

Figure 73: *No stabilization of deprotonated 1,9-DimeA ligand by intramolecular hydrogen bonding.*

2.6.3 Migration of CH_3 in 1,9-DimeAH$^+$ and Dimroth Rearrangement

In the course of our studies with 1,9-DimeAH$^+$ complexes, we frequently observed changes in the ^{1}H NMR spectra when the solution was kept for some time. As X-ray crystallography shows, these new signals are due to species arising from a “migration” of the methyl group from the N1 position to the N6 position to give 1,9-dimethyladeninium. This process is called Dimroth-rearrangement.[133] The basis of the mechanism of this reaction is shown in

Figure 74. It concerns here a relocation, in which under ring opening the N1 and N6 atoms exchange their positions. The reaction can be already introduced in weakly alkaline solution by the attack of a hydroxyl ion on the C2 atom. It can be used to produce N6-alkylated derivates of adenine.[134]

Details of this process applied to compounds (**22**) and (**23**) are reported below.

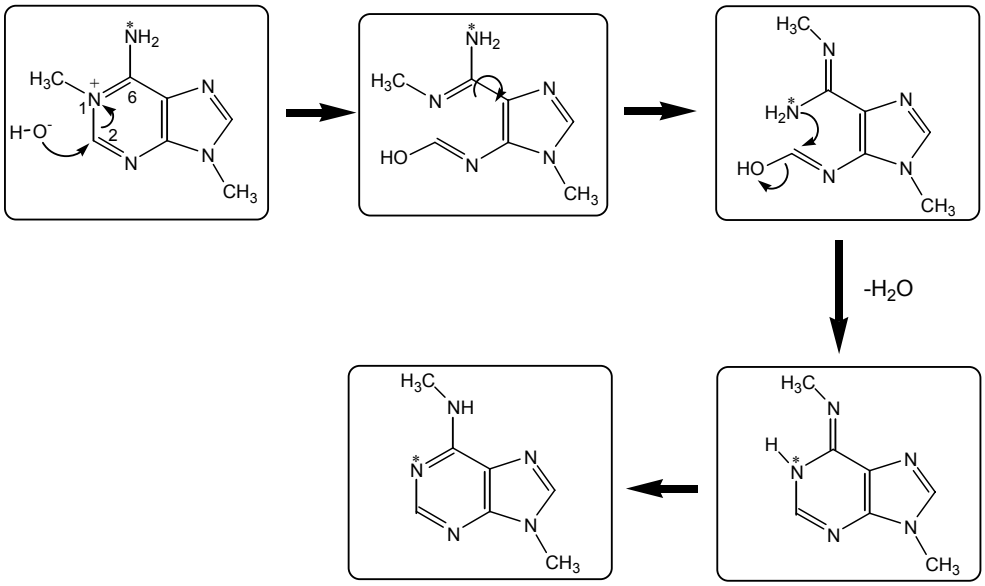

Figure 74: *Mechanism of the process Dimroth-rearrangement.*

This type of reaction involves hydrolytic cleavage of the N1–C2 bond, followed by rotation and recyclization. As, verified by ^{15}N labelling, the endocyclic nitrogen N1 bearing the alkyl group becomes the exocyclic N6 atom.[135]

2.6.3.1 Possibility of Migration in *trans*-[$(NH_3)_2$Pt(1,9-DimeAH-*N7*)(1-MeC-*N3*)]$(NO_3)_3$ (22)

The determination of the acidity constant for the deprotonation of the NH_2 position of 1,9-DimeA has been described in Section 2.6.1. In the course of the determination of this pK_a value, we noticed new signals, which have been assigned to different migration processes. As an example for the change of the

chemical shifts of the methyl groups and the appearance of new signals, a stackplot of the resonances in the aliphatic region of the ^{1}H NMR spectra of the *trans*-[$(NH_3)_2$Pt(1,9-DimeAH-*N7*)(1-MeC-*N3*)]$^{3+}$ (**22**) system at different reaction times is shown in Figure 75.

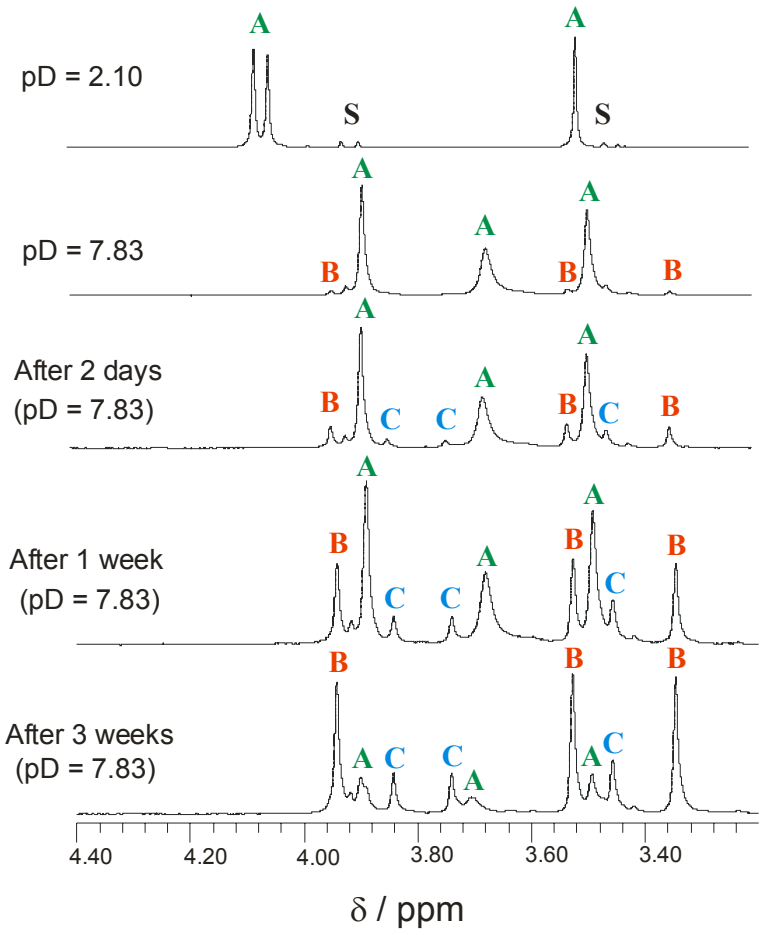

Figure 75: *Stackplot of the methyl group signals of (**22**) in D_2O at different pD values after different periods of time. A = trans-[$(NH_3)_2$Pt(1,9-DimeAH-N7)(1-MeC-N3)]$^{2+}$ (**23**); B = trans-[$(NH_3)_2$Pt(6,9-DimeA-N7)(1-MeC-N3)]$(NO_3)_2$ (**24**); C = not determined; **S** = starting compound 1,9-DimeAH$^+$.*

From pD = 2.10 to pD = 7.83 the signals corresponding to the methyl groups of the adenine, undergo upfield shifts with increasing pD. At pD = 2.10, the chemical shift difference between the CH_3-N9 and CH_3-N1 resonances is very small. However, at pD = 7.83 these resonances are more clearly separated.

It should be noted, that the resonance of the methyl group of the cytosine remains in the same region (~ 3.5 ppm). This is because the first deprotonation step corresponds to the deprotonation of the NH_2 of the adenine.

Another observation, which has been made after two days, is the appearance of new signals (C). This finding, which occurs at pD ~ 5 and higher, clearly indicates that new compounds are formed. Two different sets of signals are observed. We attribute these resonances to the migration of the *trans*-$(NH_3)Pt^{II}$ entity (compound C) and to the migration of the methyl group from N1 to N6 (compound B). Several NMR experiments have been carried out at different pD values and these indicate that the migration of the methyl group takes place first. After three weeks, the resonances of the starting compound have almost disappeared, whereas the resonances of the new compound (B) have increased in intensity.

In oder to determine if this interpretation is correct, it was decided to react 6,9-DimeA with *trans*-$[(NH_3)_2Pt$(1-MeC-*N3*)Cl$](NO_3)$.

2.6.3.2 *trans*-$[(NH_3)_2Pt$(6,9-DimeA-*N7*)(1-MeC-*N3*)$](NO_3)_2$ (24)

One equivalent of $AgNO_3$ was added to *trans*-$[(NH_3)_2Pt$(1-MeC-*N3*)Cl$]^+$, in oder to obtain the aqua species. After removal of AgCl, one equivalent of 6,9-DimeA was added. The mixture was kept at 40°C for three days. Crystals of (**24**) suitable for X-ray crystal structure analysis were obtained by slow evaporation of the solvent at 4°C. Complex (**24**) crystallizes in the monoclinic P2/n space group (see X-ray Table A-7). X-ray crystallography reveals the presence of two nitrate ions.

The solid state structure of (**24**) consists of a platinum atom coordinated to the N3 atom of the 1-methylcytosine and to the N7 atom of the 6,9-Dimethyladenine in a square-planar coordination geometry, with no observable distortions. A view of the *trans*-$[(NH_3)_2Pt$(6,9-DimeA-*N7*)(1-MeC-*N3*)$]^{2+}$ cation is

depicted in Figure 76. The angles between the platinum atom and the respectively *trans*-positioned ligands are nearly 180°: N7A-Pt-N3B, 176.5(5)° and N11-Pt-N12, 177.1(5)°. The Pt, N11 and N12 atoms are situated below (-0.005(5), -0.052(6) and -0.052(6) Å, respectively) and the N7A and N3B above (0.055(6) and 0.053(6) Å, respectively) the platinum coordination plane, with a r.m.s. eviation of 0.048. Pt-N distances range from 1.985(12) to 2.060(12) Å. A list of selected distances and angles between atoms of *trans*-[$(NH_3)_2$Pt(6,9-DimeA-*N7*)(1-MeC-*N3*)]$(NO_3)_2$ (**24**) is given in Table 16.

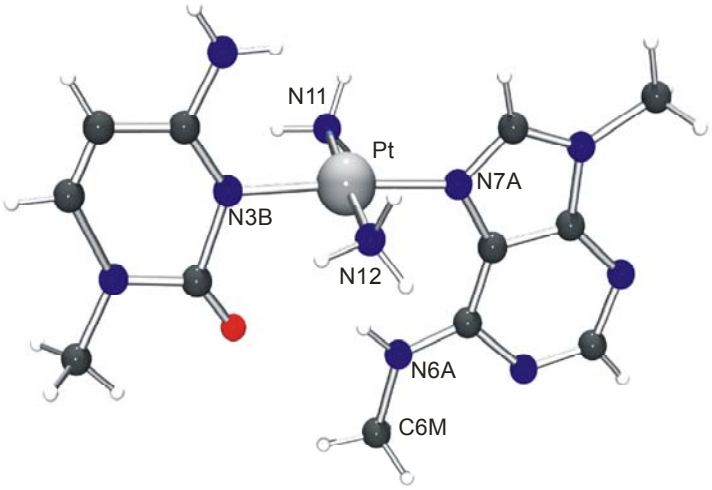

Figure 76: *X-ray structure of the cation trans-[$(NH_3)_2$Pt(6,9-DimeA-N7)(1-MeC-N3)]$^{2+}$ (**24**).*

Table 16: *Selected distances (Å) and angles (°) for non-hydrogen atoms in **24**.*

Pt-N7A	1.985(12)	N7A-Pt-N3B	176.5(5)
Pt-N3B	2.014(13)	N7A-Pt-N11	88.4(5)
Pt-N11	2.050(12)	N3B-Pt-N11	92.3(5)
Pt-N12	2.060(12)	N7A-Pt-N12	90.5(5)
N6-C6	1.328(17)	N3B-Pt-N12	89.0(5)
N6-C6M	1.418(17)	N11-Pt-N12	177.1(5)
		C2A-N1A-C6A	119.5(13)
		C8A-N7A-C5A	103.5(13)

C8A-N7A-Pt	130.2(11)
C5A-N7A-Pt	126.2(10)
C4B-N3B-C2B	120.5(15)

The adenine base bonded via N7 to the platinum atom presents normal distances and angles between atoms. The atoms of the 9-methyladenine base are coplanar, with a r.m.s. deviation of 0.018. The dihedral angle between the adenine ring and the platinum coordination plane is 89.9(3)°.The cytosine ligand in (**24**) has normal distances and angles between atoms. The two external Pt-N-C angles are significantly different: the Pt-N3B-C2B angle is 114.7(11)° and the Pt-N3B-C4B angle is larger, 124.8(11)°. This is a common feature of many 1-MeC compounds of Pt.[136] The atoms of the 1-methylcytosine base are coplanar, with a r.m.s. deviation of 0.015. The dihedral angle between the cytosine ring and the platinum coordination plane is 89.5(4)°. So both nucleobases are nearly perpendicular to the plane of Pt. As a consequence of this fact, an intramolecular hydrogen bond is observed in the cationic entity: O2B···N6A, 3.11(2) Å (Figure 77).

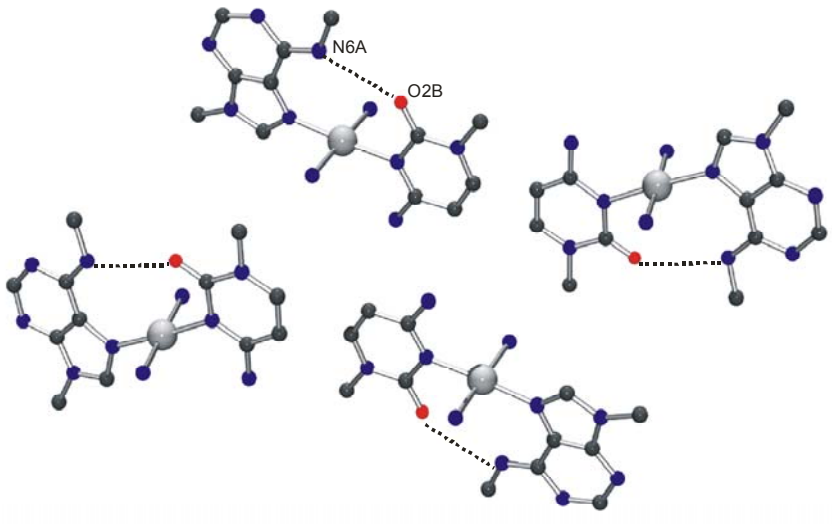

Figure 77: *View of the intramolecular (3.11 Å) H bonding.*

Complex (**24**) displays few intermolecular hydrogen bonds only. The exocyclic amino group N4B of the cytosine nucleobase of the cation of (**24**) forms hydrogen bonds only with the oxygen atom of one nitrate anion. The water molecule is bonded to another oxygen of this nitrate: N4B(H4B)···O23, 2.941 Å, and O22···O1w, 2.871 Å (Figure 78).

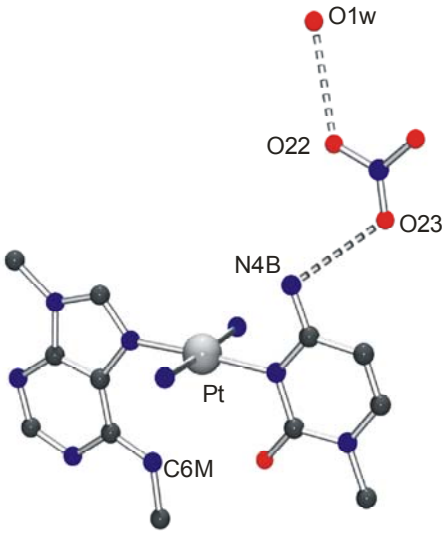

Figure 78: *Intermolecular hydrogen bonds in (**24**).*

^{1}H NMR spectra of (**24**) were recorded. In aqueous solution, the spectrum displays two sets of doublets in a 1:1 ratio in the aromatic region (H6 and H5 protons of 1-MeC) as well as a singlet corresponding to the methyl group of 1-MeC. The resonances corresponding to H8, H2, CH_3-N1 and CH_3-N9 are well separated (Figure 79). Chemical shifts of the signals are at 8.56 ppm (H8), 8.44 ppm (H2), 7.69 ppm (H6), 6.09 ppm (H5), 3.53 ppm (CH_3-N6), 3.94 ppm (CH_3-N9) and 3.35 ppm (CH_3-C) over a wide pH range. If we compare these chemical shifts with the ones for compound (B) in Section 2.6.3.1., they are identical (B = **24**).

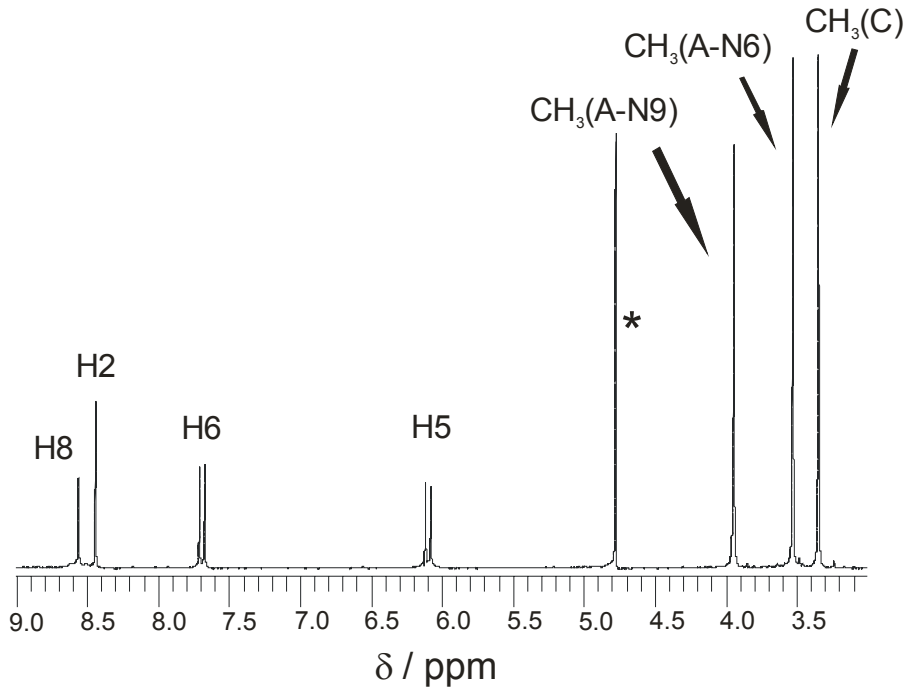

Figure 79: *^{1}H NMR spectrum of trans-[$(NH_3)_2$Pt(6,9-DimeA-N7)(1-MeC-N3)]$(NO_3)_2$ (**24**) in D_2O (pD ~ 6.3)(* = solvent).*

As expected, removal of the proton at the N1 (6,9-DimeA) position of the complex *trans*-[$(NH_3)_2$Pt(6,9-DimeA-*N7*)(1-MeC-*N3*)]$(NO_3)_2$ (**24**) produces lowfield shifts of the proton and methyl groups signals at strongly acidic pH values. The pK_a value of (**24**) (N1 position) was determined to be 2.07 ± 0.04 in D_2O, corresponding to 1.60 ± 0.04 in water. This value agrees well with the pK_{a1} value of the deprotonation of N1 of N7 platinated 9-MeAH$^+$.

A graphical representation of the pH dependence is depicted in Figure 80.

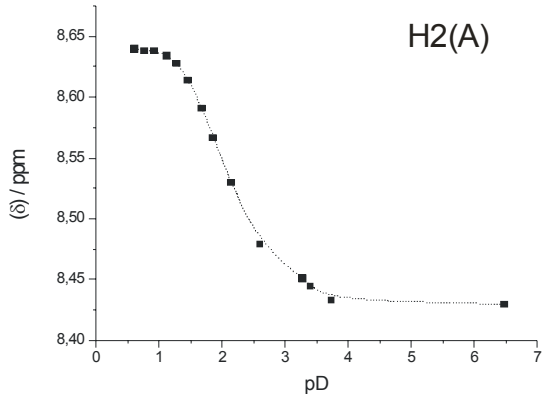

Figure 80: *Representation of the chemical shifts of H2 of the adenine ligand in trans-[(NH$_3$)$_2$Pt(6,9-DimeA-N7)(1-MeC-N3)](NO$_3$)$_2$ (**24**).*

2.6.3.3 Possibility of Migration in *trans*-[(NH$_3$)$_2$Pt(1,9-DimeAH-*N7*)(9-MeGH-*N7*)](NO$_3$)$_3$ (23)

Similar results were found for *trans*-[(NH$_3$)$_2$Pt(1,9-DimeAH-*N7*)(9-MeGH-*N7*)](NO$_3$)$_2$ (**23**). The determination of the acidity constant of (**23**) via pD dependent ^{1}H NMR spectroscopy was discussed in Section 2.6.2. Figure 81 shows several selected ^{1}H NMR spectra, which were taken at different pD values. In spectra with pD < 8 only two of the three resonances expected for the methyl groups are observed. At pD ~ 8.75 we observe the expected three resonances. With increasing pD, an increasing of number of new resonances can be observed. Formation of two novel compounds could account for this observation. On one hand, (B) could be a migration product of the methyl group from N1 to N6. On the other hand, (C) could be assigned to a migration product of the *trans*-(NH$_3$)$_2$Pt^{II} entity.

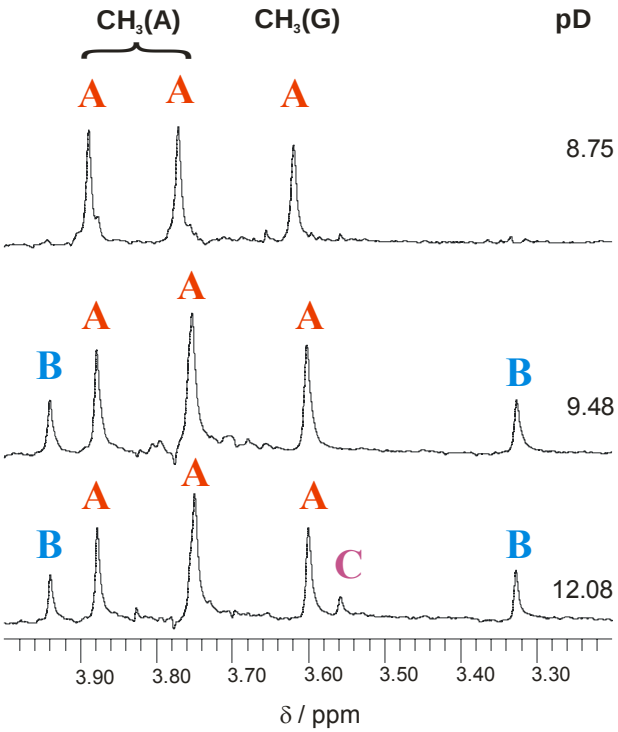

Figure 81: *Stackplot of the methyl group region of ^{1}H NMR spectra of (**23**) at different pD values.*

As can be observed, the resonances corresponding to the product, in which the methyl group has migrated, (B) appear before the (C) resonance.

2.6.3.4 *trans*-[$(NH_3)_2$Pt(6,9-DimeA-*N7*)(9-MeGH-*N7*)]$(NO_3)_2\cdot 5H_2O$ (25)

To prove that the signals of (B) correspond to the postulated product, 6,9-DimeA was reacted with *trans*-[$(NH_3)_2$Pt(9-MeGH-*N7*)(H_2O)]$^{2+}$.This reaction was successful as judged by the fact that the signals of product (**25**) corresponded to (B), consistent with methyl group migration from N1 to N6.

One equivalent of 6,9-DimeA and one equivalent of *trans*-[$(NH_3)_2$Pt(9-MeGH-*N7*)(H_2O)]$^{2+}$ were allowed to react at 40°C for three days. The solution was then kept in the refrigerator. Within one week, colourless crystals of *trans*-[$(NH_3)_2$Pt(6,9-DimeA-*N7*)(9-MeGH-*N7*)]$(NO_3)_2 \cdot 5H_2O$ (**25**) suitable for X-ray crystal structure analysis were obtained. The crystals were isolated and measured. The complex (**25**) crystallizes in the monoclinic P2(1)/c space group. Data for *trans*-[$(NH_3)_2$Pt(6,9-DimeA-*N7*)(9-MeGH-*N7*)]$(NO_3)_2 \cdot 5H_2O$ (**25**) were collected at room temperature. In the refinement process of the X-ray data, all non-hydrogen atoms of the crystal were refined anisotropically. The hydrogen atoms were placed at geometrical idealized positions and refined isotropically. Crystal data, data collection and refinement parameters for (**25**) are summarized in Table A-8 (see Appendix).

The solid state structure of (**25**) consists of a platinum atom coordinated to the N7 atom of the 9-methylguanine and to the N7 atom of the 6,9-Dimethyladenine in a square-planar coordination geometry, with no observable distortions. A view of the *trans*-[$(NH_3)_2$Pt(6,9-DimeA-*N7*)(9-MeGH-*N7*)]$^{2+}$ cation is depicted in Figure 82. The angles between the platinum atom and the four coordination sites are nearly 180°: N7G-Pt-N7A, 177.7(6)° and N11-Pt-N12, 177.4(5)°. The N11, N12 atoms are situated below (-0.041(7), -0.042(7) Å, respectively) and the Pt, N7A and N7G above (0.005(6), 0.039(7) and 0.039(7) Å, respectively) the platinum coordination plane, with a r.m.s. deviation of 0.036. Pt-N distances about the Pt center range from 1.990(14) to 2.061(14) Å. A list of selected distances and angles between atoms of *trans*-[$(NH_3)_2$Pt(6,9-DimeA-*N7*)(9-MeGH-*N7*)]$(NO_3)_2 \cdot 5H_2O$ (**25**) is given in Table 17.

Table 17: *Selected distances (Å) and angles (º) for non-hydrogen atoms in* ***25****.*

Pt-N7G	1.990(14)	N7G-Pt-N7A	177.7(6)
Pt-N7A	1.999(15)	N7G-Pt-N12	88.5(5)
Pt-N11	2.061(14)	N7A-Pt-N12	90.4(5)
Pt-N12	2.034(14)	N7G-Pt-N11	91.8(5)
N6A-C6A	1.39(2)	N12-Pt-N11	177.4(5)
N6A-C6M	1.48(2)	C8A-N7A-C5A	103.6(15)

C8a-N7A-Pt	125.5(13)
C5A-N7A-Pt	130.8(13)
C6A-N1A-C2A	119.2(17)
C2G-N1G-C6G	126.3(16)

The presence of two anions indicates that both nucleobases are neutral. Consequently, the N1 position of 6,9-DimeA is not protonated. The size of the internal ring angle C6-N1-C2 (119.2(17)°) is consistent with this view. Values for 6,9-DimeAH with protonated N1 positions have been previously published and were found to be between 122° $[(AH)_2](HPO_4)\cdot 2H_2O$[137] and 124.3º of $[AH](Br)\cdot ½H_2O$.[138]

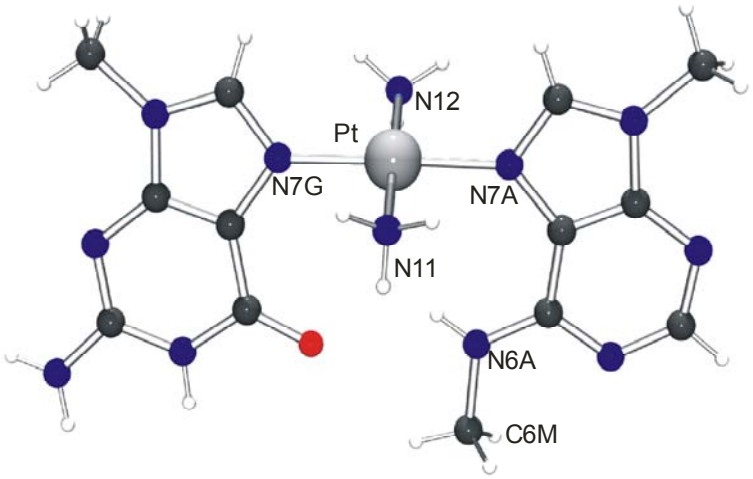

Figure 82: *View of the cation trans-$[(NH_3)_2Pt(6,9\text{-DimeA-N7})(9\text{-MeGH-N7})]^{2+}$ of* ***(25)***

The guanine base bonded via N7 to the platinum atom displays normal distances and angles between atoms. The atoms of the 9-methylguanine base are coplanar, with a r.m.s deviation of 0.020. The dihedral angle between the guanine ring and the platinum coordination plane is 65.0(3)°. The atoms of the adenine base are also practically coplanar (r.m.s. deviation, 0.011). The dihedral angle between the adenine ring and the plane containing the Pt is 73.1(3)°. There is one intramolecular hydrogen bond observed (Figure 83). This bond

takes place between the exocyclic O6 of 9-MeGH and the N6H of 6,9-DimeA. The distance between both atoms is 2.93(2) Å. There are also intermolecular hydrogen bonds, e.g. between guanine bases, giving rise to pairs of H bonds between N2G and N3G sites: The N2G(H2G)···N3Ga(-x, -y+1, -z+1), 3.02(2) Å and N3G···N2Ga(H2Ga)(-x, -y+1, -z+1), 3.02(2) Å (Figure 83). These hydrogen bonds have been also observed in other strucutres.[139]

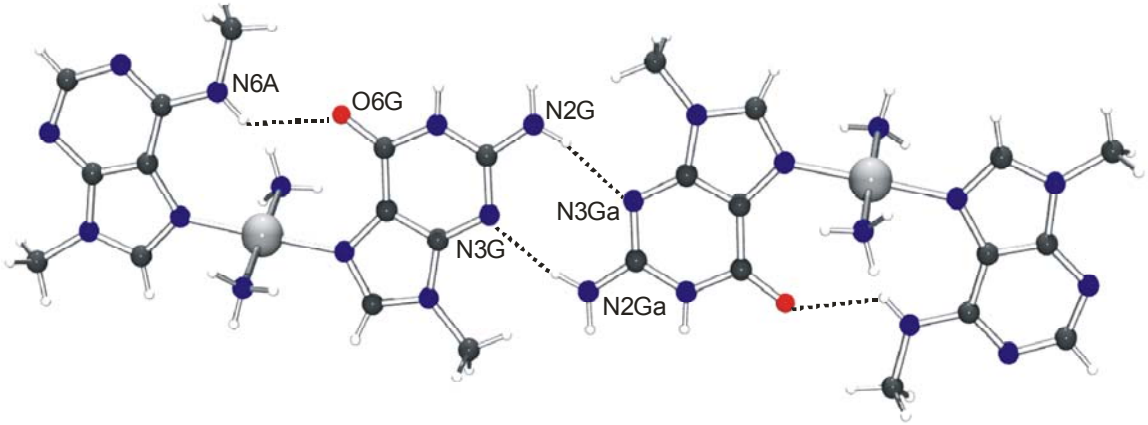

Figure 83: *View along the b axis of the packing of the cation of (**25**). Intramolecular N6A(H)···O6G and intermolecular N2G(H)···N3G hydrogen bonds are observed.*

The crystal structure also contains five water molecules of crystallization and two nitrate anions.

Crystal packing of (**25**) is based on interactions between the *trans*-[$(NH_3)_2$Pt(6,9-DimeA-*N7*)(9-MeGH-*N7*)]$^{2+}$ cation and the nitrate counter anions. As shown in Figure 84, the oxygen atoms of NO_3^- in the crystal structure are implicated in hydrogen bonding with N1G and N2G of the guanine base, and one of the ammine ligands (N12) of the platinum.

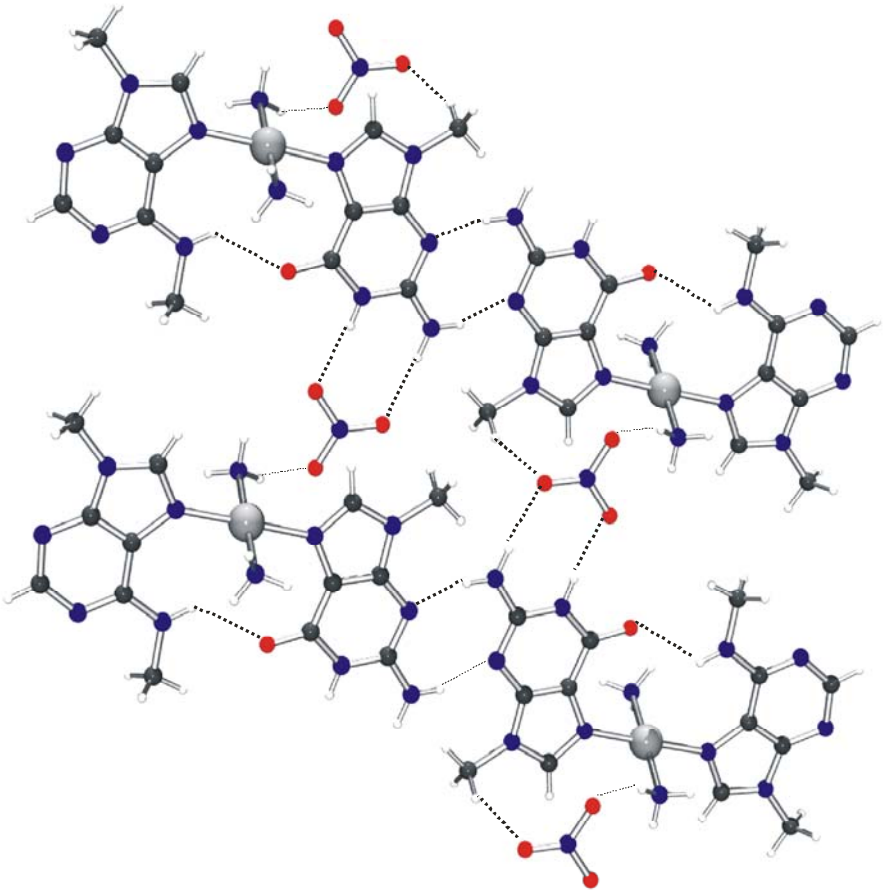

Figure 84: *Intermolecular hydrogen bonds in (**25**).*

A ^{1}H NMR spectrum of (**25**) was recorded. In aqueous solution, the spectrum displays two singlets corresponding to the methyl group of guanine and its H8 proton as well as singlets corresponding to H8, H2, CH_3-N1 and CH_3-N9 of the adenine (Figure 85). Chemical shifts of the signals are at 8.43 ppm (H8-A), 8.33 ppm (H8-G), 8.67 ppm (H2), 3.78 ppm (CH_3-N6), 3.94 ppm (CH_3-N9) and 3.32 ppm (CH_3-G) over a wide pH range. If we compare these chemical shifts with the ones for compound (B) in Section 2.6.3.3., they are identical, thereby confirming the interpretation made above.

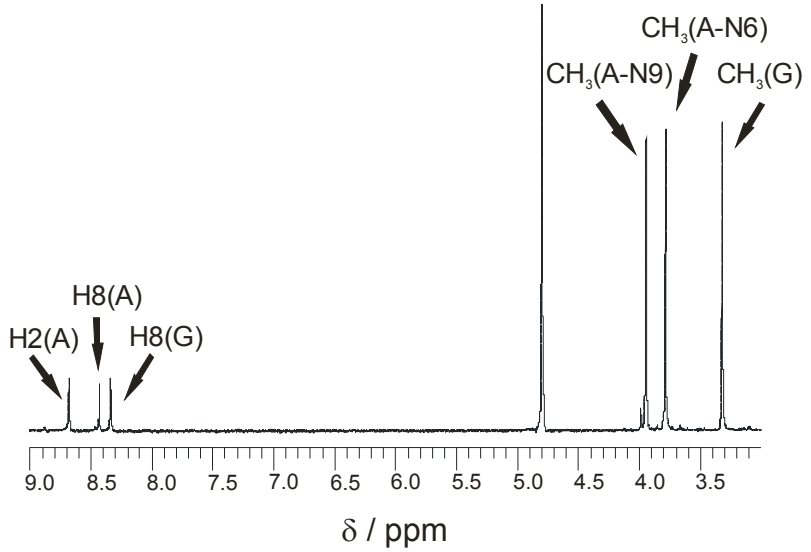

Figure 85: *^{1}H NMR spectrum of (**25**) in D_2O (pD ~ 6.4).*

2.7 1-MeC System

As demonstrated before in the case of Pt^{II} adenine compounds [17,37,132], suitably positioned hydrogen bond donor groups can stabilize the deprotonated amino group of a nucleobase and thus lower the apparent pK_a of the amino group. When comparing pK_a values of a nucleobase in dependence of the other ligands around the metal centers, it is helpful to reduce the variables as much as possible. Thus, in compounds of type *trans*-$(NH_3)_2Pt$(nucleobase)X (with X = second nucleobase or other ligand) the influence of a NH_3 ligand bound to Pt^{II} available to form a H bond, can be considered constant to a first approximation. Furthermore, keeping the charges of the compounds to be compared identical (e.g. +2) minimizes the effects of different charge. Finally, if the two *trans*-positioned ligands (nucleobase and X) do not differ too much in their *trans* influence, as should be the case with heterocyclic N-donors, we propose that any significant shifts in pK_a values of the nucleobase are to be attributed primarily due to intramolecular interactions between the nucleobase and X. In the following, this idea will be examined for the types of complexes with the *trans*-$(NH_3)_2Pt^{II}$ moiety, namely for *trans*-$[(NH_3)_2Pt$(1-MeC-*N3*)X$]^{2+}$.

The pK_a value of the exocyclic amino group of 1-methylcytosine has been reported to be 16.7.[18] Coordination of $(NH_3)_3Pt^{II}$ to the N3 position acidifies the N(4)H_2 group to pK_a = 12.9 (H_2O).[136]

With all 1-MeC compounds studied here, ^{1}H NMR spectroscopic complications occur at high pD (≥ 12) with time. These are due to a deamination reaction of the nucleobases, during which 1-methylcytosine is converted into 1-methyluracilate.[136,140] With the adenine containing complex *trans*-[$(NH_3)_2$Pt(1-MeC-*N3*)(9-MeA-*N7*)]$(ClO_4)_2$ (**27**) a similar deamination to give hypoxanthine is feasible [141], in addition to the possibility of Pt^{II} migration.[25,66,67]

2.7.1 *trans*-[$(NH_3)_2$Pt(1-MeC-*N3*)$_2$]$^{2+}$ (26)

trans-[$(NH_3)_2$Pt(1-MeC-*N3*)$_2$]$^{2+}$ (**26**) exists in aqueous solution in an equilibrium of *head-head* (*hh*) and *head-tail* (*ht*) rotamers, with the latter predominating 3:1.[142,143] The first deprotonation step of (**26**) was followed by ^{1}H NMR spectroscopy in D_2O solution.

trans-[$(NH_3)_2$Pt(1-MeC-*N3*)$_2$]$^{2+}$ ⇋ *trans*-[$(NH_3)_2$Pt(1-MeC$^-$-*N3*)(1-MeC-*N3*)]$^+$ + H^+

26

Separate H5 and H6 doublets for the two rotamers were detected throughout the pD range 7-13, whereas no separate signals were seen for the N(1)CH_3 singlet. Agreement between pK_a values obtained for the most intense signal sets N(1)CH_3, H(5)(*ht*), H(6)(*ht*) was excellent, values being 13.04, 13.04, and 13.02 (D_2O), giving an average of 13.03 in D_2O and 12.39 in H_2O, with a standard deviation of ± 0.07. For the minor rotamer agreement was less good, 13.01 (H5) and 12.90 (H6) in D_2O.[144] Although, in principle, a lower pK_a could have been expected for the *hh* rotamer, we do not consider this difference significant. The separation between the exocyclic N(4) sites in the *hh* form,

which is estimated to be around 4 Å, is certainly too large to expect any substantial interaction between these groups. Moreover, if important, the possibility of favorable interaction between -NH^- and -NH_2 probably would have caused a shift in the rotamer equilibrium toward the *head-head* form, a feature not seen in the experiments (Figure 86).

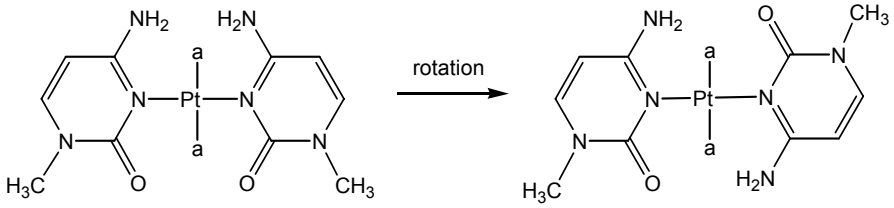

head-head ***head-tail***

Figure 86: *Rotamers (hh = head-head; ht = head-tail) of (**26**).*

Although for [(dien)Pt^{II}(1-MeC-*N3*)]$^{2+}$ we have reported also migration to N4 under conditions of high pH, with *trans*-[$(NH_3)_2$Pt(1-MeC-*N3*)$_2$]$^{2+}$ (**26**) such a process is not observed at room temperature.

2.7.2 *trans*-[$(NH_3)_2$Pt(9-MeA-*N7*)(1-MeC-*N3*)]$^{2+}$ (27)

Compound (**27**) has previously been crystallized as its ClO_4^- salt.[49] pD dependent ^{1}H NMR spectra for the individual nucleobase resonances gave pK_a values of 12.7 each for N(1)CH_3, H5, and H6 resonances of 1-MeC. Despite considerably smaller shifts, rather similar values were obtained for N(9)CH_3 and H2 resonances of the 9-MeA ligand (12.6 and 12.7), but the H8 resonance of 9-MeA (δ 8.64 at pD 6[49]) could not be evaluated due to rapid isotopic exchange. The average pK_a of (**27**), converted from D_2O to H_2O, is thus 12.0 ± 0.1 (Figure 87).

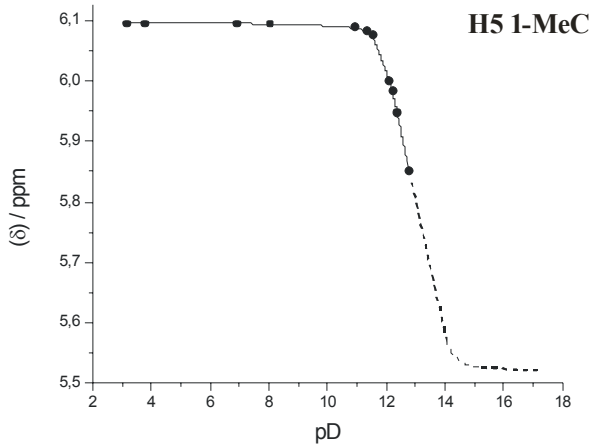

Figure 87: *pD dependence of the H5 resonance of the 1-MeC of (**27**).*

The experimental values are represented by the solid line, and the dotted line corresponds to calculated values based on a fitting of the pD dependence.
A comparison of the extent of upfield shifts of the individual proton resonances reveals that 1-MeC resonances are much more affected than those of 9-MeA: $\Delta\delta$ values (in ppm) in the pD range 7 - 12.8 are 0.38 (H6, 1-MeC), 0.24 (H5, 1-MeC) and 0.12 (CH_3, 1-MeC), as compared to 0.02 (H2, 9-MeA) and 0.01 (CH_3, 9-MeA). This finding strongly suggests that it is the cytosine nucleobase which undergoes deprotonation, rather than the adenine. We considered the existence of a tautomeric equilibrium between two species containing deprotonated cytosine and deprotonated adenine, with the former dominating, but were unable to prove such a possibility by applying Raman spectroscopy, for which characteristic differences between ring modes of the individual tautomers could have been expected. ^{1}H NMR spectra of (**27**) recorded at different pD values are shown in Figure 89. As can be seen, at pD ~ pK_a there is a definite broadening of all three 1-MeC resonances, whereas the 9-MeA resonances remain sharp. We propose that this feature is due to a dynamic process, viz. ligand rotation in order to accomplish intramolecular H bonding between –NH^- of 1-MeC^- and -NH_2 of 9-MeA (Figure 88).

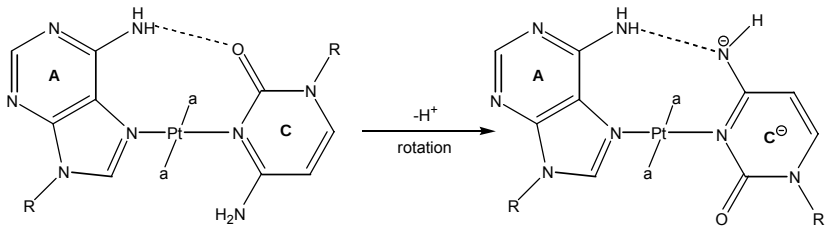

Figure 88: *Ligand rotation in order to favour intramolecular hydrogen bond between the exocyclic amino group of the 9-MeA and the –NH¯ of 1-MeC¯ in (**27**).*

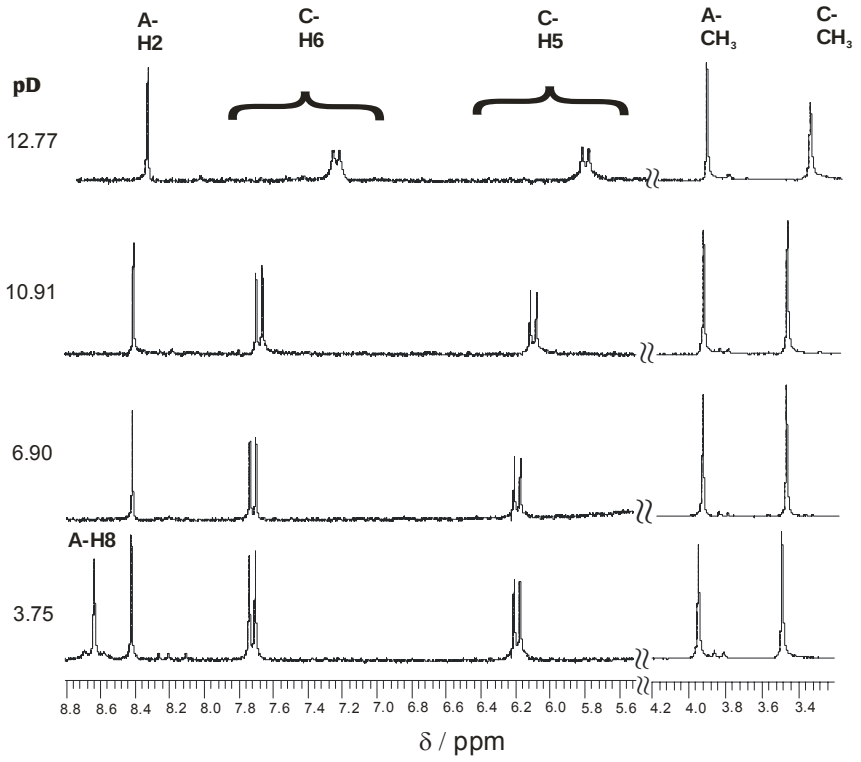

Figure 89: *^{1}H NMR spectra of (**27**) recorded at different pD values.*

2.8 Solvent Effects

It is well established that acid-base equilibria and consequently pK_a values can change considerably with variations of the environment, for example, the polarity and dielectric constant of the solvent, solvation properties, and others. This aspect is of particular significance in biological processes that occur at the interface of water and biomolecule aggregates. For example, variations in pK_a values of amino acid side chains in proteins as well as local conditions in the active site of enzymes have been intensely studied for this reason.[145] Differences in pK_a values of identical amino acid side chains are observed in the denatured and unfolded state of proteins, which provide qualitative information concerning electrostatic interactions in this state.[146] Similarly, pK_a values of acid-base indicators fixed via molecular imprinting techniques in solid matrixes can be shifted within surprinsingly large boundaries as a consequence of different local environments.[147]

Regarding the reasons for variations in pK_a values,[148] it is helpful to differentiate between cationic, neutral, and anionic acids. In Figure 90, cases relevant to nucleic acids are depicted.

Variations in pK_a values of acids can be attributed to the reason, which is going to be discussed in this chapter: polarity of the environment. A strongly hydrophobic environment inhibits solvation and hence stabilization of the ionic conjugate bases in (II) and (III). Ionization is thus suppressed in these cases, and the pK_a values increase. On the other hand, the pK_a of the cationic acid (I) is expected to decrease, hence the cationic acid becomes more acidic, since the resulting conjugate base is uncharged.

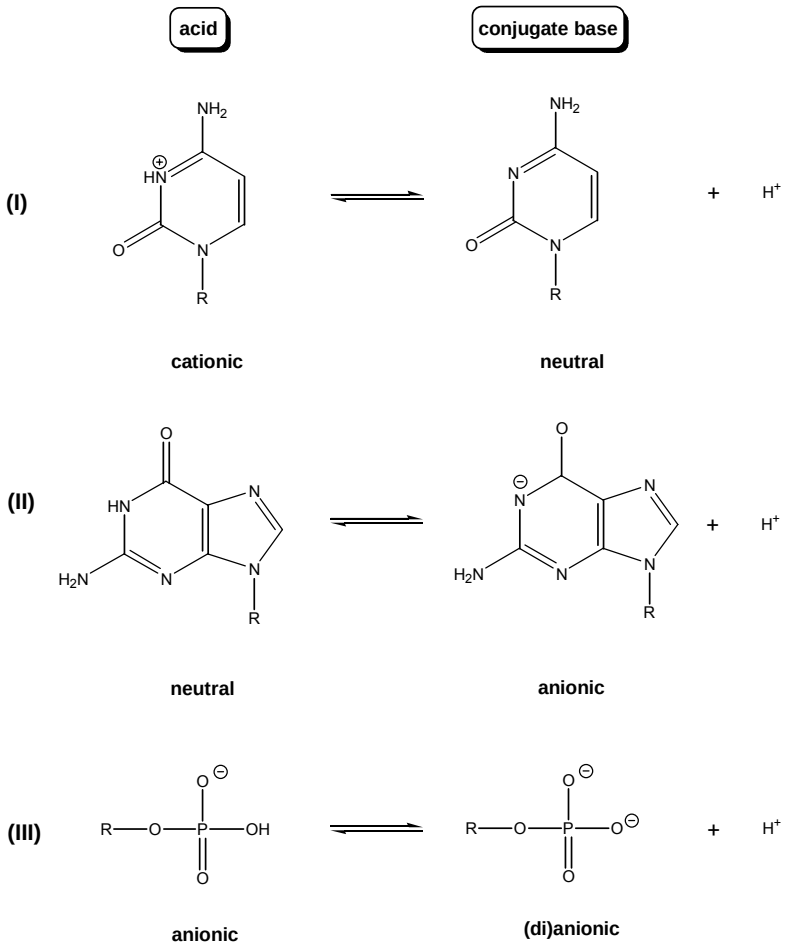

Figure 90: *Schematic representation of feasible acid-base equilibria of nucleobase components.*

The pK_{a1} value of the 9-methyladenine nucleobase has been determined in different solvents, in order to compare the resulting values. The pK_{a1} has been studied in H_2O as solvent, and the pK_a correponding to the deprotonation at N1 position was found to be 4.3[149] or 4.5.[150] When the N1 position of 9-MeA is protonated, the 9-methyladeninium (**A**) is a cation, so it acts as an acid and when it loses a proton, its conjugate base is neutral (**B**) (Figure 91).

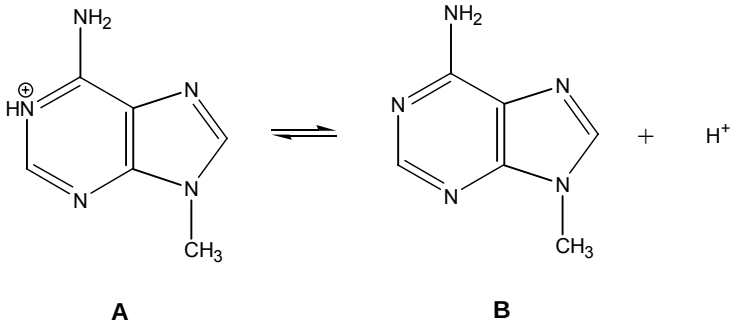

Figure 91: *Acid-base equilibria of 9-methyladenine.*

2.8.1 Mixture of Acetone and D_2O

To determine the pK_{a1} value of the 9-MeA in a mixture of acetone and deutered water, two different experiments were carried out. In the first one, the proportion acetone/D_2O was 20 to 80 and in the other case it was 80 to 20.

Water is a very polar solvent and it has a dielectric constant of 80.4.[151] Acetone is also a polar solvent, but less polar than water. Its dielectric constant is consequently lower than that of water and it has the value of 21.4.[151] As a result, when acetone is added to water, the dielectric constant of the medium decreases and the neutral 9-methyladenine is better solvated. As a consequence of the solvent mixture, the equilibrium is shifted to the right side, so the cationic specie (**A**) becomes more acidic, or in other words, the pK_a value becomes lower.

2.8.1.1 20% Acetone / 80% D_2O

The first experiment was performed with a mixture of acetone and D_2O in proportion 20 to 80 by volume. With protonated 9-methyladenine only one deprotonation step can be observed. This step at low pH refers to the deprotonation of the N1H site of the 9-methyladeninium ion. The second one, at higher pH, is due to the deprotonation of the exocyclic amino group. However,

the latter one cannot be observed as it occurs at pH>14. The ^{1}H NMR resonances of the methyl group situated at N9, of the H8 and of the H2 were measured in dependence on pD. The NMR data for each proton were evaluated by a curve-fitting procedure based on equation (2) (see Section 2.1) by taking the deprotonation step into account as can be seen in Figure 92. The individual pK_a value calculated from the different protons is given in Table 18. The final result for the deprotonation step is then obtained by calculating the mean of the mentioned individual results, giving eventually p$K_{a/D_2O,av}$.

Table 18: *Negative logarithmus of the acidity constant (pK_a) of 9-MeA in a solution 80% D_2O and 20% Acetone.*

	pK_{a/D_2O} determined from the shift of				p$K_{a/D_2O,av}$		p$K_{a/H_2O,av}$	
	CH_3		H2		H8			
$N1H^+$	4.27 ±	.0.09	4.21 ±	.0.06	4.23 ±	.0.07	4.24 ±	0.07	3.73 ±	0.07

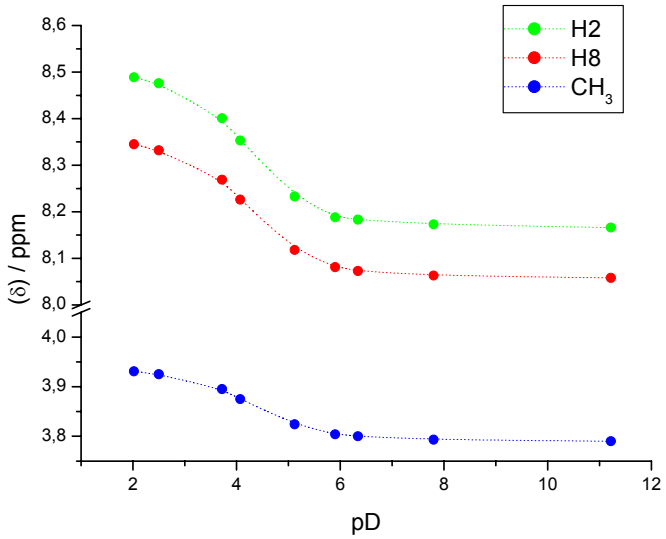

Figure 92: *pH dependence of the ^{1}H chemical shifts of 9-MeA in the pD range from 2 to 11.*

One can observe that the shift difference for H2 is the largest ones, i.e. $\Delta\delta$ = 0.323 ppm, while that for H8 is $\Delta\delta$ = 0.287 ppm and that of the methyl group is $\Delta\delta$ = 0.141 ppm. This result seems most reasonable because H2 is on the one hand spatially close to the N1 site, and on the other hand, it is also part of the aromatic purine system. Therefore the deprotonation of N1H is also more strongly reflected, whereas the methyl group protons are at the aliphatic side chain and thus are less exposed to the acid-base reaction at the purine ring.

Finally, the $pK_{a/D_2O,av}$ values determined in D_2O were also converted to aqueous solution by applying equation (3) giving the result:

$$pK_{9\text{-MeAH}} = 3.73 \pm 0.07$$

This result is in agreement with expectations, according to which a lower pK_a value is expected with acetone added.

2.8.1.2 80% Acetone / 20% D_2O

The acidity constant for the deprotonation of the N1H position of the 9-methyladenine in a solution of a mixture of acetone and D_2O in a ratio 80:20 was also determined via pD dependent ^1H NMR measurements in D_2O. The resonances of H8 as well as of H2 and of the aliphatic protons of the methyl group at N9 were used for the determination (Figure 93). The individual pK_a values calculated from the different protons are given in Table 19. The final result was then obtained by calculating the mean of the pK_a values, giving $pK_{a/D_2O,av}$ = 3.11 ± 0.08. As expected, and in agreement with the pK_a value, which was obtained below, the pK_a value in this case is lower.

Table 19: *Negative logarithmus of the acidity constant (pK_a) of 9-MeA in a solution 20% D_2O and 80% Acetone.*

	pK_{a/D_2O} determined from the shift of						$pK_{a/D_2O,av}$		$pK_{a/H_2O,av}$	
	CH_3		H2		H8					
$N1H^+$	3.61 ±	0.08	3.61 ±	0.08	3.61 ±	0.08	3.61 ±	0.08	3.11 ±	0.08

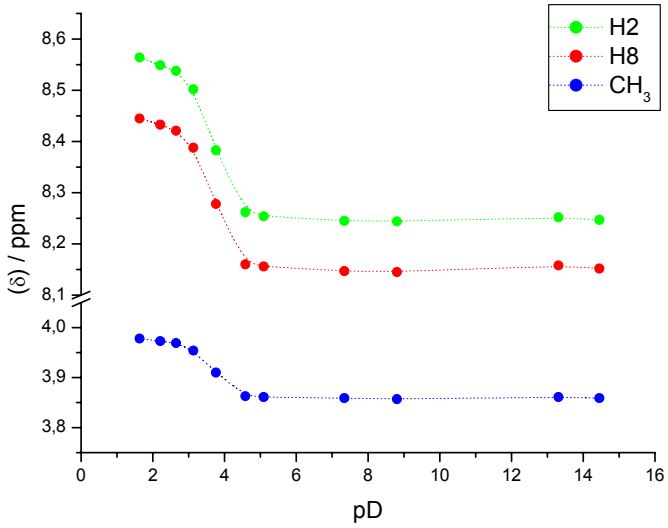

Figure 93*: pH dependence of the ^1H chemical shifts of 9-MeA in the pD range from 2 to 11. For the exact chemical shifts of the species see Tables of the pD dependences.*

2.8.2 Mixture of Methanol and D_2O

Next, methanol was used as a cosolvent with D_2O. Methanol is a polar solvent, more polar than acetone, with a dielectric constant of 33.7.[151] 9-methyladenine was dissolved in a mixture of 80% of methanol and 20% D_2O. The determination of the pK_a value corresponding to deprotonation of N1 position of the 9-MeA was followed by ^1H NMR spectroscopy. Table 20 contains the various pK_a values obtained for the different protons.

Table 20: *Negative logarithmus of the acidity constant (pK_a) of 9-MeA in a solution 20% D_2O and 80% Methanol.*

	pK_{a/D_2O} determined from the shift of						$pK_{a/D_2O,av}$		$pK_{a/H_2O,av}$	
	CH_3		H2		H8					
$N1H^+$	3.68 ±	0.02	3.70 ±	0.01	3.69 ±	0.02	3.69 ±	0.02	3.19 ±	0.02

Figure 94 shows the different curves corresponding to the different protons. The final result, $pK_{a/D_2O,av}$ = 3.19 ± 0.02, is slightly higher than the $pK_{a/D_2O,av}$ = 3.11 ± 0.08 for the mixture 80% acetone and 20% D_2O. This finding is in agreement with qualitative conclusions, according to which a lowering of the dielectric constant of the solvent lowers the pK_a value.

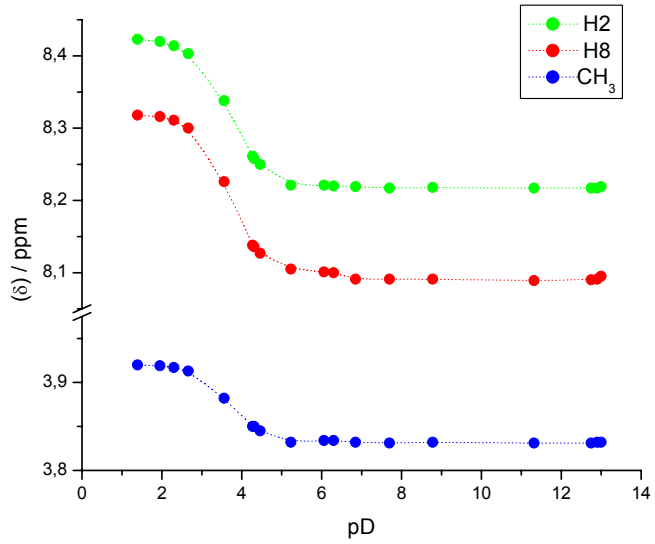

Figure 94: *pD dependence of 9-MeA in a mixture of methanol/D_2O (80%/20%).*

In Table 21, the acidity constants $pK_{a/D_2O,av}$ and its corresponding one in water of the different experiments are summerized. It is evident that these values agree well within expectations pointed out at the beginning of this chapter. By comparing the $pK_{a/H_2O,av}$, one can conclude that the lower the acidity

constant is ($\varepsilon_{D_2O} > \varepsilon_{Methanol} > \varepsilon_{Acetone}$), the more acidic the cationic specie is (see **A** in Figure 91). Therefore, there is a decrease in pK_a value.

Table 21: *Summary of the pK_a value of 9-MeA in different solutions.*

Solution	p$K_{a/D_2O,av}$	p$K_{a/H_2O,av}$
D_2O	4.81[149] or 5.02[150]	4.30[149] or 4.50[150]
D_2O / Aceton (80/20)	4.24	3.73 ± 0.07
D_2O / Methanol (20/80)	3.69	3.19 ± 0.02
D_2O / Aceton (20/80)	3.61	3.11 ± 0.08

2.9 Acidity of Aqua Ligands in $[(NH_3)_2Pt(nucleobase)(H_2O)]^{n+}$

The simplest reaction of an aqua-cation in solution is the loss of a proton to give a hydroxo-aqua-species, according to:

$$[M(OH_2)_x]^{n+} \rightleftharpoons [M(OH_2)_{x-1}(OH)]^{(n-1)+} + H^+aq$$

This behaviour leads to the complicated field of oligomerization. Most of the hydroxo-aqua cations display pronounced tendencies to form hydroxo-, and eventually even oxo- bridged species, for example:

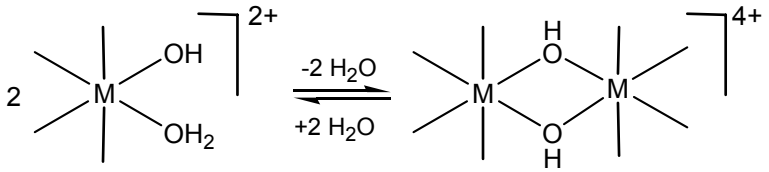

At the simplest level, the coordination of a metal ion to a water molecule will, through electrostatics, make proton loss easier (Figure 95).[152] The greater the positive charge on the ion, the easier it should be for the proton to dissociate from an attached water molecule.

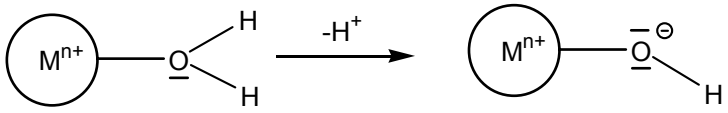

Figure 95: *Acidity of a hydrated cation.*

In this chapter, the acidity of a water molecule coordinated to a platinum ion will be discussed. A possible effect of intramolecular H bonding between the OH^- group and the exocyclic amino group of a nucleobase on the acidity and reactivity of a metal-bound hydroxide will also be discussed.

2.9.1 Acidity Constants of *trans*-$[Pt(NH_3)_2(H_2O)_2]^{2+}$

pK_a values of the aqua ligands in *trans*-$[Pt(NH_3)_2(H_2O)_2]^{2+}$ were reported by Appleton et al[153] applying ^{195}Pt as well as ^{15}N NMR spectroscopy (of ^{15}N labelled NH_3 ligands). The NMR spectroscopic changes were smaller in magnitude than the corresponding changes when water coordinated trans to ammine in *cis*-$[Pt(H_2O)_2(^{15}NH_3)_2]^{2+}$ is deprotonated.[154-158] The acid dissociation constants K_{a1} and K_{a2} correspond to:

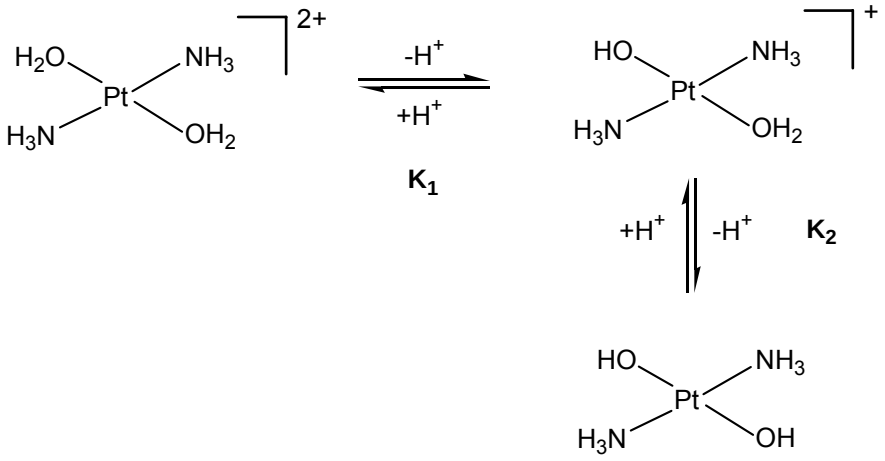

pK_a values were found to be pK_{a1} = 4.35 and pK_{a2} = 7.40 for the two steps (no standard deviations given).

2.9.2 Comparison with its *cis*-Isomer

In a similar way, pK_a values were determined for the cis isomer. With the use of an iterative program,[159] the parameters K_{a1} and K_{a2} were varied to give the best least-squares fit to the experimental data over the pH range 4.3-9.1. The values obtained were pK_{a1} = 5.93 ± 0.10 and pK_{a2} = 7.87 ± 0.10.

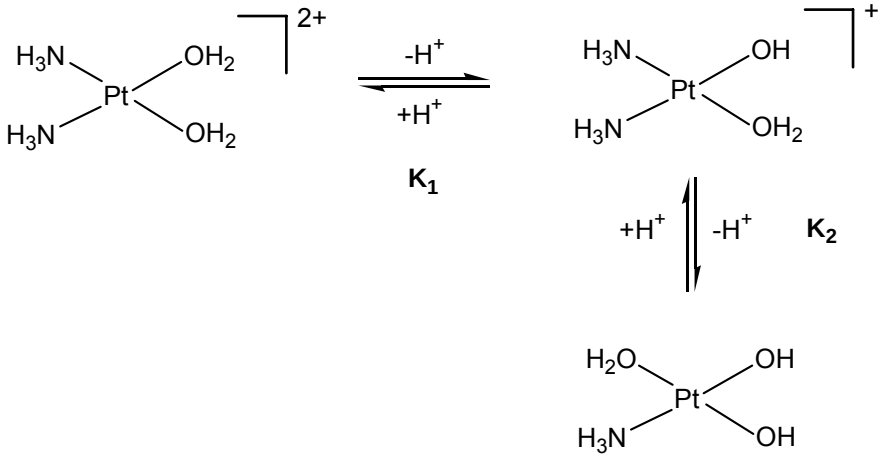

The two acid dissociation constants are more difficult to determine, because of the formation of hydroxo-bridged oligomers like $[Pt(NH_3)_2(\mu\text{-}OH)]_n^{n+}$. For *trans* complexes, formation of μ-OH species is much less pronounced.

Comparison of the results of the two isomers reveal that the *trans* isomer is more acidic, most likely a consequence of differences in *trans* influence, with that of H_2O in the *trans*-isomer being larger than that of NH_3.

If chloro species of the two isomers are included in the comparison, viz. *cis*- and *trans*-$[PtCl(NH_3)_2(H_2O)]^+$, the following picture emerges (Figure 96):

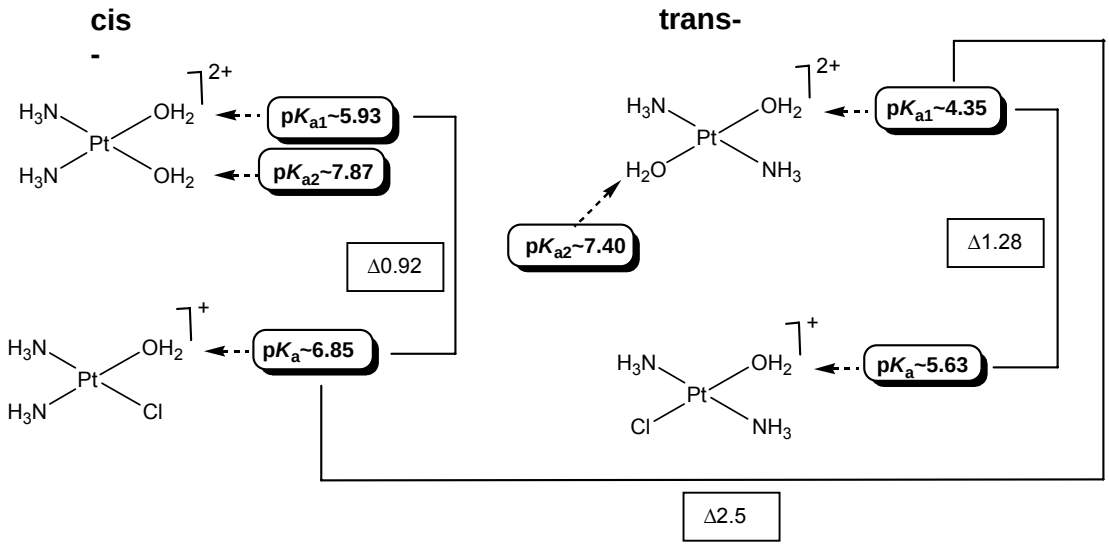

Figure 96: *Comparison of the acidity constants of cis- and trans-$[Pt(H_2O)_2(NH_3)_2]^{2+}$ with cis- and trans-$[PtCl(H_2O)(NH_3)_2]^{+}$.*

In the next chapter, the acidity of a water molecule coordinated to a platinum ion, carrying a nucleobase, will be studied.

2.9.3 Effect of Intramolecular H Bonding on the Basicity of a Metal-Bound Hydroxide

In order to study the hydrolysis of biologically important phosphate diesters with poor leaving groups (e.g., DNA), the reactivity of three Cu(II) complexes for hydrolizing 2´,3´-cAMP was studied by Chin et al.[160] It was found by these authors, that one amino group in close proximity to the aqua ligand lowers the pK_a of the metal-bound water molecule. It appears that the amino group is acting as a hydrogen bond donor to the metal-bound hydroxide, thereby stabilizing it and lowering the pK_a of the H_2O ligand. If the amine nitrogen was acting as a hydrogen bond acceptor, the pK_a of the coordinated water molecule should have increased.

It was proposed that the mechanism for promoted hydrolysis of 2´,3´-cAMP involves intramolecular nucleophilic attack by the metal-hydroxide on the coordinated phosphate diester.[161] Hydrogen bonds between the amino group and the OH group of the copper complex, should acidify the OH group, making it easier for this group to deprotonate and thus facilitate the expulsion of the leaving-group (Figure 97).

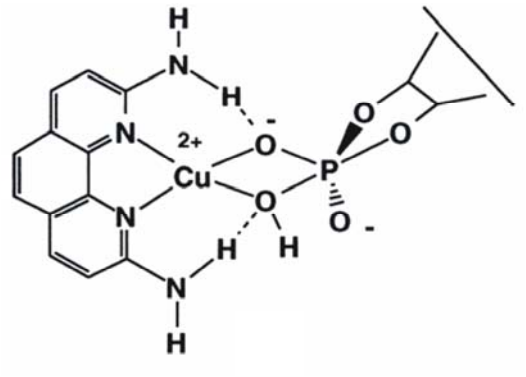

Figure 97: *Intramolecular nucleophilic attack by the metal-hydroxide on the coordinated phosphate diester. Hydrogen bonds between the amino group and the OH group are also observed.*

2.9.3.1 *cis*- and *trans*-$[(NH_3)_2Pt(1\text{-}MeC\text{-}N3)(H_2O)]^{2+}$

In order to study the possibility of hydrogen bonds between the exocyclic amino group of the cytosine and the OH group, selected nucleobase compounds were studied by ^1H NMR spectroscopy. Measurement of the pD dependence was carried out using identical samples, in which the pD of the solutions was changed in small increments by addition of small amounts of DNO_3 and NaOD, respectively. ^1H NMR spectra were recorded immediately after adjusting the pD.

pD-dependent ^1H NMR spectra (2 < pD < 14) of *cis*-$[(NH_3)_2Pt(1\text{-}MeC\text{-}N3)(H_2O)]^{2+}$ reveal two deprotonation steps. The first one occurs with pK_{a1} = 5.78 ± 0.03 (calculated for H_2O). The second one takes place at pD > 13. The first one is assigned to the deprotonation of the water molecule. In this case, a

hydrogen bond between the NH_2 of the cytosine and OH^- could be possible, in principle (Figure 98). Under strongly basic conditions *cis*-$[(NH_3)_2Pt(1\text{-}MeC\text{-}N3)(OH)]^+$ becomes deprotonated also at the exocyclic amino group of the cytosine. The graphical representation of the pD dependence is depicted in Figure 99 (on the right side). A significant upfield shift of the CH_3-signals at basic pH values can be observed, due to the deprotonation of the cation.

In order to study the deprotonation of the water molecule, the pK_{a1} value was compared to its *trans*-isomer, *trans*-$[(NH_3)_2Pt(1\text{-}MeC\text{-}N3)(H_2O)]^{2+}$. In this case, deprotonation of H_2O occurs earlier: pK_{a1} = 5.17 ± 0.1 (Figure 99, on the left side). As there is no intramolecular stabilization possible of the hydroxo ligand in the trans isomer, yet *trans*-$[(NH_3)_2Pt(1\text{-}MeC\text{-}N3)(H_2O)]^{2+}$ is more acidic, one has to conclude that differences in trans-influence rather than a differential stabilization of the hydroxo species is dominating. It may be added that the crystal structure analysis of *cis*-$[(NH_3)_2Pt(1\text{-}MeC\text{-}N3)(OH)]^+$ provides no evidence for the kind of H bond between the OH^- ligand and the exocyclic amino group of cytosine discussed above.[162]

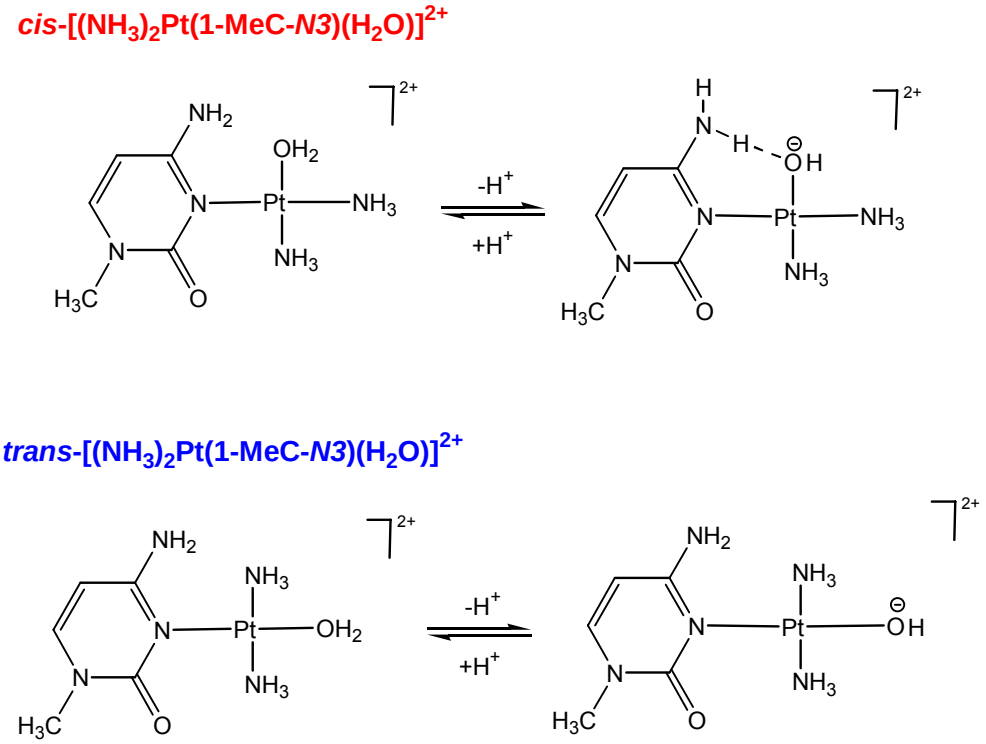

Figure 98: *Possibility of intramolecular hydrogen bond between the NH_2 of the cytosine and the OH^- in cis-$[(NH_3)_2Pt(1\text{-}MeC\text{-}N3)(H_2O)]^{2+}$.*

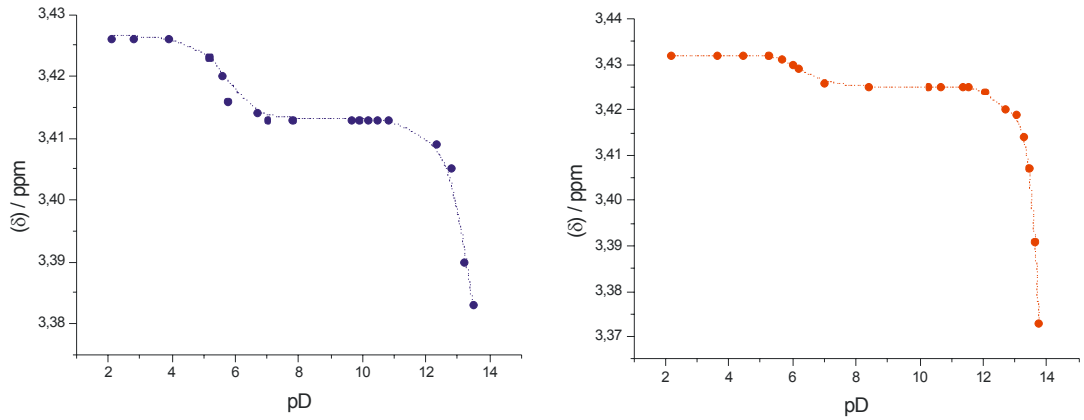

Figure 99: *pD dependence (δ, ppm) of the CH_3 resonance in D_2O of the cation cis-$[(NH_3)_2Pt(1\text{-}MeC\text{-}N3)(H_2O)]^{2+}$ (right) and for trans-$[(NH_3)_2Pt(1\text{-}MeC\text{-}N3)(H_2O)]^{2+}$ (left).*

2.9.3.2 *cis*- and *trans*-$[L_2Pt(9\text{-}MeGH\text{-}N7)(H_2O)]^{2+}$

In order to get some more insight into the question of a stabilizing hydrogen bond between the exocyclic amino group of a nucleobase and the hydroxo group, a similar experiment was carried out with guanine. In this case, 9-methylguanine was used as nucleobase, because an intramolecular hydrogen bond of the kind discussed is not possible (Figure 100).

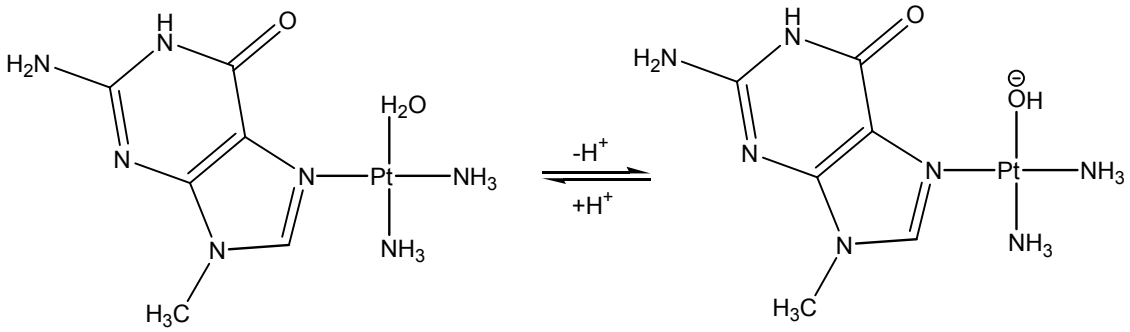

Figure 100: *Acid-base equilibrium of cis-*$[(NH_3)_2Pt(9\text{-}MeGH\text{-}N7)(H_2O)]^{2+}$.

The acidity of the water molecule in *trans*-$[(NH_3)_2Pt(9\text{-MeGH-}N7)(H_2O)]^{2+}$ was determined by ^1H NMR spectroscopy (pD dependence of CH_3 and H8 of guanine) and found to be 5.27 ± 0.05 (calculated for H_2O) (Figure 101). This value is practically identical with the one obtained for *trans*-$[(NH_3)_2Pt(1\text{-MeC-}N3)(H_2O)]^{2+}$ (pK_{a1} = 5.17 ± 0.1). *Cis*-$[(NH_3)_2Pt(9\text{-MeGH-}N7)(H_2O)]^{2+}$ was not studied because of its high reactivity, leading to multiple products.[163] Instead, the pK_{a1} value in the complex *cis*-$[\{NH(CH_3)_2\}_2Pt(9\text{-MeGH-}N7)(H_2O)]^{2+}$ was determined (5.81 ± 0.03). Again, this value is almost identical with the one obtained for *cis*-$[(NH_3)_2Pt(1\text{-MeC-}N3)(H_2O)]^{2+}$ (pK_{a1} = 5.78 ± 0.03), despite having different am(m)ine ligands.

To conclude, the pK_a values corresponding to the deprotonation of the water molecule in *trans* complexes are lower than in *cis* complexes, due to the *trans* influence. A definitive effect of a neighbour group effect on H_2O ligand acidity via H bond formation between the OH^- ligand and a nucleobase was not observed. Table 22 summerizes the finding results.

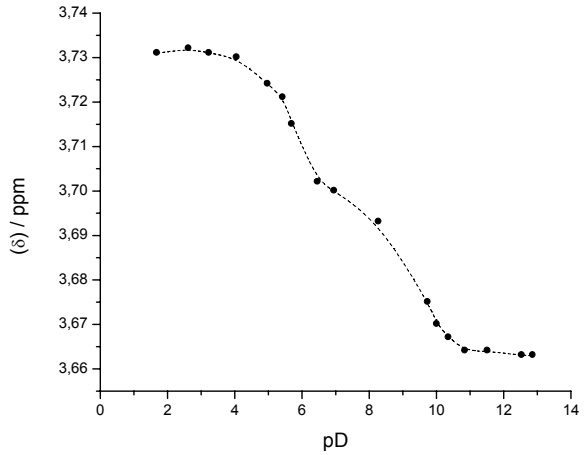

Figure 101: *pD dependence (δ, ppm) of the CH_3 resonance of 9-MeGH in trans-$[(NH_3)_2Pt(9\text{-MeGH-}N7)(D_2O)]^{2+}$. The first step corresponds to the deprotonation of the water molecule and the second one to the deprotonation of the N1H position of the 9-methylguanine.*

Table 22: *Negative logarithmus of the acidity constant (pK_{a1}) of a water molecule in different complexes, involving Pt atom and a nucleobase. X corresponds to a nucleobase and L to an am(m)ine ligand.*

	***cis*-$[L_2PtX(H_2O)]^{2+}$**		***trans*-$[L_2PtX(H_2O)]^{2+}$**	
	X = 1-MeC L = NH_3	**X = 9-MeGH L = $NH(CH_3)_2$**	**X = 1-MeC L = NH_3**	**X = 9-MeGH L = NH_3**
pK_{a1H_2O}	5.78 ± 0.03	5.81 ± 0.00	5.17 ± 0.1	5.27 ± 0.05

2.10 Pyrazole System

The heterocycle pyrazole (pzH) and the pyrazolate anion (pz) are particularly suitable for bringing together metal centers at close distance, due to their good ligating properties and their geometry. The synthesis of polynuclear transition metal complexes, in which the metals are brought to a fixed distance to each other, is an important area of research for the catalysis in biological and industrial reactions.[164,165] In recent years, several elegant examples of polynuclear systems of bonded pyrazolate anions were described,[166] including that of dinuclear complexe with the structure [{Ru(μ-pz)($CNBu^t$)$_2$}$_2$]. Moreover, these complexes were described as “Supernucleophiles”, when used for the activation of X-CH (with X being a halogen).[167] Apart from the bridging species, pyrazole can still coordinate in chelating or monofunctional fashion. The latter is important for the design of polynuclear compounds. Selected metal binding patterns are shown in the following table (Table 23).

The idea to involve pyrazole ligands in a study concerned primarily with nucleobase acidification as a consequence of metal coordination and of neighbour group effects was very simple: The pyrazole should act as a “helper” ligand to bring two different nucleobases into close proximity (Figure 102), thereby facilitating H bonding interactions between functional groups in different protonation states (see, in particular 2.10.1.6).

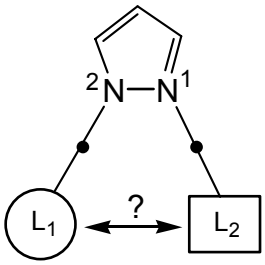

Figure 102: *Pyrazolate as "helper" ligand. L_1 and L_2 = different nucleobases.*

Table 23: *Different ways of coordination of a metal to the pyrazole ligand.*

Position of coordination	Complexes	Lit.
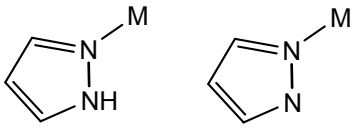	$(DPPF)Pt(pz)_2$	[168]
	cis-$Pt(pzH)_2Cl_2$	[169]
	$[Pt(pz)_2(Hpz)_2]_2$	[170]
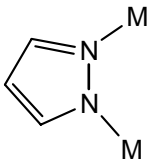	$[(DPPF)Pt(\mu\text{-}pz)_2CdI_2]$	[168]
	$[Pt_2Cl_2(\mu\text{-}pz)_2(PEt_3)_2]$	[171]
	$[Pt(pz)_2]_3$	[172]
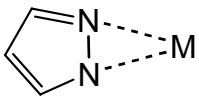	$[(C_5H_5)_2Zr(thf)(\eta^2\text{-}pz)]^+$	[173]

Dissociation equilibria of pyrazole are shown in Figure 103. Pyrazole can be protonated at the N1 position in acidic solution (pK_{a1} = 2.56).[174] Under strongly basic conditions, for example in the reactions with alkali metals,[175,176] the second endocyclic nitrogen N2 is deprotonated (pK_{a2} = 14.21)[177] When a metal becomes coordinated to the N1 position, the electronic density of the ring system decreases and N2H becomes more acidic, so that the second coordination position can also be metalled under relatively mild conditions.[178]

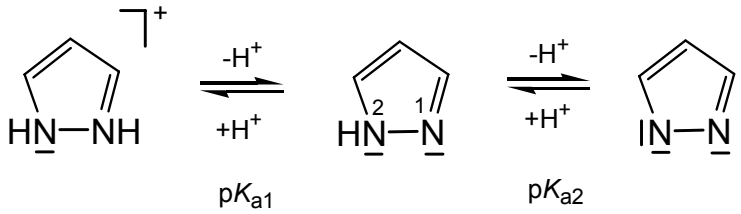

Figure 103: *Acid-base equilibria of pyrazole.*

Because of the fast tautomeric equilibrium, the H3 and H5 protons of the free pyrazole are equivalent and therefore appear as only one doublet in the ^{1}H NMR spectrum. When coordinated at the N1 position, the protons are no longer chemically equivalent and therefore give rise to two doublets in the spectrum. The electron withdrawing effect of the metal causes a downfield shift (e.g., in *trans*-[AaPt(pzH)$_2$]$^{2+}$; a = ammine, A = n-hexylamine). Further complexation under simultaneous deprotonation of the N2 position causes, however, a weak high field shift of the signals. The following table (Table 24) gives an overview of the observed chemical shifts of the discussed complexes in the case of platinum coordination.[179]

Table 24: *Chemical shifts in ppm of the resonances in ^{1}H NMR of the free and platinum coordinated pyrazole in MeOD.*[180]

Complex	H4 (t)	H3 (d)	H5 (d)
pzH	6.42	7.62	see H3
trans-[AaPt(pzH)$_2$]$^{2+}$	6.67	7.98	8.11
trans-[PtAa(pz-*N1*,*N2*)$_2${PtAaCl}$_2$]$^{2+}$	6.52	7.70	see H3

2.10.1 *trans*-[$(NH_3)_2$Pt(pzH)Cl](NO_3) (28) as Starting Compound

Addition of one equivalent of pyrazole ligand (pzH) to *trans*platin leads to the formation of the 1:1 complex (**28**) and the 2:1 complex *trans*-[$(NH_3)_2Pt(pzH)_2]^{2+}$ in high yield. In order to obtain compound (**28**), variations of the reaction were carried out in order to improve the yield. The highest content of desired 1:1 product, which makes use of an intermediate Pt^{II}-DMF species, which then reacts with pyrazole.[181] The improved yield of (**28**) in relation to similar conditions reaction in water can be attributed on the one hand to the good solubility of trans-DDP in DMF and on the other hand to the fact that further solvolysis is reduced by the coordinated DMF.

Recrystallization of the raw product in water leads to an increase of the concentration of the bis(pyrazole)complex. The same is to be observed upon dissolving the raw product and following complete removal of the water in a rotation evaporator. This behaviour was already described for other 1:1 complexes of *trans*platinum.[182] Here for aqueous solvents the following equilibrium is accepted:

$$2\ trans\text{-}[(NH_3)_2Pt(pzH)Cl]^{+} \rightleftharpoons trans\text{-}[(NH_3)_2Pt(pzH)_2]^{2+} + trans\text{-}[(NH_3)_2PtCl_2]$$

Both complexes (1:1 and 2:1) were separated following recrystallization from a mixture of isopropanol/water (2:1). Crystals of *trans*-[$(NH_3)_2$Pt(pzH)Cl](NO_3) (**28**) were collected and proved useful for X-ray crystallography. The complex crystallizes in the triclinic P-1 space group. Details concerning the crystal, X-ray measurement, and the refinement of data are listed in Tables A-9 (see Appendix).

Compound (**28**) contains two crystallographically independent cations Pt1 and Pt2. View of both cations are given in Figure 104. In both cases the pyrazole ring and the chloride ligand are trans to each other and are bonded to

Pt. The platinum is bonded via N1 to the pyrazole. The geometry about Pt is square-planar. Deviations from the ideal case are very small, as evidenced by values of the N-Pt-N and N-Pt-Cl angles: the angles between Pt and the two *trans* positioned nitrogen atoms and the chloro ligand range from 176.8(3)° to 179.4(4)°, and between Pt and the cis positioned nitrogen atoms and chloride from 89.1(3)° to 90.9(2)°. The platinum coordination sphere is coplanar with the four donors deviating by ± 0.033 Å from the mean plane. Pt-N distances range from 2.003(11) to 2.067(12) Å. In the unit cell, there are two different molecules of (**28**), which are differently oriented. The distances and angles in the pyrazole of (**28**) are not unusual (Table 25).

A differentiation between N2 and the C5 of the pyrazole ligands was made by interchanging these atoms and by determining the R values for the two situations. The solution leading to the lower R value was eventually chosen.

The two external C-N-Pt1 and C-N-C angles are slightly different. The angle on the side of the carbon atom (Pt1-N1B-C5B, 129.9(9)°) is larger than the one on the side of the nytrogen atom (Pt1-N1B-N2B), 124.4(8)°). The atoms in the pyrazole ring are almost coplanar within ± 0.0076 Å. The metal coordination plane and the pyrazole (B) ring form an dihedral angle of 52.0(4)°. In the case of the other molecule, the two external C-N-Pt2 and C-N-C angles are likewise different. The angle on the side of the carbon atom (Pt2-N1A-C5A, 130.4(9)°) is larger than the one on the side of the nytrogen atom (Pt2-N1A-N2A), 121.4(8)°). The atoms in the pyrazole ring are almost coplanar within ± 0.0137 Å. The metal coordination plane and the pyrazole (A) ring form an dihedral angle of 87.7(4)°. Thus, the two crystallographically independent cations differ primarily in the dihedral angles between Pt and pz planes.

Table 25: *Selected distances (Å) and angles (°) for non-hydrogen atoms in* ***28****.*

Pt1-N1B	2.003(11)	N1B-Pt1-N12	88.8(5)
Pt1-N12	2.041(11)	N1B-Pt1-N11	91.3(49
Pt1-N11	2.067(12)	N12-Pt1-N11	179.4(4)

Pt1-Cl1	2.294(3)	N1B-Pt1-Cl1	176.8(3)
N1B-N2B	1.340(15)	N12-Pt1-Cl1	90.9(3)
N1B-C5B	1.347(15)	N11-Pt1-Cl1	89.1(3)
C5B-C3B	1.365(19)	N2B-N1B-C5B	105.6(11)
N2B-C4B	1.372(17)	N2B-N1B-Pt1	124.4(8)
C3B-C4B	1.315(18)	C5B-N1B-Pt1	129.9(9)
		N1B-C5B-C3B	109.7(12)
		C4B-C3B-C5B	109.5(11)
		C3B-C4B-N2B	107.4(12)
Pt2-N1A	2.044(10)	N1A-Pt2-N22	90.0(4)
Pt2-N21	2.063(11)	N21-Pt1-N22	177.0(4)
Pt2-N22	2.031(12)	N1A-Pt1-N21	89.8(4)
Pt2-Cl2	2.283(3)	N22-Pt2-Cl2	89.4(3)
N1A-N2A	1.320(13)	N1A-Pt2-Cl2	178.1(3)
N1A-C5A	1.291(16)	N21-Pt2-Cl2	90.9(3)
C5A-C3A	1.38(2)	N2A-N1A-C5A	108.1(10)
N2A-C4A	1.308(17)	N2A-N1A-Pt2	121.4(8)
C3A-C4A	1.33(2)	C5A-N1A-Pt2	130.4(9)
		N1A-C5A-C3A	108.1(13)
		C4A-C3A-C5A	106.0(13)
		C3A-C4A-N2A	108.0(13)

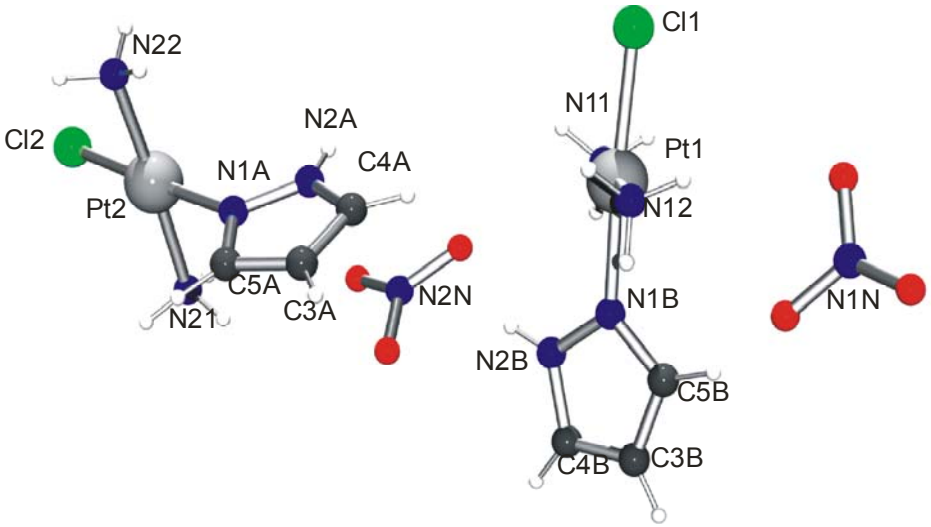

Figure 104: *View of two independent cations trans-[$(NH_3)_2$Pt(pzH)Cl](NO_3) (**28**) with NO_3^- anions in the unit cell.*

Cations of (**28**) are arranged in layers (Figure 105).

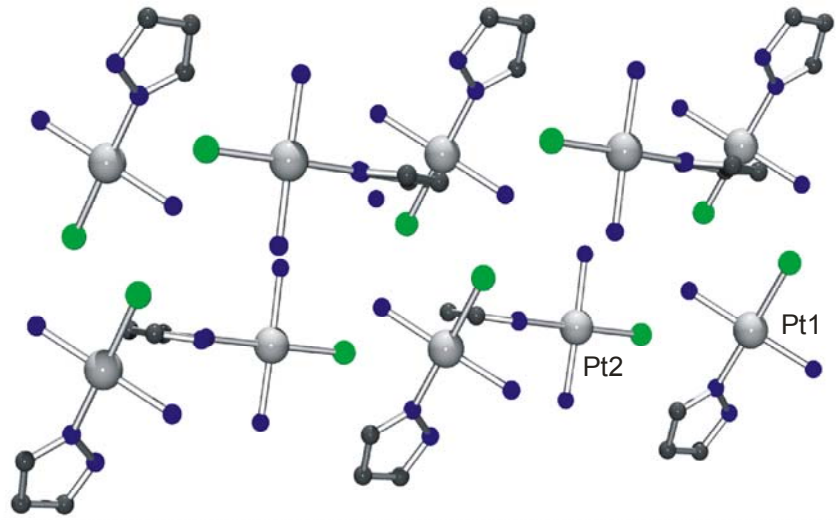

Figure 105: *Detail of packing of trans-[$(NH_3)_2$Pt(pzH)Cl](NO_3) (**28**) with nitrates omitted.*

There are no intramolecular hydrogen bond interactions possible within the cations of (**28**). However, there are intermolecular H bonding interactions between ligands of neighbouring cations and also with nitrate anions. Distances between Cl and the ammine ligands of the platinum atom are: Cl-N (1-x, 1-y, 1-z), 3.28(1) Å. This situation is shown in Figure 106. Intermolecular Pt···Cl distances are 3.79 Å, which is considered too long for any bonding interaction.

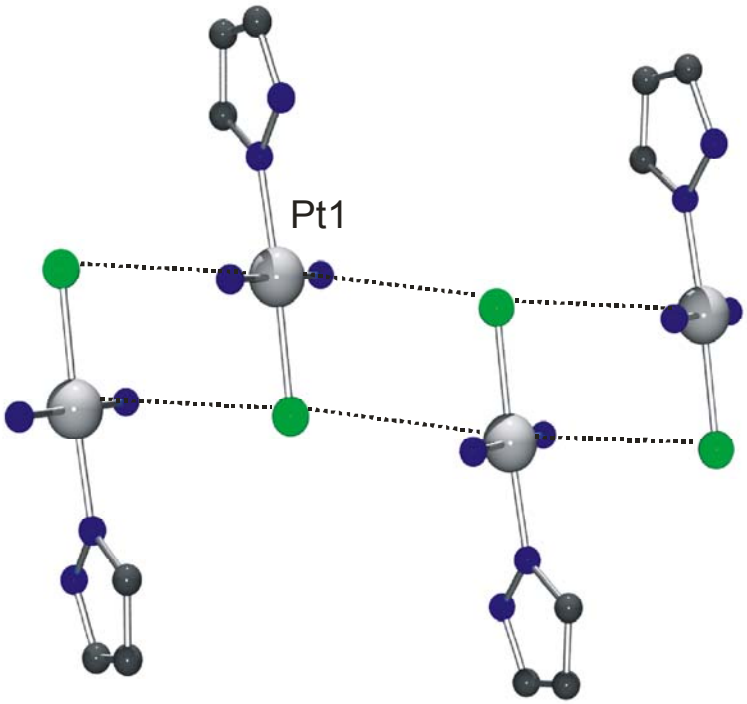

Figure 106: *Weak interaction between Cl and the NH_3 ligands of cations (**28**).*

The crystal packing of (**28**) is based on interactions between the *trans*-$[(NH_3)_2Pt(pzH)Cl]^+$ cation and the nitrate counter anions in the unit cell. As shown in Figure 107, the oxygen atoms of the nitrate form hydrogen bonds with the protons of the ammine ligand of the platinum and when the other endocyclic nitrogen atom of the pyrazole ligand: O1N···N12, 2.96(1) Å; O2N···N12, 3.30(2) Å; O7N···N2B, 3.05(2) Å; O7N···N2A, 3.32(2) Å; O5N···N2B, 2.97(2) Å; O5N···N11, 2.93(1) Å and O6N···N21, 3.06(1) Å.

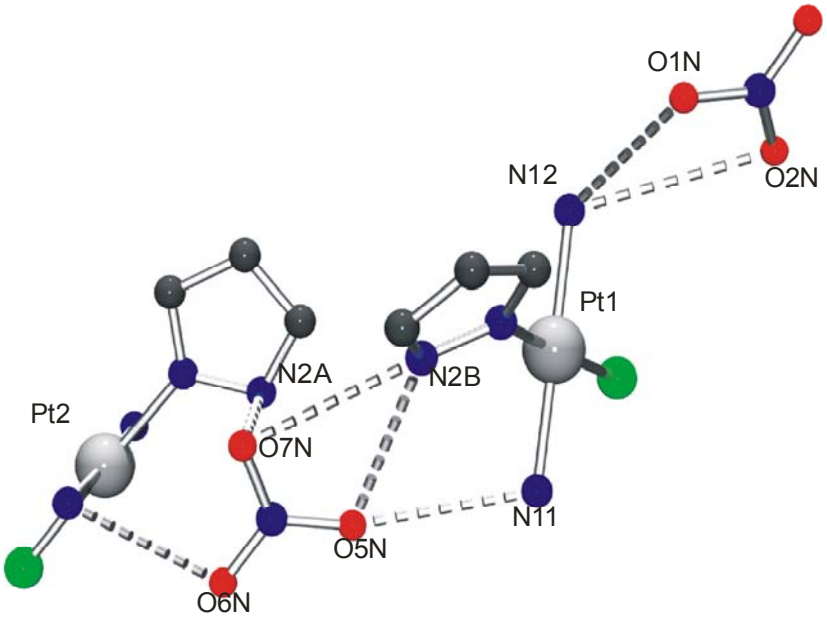

Figure 107: *Interactions between the cation and the nitrate anions in (**28**).*

2.10.1.1 NMR Studies

The complex *trans*-$[(NH_3)_2Pt(pzH)Cl]^+$ was also studied by ^1H NMR spectroscopy. In comparison to the bis(pyrazole) complex the 7.90/7.81 ppm resonances for H3/H5 and the signal at 6.53 (H4) ppm (pD = 7.4) are slightly highfield shifted (Figure 108). Due to the coordination of the platinum atom to the N1 site of the pyrazole ligand, the ^{195}Pt satellites of 18.1 Hz of the H5 resonance are observed. During the observation of the signals of (**28**) over the time, the equilibrium mentioned above is confirmed, since after few hours the signals of the 2:1 complex are detectable.[181] In the IR spectrum, the bands corresponding to the 2:1 complex and (**28**) differ not so much. Only the band υ (Pt-Cl) at 340 cm^{-1} was found for the complex *trans*-$[(NH_3)_2Pt(pzH)Cl]^+$.

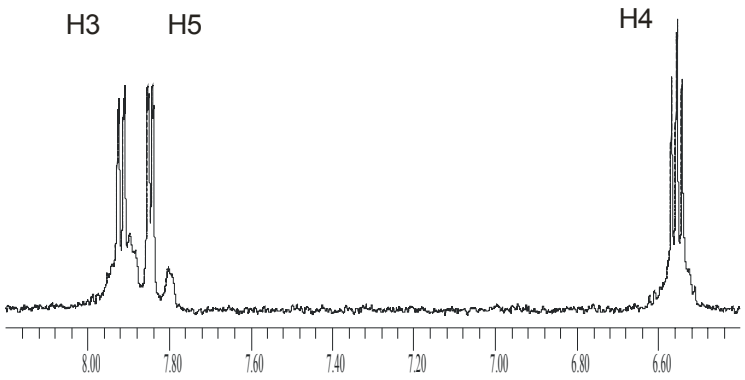

Figure 108: *^{1}H NMR spectrum of the complex trans-[$(NH_3)_2$Pt(pzH)Cl]$^+$ in D_2O at pD = 7.4.*

2.10.1.2 Reaction of *trans*-[$(NH_3)_2$Pt$(pzH)_2$]$(NO_3)_2$ with *trans*-[$(NH_3)_2$Pt(1-MeC-*N3*)(H_2O)]$^{2+}$

Synthesis of trinuclear *trans*,*trans*,*trans*-{$(NH_3)_2$Pt(*N1*-pz-*N2*)$_2$[$(NH_3)_2$Pt(1-MeC-*N3*)]$_2$}$^{6+}$ complexes was achieved using the complex *trans*-[$(NH_3)_2$Pt$(pzH)_2$]$^{2+}$, which is obtained in a high yield in the preparation of the 1:1 complex (**28**). Two equivalents of *trans*-[$(NH_3)_2$Pt(1-MeC-*N3*)(H_2O)]$^{2+}$ were added to a solution containing *trans*-[$(NH_3)_2$Pt$(pzH)_2$]$^{2+}$ and the mixture was brought to pH 8. Under these conditions, the deprotonation of the endocyclic nitrogen of the pyrazole ligand (N2) takes place. The reaction was carried out during three days at 40°C and the sample was left in the refrigerator. After several days, a precipitate formed which was filtered off and disolved in D_2O in order to identify the complex. As can be seen in Figure 109, the ^{1}H NMR spectrum of the product (**29**) is consistent with a complex containing pz and 1-MeC in a 1:1 ratio (integrals of signals) and with pyrazole resonances being different from those of the bis(pyrazole) complex.[181] As expected from the anticipated structure (Figure 110), H3 and H5 are still inequivalent and therefore give rise to two different sets of resonances, centered at 8.00 (H3) and 7.72 ppm (H5). The H4 resonance of pz is at 6.50 ppm. The 1-MeC resonances are observed at 3.51 (s, CH_3), 6.09 ppm (d, ^{3}J = 7.5 Hz, H5) and 7.68 ppm (d, H6).

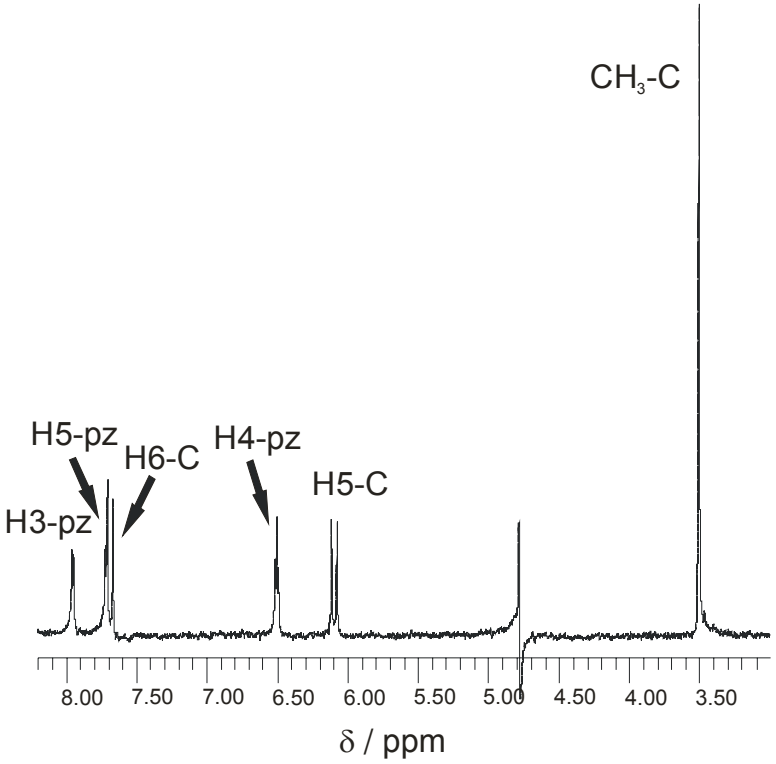

Figure 109: *^{1}H NMR spectrum of trans,trans,trans-{$(NH_3)_2Pt(N1\text{-}pz\text{-}N2)_2[(NH_3)_2Pt(1\text{-}MeC\text{-}N3)]_2\}^{6+}$ (**29**).*

Unfortunately, attempts to crystallize this complex were not successful.

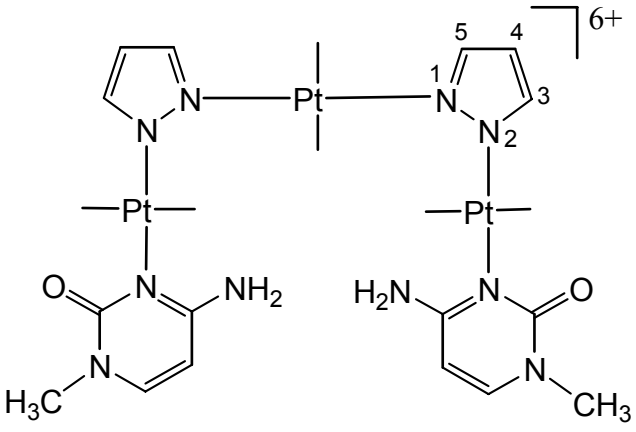

Figure 110: *trans,trans,trans-{$(NH_3)_2Pt(N1\text{-}pz\text{-}N2)_2[(NH_3)_2Pt(1\text{-}MeC\text{-}N3)]_2\}^{6+}$ (**29**).*

2.10.1.3 Reaction of *trans*-$[(NH_3)_2Pt(pzH)Cl]^+$ with $AgNO_3$

Treatment of *trans*-$[(NH_3)_2Pt(pzH)Cl]^+$ with one equivalent of $AgNO_3$ in D_2O, pD ~ 9, was carried out on an NMR scale. The objective of this experiment was to observe the possibility of obtaining cyclic pyrazole complexes. Once the N2 position of the ligand is deprotonated, another *trans*-$[(NH_3)_2Pt(pzH)(H_2O)]^{2+}$ entity could be coordinated. The reaction was followed by ^1H NMR spectroscopy (Figure 111). The spectrum on the top was measured immediately after addition of NaOD. The spectrum in the middle was recorded five days later, and new signals of the protons appeared. The spectrum on the bottom was measured one month later, and as can be seen, the signals of the protons are very complicated. Attempts to isolate any of these new species were not successful. What can be concluded is that there is indeed oligomerization with pz-bridging going on, even though it is unclear whether cyclic species and/or open chains are formed.

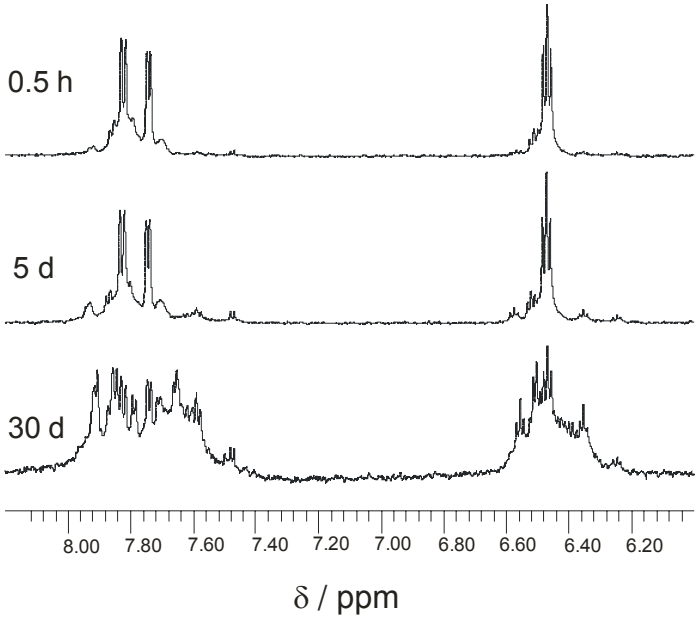

Figure 111: *Lowfield section of ^1H NMR of trans-$[(NH_3)_2Pt(pzH)(H_2O)]^{2+}$ in basic conditions with time.*

2.10.1.4 Oxidation of Pt(II) to Pt(IV) in *trans*-$[(NH_3)_2Pt(pzH)Cl]^+$

When a solution containing the complex *trans*-$[(NH_3)_2Pt(pzH)Cl]^+$ (**28**) was heated at 50°C until dryness and posterior disolution in water, yellow crystals appeared. This new complex was characterized by ^1H NMR spectroscopy and by X-ray crystallography. The ^1H NMR spectrum of this compound displays two doublets of doublets corresponding to H3/H5 protons and a triplet (H4) (Figure 112, spectrum B). Due to the coordination of Pt to the N1 site of the pyrazole, the ^{195}Pt satellites of 11.5 Hz and 11Hz of the H3 and H5 resonances are observed. The chemical shifts of these signals are downfield related to (**28**) and the 2:1 complex *trans*-$[(NH_3)_2Pt(pzH)_2]^{2+}$. The ^{195}Pt NMR spectrum was recorded, which displayed a single signal at -385 ppm, suggesting the existence of a Pt(IV) complex. The crystal proved of poor quality, but a preliminary the structure corresponding to *trans*-$[(NH_3)_2Pt(pzH)_2Cl_2](NO_3)_2 \cdot H_2O$ (**30**) could be established. In order to obtain crystals of Pt(IV) of better quality, these crystals were disolved in water at 40°C and $HClO_4$ was added. After several days in the refrigerator, red and yellow crystals appeared. The red crystals were also studied by X-ray crystallography, but the structure solution proved very difficult. This complex was also characterized by elemental analysis and ^1H NMR spectroscopy. The ^1H NMR spectrum shows a mixture of two different complexes, containing two platinum species in a 1:1 ratio. As shown in Figure 112, spectrum C represents a superposition of signals corresponding to the Pt(II) complex *trans*-$[(NH_3)_2Pt(pzH)_2]^{2+}$ (spectrum A) and signals corresponding to the Pt(IV) complex *trans*-$[(NH_3)_2Pt(pzH)_2Cl_2]^{2+}$ (spectrum B). According to the elemental analysis, the composition of the red crystals corresponds to *trans*,*trans*-$[(NH_3)_2Pt(pzH)_2Cl_2][(NH_3)_2Pt(pzH)_2](ClO_4)_4 \cdot H_2O$ (**31**).

The structure of (**31**) is proposed to consist of chains of *trans*-$[(NH_3)_2Pt(pzH)_2Cl_2]^{2+}$ entities linked to *trans*-$[(NH_3)_2Pt(pzH)_2]^{2+}$, by a weak interaction between the Pt(II) atom and the chloro atom of Pt(IV) (Figure 113). The charge of the smallest unit is 4+. This kind of structure has been already observed in other publications.[183-186]

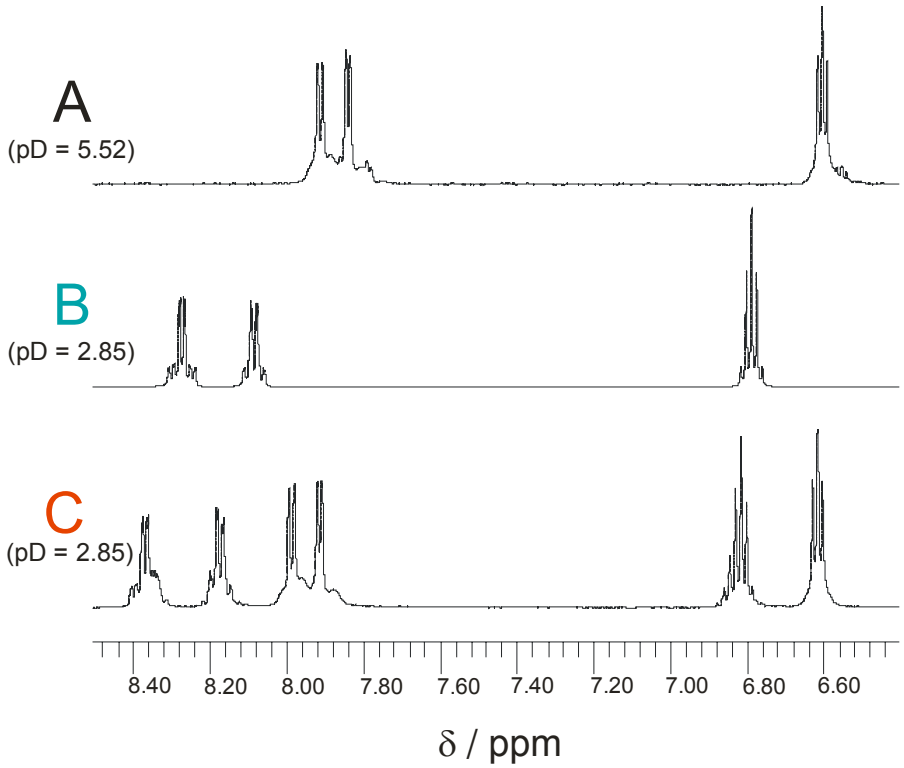

Figure 112: *Lowfield section of ^{1}H NMR of different compounds: A: trans-$[(NH_3)_2Pt(pzH)_2](NO_3)_2$; B: trans-$[(NH_3)_2Pt(pzH)_2Cl_2](NO_3)_2 \cdot H_2O$ (**30**) and C: trans,trans-$[(NH_3)_2Pt(pzH)_2Cl_2][(NH_3)_2Pt(pzH)_2](ClO_4)_4 \cdot H_2O$ (**31**).*

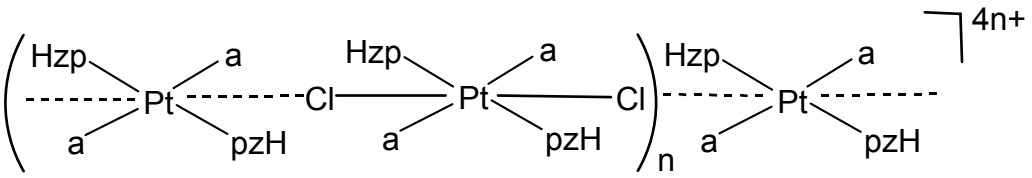

Figure 113: *Structure of (**31**) forming chains.*

2.10.1.4.1 *trans,trans,trans*-$[(NH_3)_2Pt(pzH)_2Cl_2](ClO_4)_2 \cdot H_2O$ (32)

Yellow crystals obtained after recrystallization of (**30**) from dilute $HClO_4$ were obtained. Compound (**32**) crystallizes in a centrosymmetrical space group. After refinement of the measured crystal data, the molecule was found to be in the P2(1)/c space group, having the platinum atom located in the inversion

center. All the hydrogen atoms were found in the Fourier difference and refined isotropically. Details concerning the crystal, X-ray measurement, and the refinement of data are listed in Table A-10 (see Appendix).

In (**32**) the platinum atom is coordinated to the N1 site of two pyrazole ligands, to two chloride ion and to two ammine ligand in a non-distorsioned octahedral coordination. The pyrazole ring, and its symmetry related (-x+1, -y+1, -z+1) ring are almost coplanar (Figure 114). N2 and C5 of the pyrazole were differentiated by the R value of the refinement of the data in the crystallography method.

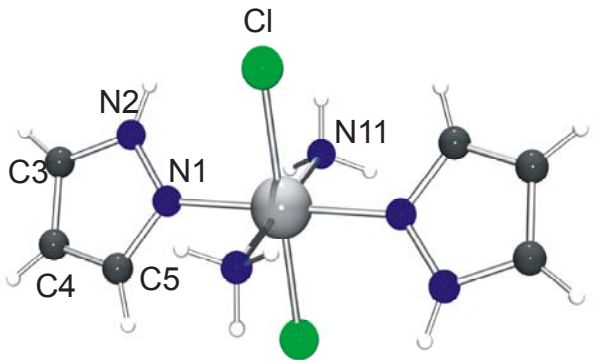

Figure 114: *View of the cation trans,trans,trans-$[(NH_3)_2Pt(pzH)_2Cl_2]^{2+}$ of (**32**) with atom numbering scheme.*

As shown in Table 26, distances and angles in the complex are not unusual. The Pt-N1 distance is 2.013(10) Å and thus similar to the corresponding distances in the N1 coordinated pyrazole ring of (**28**) (2.003(11) Å), and comparable to other Pt-N1 coordinated pyrazole ligands.[180] Also, the angle between the Pt-N_4 coordination plane and the pyrazole plane is similar to the angle between Pt-N_3Cl and the N1 coordinated pyrazole ring B in (**28**), 54.2(3)° vs. 52.0(4)°. The two pyrazole ligands are coplanar to each other. The plane containing Pt-N and the plane containing Pt-Cl are almost perpendicular (89.7(3)°). Distances and angles are compiled in Table 26.

Table 26: *Selected distances (Å) and angles (°) for non-hydrogen atoms in* ***32****.*

Pt1-N1	2.013(10)	N1-Pt-Cl	88.7(3)
Pt1-N11	2.048(9)	N11-Pt-Cl	90.3(3)
Pt1-Cl1	2.310(3)	Cl-Pt1-Cl(i)	180.0(0)
N1-N2	1.347(15)	Cl-Pt-N1(i)	91.3(3)
N1-C5	1.381(13)	Cl-Pt-N11(i)	89.7(3)
C5-C4	1.322(15)	N11-Pt-N1	90.3(4)
N2-C3	1.393(19)	N1-Pt-N11(i)	89.7(4)
C3-C4	1.354(19)		

Symmetry code: (i) -x+1, -y+1, -z+1.

As required by the centrosymmetry of (**32**), the two trans-positioned pyrazoles are in a head-tail arrangement (Figure 114). With regard to the intramolecular interactions in *trans,trans,trans*-$[(NH_3)_2Pt(pzH)_2Cl_2](ClO_4)_2 \cdot H_2O$ (**32**), the distance between N2 of the pyrazole and the chloro ligand is 3.24(1) Å, which is suitable for a H-bonding. Cl···N11 (3.09(1) Å) and Cl···C5(i) (3.21(1) Å) contacts are relatively short, but angles are unfavourable for H bonding. Intermolecular hydrogen bonds are also possible. The distance between the water molecule and the ammine group is 2.94(1) Å and the closest intermolecular contact (2.84(1) Å) is between one oxygen atom of the perchlorate anion and the water molecule (Figure 115).

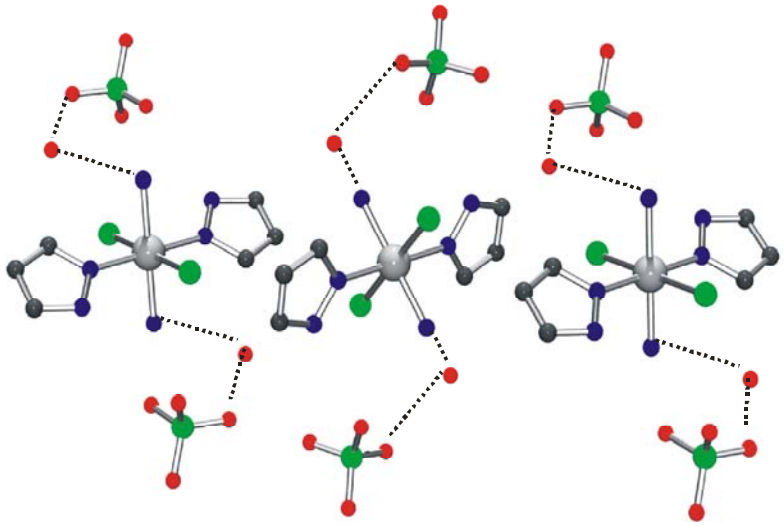

Figure 115: *View of the intermolecular hydrogen bonds in (**32**).*

The molecules are arranged in infinite chains along the a axis. There is no possibility for π-stacking interactions between the pyrazole rings (Figure 116).

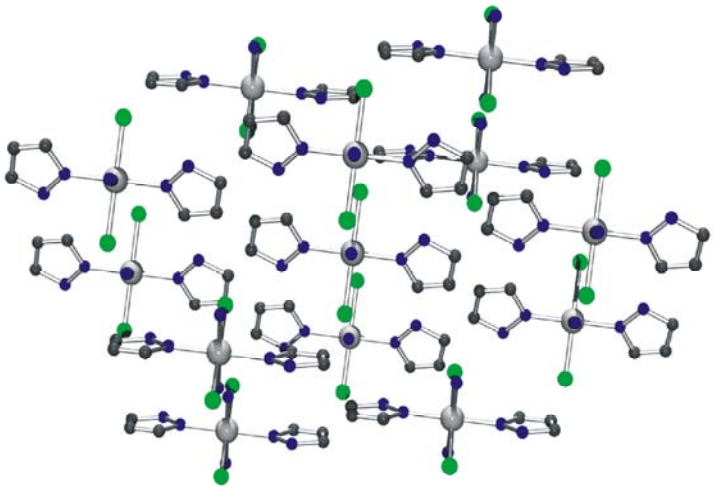

Figure 116: *View of the packing of the cations of (**32**).*

A view of the crystal packing of (**32**) with the nitrate anions and the water molcule is given in Figure 117.

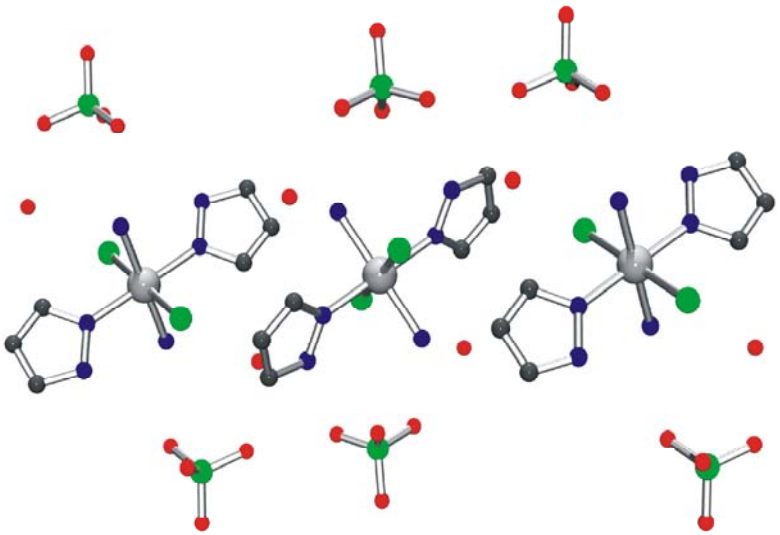

Figure 117: *View of the packing of (**20**) along the a axis.*

2.10.1.5 Reaction of *trans*-$[(NH_3)_2Pt(pzH)Cl]^+$ with 9-MeGH

Trans-$[(NH_3)_2Pt(pzH)(9\text{-MeGH-}N7)](NO_3)_2$ (**33**) was prepared by reaction of *trans*-$[(NH_3)_2Pt(pzH)(H_2O)]^{2+}$ and 9-MeGH during two days at 40°C. The ^1H NMR spectrum of a solution containing the cationic *trans*-$[(NH_3)_2Pt(pzH)(9\text{-MeGH-}N7)]^{2+}$ entity displays a singlet corresponding to the H8 proton of the guanine, two sets of doublets in corresponding to the H3 and H5 protons of the pyrazole ligand and a triplet corresponding to the H4 proton of the pyrazole in the aromatic region and a singlet corresponding to the methyl group of 9-MeGH. When the solution is in pH range from 2 to 7, the signals corresponding to the protons as well as the CH_3 singlet of 9-MeGH have chemical shifts of δ = 8.32, 7.98, 7.94, 6.61, and 3.76 ppm, respectively (Figure 118).

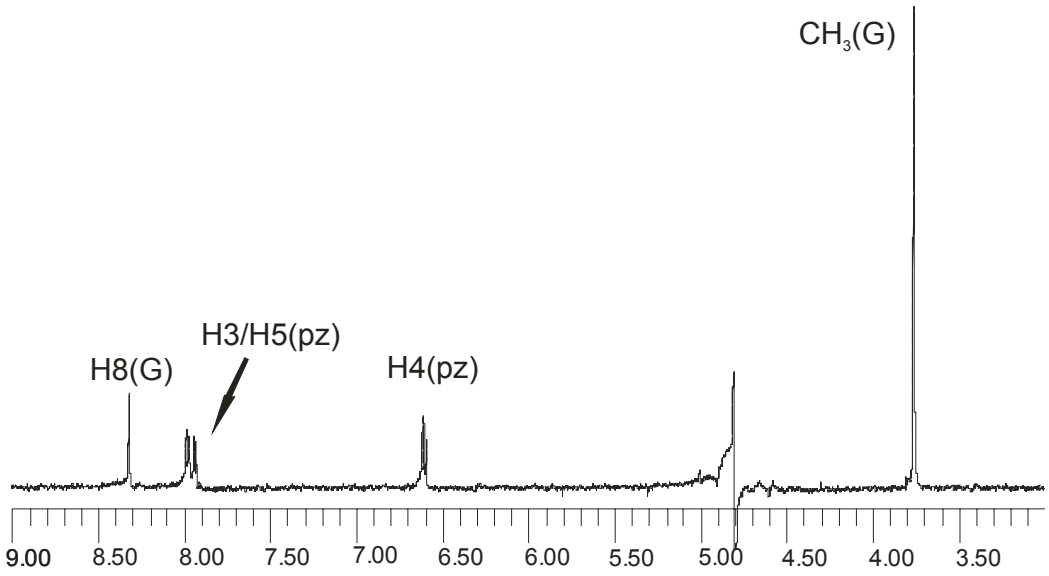

Figure 118: *Section of the ^{1}H NMR spectrum of (**33**).*

The simplicity of the ^{1}H NMR spectrum rules out any slow ligand rotation, and hence the existence of individual rotamers in solution (Figure 119).

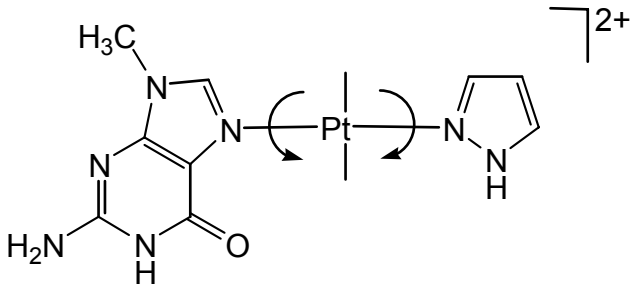

Figure 119: *View of the cation of (**33**).Possibility of rotation of the pyrazole ligand around Pt-N1 bond or rotation of the guanine nucloebase around Pt-N7.*

pD dependent ^{1}H NMR measurements have been performed with (**33**) with the aim of determining the pK_a values of the N1H position of the guanine base and the N2H site of the pyrazole. The pD dependence of the H5 proton of the pyrazole is shown in Figure 120. This resonance is practically unaffected in the pD range from 2 to 7; only above pD 7 upfield shifts are observed.

The ^{1}H NMR data for each proton were evaluated with equation (1) (see Section 2.1), which takes into account two deprotonation steps. The first one corresponds to the deprotonation of the N1H position of the 9-methylguanine and the second one corresponds to the deprotonation of the N2H of the pyrazole. The individual acidity constants pK_{a1} (for the deprotonation of N1H of guanine) and pK_{a2} (for the deprotonation of N2H of pyrazole) are displayed in Table B-25 (see Tables of pD dependences). The acidity constants, valid for the situation in D_2O, were obtained by taking the weighted mean of the individual constants pK_{a1} and pK_{a2} to give pK_{a1/D_2O} = 8.44 ± 0.09 and pK_{a2/D_2O} = 9.61 ± 0.06. The values for the situation in water were then converted to the situation in water:

$$pK_{a1/H_2O} = 7.87 \pm 0.09$$

$$pK_{a2/H_2O} = 9.03 \pm 0.06$$

Due to the platination of N1 of the pyrazole ligand, the pK_{a2/H_2O} value of N2H [180] drops by ΔpK_a = 14.21 – 9.03 = 5.18. This increase in acidity does not ensure a second platination at this site, because even at pH of 9 (where about 50% of the pyrazole ligand will be deprotonated at the N2 position) platinum (II) is still present as the hydroxo species in aqua solution. The known inertness of Pt(II)OH species probably is responsible for this lack.

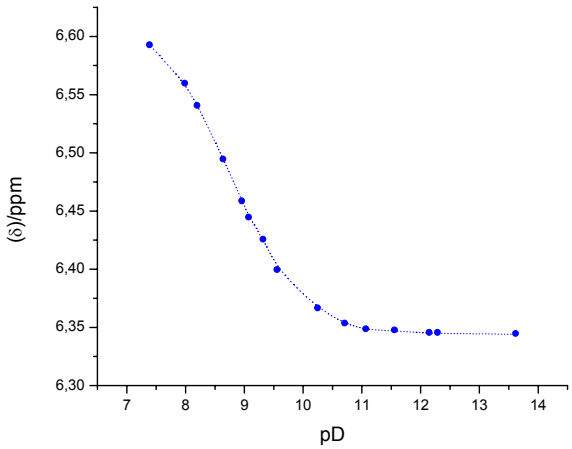

Figure 120: *pD dependent chemical shift of H5 of the pyrazole in the complex trans-[(NH$_3$)$_2$Pt(pzH)(9-MeGH-N7)](NO$_3$)$_2$ (**33**) as determined by pD dependent ^{1}H NMR measurements in D$_2$O.*

2.10.1.6 *trans,trans*-[$(NH_3)_2$Pt(9-MeGH-*N7*)(*N1*-pz-*N2*)$(NH_3)_2$Pt(1-MeC-*N3*)]$(NO_3)_3$ (34)

Unlike in the case of metalated adenine complexes, where effects of neighbour groups on the acidity of the exocyclic amino group have now been rationalized, variations in pK_a values of the N(1)H proton of N7 platinated guanine ligands are practically not understood. We hypothesized, that in analogy to the situation with deprotonated amino groups of adenine, a suitably positioned H bonding donor might lower the pK_a also of guanine – N(1)H.

For this purpose, and based on model building, the mixed guanine/pyrazolate/cytosine complex (**34**) (Figure 121) was designed and synthesized. Thus, one equivalent of *trans*-[$(NH_3)_2$Pt(1-MeC-*N3*)(H_2O)]$^{2+}$ was added to a solution containing *trans*-[$(NH_3)_2$Pt(pzH)(9-MeGH-*N7*)]$^{2+}$ and subsequent was added NaOH until pH ~ 7.5 was reached. At this pH, the pyrazole ligand is not completely deprotonated at the N2 position (pK_{a2/H_2O} ~ 9.03), but at higher pH´s there is a competition between the platination at N2 and the formation of substitutionally inert hydroxo species.

The reaction was followed by ^{1}H NMR spectroscopy. Complex *trans,trans*-[$(NH_3)_2$Pt(9-MeGH-*N7*)(*N1*-pz-*N2*)$(NH_3)_2$Pt(1-MeC-*N3*)]$(NO_3)_3$ (**34**) could be identified by ^{1}H spectroscopy in D_2O. The resonances show the existence of rotamers, which are either due to the rotation of the cytosine ligand around bond Pt-N2 (pyrazole) or to the rotation of the guanine ligand Pt-N7 (Figure 121). It was not possible to isolate (**34**) in pure form, but only in a mixture with the starting compound *trans*-[$(NH_3)_2$Pt(pzH)(9-MeGH-*N7*)]$^{2+}$ (**33**). The resonances of (**34**) are summerized in Table 27.

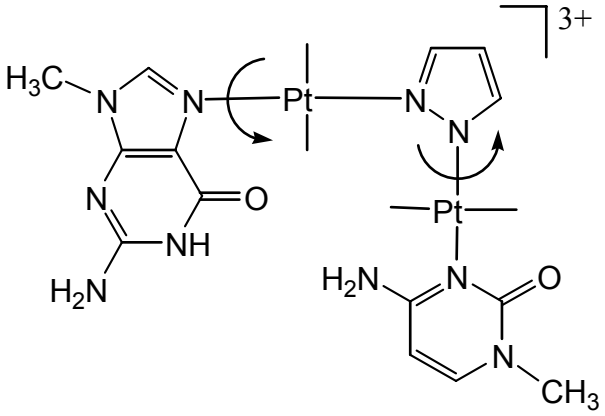

Figure 121: *Possible rotation of guanine or cytosine ligand, which leads to the formation of rotamers.*

Table 27: *Chemical shifts of the resonances corresponding to the complex (**34**) in D_2O, pD ~ 7.8.*

Signals	ppm	
CH_3(C)	3.49 / 3.47	s
CH_3(G)	3.78 / 3.75	s
H5(C)	6.12 / 6.09	d
	6.08 / 6.06	d
H6(C)	7.68 / 7.65	d
	7.67 / 7.63	d
H5(pz)	6.47	m
H6(pz)	7.93	m
H8(G)	8.20 / 8.42	s

The pD dependent ^{1}H NMR spectra of (**34**) were recorded (in the mixture with (**33**)). Although not carried out in an extensive way, it was clearly evident, that there was no significant deprotonation of the guanine ligand in (**34**) below pH 8 (calculated for H_2O). This means that it is in the normal range of N7 platinated guanine ligands, and there is no effect of the cytosine ligand at “the other end” of the pyrazolate ligand. Hence, one has to conclude that there is no

close distance between N1 of guanine and N(4)H_2 of cytosine. The original hope (see Chapter 2.10) of markedly reducing the pK_a of guanine – N(1)H thus did not realize.

3 EXPERIMENTAL SECTION

3.1 Instrumentation and Measurements

3.1.1 Determination of pH- and pD-values

The pH (uncorrected pH*) of a D_2O solution was determined by use of a glass electrode on a Metrohm 6321 pH meter. pD values were obtained after addition of 0.4 units to the value displayed on the pH meter[28]. Measurement of the pD dependences were carried out using identical samples, in which the pD of the solutions was modified in small increments by addition of small amounts of DNO_3 and/or NaOD. Due to the limitations of the AgCl glass electrodes, it was not possible to get reliable measurements at pH values close to 14.

3.1.2 NMR Spectroscopy

One- and two-dimensional ^1H NMR spectra were recorded on a Varian Mercury 200 FT NMR, on a Bruker DRX 300, on a Bruker DRX 400 and on a Varian Inova 600 MHz by or with the collaboration of Prof. Burkhard Costisella and Anette Danzmann. TSP (sodium 3-trimethylsilyl-propanesulfonate) (δ = 0 ppm) and/or TMA (tetramethylammonium bromide) (δ = 3.18 ppm) were used as internal standards.

^{195}Pt NMR spectra were recorded by Dr. Pablo Sanz on a Bruker DRX 300. Na_2PtCl_6 and/or K_2PtCl_4 were used as external and/or internal standards, respectively. In the case of internal standards for ^{195}Pt NMR (in D_2O), a capillary tube containing a solution of K_2PtCl_4 (or Na_2PtCl_6) in H_2O was introduced in the sample acting as standard. To fill up a capillary tube of glass ($\varnothing$ = 0.5mm), a tube closed at the bottom was slightly heated and face down introduced in a solution containing the standard. After filling, the tube had to be centrifuged and closed at the top. The standard Na_2PtCl_6 displays a signal at 0 ppm. However,

K_2PtCl_4 displays rapidly two signals due to hydrolysis in water. These are at -1625 ppm ($[PtCl_4]^{2-}$) and at -1181 ppm ($[PtCl_3(H_2O)]^-$).

The pK_a value was obtained after evaluating the chemical shift (δ) data at different pD with a Newton-Gauss non-linear least-squares curve fitting procedure as described in Section 2.1.[30]

3.1.3 IR Spectroscopy

IR spectra were taken on a Perkin-Elmer 580 B FT spectrometer. Measurements (KBr) were performed from 4000 to 250 cm^{-1}. The treatment and evaluation of the spectra was done with the help of the program Opus-IR.

3.1.4 Elemental Analysis

The contents of carbon, hydrogen and nitrogen were determined on a Carlo-Erba-Strumentazione 1106 Element Analyzer by Markus Hüffner.

3.1.5 X-Ray Crystallography

Data collection was performed on an Enraf-Nonius Kappa CCD diffractometer at the University of Dortmund using graphite-monochromated Mo-Kα radiation (λ= 0.71069 Å)[187]. Data reduction and cell refinement were carried out using the programs DENZO and SCALE-PACK[188]. Intensities of reflections were collected at room temperature, 293(2)º. All the structures were solved by standard Patterson methods[189] and refined by full-matrix least-squares methods based on F^2 using the SHELXTL-PLUS[190], SHELXL-97[191] and WinGX[192] programs. In the refinement process of the X-ray data, if not

specified, all non-hydrogen atoms of the crystal were refined anisotropically, and all the hydrogen atoms except those of the water molecules were included in geometrically calculated positions and refined with isotropic displacement parameters according to the riding model.

The production of the diagrams was achieved with the programs "Ortep-3 for Windows"[193], and "Persistence of Vision Raytracer (POV-Ray)"[194].

3.1.6 DFT Calculations

The DFT calculations for the gas-phase optimized structures were performed by Patrick Lax using the computer program Gaussian 98.[57] The optimization was followed by a frequency calculation in order to confirm every structure to be a minimum structure. The built in combination of Becke's three-parameter hybrid function [195] with Lee-Yang-Parr's exchange functional[196] was applied. Pt atom was described with the LANL2DZ basis set. For the lighter atoms H, C, N and O a 6-31G* basis set was used.

3.2 Synthesis of Complexes

3.2.1 Materials

The model nucleobases 9-methylguanine and 9-ethylguanine were purchased from Fa. Chemogen, Konstanz (Germany). 9-Ethyladenine,[197] 1-methylcytosine,[198] 6,9-Dimethyladenine[134] and 9-methyladenine[46] were synthesized as described. All the other chemicals used (either *puriss* or *pro analysi*) were from Merck GmbH, Darmstadt (Germany), Fluka AG, Buchs (Switzerland) or Aldrich-Chemical Co. Ltd., Gillingham-Dorset (UK).

K_2PtCl_4, from which *trans*-$(NH_3)_2PtCl_2$,[199] *cis*-$(NH_3)_2PtCl_2$,[200] and [dienPtI]I[201] were prepared according to the literature, was from Heraeus

GmbH, Hanau (Germany). [dienPdI]I was synthesized according to ref. 201, but using K_2PdCl_4.

The following Pt^{2+} complexes were needed for further syntheses (see Section 3.2.2): *trans*-[$(NH_3)_2$Pt(1-MeC-*N3*)Cl]NO_3 was obtained in aqueous solution following the procedure described in ref 202. The complex [Pt(1-MeC-*N3*)$_3$Cl](NO_3) was synthesized according to a prescription in ref. 94. The compounds [(dien)Pt(9-MeA-*N1*)]$(NO_3)_2$ (**1**), *trans*-[$(NH_3)_2$Pt(9-EtA-*N1*)(9-MeGH-*N7*)]$(NO_3)_2$ and *trans*-[{$(NH_3)_2$Pt(1-MeC-*N3*)}$_2$(9-MeA-*N1*,*N7*)]$(ClO_4)_4$ (**7**) were kindly provided by Prof. Dr. Bernhard Lippert. The synthesis of *trans*-[$(NH_3)_2$Pt(9-MeA-*N7*)$_2$]$(ClO_4)_2\cdot 2H_2O$ (**2**) is described in ref. 203. *Cis*-[$(NH_3)_2$Pt(9-MeA-*N7*)$_2$]$(NO_3)_2\cdot 2H_2O$ (**4**) was obtained according to the method given in ref. 204, whereas *trans*-[$(NH_3)_2$Pt(9-MeGH-*N7*)Cl]Cl was prepared analogously to ref. 205. The compounds (1,9-DimeAH)(ClO_4) and 6,9-DimeA were kindly provided by Dr. Michael Roitzsch. *Trans*-[$(NH_3)_2$Pt(pzH)$_2$]$(NO_3)_2$ and *trans*-[$(NH_3)_2$Pt(pzH)Cl](NO_3) (**28**) were synthesized according to ref. 181.

The deuterated solvents DMSO-*d6*, DMF-*d7* and D_2O were obtained from Deutero GmbH, Kastellaun (Germany), Cambridge Isotope Laboratories (CIL) and from Andoner (USA), respectively.

3.2.2 Preparation of Compounds

3.2.2.1 *cis*-[$(NH_3)_2$Pt(1-MeC-*N3*)(*N7*-9-MeA-*N1*)(dienPt)]$(ClO_4)_4$ (5)

This compound was prepared on an NMR spectroscopy scale in D_2O solution from *cis*-[$(NH_3)_2$Pt(9-MeA-*N7*)(1-MeC-*N3*)]$(ClO_4)_2\cdot H_2O$ (**2**) by treating it with [(dien)Pt(D_2O)]$^{2+}$ (1:1, 3 days, 40°C). At this stage formation of a single new species was evident, clearly separted from signals of the starting compound, the resonances of which had dissapeared.

^{1}H NMR:

9-MeA: (D_2O, pD = 4.8, δ/ppm): 8.76,brs, H2; 8.70, s, H8; 3.89, s, CH_3

1-MeC: (D_2O, pD = 4.8, δ/ppm): 7.56, d (^3J = 7.2 Hz), H6; 6.22, d (^3J = 7.2 Hz), H5, 3.36, s, CH_3
dienPt: (D_2O, pD = 4.8, δ/ppm): 3.35, 3.29, 3.12, 3.09, 2.93, 2.90, m, CH_2

The assigment of H8 of 9-MeA was confirmed by a 1D NOE experiment; the relative intensities of all resonances are as expected for the composition.

3.2.2.2 *trans*-[$(NH_3)_2$ClPt(*N7*-9-MeA-*N1*)(dienPt)]$(ClO_4)_3$ (8)

[(dien)Pt(9-MeA-*N1*)]$(NO_3)_2$ (**1**) (760.57 mg, 1.33 mmol) and *trans*-$(NH_3)_2PtCl_2$ (798.7 mg, 3.66 mmol) were dissolved in 50 ml of water at pH 4.13. The solution was stirred at 45°C for one day. Then the solution was cooled to 4°C and the precipitated excess of *trans*-$(NH_3)_2PtCl_2$ was removed. After addition of 2 eq. of $NaClO_4 \cdot H_2O$, the solution was concentrated to 20 ml by rotaevaporation. The residue remaining after evaporation was recrystallized from water to give 204 mg (0.21mmol) of (**8**) in 15.8 % yield.

Elemental analysis:
$C_{10}H_{26}N_{10}Pt_2Cl_4O_{12}$, M = 1010.35 g·mol^{-1}
Calculated: C 11.9 %, H 2.6 %, N 13.9 %
Obtained: C 11.8 %, H 2.6 %, N 14.3 %

^{1}H NMR:
(D_2O, pD = 4.9, δ/ppm): 8.86, s, H8; 8.8, brs, H2; 3.95, s, CH_3

3.2.2.3 *trans*-[$(NH_3)_2$Pt(*N7*-9-MeA)(*N7*-9-MeA-*N1*)(dienPt)]$^{4+}$ (9)

This compound was prepared on an NMR spectroscopy scale in D_2O solution from *trans*-[$(NH_3)_2$Pt(9-MeA-*N7*)$_2$]$(ClO_4)_2 \cdot 2H_2O$ (**2**) by treating it with [(dien)Pt(D_2O)]$^{2+}$ (1:1). After stirring the solution one day at 40°C, a mixture of three compounds was obtained: (**2**), (**10**) and (**9**). This assignment of the three compounds was done according to the pD dependence of the different

compounds. The differentation of species was easy if resonances of the methyl group protons were evaluated, yet difficult for the heteroaromatic protons.

^{1}H NMR:
Pt(*N7*-9-MeA-*N1*): (D_2O, pD = 10.3, δ/ppm): 3.97, s, CH_3
Pt(*N7*-9-MeA): (D_2O, pD = 10.3, δ/ppm): 3.88, s, CH_3

3.2.2.4 *trans*-$[(NH_3)_2Pt\{(N7\text{-}9\text{-}MeA\text{-}N1)(dienPt)\}_2]^{6+}$ (10)

This compound was prepared on an NMR spectroscopy scale in D_2O solution from *trans*-$[(NH_3)_2Pt(9\text{-}MeA\text{-}N7)_2](ClO_4)_2 \cdot 2H_2O$ (**2**) by treating it with $[(dien)Pt(D_2O)]^{2+}$ (1:2). After stirring the solution three days at 40°C, compound (**10**) had formed. The relative intensities of all resonances are as expected for the composition. The yield was 85%.

^{1}H NMR:
(9-MeA): (D_2O, pD = 8.30, δ/ppm): 8.86, s, H8; 8.80, brs; 4.00 s, CH_3

3.2.2.5 *cis*-$[(NH_3)_2Pt\{(N1\text{-}9\text{-}MeA\text{-}N7)Pt(NH_3)_3\}_2](NO_3)_6 \cdot 2H_2O$ (11)

$[(NH_3)_3Pt(9\text{-}MeA\text{-}N7)]Cl(NO_3) \cdot H_2O$[206] (0.62 mmol) was initially converted into the NO_3^- salt by treatment with $AgNO_3$ (0.62 mmol) in water. After stirring for one day at room temperature, the precipitated AgCl was removed. The solution was combined with *cis*-$[(NH_3)_2Pt(H_2O)_2](NO_3)_2$, which was prepared from *cis*-$(NH_3)_2PtCl_2$ (0.31 mmol) and $AgNO_3$ (0.62 mmol) in water.

In order to isolate this compound, the solution was allowed to evaporate at RT. Thus, colourless crystals were obtained.

This compound has previously been characterized by ^{1}H NMR, Raman spectroscopy and X-ray crystallography.[53]

^{1}H NMR:

9-MeA: (D_2O, pD = 5.97, δ/ppm): 9.10, s, H2; 8.78, s, H8 and 9.00, s, H2 (rotamers); 3.88, s, CH_3

3.2.2.6 *cis*-[$(NH_3)_2$Pt{(*N7*-9-MeA-*N1*)(dienPt)}$_2$]$(NO_3)_6$ (12)

4,2 mg of *cis*-[$(NH_3)_2$Pt(9-MeA-*N7*)$_2$]$(NO_3)_2 \cdot 2H_2O$ (0.0061 mmol), 0.066 g of [(dien)PtI]I (0.12 mmol), and 0.041 g of $AgNO_3$ (0.24 mmol) were stirred in 50 ml of water at 40°C for three days. The AgI formed was eliminated by centrifugation. The resulting solution was brought to dryness by rotary evaporation. The compound was pure according to ^{1}H NMR (relative intensities).

The yield was 15.3% (0.0302 g).

^{1}H NMR:

9-MeA: (D_2O, pD = 5.6, δ/ppm): 8.80, brs, H2; 8.72, s, H8; 3.84, s, CH_3

dienPt: (D_2O, pD = 5.6, δ/ppm): 3.34, 3.29, 3.12, 3.09, 2.93, 2.90, m, CH_2

The assigment of H8 of 9-MeA was again established by an NOE experiment; at pD > 8.2, the H2 resonance disappears because of isotopic exchange.

3.2.2.7 *trans,trans,trans*-[$(NH_3)_2$Pt(*N7*-9-MeA-*N1*)(dienPt)(*N7*-9-EtA-*N1*){$(NH_3)_2$Pt(9-MeGH-*N7*)}]$^{6+}$ (13)

Complex (**8**) (136.13 mg, 0.13 mmol), *trans*-[$(NH_3)_2$Pt(9-EtA-*N1*)(9-MeGH-*N7*)]$(NO_3)_2$ (91.77 mg, 1 eq) and $AgNO_3$ (22.88 mg, 1 eq) were stirred for five days at 40°C in 80 ml of water. After removal of AgCl, the solution was slowly concentrated at room temperature. A few small colourless needles of (**13**) were obtained, which were suitable for X-ray analysis. The solution contained also a white precipitate, which according to ^{1}H NMR was also (**13**).

^{1}H NMR:

9-MeA: (D_2O, pD = 8.0, δ/ppm): 4.04, s, CH_3

9-EtA: (D_2O, pD = 8.0, δ/ppm): 4.49, q, CH_2; 1.61, t, CH_2
9-MeG: (D_2O, pD = 8.0, δ/ppm): 3.80, s, CH_3

No attempt to assign the heteroaromatic protons was made.

3.2.2.8 *trans*-[{$(NH_3)_2$Pt(1-MeC-*N3*)}$_2$(9-MeA-*N7*,*N6*)]$(ClO_4)_3 \cdot 3.5H_2O$ (15)

trans-[{$(NH_3)_2$Pt(1-MeC-*N3*)}$_2$(9-MeA-*N1*,*N7*)]$(ClO_4)_4$ (**7**) (50 mg, mmol) was dissolved in water (2 ml, brief heating) and the pH value was raised from 4.4 to 11 by adding 1M NaOD. The sample was lyophilized and subsequently dissolved in D_2O (1ml), and then the solution was kept in a closed vial until crystals of (**15**) appeared after several days.

The complex was characterized by X-ray crystallography.

3.2.2.9 [(9-MeA-*N7*)Pt$(NH_3)_3$]$Cl_2 \cdot 2H_2O$ (16)

9-MeA (4 mmol) was reacted with K_2PtCl_4 (4 mmol) in 250 ml of water at 55°C for 20 min.[206] After that, the mixture was stirred for 6 hours at room temperature. The yellow precipitate was removed by filtration and washed with 5 ml of cold water. The yellow compound was [$PtCl_3$(9-MeAH-*N7*)]. This compound was dissolved in water and 80 ml of NH_3 (25%) were added. After stirring for one day, the precipitate was removed and the volume was reduced to 30 ml. The pH of the solution was adjusted to pH 4.0 (HNO_3, 0.1N). The solution was allowed to evaporate at 4°C. Colourless crystals of (**16**) were isolated from it and characterized by X-ray crystallography. The yield was 82%.

Elemental analysis:
$C_6N_8H_{20}PtCl_2O_2$, M = 502.26 g·mol^{-1}
Calculated: C 14.3 %, H 4.0 %, N 22.3 %
Obtained: C 14.3 %, H 4.0 %, N 22.5 %

3.2.2.10 *cis*-[$(NH_3)_2$Pt(*N1*-9-MeA-*N7*)(*N6*-9-MeA-*N7*){Pt$(NH_3)_3\}_2]^{5+}$ (17)

To a solution of *cis*-[$(NH_3)_2$Pt{(*N1*-9-MeA-*N7*)Pt$(NH_3)_3\}_2](NO_3)_6 \cdot 2H_2O$ (**11**) in 1ml of D_2O was added 1M NaOH. When the pH was ca. 9, the solution was kept at room temperature. After one month, a ^1H NMR spectrum was recorded and the signals observed were assigned to compound (**17**), due to the two different signals of the methyl groups and their relative intensities. (**17**) has not been isolated.

3.2.2.11 *cis*-[$(NH_3)_2$Pt(*N6*-9-MeA-*N7*)$_2${Pt$(NH_3)_3\}_2](NO_3)_4 \cdot 6H_2O$ (18)

cis-[$(NH_3)_2$Pt{(*N1*-9-MeA-*N7*)Pt$(NH_3)_3\}_2](NO_3)_6 \cdot 2H_2O$ (**11**) (60mg) was dissolved in 1.2 ml D_2O. The pH value was raised from 5.4 to 10 by adding 1M NaOD. The sample was lyophilized and subsequently dissolved in D_2O (1ml), and then the solution was kept in a closed vial until crystals of (**18**) appeared after several weeks. The composition of (**18**) was confirmed by X-ray crystallography.

3.2.2.12 [{(dien)Pd$\}_3$(9-MeA-*N1*,*N7*,*N6*)]$Cl_{3.5}(PF_6)_{1.5} \cdot 3H_2O$ (19)

[dienPdI]I (85.8 mg, 0.18 mmol) and $AgPF_6$ (89 mg, 0.36 mmol) were suspended in 10 ml of water and stirred in the dark for 24 hours at 40°C. After removal of AgI,1/2 eq of 9-MeA (13.8 mg, 0.09 mmol) in 5 ml water was added. The pH of the solution was adjusted to 11 with a solution of NaOH/NaCl. After stirring for one hour at 40°C, another equivalent of $[dienPd(H_2O)]^{2+}$ was added. The mixture was stirred for two more hours at 40°C. The solution was subsequently allowed to crystallize (4°C). Formation of small yellow crystals was observed. After isolation, the crystals were characterized by X-ray crystallography.

3.2.2.13 [Pt(1-MeC-*N3*)$_3$(OH)]$(ClO_4)_{0.5}(OH)_{0.5} \cdot 7H_2O$ (21)

[Pt(1-MeC-*N3*)$_3$Cl](NO_3) (160 mg, 0.23 mmol) and 9-MeA (34.3 mg, 0.23 mmol) were combined in 30 ml of water and $AgNO_3$ (39.07 mg, 0.23 mmol) was added.

Then 1N HNO_3 was added dropwise to reach pH 1-2. The mixture was stirred at 40°C for 7 days in the dark. Then AgCl was filtered off and the resulting solution was concentrated to 10 ml volume by rotary evaporation. Then the pH was adjusted to 10 (1M NaOH) and the solution was kept in a closed vial in the refrigerator. After several days, a small amount of unreacted [Pt(1-MeC-*N3*)$_3$Cl](NO_3) was filtered off. Further evaporation led to colourless needles of (**21**).

^{1}H NMR

1-MeC (*trans* to OH group): (D_2O, pD = 7.1, δ/ppm): 7.43, d, (^{3}J = 7.4 Hz) H6; 5.89, d, H5; 3.35, s, CH_3; 1-MeC (*cis* to OH group): 7.54, d, (^{3}J = 7.4 Hz) H6; 5.96, d, H5; 3.41, s, CH_3

3.2.2.14 *trans*-[$(NH_3)_2$Pt(1,9-DimeAH-*N7*)(9-MeGH-*N7*)]$(NO_3)_2$ (23)

trans-[$(NH_3)_2$Pt(9-MeGH-*N7*)Cl]Cl (3.5 mg, 7.5 mmol) was stirred in 60 µl of D_2O at 40°C in the dark overnight. After removal of AgCl, (1,9-DimeAH)(ClO_4) (1.99 mg, 1 eq) was added, the pH of the solution adjusted to 1.3 (NaOD) and stirred at 40°C for three days. The signals of the resonances in the ^{1}H NMR spectrum were assigned to (**23**), according to the relative intensities.

^{1}H NMR:

1,9-DimeAH: (D_2O, pD = 8.7, δ/ppm): 8.61, s, H8; 8.34, s, H2; , s, 3.89, s, N9-CH_3; 3.77, s, N1-CH_3

9-MeGH: (D_2O, pD = 8.7, δ/ppm): 8.22, s, H8; 3.62, s, CH_3

3.2.2.15 *trans*-[$(NH_3)_2$Pt(6,9-DimeA-*N7*)(1-MeC-*N3*)]$(NO_3)_2$ (24)

trans-[$(NH_3)_2$Pt(1-MeC-*N3*)Cl](NO_3) (145.94 mg, 0.32 mmol), 6,9-DimeA (52.72 mg, 1 eq) and $AgNO_3$ (54.88 mg, 1 eq) were stirred in 50 ml water at 40°C for 3 days in the dark. After filtration of AgCl, the filtrate was evaporated slowly by

rotary evaporation to 10 ml volume. The solution was then allowed to evaporate at 4°C. Eventually, colourless crystals were obtained. The yield was 65%.

Elemental analysis:

$C_{12}N_{12}H_{24}PtO_9$, M = 675.48 g·mol^{-1}

Calculated: C 21.3 %, H 3.6 %, N 24.9 %

Obtained: C 21.3 %, H 3.8 %, N 24.8 %

^{1}H NMR:

6,9-DimeA: (D_2O, pD = 6.3, δ/ppm): 8.56, s, H8; 8.44, s, H2; , s, 3.94, s, N9-CH_3; 3.53, s, N6-CH_3

1-MeC: (D_2O, pD = 6.3, δ/ppm): 7.69, d, H6; 6.09, d, H5; 3.35, s, CH_3

3.2.2.16 *trans*-[$(NH_3)_2$Pt(6,9-DimeA-*N7*)(9-MeGH-*N7*)]$(NO_3)_2$·5H_2O (25)

trans-[$(NH_3)_2$Pt(9-MeGH-*N7*)Cl]Cl (159.816 mg, 0.34 mmol) was stirred together with 6,9-DimeA (56.06 mg, 0.34 mmol) and AgCl (116.72 mg, 0.68 mmol) in 50 ml of water at 40°C in the dark for three days. The initial pH was 5.8. AgCl was then removed by filtration and the resulting solution was concentrated to 10 ml volume by rotary evaporation. After cooling the solution to 4°C for one week, a white precipitate was filtered off and recrystallized from water. Crystals suitable for X-ray crystallography were obtained. The yield was 32%.

^{1}H NMR:

6,9-DimeA: (D_2O, pD = 6.4, δ/ppm): 8.43, s, H8; 8.67, s, H2; , s, 3.94, s, N9-CH_3; 3.78, s, N6-CH_3

9-MeGH: (D_2O, pD = 6.4, δ/ppm): 8.33, s, H8; 3.32, s, CH_3

3.2.2.17 *trans*,*trans*,*trans*-{$(NH_3)_2Pt(N1\text{-pz-}N2)_2[(NH_3)_2Pt(1\text{-MeC-}N3)]_2\}^{6+}$ (29)

A solution containing *trans*-$[(NH_3)_2Pt(pzH)_2](NO_3)_2$ (52 mg, 0.11 mmol), *trans*-$[(NH_3)_2Pt(1\text{-MeC-}N3)Cl]NO_3$ (96 mg, 0.22 mmol) and $AgNO_3$ (36 mg, 0.11 mmol) were brought to pH 8.3 with 1M NaOH. The mixture was then stirred at 40°C in the dark for 7 days in 50 ml of H_2O. After removal of AgCl, the solution was concentrated to 10 ml volume and cooled to 4°C. Excess of *trans*-$[(NH_3)_2Pt(1\text{-MeC-}N3)Cl]NO_3$ was filtered off, and the solution was concentrated by slow evaporation. A precipitate was obtained, which was assigned to complex (**29**), based on the relative intensities of the ^{1}H NMR resonances.

^{1}H NMR:

1-MeC: (D_2O, pD = 5.6, δ/ppm): 7.68, d, (^3J = 7.5 Hz) H6; 6.09, d, H5; 3.51, s, CH_3

pzH: (D_2O, pD = 5.6, δ/ppm): 7.96, d, H3; 7.72, d, H5; 6.50, t, H4

3.2.2.18 *trans*-$[(NH_3)_2Pt\{(pzH)Cl\}_2](NO_3)_2\cdot H_2O$ (30)

A solution containing *trans*-$[(NH_3)_2Pt(pzH)Cl](NO_3)$ (**28**) was heated at 50°C to dryness and subsequently dissolved in water. Yellow crystals were collected by filtration and characterized by X-ray crystallography. The yield was 64%.

Elemental analysis:

$PtCl_2C_6H_{16}N_8O_9$, M = 596.24 g·mol^{-1}

Calculated:	C 12.1 %,	H 3.0 %,	N 18.8 %
Obtained:	C 12.0 %,	H 3.0 %,	N 19.1 %

^{195}Pt NMR: -385 ppm

3.2.2.19 *trans*,*trans*-$[(NH_3)_2Pt(pzH)_2Cl_2][(NH_3)_2Pt(pzH)_2](ClO_4)_4 \cdot H_2O$ (31) and *trans*-$[(NH_3)_2Pt\{(pzH)Cl\}_2](ClO_4)_2 \cdot H_2O$ (32)

Compound (**30**) (20 mg, 0.03 mmol) was dissolved in 30 ml of water at 40°C. After addition of 1M $HClO_4$, the solution was allowed to evaporate at 4°C. Red crystals and subsequently yellow crystals appeared, which were separated mechanically under a microscope. The red ones correspond to compound (**31**) and the yellow ones to (**32**). The yield was 71%.

Elemental analysis: (**31**)

$PtC_6H_{14}N_6Cl_3O_9$, M = 615.65 g·mol^{-1}

Calculated:	C 11.7 %,	H 2.3 %,	N 13.6 %
Obtained:	C 11.8 %,	H 2.3 %,	N 13.7 %

Elemental analysis: (**32**)

$PtCl_4C_6H_{16}N_6O_9$, M = 653.12 g·mol^{-1}

Calculated:	C 11.0 %,	H 2.5 %,	N 12.9 %
Obtained:	C 11.1 %,	H 2.7%,	N 13.2%

3.2.2.20 *trans*-$[(NH_3)_2Pt(pzH)(9\text{-MeGH-}N7)](NO_3)_2$ (33)

trans-$[(NH_3)_2Pt(pzH)Cl](NO_3)$ (**28**) (142 mg, 0.36 mmol), $AgNO_3$ (61 mg, 0.36 mmol) and 9-MeGH (59.4 mg, 0.36 mmol) were dissolved in 200 ml of water. The pH was brought from 3.5 to 4.5 with 1 NaOH. The mixture was stirred at 40°C in the dark for two days. AgCl was filtered off and the solution was evaporated to near dryness. The yield was about 85%. The white solid was characterized by ^{1}H NMR and elemental analysis.

Elemental analysis:

$C_9H_{17}N_{11}O_7Pt$, M = 586.38 g·mol^{-1}

Calculated:	C 18.4 %,	H 2.9 %,	N 26.3 %
Obtained:	C 18.2 %,	H 3.0 %,	N 26.2 %

^{1}H NMR:

9-MeGH: (D_2O, pD = 4.3, δ/ppm): 8.32, s, H8; 3.76, s, CH_3

pzH: (D_2O, pD = 4.3, δ/ppm): 7.98, d, (^3J = 8.8 Hz) H3; 7.94, d, H5; 6.61, t, H4

3.2.2.21 *trans,trans*-[$(NH_3)_2$Pt(9-MeGH-*N7*)(*N1*-pz-*N2*)$(NH_3)_2$Pt(1-MeC-*N3*)]$(NO_3)_3$ (34)

This compound was prepared on an NMR scale in D_2O solution from *trans*-[$(NH_3)_2$Pt(pzH)(9-MeGH-*N7*)]$(NO_3)_2$ (**33**) by treating it with *trans*-[(NH_3)Pt(1-MeC-*N3*)$(D_2O)]^{2+}$ (1:1). The pH was adjusted to 7.5. After stirring the solution three days at 40°C, signals corresponding to (**34**) appeared, which relative intensities were as expected.

4 Appendix; X-Ray Tables

Table A-1: *Crystallographic data for compound* ***8****.*

Compound	*trans*-[$(NH_3)_2$ClPt(*N7*-9-MeA-*N1*)(dienPt)]$(ClO_4)_3$
Formula	C_{10} H_{27} Cl_4 N_{10} O_{12} Pt_2
Formula weight (g mol^{-1})	1011.4
Crystal color and habit	yellow blocks
Space system	triclinic
Space group	P-1
a (Å)	8.8200(18)
b (Å)	10.749(2)
c (Å)	28.322(6)
α (º)	90.01(3)
β (º)	93.32(3)
γ (º)	92.02(3)
Z	4
V ($Å^3$)	2678.9(9)
ρ_{calc} (g cm^{-1})	2.508
μ (Mo Kα) (mm^{-1})	10.904
F(000)	1908
θ range (º)	3 - 28
No. reflections collected	11428
No. reflections observed I>2σ(I)	7412
No. parameters refined	685
R_1 (obs. data)	0.054
wR2 (obs. data)	0.1079
Goodness-of-fit, S	1.06
Residual ρ_{max}, ρ_{min} (e $Å^{-3}$)	1.562, -1.281

Table A-2: *Crystallographic data for compound* ***15***.

Compound	*trans*-[{$(NH_3)_2Pt(1\text{-}MeC\text{-}N3)$}$_2$(9-MeA-*N7*,*N6*)]$(ClO_4)_3 \cdot 3.5H_2O$
Formula	$C_{16}\ H_{39}\ Cl_3\ N_{15}\ O_{17.5}\ Pt_2$
Formula weight (g mol^{-1})	1211.04
Crystal color and habit	colourless blocks
Space system	monoclinic
Space group	$P2_1/c$
a (Å)	11.845(2)
b (Å)	15.317(3)
c (Å)	21.292(4)
α (º)	90.00
β (º)	94.43(3)
γ (º)	90.00
Z	2
V (Å^3)	3851.5(12)
ρ_{calc} (g cm^{-1})	2.101
μ (Mo Kα) (mm^{-1})	7.551
F(000)	2348
θ range (º)	3 - 27
No. reflections collected	9662
No. reflections observed I>2σ(I)	6064
No. parameters refined	512
R_1 (obs. data)	0.0476
wR2 (obs. data)	0.1097
Goodness-of-fit, S	0.967
Residual ρ_{max}, ρ_{min} (e Å^{-3})	2.486, -2.141

Table A-3: *Crystallographic data for compound* ***16***.

Compound	[(9-MeA-*N7*)$Pt(NH_3)_3$]$Cl_2 \cdot 2H_2O$
Formula	$C_6\ H_{20}\ Cl_2\ N_8\ O_2\ Pt$
Formula weight (g mol^{-1})	502.29
Crystal color and habit	colourless blocks
Space system	monoclinic
Space group	C2/c
a (Å)	28.133(6)
b (Å)	7.1110(14)
c (Å)	17.814(4)
α (º)	90.00
β (º)	118.27(3)
γ (º)	90.00
Z	8
V (Å^3)	3138.6(11)
ρ_{calc} (g cm^{-1})	2.126
μ (Mo Kα) (mm^{-1})	9.293
F(000)	1920
θ range (º)	3.08 – 27.48
No. reflections collected	3591
No. reflections observed I>2σ(I)	2764
No. parameters refined	253
R_1 (obs. data)	0.0283
wR2 (obs. data)	0.0856
Goodness-of-fit, S	1.105
Residual ρ_{max}, ρ_{min} (e Å^{-3})	1.560, -2.904

Table A-4: *Crystallographic data for compound **18**.*

Compound	*cis*-$[(NH_3)_2Pt(N6\text{-}9\text{-}MeA\text{-}N7)_2\{Pt(NH_3)_3\}_2](NO_3)_4\cdot 6H_2O$
Formula	$C_{12}\ H_{36}\ N_{22}\ O_{17}\ Pt_3$
Formula weight (g mol^{-1})	1345.9
Crystal color and habit	colourless blocks
Space system	monoclinic
Space group	C2/c
a (Å)	24.753(5)
b (Å)	10.812(2)
c (Å)	14.514(3)
α (º)	90
β (º)	95.80(3)
γ (º)	90
Z	4
V (Å^3)	3864.6(14)
ρ_{calc} (g cm^{-1})	2.313
μ (Mo Kα) (mm^{-1})	10.924
F(000)	2528
θ range (º)	3.12 – 27.5
No. reflections collected	4435
No. reflections observed I>2σ(I)	3624
No. parameters refined	244
R_1 (obs. data)	0.0273
wR2 (obs. data)	0.0632
Goodness-of-fit, S	1.057
Residual ρ_{max}, ρ_{min} (e Å^{-3})	1.112, -0.958

Table A-5: *Crystallographic data for compound **19**.*

Compound	$\{[(dien)Pd]_3(9\text{-}MeA\text{-}N1,N7,N6)\}Cl_{3.5}(PF_6)_{1.5}\cdot 3H_2O$
Formula	$C_{18}\ H_{45}\ Cl_{3.5}\ F_9\ N_{14}\ O_3\ P_{1.5}\ Pd_3$
Formula weight (g mol^{-1})	1166.41
Crystal color and habit	yellow blocks
Space system	monoclinic
Space group	$P2_1/c$
a (Å)	12.659(3)
b (Å)	16.193(3)
c (Å)	20.720(4)
α (º)	90
β (º)	105.52(3)
γ (º)	90
Z	4
V (Å^3)	4092.5(14)
ρ_{calc} (g cm^{-1})	1.893
μ (Mo Kα) (mm^{-1})	1.675
F(000)	2304
θ range (º)	2.09 – 27.08
No. reflections collected	8970
No. reflections observed I>2σ(I)	4845
No. parameters refined	472
R_1 (obs. data)	0.035
wR2 (obs. data)	0.0613
Goodness-of-fit, S	0.776
Residual ρ_{max}, ρ_{min} (e Å^{-3})	1.056, -0.592

Table A-6: *Crystallographic data for compound **21**.*

Compound	$[Pt(1\text{-}MeC\text{-}N3)_3(OH)](ClO_4)_{0.5}(OH)_{0.5}\cdot 7H_2O$
Formula	$C_{15}\ H_{37.5}\ Cl_{0.5}\ N_9\ O_{14}\ Pt$
Formula weight (g mol^{-1})	780.85
Crystal color and habit	colourless prisms
Space system	monoclinic
Space group	C2/c
a (Å)	30.454(6)
b (Å)	14.558(3)
c (Å)	13.471(3)
α (º)	90
β (º)	99.28(3)
γ (º)	90
Z	8
V (Å^3)	5894(2)
ρ_{calc} (g cm^{-1})	1.76
μ (Mo Kα) (mm^{-1})	4.882
F(000)	3112
θ range (º)	2.47 – 27.5
No. reflections collected	6150
No. reflections observed I>2σ(I)	3319
No. parameters refined	356
R_1 (obs. data)	0.043
wR2 (obs. data)	0.1026
Goodness-of-fit, S	0.897
Residual ρ_{max}, ρ_{min} (e Å^{-3})	1.492, -0.861

Table A-7: *Crystallographic data for compound **24**.*

Compound	*trans*-$[(NH_3)_2Pt(6,9\text{-}DimeA\text{-}N7)(1\text{-}MeC\text{-}N3)](NO_3)_2\cdot H_2O$
Formula	$C_{12}\ H_{24}\ N_{12}\ O_8\ Pt$
Formula weight (g mol^{-1})	659.52
Crystal color and habit	colourless blocks
Space system	monoclinic
Space group	P2/n
a (Å)	13.374(3)
b (Å)	13.183(3)
c (Å)	26.970(5)
α (º)	90
β (º)	103.34(3)
γ (º)	90
Z	8
V (Å^3)	4626.8(16)
ρ_{calc} (g cm^{-1})	1.894
μ (Mo Kα) (mm^{-1})	6.129
F(000)	2576
θ range (º)	3.09 – 27.59
No. reflections collected	10624
No. reflections observed I>2σ(I)	4595
No. parameters refined	540
R_1 (obs. data)	0.082
wR2 (obs. data)	0.2227
Goodness-of-fit, S	0.998
Residual ρ_{max}, ρ_{min} (e Å^{-3})	2.286, -0.714

Table A-8: *Crystallographic data for compound **25**.*

Compound	*trans*-[$(NH_3)_2$Pt(6,9-DimeA-*N7*)(9-MeGH-*N7*)]$(NO_3)_2 \cdot 5H_2O$
Formula	C_{13} H_{32} N_{14} O_{12} Pt
Formula weight (g mol^{-1})	771.53
Crystal color and habit	colourless blocks
Space system	monoclinic
Space group	$P2_1/c$
a (Å)	9.6160(19)
b (Å)	13.392(3)
c (Å)	20.301(4)
α (º)	90
β (º)	86.64(3)
γ (º)	90
Z	4
V (Å^3)	2609.8(9)
ρ_{calc} (g cm^{-1})	1.938
μ (Mo Kα) (mm^{-1})	5.461
F(000)	1488
θ range (º)	1.82 – 22.94
No. reflections collected	3545
No. reflections observed I>2σ(I)	1713
No. parameters refined	363
R_1 (obs. data)	0.0467
wR2 (obs. data)	0.1556
Goodness-of-fit, S	0.855
Residual ρ_{max}, ρ_{min} (e Å^{-3})	1.869, -1.004

Table A-9: *Crystallographic data for compound **28**.*

Compound	*trans*-[$(NH_3)_2$Pt(pzH)Cl](NO_3)
Formula	C_3 H_{10} Cl N_5 O_3 Pt
Formula weight (g mol^{-1})	394.7
Crystal color and habit	yellow plates
Space system	triclinic
Space group	P-1
a (Å)	7.9570(16)
b (Å)	9.789(2)
c (Å)	13.267(3)
α (º)	77.22(3)
β (º)	85.61(3)
γ (º)	77.38(3)
Z	4
V (Å^3)	983.0(3)
ρ_{calc} (g cm^{-1})	2.667
μ (Mo Kα) (mm^{-1})	14.533
F(000)	728
θ range (º)	2.18 – 26.73
No. reflections collected	4131
No. reflections observed I>2σ(I)	3011
No. parameters refined	237
R_1 (obs. data)	0.0613
wR2 (obs. data)	0.153
Goodness-of-fit, S	1.041
Residual ρ_{max}, ρ_{min} (e Å^{-3})	3.062, -4.075

Table A-10: *Crystallographic data for compound* ***32****.*

Compound	*trans*-$[(NH_3)_2Pt\{(pzH)Cl\}_2](ClO_4)_2 \cdot H_2O$
Formula	$C_6\ H_{14}\ Cl_4\ N_6\ O_{10}\ Pt$
Formula weight (g mol^{-1})	667.12
Crystal color and habit	yellow blocks
Space system	monoclinic
Space group	$P2_1/c$
a (Å)	9.4960(19)
b (Å)	10.621(2)
c (Å)	10.474(2)
α (º)	90
β (º)	115.67(3)
γ (º)	90
Z	2
V ($Å^3$)	952.1(3)
ρ_{calc} (g cm^{-1})	2.327
μ (Mo Kα) (mm^{-1})	7.989
F(000)	636
θ range (º)	3.06 – 27.5
No. reflections collected	2159
No. reflections observed I>2σ(I)	1502
No. parameters refined	124
R_1 (obs. data)	0.055
wR2 (obs. data)	0.1565
Goodness-of-fit, S	1.087
Residual ρ_{max}, ρ_{min} (e $Å^{-3}$)	5.585, -1.247

5 Summary

Acid-base equilibria involving nucleobases at physiological pH value have recently been recognized as being possible and biorelevant in catalytic reactions, in particular of RNA. Reasons for “shifted” pK_a values, hence for pK_a values shifted from high or from low values to ~ 7, are beginning to emerge. It is obviously a combination of effects of the medium, of the microenvironment, and of charge distribution in the vicinity of the site involved in acid-base chemistry, which contributes to the shift. The influence of a coordinated metal ion on acid-base equilibria of nucleobases has been studied since quite some time, but it had been the impression that, within narrow limits, the effect of the metal is “constant”, depending mainly on its oxidation state, its vicinity to the acidic/basic group and on coligands in that they determine the overall charge of the complex. It was the observation of M. S. Lüth in our group in 2001, that twofold Pt coordination to 9-methyladenine (9-MeA) not only acidifies the exocyclic N(6)H_2 group, but that apparently the microenvironment (intramolecular H bonding leading to a stabilization of the deprotonated form) had an influence on pK_a reaching that of the two metal ions.

Based on this observation, it was the aim of the present thesis to place these findings into a wider perspective by systematically studying 9-methyladenine complexes of Pt^{II} with different coligands capable or incapable of interacting with the deprotonated species and determining relevant pK_a values. These studies have been extended to 1,9-dimethyladenine complexes, hence to compounds, in which the adenine base had been chemically modified.

Next, the question of NH_2 acidification in complexes of 1-methylcytosine was studied, followed by the question of acidification of the aqua ligand in simple nucleobase compounds of composition *cis*-$[(NH_3)_2Pt(nucleobase)(H_2O)]^{2+}$. Moreover, by employing 9-methyladenine, the pK_a of the protonated species in dependence of the solvent (water and mixtures of acetone/water as well as methanol/water) was investigated. In the final chapter, a preliminary study was

undertaken with the aim of extending this work to the deprotonation of N7-platinated guanine. In order to bring the N1 position of the guanine base into reach of the a second nucleobase capable of stabilizing the guanine anion, the bidentate pyrazolate ligand was applied, which was additionally linked via a *trans*-a_2Pt^{II} entity to a cytosine nucleobase.

Concerning the most important findings of the present thesis, the following points can be listed.

(1) A considerable number of complexes of 9-methyladenine with N1 and N7 sites platinated confirms the concept that not only the positive charge of the metals but that in particular favourable hydrogen bonding between the deprotonated exocyclic NH_2 group of 9-MeA is extremely important to lower the pK_a from 10 – 11 (effect of two metals only) into the pK_a range of 7 – 8. This value is close to physiological pH. For example, in *trans,trans,trans*-$[(NH_3)_2Pt(N7\text{-}9\text{-}MeA\text{-}N1)(dienPt)(N7\text{-}9\text{-}EtA\text{-}N1)\{(NH_3)_2Pt(9\text{-}MeGH\text{-}N7)\}]^{6+}$ (**13**), the deprotonation of the NH_2 of the adenine nucleobase occurs at pK_a 7.14. The pK_a shift is due to the combined effects of twofold metal coordination *and* a favourable intramolecular hydrogen bond between an anionic and a neutral adenine nucleobase.

(2) The most dramatic shifts in pK_a values of platinated 9-MeA complexes were observed, when there was formation of a “metal-stabilized” rare tautomer of 9-MeA (A*). By this term we mean that in this case a metal is bonded to N6 of the nucleobase and one of the protons that used to be at $N(6)H_2$, has been transferred to N1.

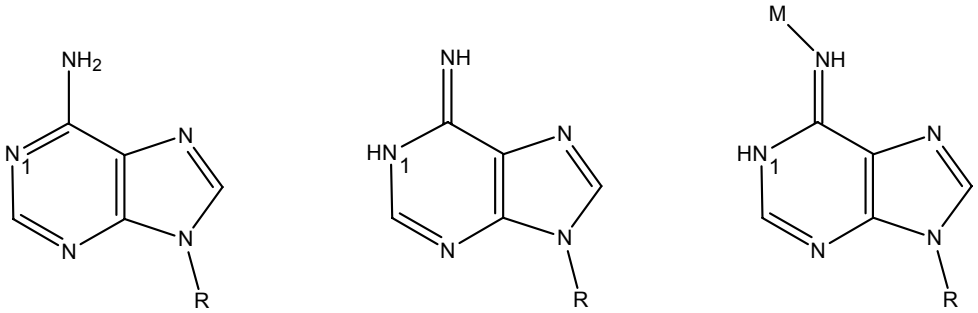

Formation of this M-A* species occurs via a metal migration process from N1 to N6, which is greatly facilitated, if there is a second metal coordinated to N7. Thus, starting from *trans*-[{$(NH_3)_2$Pt(1-MeC-*N3*)}$_2$(9-MeA-*N1,N7)*]$^{4+}$ (**7**), the migration product *trans*-[{$(NH_3)_2$Pt(1-MeC-*N3*)}$_2$(9-MeA-*N7*,*N6*)]$^{3+}$ (**15**) has been isolated and characterized, with a pK_a of 5.0 for N(1)H of adenine. Similarly, the double migration product *cis*-[$(NH_3)_2$Pt(*N6*-9-MeA-*N7)*$_2${Pt$(NH_3)_3$}$_2$]$^{4+}$ (**18**) has been derived from *cis*-[$(NH_3)_2$Pt{(*N1*-9-MeA-*N7*)Pt$(NH_3)_3$}$_2$]$^{6+}$ (**11**). The first pK_a value of (**18**) is 4.9, as compared to 8.7 in (**11**).

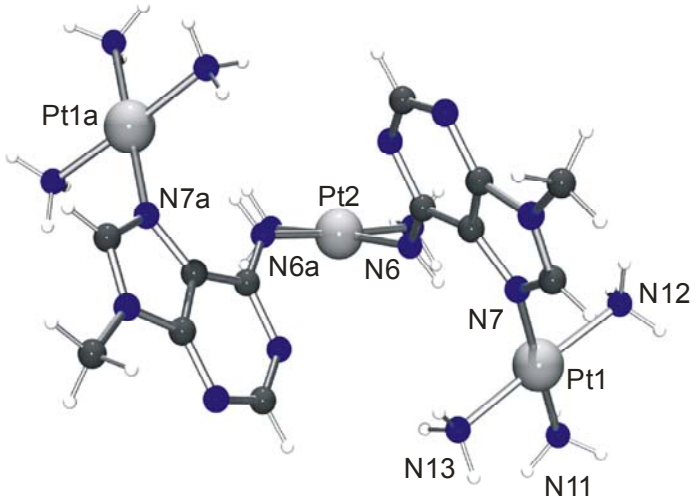

*View of the cation cis-[(NH$_3$)$_2$Pt(N6-9-MeA-N7)$_2${Pt(NH$_3$)$_3$}$_2$]$^{4+}$ of (**18**)*

(3) By synthesizing mixed nucleobase complexes containing 6,9-DimeA, *trans*-[$(NH_3)_2$Pt(6,9-DimeA-*N7*)(1-MeC-*N3*)]$^{2+}$ (**24**) and *trans*-[$(NH_3)_2$Pt(6,9-DimeA-*N7*)(9-MeGH-*N7*)]$^{2+}$ (**25**) and by structurally characterizing these, it was unambiguously demonstrated that the complications seen in spectra of the

corresponding 1,9-DimeA complexes *trans*-[$(NH_3)_2$Pt(1,9-DimeAH-*N7*)(9-MeGH-*N7*)]$^{3+}$ (**22**) and *trans*-[$(NH_3)_2$Pt(1,9-DimeAH-*N7*)(9-MeGH-*N7*)]$^{3+}$ (**23**) at alkaline pH was due to Dimroth rearrangements.

(4) The effect of the solvent (mixture) on the pK_a of 9-MeAH$^+$ was relatively minor, even though it displayed the expected direction, viz. when the dielectric constant of the medium decreases, the pK_a decreases as well. The fact that the changes were not dramatical may be due to the fact that even in the solvent mixtures applied, there was still a sufficient number of H_2O molecules present to properly solvate all the charged species present in equilibrium.

(5) The pK_a values for the mono(nucleobase) complexes of *cis*-$(NH_3)_2Pt^{II}$, *cis*-[$(NH_3)_2$Pt(nucleobase)(H_2O)]$^{2+}$, did not display the expected difference in pK_a of the aqua ligand for nucleobase = guanine-*N7* and cytosine-*N3*, even though from model building a stabilizing H bonding effect between the hydroxo ligand and the exocyclic amino group of cytosine could have been anticipated.

6 Zusammenfassung

Säure-Base-Gleichgewichte von Nukleobasen bei physiologischem pH-Wert wurden erst kürzlich als möglich und als biorelevant in katalytischen Reaktionen angesehen, insbesondere solcher der RNA. Ursachen veränderter pK_s-Werte, also Verschiebungen von niedrigen oder hohen Werten zu Werten von 7 ± 1 beginnt man gerade erst zu verstehen. Es ist offensichtlich, dass hier eine Reihe verschiedener Effekte eine Rolle spielen, wie z. B. das Medium, die Mikroumgebung oder die Ladungsverteilung. Säure-Base-Gleichgewichte von Nukleobasen unter dem Einfluss koordinierter Metalle werden schon seit einiger Zeit untersucht, wobei man aber bisher meist davon ausgegangen ist, dass der Effekt des Metalls konstant ist und hauptsächlich von der Oxidationsstuffe und der Nähe zur Säure/Base Gruppe abhängt. M. S. Lüth beobachtete 2001, dass die zweifache Pt-Koordination über N1 and N7 an 9-Methyladenin (9-MeA) nicht nur die exozyklische N(6)H_2-Gruppe acider macht, sondern dass anscheinend auch die nähere Umgebung (eine intramolekulare Wasserstoffbrücke führt zur Stabilisierung der deprotonierten Form), einen gravierenden Einfluss auf den pK_s-Wert hat.

Ziel dieser Dissertation war es, aufbauend auf dieser Beobachtung, zu einem tieferen Verständnis der Einflüsse der genannten Faktoren zu gelangen. Hierfür wurden systematisch 9-Methyladenin-Komplexe von Pt^{II} studiert, welche unterschiedliche Co-Liganden enthalten, die mit der deprotonierten Adenin-Base entweder interagieren können oder auch nicht. Diese Studie wurde auch auf 1,9-Dimethyladenin-Komplexe ausgeweitet.

Weiterhin wurde der Einfluss von Nachbarliganden auf die Acidität der exocyclischen Aminogruppe in N3-platiniertem 1-Methylcytosin sowie auf die Acidität von Aqua-Liganden in Verbindungen der Zusammensetzung *cis*-$[(NH_3)_2Pt(Nukleobase)(H_2O)]^{2+}$ untersucht. Schließlich wurde am Beispiel von protoniertem 9-Methyladenin der Einfluss des Lösungsmittels (Wasser sowie Aceton/Wasser- und Methanol/Wasser-Gemische) auf den pK_s-Wert studiert. Im

abschließenden Kapitel wurde eine erste orientierende Untersuchung hinsichtlich der Übertragbarkeit des Konzepts der intramolekularen Stabilisierung anionischer Nukleobasen auf die N1-Position N7 platinierter Guanin-Liganden durchgeführt. Ziel war es hierbei, eine zweite Nukleobase (hier: Cytosin) über einen verbrückenden Pyrazolat-Hilfsliganden so zu positionieren, dass eine Wechselwirkung zwischen N(4)H_2 des Cytosins und N1 des Guanins prinzipiell möglich ist.

Nachfolgend seien die wichtigsten Ergebnisse dieser Dissertation noch einmal zusammengefasst:

(1) Es wurde eine größere Anzahl ein- und mehrkerniger 9-Methyladenin-Komplexe des Pt mit N1 und N7-Koordination hinsichtlich ihrer N(6)H_2-Acidität untersucht. Die Ergebnisse bestätigen das Konzept wonach nicht nur die positive Ladung der koordinierten Metalle, sondern in besonderer Weise auch intramolekulare Wasserstoffbrücken äußerst wichtig sind, um den pK_s-Wert der NH_2-Gruppe auf ca. 7-8 abzusenken. Zum Beispiel findet in *trans,trans,trans*-[$(NH_3)_2$Pt(*N7*-9-MeA-*N1*)(dienPt)(*N7*-9-EtA-*N1*){$(NH_3)_2$Pt(9-MeGH-*N7*)}]$^{6+}$ (**13**) die Deprotonierung der NH_2-Gruppe des einen Adenins mit einem pK_s-Wert von 7.14 statt, was neben der zweifachen Platinierung vor allem auch auf die intermolekulare Wasserstoffbrücke der NH^- -Funktion mit der NH_2-Gruppe der zweiten Adeninbase zurück zu führen ist.

(2) Die drastischste Veränderung des pK_s-Wertes eines platinierten 9-Methyladenin-Liganden tritt bei Ausbildung eines sog. Metall-stabilisierten Tautomers, M-A*, auf. In diesem Fall ist das Metall an der N6-Position der Nukleobase gebunden und eines der beiden Protonen der NH_2-Gruppe ist zum N1 gewechselt.

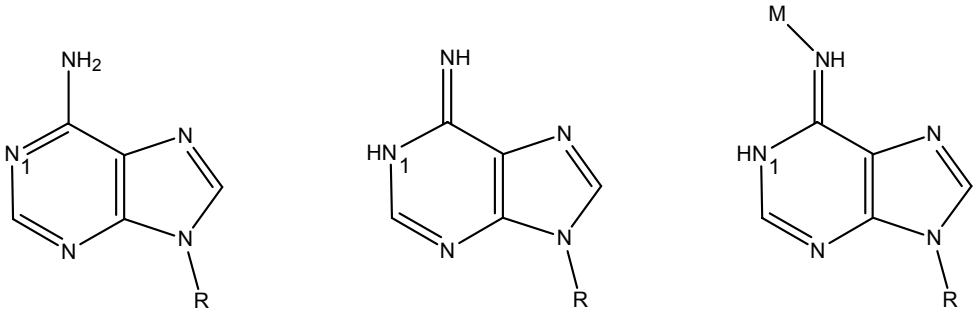

Die Bildung der M-A* Spezies geht auf eine Metallwanderung von N1 nach N6 zurück, welche durch ein zweites Metall, koordiniert an N7, deutlich erleichtert wird. Ausgehend von *trans*-[{$(NH_3)_2$Pt(1-MeC-*N3*)}$_2$(9-MeA-*N1,N7)*]$^{4+}$ (**7**), wurde z. B. das Umlagerungsprodukt *trans*-[{$(NH_3)_2$Pt(1-MeC-*N3*)}$_2$(9-MeA-*N7*,*N6*)]$^{3+}$ (**15**) isoliert und charakterisiert. Ein pK_s-Wert von 5.0 wurde für N(1)H von Adenin bestimmt. Gleichermaßen wurde das Umlagerungsprodukt *cis*-[$(NH_3)_2$Pt(*N6*-9-MeA-*N7)*$_2${Pt$(NH_3)_3$}$_2$]$^{4+}$ (**18**) aus *cis*-[$(NH_3)_2$Pt{(*N1*-9-MeA-*N7*)Pt$(NH_3)_3$}$_2$]$^{6+}$ (**11**) hergestellt. Der pK_s-Wert verschiebt sich hierbei von 8.7 (**11**) nach 4.9 (**18**).

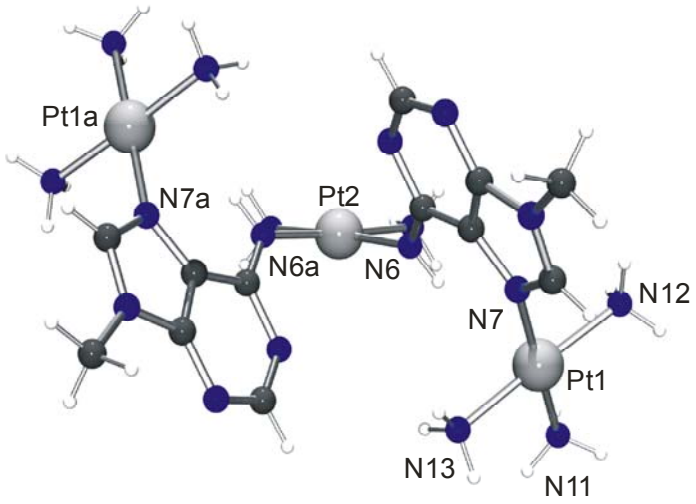

*Ansicht des Kations cis-[$(NH_3)_2$Pt(N6-9-MeA-N7)$_2${Pt$(NH_3)_3$}$_2$]$^{4+}$ von (**18**)*

(3) Durch die Synthese und vollständige strukturelle Charakterisierung der gemischten Nukleobase-Komplexe des 6,9-DimeA, *trans*-[$(NH_3)_2$Pt(6,9-

DimeA-*N7*)(1-MeC-*N3*)]$^{2+}$ (**24**) und *trans*-[$(NH_3)_2$Pt(6,9-DimeA-*N7*)(9-MeGH-*N7*)]$^{2+}$ (**25**) konnte der Nachweis erbracht werden, dass die in Spektren der 1,9-DimeA-haltigen Verbindungen *trans*-[$(NH_3)_2$Pt(1,9-DimeAH-*N7*)(9-MeGH-*N7*)]$^{3+}$ (**22**) und *trans*-[$(NH_3)_2$Pt(1,9-DimeAH-*N7*)(9-MeGH-*N7*)]$^{3+}$ (**23**) bei alkalischen pH beobachteten Komplikationen auf Dimroth-Umlagerungen zurück zu führen sind.

(4) Der Effekt von Lösungsmittelgemischen auf den pK_s-Wert von 9-MeAH$^+$ ist verhältnismäßig gering, bestätigt aber den prognostizierten Trend: Wenn die Dielektrizitätskonstante des Lösungsmittels sinkt, verringert sich auch der pK_s-Wert. Der relativ kleine Effekt kann damit erklärt werden, dass der Gehalt an H_2O in den verwendeten Gemischen noch immer zu hoch ist, um eine effiziente Solvatisierung der ionogenen Spezies zu gewährleisten.

(5) Die pK_s-Werte von Aqua-Liganden in Verbindungen des Typs *cis*-[$(NH_3)_2$Pt(Nukleobase)(H_2O)]$^{2+}$ zeigten nicht die erwarteten Unterschiede für Guanin-*N7* und Cytosin-*N3*, obwohl man eigentlich von einem stabilisierenden Effekt durch eine Wasserstoffbrücke zwischen dem Hydroxoliganden und der exozyklischen Aminogruppe von Cytosin hätte ausgehen können.

7 Resumen

Los equilibrios ácido-base que implican nucleobases en el rango del pH fisiológico se han estudiado recientemente como posibles y biorelevantes en reacciones catalíticas, en particular en el caso del ARN. Las razones de los cambios en los valores de pK_a, desde valores ácidos y básicos a valores próximos a 7, están saliendo a la luz. Una combinación de los efectos del medio, del entorno y de la distribución de la carga en la posición a estudiar, contribuyen a estos cambios. En estos equilibrios ácido-base ha sido estudiada desde hace bastante tiempo, la influencia de un ion metálico coordinado a una nucleobase, pero se tenía la impresión de que, dentro de pequeños límites, el efecto del metal era constante, dependiendo principalmente de su estado de oxidación, su cercanía al grupo ácido/básico y de otros ligandos. M. S. Lüth, en nuestro grupo en 2001, observó que una doble coordinación de Pt a 9-metiladenina (9-MeA), acidifica no solamente el grupo exocíclico N(6)H_2, sino que también el entorno (puentes de hidrógeno intramoleculares que conducen a una estabilización de la forma desprotonada) tenía al parecer una influencia semejante en el valor de pK_a.

De acuerdo con esta observación, el objetivo de esta tesis es ampliar estos resultados, estudiando complejos de Pt^{II} con 9-metiladenina y con diversos co-ligandos, capaces o incapaces de interaccionar con especies desprotonadas y la posterior determinación de los valores de pK_a. Estos estudios han sido extendidos a complejos de 1,9-dimetiladenina, por lo tanto a compuestos, en los cuales la adenina había sido modificada químicamente.

Además, ha sido estudiada la acidificación del grupo NH_2 en complejos de 1-metilcitosina y también la del ligando H_2O en compuestos con nucleobases simples, de composición *cis*-$[(NH_3)_2Pt(nucleobase)(H_2O)]^{2+}$. Por otra parte, ha sido investigado el pK_a de especies protonadas en dependencia del solvente (agua y mezclas de acetona/agua así como metanol/agua) empleando 9-metiladenina. En el capítulo final, un estudio preliminar fue llevado a cabo con la

idea de extender este trabajo a la desprotonación de la guanina con Pt coordinado en N7. Para acercar la posición N1 de ésta a otra segunda nucleobase, capaz de estabilizar el anión de la guanina, se utilizó el ligando pirazolato, el cual se unió a través de la entidad *trans*-a_2Pt^{II} a una citosina.

Los resultados más importantes de esta tesis se enumeran a continuacón:

(1) un número considerable de complejos de 9-metiladenina con Pt coordinado en las posiciones N1 y N7 confirma el hecho de que no solamente las cargas positivas de los metales, sino también en particular los puentes de hidrógeno que afectan a grupo desprotonado NH_2, son muy importantes a la hora de disminuir el pK_a desde 10 - 11 (sólo dos metales) hasta 7 - 8, valor cercano del pH fisiológico. Por ejemplo, en *trans,trans,trans*-[$(NH_3)_2$Pt(*N7*-9-MeA-*N1*)(dienPt)(*N7*-9-EtA-*N1*){$(NH_3)_2$Pt(9-MeGH-*N7*)}]$^{6+}$(**13**),la desprotonación del NH_2 de la adenina ocurre a pK_a 7.14. Este valor bajo de pK_a se debe a la combinación de dos efectos: la coordinación de dos átomos de platino y un puente de hidrógeno intramolecular entre la adenina aniónica y la neutral.

(2) los cambios más drásticos en los valores del pK_a de complejos de 9-MeA con Pt fueron observados en la formación de un tautómero no muy común de 9-MeA (M-A*), que recibe el nombre de “metal-estabilizado”. Este nombre significa, que un metal está enlazado a la posición N6 de la nucleobase y uno de los protones que suelen estar en $N(6)H_2$ se transfiere a N1.

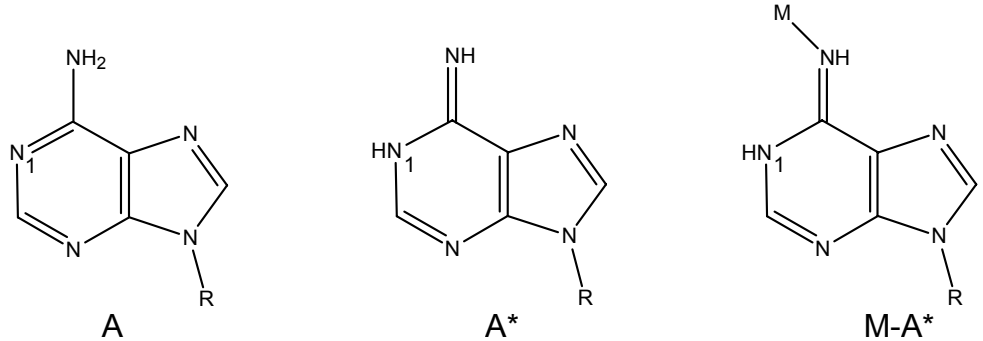

A A* M-A*

La formación de esta especie M-A* ocurre a través de un proceso de migración del metal de N1 a N6, que está favorecida por la presencia de un segundo metal coordinado a N7. Partiendo del complejo *trans*-[{$(NH_3)_2$Pt(1-MeC-*N3*)}$_2$(9-MeA-*N1,N7)*]$^{4+}$ (**7**), el producto *trans*-[{$(NH_3)_2$Pt(1-MeC-*N3*)}$_2$(9-MeA-*N7*,*N6*)]$^{3+}$ (**15**), ha sido aislado y caracterizado, obteniendo un pK_a de 5.0 para el N(1)H de la adenina. De modo parecido, el producto de la doble migración *cis*-[$(NH_3)_2$Pt(*N6*-9-MeA-*N7)*$_2${Pt$(NH_3)_3$}$_2$]$^{4+}$ (**18**) se obtuvo a partir del compuesto de partida *cis*-[$(NH_3)_2$Pt{(*N1*-9-MeA-*N7*)Pt$(NH_3)_3$}$_2$]$^{6+}$ (**11**). Sin embargo, el valor de pK_a de (**18**) es 4.9 en comparación con el valor de 8.7 del compuesto (**11**).

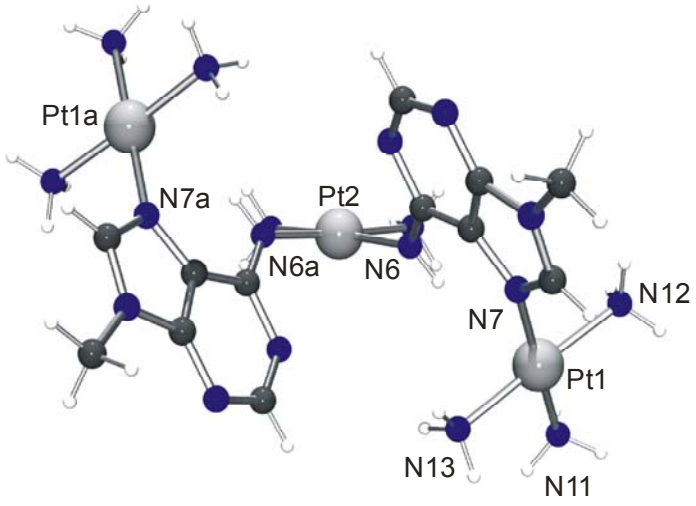

*Vista del catión cis-[$(NH_3)_2$Pt(N6-9-MeA-N7)$_2${Pt$(NH_3)_3$}$_2$]$^{4+}$ de (**18**)*

(3) En complejos formados por 1,9-DimeA y otra nucleobase: *trans*-[$(NH_3)_2$Pt(1,9-DimeAH-*N7*)(9-MeGH-*N7*)]$^{3+}$ (**22**) y *trans*-[$(NH_3)_2$Pt(1,9-DimeAH-*N7*)(9-MeGH-*N7*)]$^{3+}$ (**23**) se observaron complicaciones de las señales en los espectros a pH básico. Se ha demostrado gracias a la síntesis de compuestos como *trans*-[$(NH_3)_2$Pt(6,9-DimeA-*N7*)(1-MeC-*N3*)]$^{2+}$ (**24**) y *trans*-[$(NH_3)_2$Pt(6,9-DimeA-*N7*)(9-MeGH-*N7*)]$^{2+}$ (**25**), que estas complicaciones son debidas a un proceso llamado “Dimroth rearrangement”.

(4) el efecto del disolvente (mezcla) en los valores de pK_a en 9-MeAH$^+$ es relativamente pequeño. Aunque los resultados fueron los previstos, es decir, se observó que cuando la constante dieléctrica del medio disminuye, el valor de pK_a también lo hace. El hecho de que los cambios en los valores de pK_a no fueran drásticos, puede ser debido a que en las mezclas de disolventes utilizadas, había suficiente moléculas de H_2O como para solvatar las especies presentes en equilibrio.

(5) Aunque sería esperada una estabilización mediante puentes de hidrógeno entre el ligando OH^- y el NH_2 de la citosina, los valores de pK_a para complejos del tipo *cis*-[$(NH_3)_2$Pt(nucleobase)(H_2O)]$^{2+}$, no mostraron la diferencia esperada en el pK_a del ligando H_2O, para el caso en que la nucleobase fuera guanina-*N7* y citosina-*N3*.

8 References

[1] W. Saenger, *Principles of Nucleic Acid Structure*, Springer-Verlag, New York, **1984**, p.107.

[2] G. Kampf, L. E. Kapinos, R. Griesser, B. Lippert, H. Sigel, *J. Chem. Soc*. *Perkin Trans*. 2, **2002**, 1320.

[3] B. Song, J. Zhao, R. Griesser, C. Meiser, H. Sigel, B. Lippert, *Chem. Eur. J*., **1999**, *5*, 2374.

[4] R. K. O. Sigel, E. Freisinger, B. Lippert, *J. Biol. Inorg. Chem*., **2000**, *5*, 287.

[5] a) K. Gehring, J.-L. Leroy, M. Guerson, *Nature,* **1993**, *363*, 561; b) D. Leitner, W. Schröder, K. Weisz, *Biochemistry,* **2000**, *39*, 5886.

[6] a) A. M. Pyle, *J. Biol. Inorg. Chem.,* **2002**, *7*, 679, and references therein; b) E. Westhoff, *Science,* **1999**, *286*, 61, and references therein; c) A. T. Perrotta, I.-h. Shih, M. D. Been, *Science,* **1999**, *286*, 123.

[7] G. W. Muth, L. Ortoleva-Donnelly, S. A. Strobel, *Science,* **2000**, *289*, 947.

[8] A. K. Oyelere, J. R. Kardon, S. A. Strobel, *Biochemistry,* **2002**, *41*, 3667.

[9] P. Legault, A. Pardi, *J. Am. Chem. Soc*., **1997**, *119*, 6621.

[10] a) M. J. Clarke, *J. Am. Chem. Soc.*, **1978**, *100*, 5068; b) E. M. Kastner, K. F. Coffey, M. J. Clarke, S. E. Edmonds, K. Eriks, *J. Am. Chem. Soc.,* **1981**, *103*, 5747; c) V. M. Rodriguez-Bailey, M. J. Clarke, *Inorg. Chem*., **1997**, *36*, 1611.

[11] J. H. J. den Hartog, H. van den Elst, J. Reedijk, *J. Inorg. Biochem*., **1984**, *21*, 83.

[12] K. Inagaki, M. Kuwayama, Y. Kidani, *J. Inorg. Biochem*., **1982**, *16*, 59.

[13] a) R. Griesser, G. Kampf, L. E. Kapinos, S. Komeda, B. Lippert, J. Reedijk, H. Sigel, *Inorg. Chem.,* **2003**, *42*, 32, and references therein; b) B. Lippert, H. Schöllhorn, U. Thewalt, *Inorg. Chim. Acta,* **1992**, 198, 723.

[14] J. E. Sponer, J. Leszczynski, F. Glahé, B. Lippert, J. Sponer, *Inorg. Chem.,* **2001**, *40*, 3269.

[15] H. Schöllhorn, U. Thewalt, B. Lippert, *J. Am. Chem. Soc.,* **1989**, *111*, 7213.

[16] a) J. Müller, E. Zangrando, N. Pahlke, E. Freisinger, L. Randaccio, B. Lippert, *Chem. Eur. J.,* **1998**, *4*, 397; b) J. Müller, F. Glahé, E. Freisinger, B. Lippert, *Inorg. Chem*., **1999**, *38*, 3160.

[17] M. S. Lüth, M. Willermann, B. Lippert, *Chem. Commun*., **2001**, 2058.

[18] R. Stewart, M. G. Harris, *Can. J. Chem*., **1977**, *55*, 3807.

[19] a) L. Heck, M. Ardon, A. Bino, J. Zapp, *J. Am. Chem. Soc*., **1988**, *110*, 2691; b) W. Frank, L. Heck, S. Müller-Becker, T. Raber, *Inorg. Chim. Acta,* **1997**, *265*, 17.

[20] G. M. Blackburn and M. J. Gait, Eds., *Nucleic Acids in Chemistry and Biology*, Oxford

University Press, Oxford, **1996**.

[21] F. Basolo, R. G. Pearson, *'Mechanism of Inorganic Reactions'*, Wiley, New York, **1967**, Chapter 5.

[22] R. B. Martin in 'Platinum, *Gold and Other Metal Chemotherapeutic Agents',* Ed. S. J. Lippard, ACS Symposium Series 209, American Society, Washington DC, **1983**, p. 231.

[23] J. Arpalahti, K. D. Klika, R. Sillanpää, R. Kivekäs, *J. Chem. Soc., Dalton Trans.,* **1998**, 1397.

[24] J. L. Van der Veer, H. Van der Elst, J. Reedijk, *Inorg. Chem*., **1987**, *26*, 1536.

[25] J. Arpalahti and K.D. Klika, *Eur. J. Inorg. Chem*., **1999**, 1199.

[26] T. Fujii, I. Itaya, C. C. Wu, F. Tanaka, *Tetrahedron,* **1971**, *27*, 2415.

[27] A. Albert and E. P. Serjeant, *The Determination of ionization Constants*, Chapman and Hall, London, **1984**.

[28] R. Lumry, E. L. Smitz, R. R. Glantz, *J. Am. Chem. Soc*., **1951**, *73*, 4335.

[29] P. K. Glasoe, F. A. Long, *J. Phys. Chem*., **1960**, *64*, 188.

[30] R. Tribolet, H. Sigel *Eur. J. Biochem*., **1987**, *163*, 353.

[31] Press, W.H.; Flannery, B.P.; Teukolsky, S.A.; Vetterling, W.T. *Numerical recipes in C*, Cambridge Univ. Press, Cambridge, **1988**.

[32] J. V. Burda, J. Sponer, P. Hobza, *J. Phys. Chem.*, **1996**,*100*, 7250.

[33] a) J. Vinje, J. A. Parkinson, P. J. Sadler, T. Brown, E. Sletten, *Chem. Eur. J.*, **2003**, *9*, 1620. b) V. Monjardet-Bas, M. A. Elizondo-Riojas, J. C. Chottard, J. Kozelka, *Angew. Chem. Int. Ed.*, **2002**, *41*, 2998.

[34] C. B. Black and J. A. Cowan, *J. Am. Chem. Soc.*, **1994**, *116*, 1174.

[35] a) J. Sponer, J. V. Burda, M. Sabat, J. Leszczynski, P. Hobza, *J. Phys. Chem. A*, **1998**, *102*, 5951. b) J. Sponer, J. V. Burda, M. Sabat, J. Leszczynski, P. Hobza, *J. Biomol. Struct. Dyn.*, **1999**, *17*, 61.

[36] J. Sponer, M. Sabat, L. Gorb, J. Leszczynski, B. Lippert, P. Hobza, *J. Phys. Chem. B*, **2000,** *104*, 7535.

[37] M. Garijo Añorbe, M. S. Lüth, M. Roitzsch, M. Morell Cerdà, P. Lax, G. Kampf, H. Sigel, B. Lippert, *Chem. Eur. J.,* **2004**, *10*, 1046.

[38] a) M. Wall, B. Linkletter, D. Williams, A.-M. Lebuis, R. C. Hynes, J. Chin, *J. Am. Chem. Soc.,* **1999**, *121*, 4710. b) J. C. Mareque-Rivas, R. Prahabaran, R. Torres Martin de Rosales, *Chem. Commun.*, **2004**, 76.

[39] J. V. Burda, J. Sponer, J. Leszczynski, B. Lippert, *J. Phys. Chem. B*, **1997**, *101*, 9670.

[40] B. Lippert, *Coor. Chem. Rev*., **2000**, *487*, 200.

[41] a) R. K. O. Sigel, E. Freisinger, M. Abbate, B. Lippert, *Inorg. Chim. Acta*. **2002**, *339*, 355. b) E. Freisinger, A. Schimanski, B. Lippert, *J. Biol. Inorg. Chem*., **2001**, *6*, 378.

[42] a) K. Aoki, *Met. Ions Biol. Syst*., **1996**, *32*, 91. b) S. Mansy, R. S. Tobias, *Inorg. Chem*.

1975, *14*, 287. c) J. A. Carrabine, M. Sundaralingam, *Biochemistry*, **1971**, *10*, 292. d) M. Goodgame, D. A. Jakubovic, *Coord. Chem. Rev*., **1987**, *79*, 97.

[43] D. W. Abbot, C. Woods, *Inorg. Chem*., **1983**, *22*, 2918.

[44] F. Zamora, M. Sabat, *Inorg. Chem*., **2002**, *41*, 4976.

[45] L. G. Marzilli, R. C. Stewart, C. P. van Vuuren, B. de Castro, J. P. Caradonna, *J. Am. Chem. Soc*., **1978**, *100*, 3967.

[46] G. Krüger, *Hoppe Seyler's Z. Physiol. Chemie,* **1894**, *18*, 434.

[47] M.S. Lüth, *Dissertation*; Universität Dortmund, Dortmund **2001**.

[48] R.B. Martin, in: B. Lippert (Ed), *Cisplatin: Chemistry and Biochemistry of a Leading Anticancer Drug* , VHCA Zürich and Wiley-VCH Weinheim, **1999**, 183.

[49] R. Beyerle-Pfnür, B. Brown, R. Faggiani, B. Lippert, C. J. L. Lock, *Inorg. Chem*., **1985**, *24*, 4001.

[50] C. Meiser, B. Song, E. Freisinger, M. Peilert, H. Sigel, B. Lippert, *Chem. Eur. J.,* **1997**, *3*, 388.

[51] R. K. O. Sigel, S. M. Thompson, E. Freisinger, F. Glahé, B. Lippert, *Chem. Eur. J.,* **2001**, *7*, 1968.

[52] J. F. Britten, C. J. L. Lock, W. M. C. Pratt, *Acta Cryst.*, **1982**, *B38*, 2148.

[53] S. Jaworski, S. Menzer, B. Lippert, M. Sabat, *Inorg. Chim. Acta,* **1993**, *205*, 31 .

[54] H. Schöllhorn, G. Raudaschl-Sieber, G. Müller, U. Thewalt, B. Lippert, *J. Am. Chem. Soc.,* **1985**, *107*, 5932.

[55] R. Faggiani, C. J. L. Lock, B. Lippert, *J. Am. Chem. Soc.,* **1980**, *102*, 5418.

[56] C. F. Moreno-Luque, E. Freisinger, R. Griesser, J. Ochocki, B. Lippert, H. Sigel, *J. Chem. Soc. Perkin Trans. 2,* **2001,** 2005.

[57] Gaussian 98 (Revision A.7), M. J. Frisch, G. W. Trucks, H. B. Schlegel, G. E. Scuseria, M. A. Robb, J. R. Cheeseman, V. G. Zakrzewski, J. A. Montgomery, Jr., R. E. Stratmann, J. C. Burant, S. Dapprich, J. M. Millam, A. D. Daniels, K. N. Kudin, M. C. Strain, O. Farkas, J. Tomasi, V. Barone, M. Cossi, R. Cammi, B. Mennucci, C. Pomelli, C. Adamo, S. Clifford, J. Ochterski, G. A. Petersson, P. Y. Ayala, Q. Cui, K. Morokuma, D. K. Malick, A. D. Rabuck, K. Raghavachari, J. B. Foresman, J. Cioslowski, J. V. Ortiz, A. G. Baboul, B. B. Stefanov, G. Liu, A. Liashenko, P. Piskorz, I. Komaromi, R. Gomperts, R. L. Martin, D. J. Fox, T. Keith, M. A. Al-Laham, C. Y. Peng, A. Nanayakkara, C. Gonzalez, M. Challacombe, P. M. W. Gill, B. Johnson, W. Chen, M. W. Wong, J. L. Andres, C. Gonzalez, M. Head-Gordon, E. S. Replogle, J. A. Pople, Gaussian, Inc., Pittsburgh, PA, **1998**.

[58] a) I. Dieter-Wurm, M. Sabat, B. Lippert, *J. Am. Chem. Soc.,* **1992**, *114*, 357; b) S. Menzer, M. Sabat, B. Lippert, *J. Am. Chem. Soc*., **1992**, *114*, 4644; c) O. Krizanovic, M. Sabat, R. Beyerle-Pfnür, B. Lippert, *J. Am. Chem. Soc*., **1993**, *115*, 5538; d) A. Schreiber, M. S. Lüth, A. Erxleben, E. C. Fusch, B. Lippert, *J. Am. Chem. Soc*., **1999**,

121, 3248; e) S. Metzger, A. Erxleben, B. Lippert, *J. Biol. Inorg. Chem*., **1997**, *2*, 256; f) M. S. Lüth, E. Freisinger, F. Glahé, J. Müller, B. Lippert, *Inorg, Chem*., **1998**, *37*, 3195; g) M. S. Lüth, E. Freisinger, F. Glahé, J. Müller, B. Lippert, *Inorg, Chem.*, **1998**, *37*, 5044; h) R. K. O. Sigel, S. M. Thompson, E. Freisinger, B. Lippert, *Chem. Commun*., **1999**, 19.

[59] B. Lippert, *Coord. Chem. Rev.,* **1999**, *182*, 263.

[60] a) B. Andersen, E. Bernal-Méndez, M. Leng, E. Sletten, *Eur. J. Inorg. Chem.,* **2000**, 1201; b) Y. A. Shin, G. L. Eichhorn, *Biopolymers,* **1980**, *19*, 539.

[61] B. Lippert, M. Leng in *Topics Biol. Inorg. Chem. Vol. I.* (Eds.: M. J. Clarke, P. J. Sadler), Springer, Berlin, **1999**, pp. 117-142.

[62] a) P. Aich, S. L. Labiuk, L. W. Tari, L. J. T. Delbaere, W. J. Roesler, K. J. Falk, R. P. Steer, J. S. Lee, *J. Mol. Biol*., **1999**, *294*, 477.

[63] M. S. Lüth, E. Freisinger, B. Lippert, *Chem. Eur. J.*, **2001**, *7*, 2104 and references cited therein.

[64] M. S. Lüth, E. Freisinger, M. Drumm, G. Kampf, H. Sigel, B. Lippert, unpublished results.

[65] a) R. T. Wheelhouse, D. Sun, H, Han, F. X. Han, L. H. Hurley. *J. Am. Chem. Soc*., **1998**, *120*, 3261; b) H. Han, C. L. Cliff, L. H. Hurley, *Biochemistry*, **1999**, *38*, 6981.

[66] J. Viljanen, K. D. Klika, R. Sillanpää, J. Arpalahti, *Inorg. Chem.,* **1999**, *38*, 4924.

[67] J. Arpalahti, K. D. Klika, S. Molander, *Eur. J. Inorg. Chem.,* **2000**, 1007.

[68] J. Šponer, J. E. Šponer, L. Gorb, J. Leszczynski, B. Lippert, *J. Phys. Chem. A.,* **1999**, *103*, 406.

[69] F. Zamora, M. Kunsman, M. Sabat, B. Lippert, *Inorg. Chem*., **1997**, *36*, 1583.

[70] T. J. Kistenmacher, M. Rossi, *Acta Crystallogr*. Sect. B, **1977**, *33*, 253.

[71] a) J.-P. Charland, M. T. P. Viet, M. St-Jacques, A. L. Beauchamp, *J. Am. Chem. Soc*., **1985**, *107*, 8203; b) S. E. Taylor, E. Buncel, A. R. Norris, *J. Inorg. Biochem.,* **1981**, *15*, 131.

[72] K. V. Catalan, D. J. Mindiola, D. L. Ward, K. R. Dunbar, *Inorg. Chem*., **1997**, *36*, 2458.

[73] E. F. Day, C. A. Crawford, K. Folting, K. R. Dunbar, G. Christou, *J. Am. Chem. Soc*., **1994**, *116*, 9339.

[74] A. C. G. Hotze, M. E. T. Broekhuisen, A. H. Velders, K. van der Schilden, J. G. Haasnoot, J. Reedijk, *Eur. J. Inorg. Chem.,* **2002**, 369.

[75] The authors in ref. [10 c] use the designation E (entgegen) for the syn rotamer and Z (zusammen) for the anti rotamer and refer to the arrangement of the metal with respect to the imidazole part of the purine ring.

[76] J. Arpalahti in *Perspectives on Bioinorganic Chemistry*, Vol. 4., (Eds. R. W. Hay, J. R. Dilworth, K. B. Nolan), JAI Press Inc., Stamford, Connecticut, **1999**, pp. 165-208.

[77] J. Reedijk, *Proc. Natl. Acad. Sci*, **2003**, *100*, 3611.

[78] M. Boudvillain, R. Dalbiès and M. Leng, *Met. Ions Biol. Syst*., **1996**, *33*, 87.

[79] a) D. Yang, S. S. G. E. van Boom, J. Reedijk, J. H. van Boom, A. H.-J. Wang,

Biochemistry, **1995**, *34*, 12912; b) S. L. Bruhn, J. H. Toney, S. J. Lippard, *Prog. Inorg. Chem.*, **1990**, *38*, 477.

[80] S. Komeda, M. Lutz, A. L. Spek, Y. Yamanaka, T. Sato, M. Chikuma, J. Reedijk, *J. Am. Chem. Soc.*, **2002**, *124*, 4738.

[81] F. Pichierri, D. Holthenrich, E. Zangrando and B. Lippert and L. Randaccio, *J. Biol. Inorg. Chem.*, **1996**, 1, 439.

[82] J. Müller, E. Zangrando, N. Pahlke, E. Freisinger, L. Randaccio, B. Lippert, *Chem. Eur. J.*, **1998**, *4*, 397.

[83] J. Arpalahti and K. D. Klika, Eur. *J. Inorg. Chem.*, **2003**, 4195.

[84] B. Lippert, H. Schöllhorn, U. Thewalt, *J. Am. Chem. Soc.*, **1986**, *108*, 6616.

[85] R. Beyerle-Pfnür, S. Jaworski, B. Lippert, *Inorg. Chim. Acta*, **1985**, *107*, 217.

[86] J. A. R. Navarro, B. Lippert, *Coord. Chem. Rev.*, **1999**, *653*, 185 and refs. cited

[87] I. Rother, E. Freisinger, A. Erxleben, B. Lippert, *Inorg. Chim. Acta*, **2000**, *300-302*, 339.

[88] a) G. Lowe, T. Vilaivan, *J. Chem. Soc., Perkin Trans.*, **1996**, *1*, 1499; b) M. J. Clarke, *J. Am. Chem. Soc.,* **1978**, *100*, 5068.

[89] J. Müller, R. K. O. Sigel, B. Lippert, *J. Inorg. Biochem.*, **2000**, *79*, 261.

[90] a) H. Chen, S. Ogo, R. H. Fish, *J. Am. Chem. Soc.,* **1996**, *118*, 4993; b) H. Chen, M. M. Olmstead, D. P. Smith, M. F. Maestre, R. H. Fish, *Angew. Chem. Int. Ed. Engi.*, **1995**, *34*, 1514; c) D. P. Smith, E. Baralt, B. Morales, M. M. Olmstead, M. F. Maestre, R. H. Smith, *J. Am. Chem. Soc.,* **1992**, *114*, 10647.

[91] S. Korn, W. S. Sheldrick, *Inorg. Chim. Acta*, **1997**, *254*, 85.

[92] S. Cosar, M. Flock, E. Freisinger, B. Lippert, unpublished results.

[93] J. Arpalahti, K. D. Klika, R. Sillinpää, R. Kivekäs, *J. Chem. Soc.*, *Dalton Trans.*, **1998**, 1397.

[94] A. Hegmans, E. Freisinger, E. Zangrando, A. Ashfar, E. Hübener, T. G. Appleton, B. Lippert, *Inorg. Chim. Acta*, **1998**, *279*, 152.

[95] M. B. L. Janik, A. Hegmans, E. Freisinger, B. Lippert, *JBIC*, **1999**, *4*, 130.

[96] D. Holthenrich, E. Zangrando, F. Pichierri, L. Randaccio, B. Lippert, *Inorg. Chim. Acta*, **1996**, *248*, 175.

[97] R. Ludwig, *Angew. Chem. Int. Ed.*, **2001**, *40*, 1808 and refs. cited.

[98] D. F. Brougham, R. Caciuffo and A. J. Horsewill, *Nature*, **1999**, *397*, 241.

[99] M. Yoshizawa, T. Kusukawa, M. Kawano, T. Ohhara, I. Tanaka, K. Kurihara, N. Niimura, M. Fujita, *J. Am. Chem. Soc.*, **2005**, *127*, 2798.

[100] a) A. Abo-Rizig, B. Crews, L. Grace and M. S. De Vries, *J. Am. Chem. Soc.*, **2005**, *127*, 2374. b) H. M. Berman and B. Schneider, in *Oxford Handbook of Nucleic Acid Structure*, ed. S. Neidle, Oxford University Press, Oxford, **1999**, pp. 295-312.

[101] E. D. Sloan, *Clathrate Hydrates of Natural Gases*, Marcel Dekker, New York, **1990**.

[102] a) L. J. Barbour, G. W. Orr and J. L. Atwood, *Nature*, **1998**, *393*, 671. b) S. K. Ghosh and P. K. Bharadwaj, *Inorg. Chem.*, **2004**, *43*, 5180. c) P. Rodríguez-Cuamatzi, G. Vargas-Díaz and H. Höpfl, *Angew. Chem. Int. Ed.*, **2004**, *43*, 3041. d) B. Creenivasulu and J. J. Vittal, *Angew. Chem. Int. Ed.*, **2004**, *43*, 5769. e) J. Tao, Z.-J. Ma, R.-B. Huang and L.-S. Zheng, *Inorg. Chem.*, **2004**, *43*, 6133.

[103] a) L. Randaccio, E. Zangrando, A. Cesáro, D. Holthenrich, B. Lippert, *J. Mol. Structure*, **1998**, *440*, 221. b) I. B. Rother, M. Willermann, B. Lippert, *Supramol. Chem.*, **2002**, *14*, 189.

[104] K. Liu, M. G. Brown, C. Carter, R. J. Saykally, J. K. Gregory, D. C. Clary, *Nature*, **1996**, *381*, 501.

[105] K. Nauta, R. E. Miller, *Science*, **2000**, *287*, 293.

[106] F. Weinhold, *J. Chem. Phys.*, **1998**, *109*, 367.

[107] J. M. Ugalde, I. Alkorta, J. Elguero, *Angew. Chem., Int. Ed.*, **2000**, *39*, 717.

[108] J. Kim, D. Majumdar, H. M. Lee, K. S. Kim, *J. Chem. Phys.*, **1999**, *110*, 9128.

[109] K. Liu, J. D. Cruzan, R. J. Saykally, *Science*, **1996**, *271*, 929.

[110] S. Supriya, S. Manikumari, P. Raghavaiah, S. K. Das, *New J. Chem.*, **2003**, *27*, 218.

[111] L.-S. Long, Y.-R. Wu, R.-B. Huang, L.-S. Zheng, *Inorg. Chem.*, **2004**, *43*, 3798.

[112] B.-Q. Ma, H.-L. Sun, S. Gao, *Chem. Commun.*, **2004**, 2220.

[113] C. Foces-Foces, F. H. Cano, M. Martinez-Ripoll, R. Faure, C. Roussel, R. M. Claramunt, C. Lopez, D. Sanz, *Tetrahedron: Asymmetry*, **1990**, *1*, 65.

[114] R. J. Doedens, E. Yphannes, M. I. Khan, *Chem. Commun.*, **2002**, 62.

[115] J. N. Moorthy, R. Natarajan, P. Venugopalan, *Angew. Chem., Int. Ed.*, **2002**, *41*, 3417.

[116] S. K. Ghosh, P. K. Bharadwaj, *Inorg. Chem.*, **2004**, *43*, 6887.

[117] J. L. Atwood, L. J. Barbour, T. J. Ness, C. L. Raston, P. L. Raston, *J. Am. Chem. Soc.*, **2001**, *123*, 7192.

[118] W. B. Blanton, S. W. Gordon-Wylie, G. R. Clark, K. D. Jordan, J. T. Wood, U. Geiserand, T. J. Collins, *J. Am. Chem. Soc.*, **1999**, *121*, 3551.

[119] L. J. Barbour, G. W. Orr, J. L. Atwood, *Chem. Commun.*, **2000**, 859.

[120] R. Custelcean, C. Afloroaei, M. Vlassa, M. Polverejan, *Angew. Chemie. Int. Ed.*, **2000**, *39*, 3094.

[121] S. Pal, N. B. Sankaran, A. Samanta, *Angew. Chem., Int. Ed.*, **2003**, *42*, 1741.

[122] B. H. Ye, B. B. Ding, Y. Q. Weng, X. M. Chen, *Inorg. Chem.*, **2004**, *43*, 6866.

[123] B. Sreenivalusu, J. J. Vittal, *Angew. Chem., Int. Ed.*, **2004**, *116*, 5893.

[124] K. M. Park, R. Kuroda, T. Iwamoto, *Angew. Chem., Int. Ed.*, **1993**, *32*, 884.

[125] K. Raghuraman, K. K. Katti, L. J. Barbour, N. Pillarsetty, C. L. Barnes, K. V. Katti, *J. Am. Chem. Soc.*, **2003**, *125*, 6955.

[126] C. Janiak, T. G. Scharman, *J. Am. Chem. Soc.*, **2002**, *124*, 14010.

[127] B. Q. Ma, H. L. Sun, S. Gao, *Angew. Chem., Int. Ed.*, **2004**, *43*, 1374.

[128] R. Faggiani, C. J. L. Lock, B. Lippert, *Inorg. Chim. Acta*, **1985**, *106*, 75.

[129] T. Itaya, F. Tanaka, T. Fujii, *Tetrahedron*, **1972**, *28*, 535.

[130] a) J. A. McCloskey, S. Nishimura, *Acc. Chem. Res.,* **1977**, *10*, 403; b) A. Rich, *Acc. Chem. Res*., **1977**, *10*, 388.

[131] B. E. H. Maden, *Prog. Nucleic Acid Res. Mol. Biol.,* **1990**, *39*, 241.

[132] M. Roitzsch, B. Lippert, *J. Am. Chem. Soc.,* **2004**, *126*, 2421.

[133] D. J. Brown, J. S. Harper, *J. Chem. Soc.,* **1963**, 1276; T. Fujii, T Itaya, *Heterocycles,* **1998**, *48*, 359.

[134] T. Itaya, F.Tanaka,T Fujii, *Tetrahedron,* **1972**, *28*, 535.

[135] D. J. Brown, *Nature,* **1961**, *189*, 828.

[136] P. J. Sanz Miguel, P. Lax, B. Lippert, unpublished results.

[137] R. J. Walker, P. Tollin, J. N. Low, *Cryst. Struct. Commun.*, **1987**, B37, 140.

[138] V. Lager, K. Huml, *Acta Crystallogr.*, **1978**, B34, 1881.

[139] E. Freisinger, I. B. Rother, M. S. Lüth, B. Lippert, *PNAS*, **2003**, *100*, 3748.

[140] J. E. Šponer, P. J. Sanz Miguel, L. Rodriguez-Santiago, A. Erxleben, M. Krumm, M.

Sodupe, J. Sponer, B. Lippert, *Angew. Chem Int. Ed.,* **2004**, *43*, 5396.

[141] K. D. Klika, J. Arpalahti, *Chem. Commun*., **2004**, 666.

[142] B. Lippert, C. J. L. Lock, R. A. Speranzini, *Inorg. Chem*., **1981**, *28*, 808.

[143] E. Freisinger, A. Schneider, M. Drumm, A. Hegmans, S. Meier, B. Lippert, *J. Chem. Soc. Dalton*, **2000**, 2381.

[144] M. Roitzsch, M. Garijo Añorbe, P. J. Sanz Miguel, B. Müller, B. Lippert, *J. Biol. Inorg. Chem*., **2005**, *10*, 800.

[145] D. W. Urry, S. Q. Peng, T. M. Parker, D. C. Gowda, and R. D. Harris, *Angew. Chem., Int. Ed. Engl.*, **1993**, *32*, 1440.

[146] M. Tolinger, J. D. Forman-Kay, and E. Kay, *J. Am. Chem. Soc.,* **2002**, *124*, 5714.

[147] C. Liang, M. J. Weaver, and S. Dai, *Chem. Commun.*, **2002**, 1620.

[148] F. C. Kokesh, F. H. Westheimer, *J. Am. Chem. Soc.,* **1971**, *93*, 7270.

[149] F. Schwarz, Dissertation, Universität Dortmund, Dortmund, **1990**.

[150] F. Schwarz, B. Lippert, H. Schöllhorn, U. Thewalt, *Inorg. Chim. Acta*, **1990**, *176*, 113.

[151] W. D. Kumler et al., *J. Am. Chem. Soc.,* **1942**, *64*, 1941.

[152] John Burgess, *Ions in solution: Basic principles of chemical interactions*, Halsted Press, **1988**.

[153] T. G. Appleton, A. J. Bailey, K. J. Barnham, J. R. Hall, *Inorg. Chem*., **1992**, *31*, 3077.

[154] C. J. Boreham, J. A. Broomhead, D. P. Fairlie, *Aust. J. Chem.*, **1981**, *34*, 659.

[155] M. Chikuma, R. J. Pollock, *J. Magn. Reson.*, **1982**, *47*, 324.

[156] T. G. Appleton, R. D. Berry, C. A. Davis, J. R. Hall, H. A. Kimlin, *Inorg. Chem.*, **1984**, *23*, 3514.

[157] T. G. Appleton, J. R. Hall, S. F. Ralph, *Inorg. Chem*., **1985**, *24*, 4685.

[158] T. G. Appleton, J. R. Hall, S. F. Ralph, C. S. M. Thompson, *Inorg. Chem.*, **1989**, *28*, 1989.

[159] NAG FORTRAN Library, Routine E04FDF, Numerical Algorithm Group, Oxford, UK; **1982**.

[160] M. Wall, B. Linkletter, D. Williams, A-M. Lebuis, R. C. Hynes, J. Chin, *J. Am. Chem. Soc.,* **1999**, *121*, 4710.

[161] a) E. Kovari, R. Kramer, *J. Am. Chem. Soc.,* **1996**, *118*, 12704. b) J. R. Morrow, W. C. Trogler, *Inorg. Chem.,* **1988**, *27*, 3387. c) M. K. Stern, J. K. Bashkin, *Inorg. Chim. Acta*, **1997**, *263*, 49. d) S. Liu, A. D. Hamilton, *Tetrahedron Lett.,* **1997**, *38*, 1107. e) J. N. Burstyn, K. A. Deal, *Inorg. Chem*., **1993**, *32*, 3585.

[162] J. F. Britten, B. Lippert, C. J. L. Lock, P. Pilon, *Inorg. Chem.,* **1982**, *21*, 1936.

[163] B. Lippert, *Inorg. Chem.,* **1985**, *24*, 989.

[164] K. D. Karlin, J. Zubieta, Eds., *Biological and Inorganic Copper Chemistry*, Adenine Press, New York, **1986**.

[165] G. La Monica, G. Attilio Ardizzoia, *Prog. Inorg. Chem.,* **1997**, *46*, 151.

[166] S. Trofimenko, *Prog. Inorg. Chem.,* **1986**, *34*, 115.

[167] L. A. Oro, M. A. Ciriano, C. Tejel, *Pure & Appl. Chem.,* **1998**, *70*, 779.

[168] C. Pettinari, F. Marchetti, A. Cigolani, S. I. Troyanov, A. Drozdow, *J. Chem. Soc.*, *Dalton Trans.*, **1998**, 3335.

[169] M. A. Cinellu, S. Stoccoro, G. Minghetti, A. L. Bandini, G. Banditelli, B. Bovio, *J. Organomet. Chem.,* **1989**, *372*, 311.

[170] W. Burger, J. Strähle, *Z. Anorg. Allg. Chem.,* **1986**, *539*, 27.

[171] V. K. Jain, S. Kannan, E. R. T. Tiekink, *J. Chem. Soc.*, *Dalton Trans*. **1993**, 3625.

[172] W. Burger, J. Strähle, *Z. Anorg. Allg. Chem.,* **1985**, *529*, 111.

[173] D. Röttger, G. Erker, M. Grehl, R. Fröhlich, *Organometallics,* **1994**, *13*, 3897.

[174] M. Blais, *Thermodinamic. Acta,* **1977**, *20*, 335.

[175] W. Hückel, H. Bretschneider, *Chem. Ber*., **1937**, *71*, 2024.

[176] S. Reimlinger, K. Noels, *Chem. Ber.,* **1970**, *103*, 1957.

[177] G. Yagil, *Tetrahedron,* **1967**, *23*, 2855.

[178] M. Krumm, *Dissertation*, Universität Dortmund, **1992**.

[179] K. Inagaki, Y. Kidani, *Bioinorg. Chem*., **1986**, *9*, 157.

[180] A. Fichtel, *Diplomarbeit*, Universität Dortmund, **1997**.

[181] A. Schneider, *Dissertation*, Universität Dortmund, **2002**.

[182] O. Krizanovic, F. J. Pesch, B. Lippert, *Inorg. Chim. Acta*, **1989**, *165*, 145.

[183] G. C. Papavassiliou, T. Theophanides, *Journal of Raman Spectroscopy*, **1978**, *7*, 230.

[184] M. Cannas, G. Marongiu, R. Martin, H. J. Keller, *Naturforsch.*, **1983**, *38b*, 1346.

[185] S. C. Huckett, B. Scott, S. P. Love, R. J. Donohoe, C. J. Burns, E. Garcia, T. Frankcom, B. I. Swanson, *Inorg. Chem.*, **1993**, *32*, 2137.

[186] E. J. W. Austin, P. J. Barrie, R. J. H. Clark, *Inorg. Chem.*, **1995**, *34*, 3859.

[187] KappaCCD package, Nonius, Delft, The Netherlands, **1997**.

[188] Z. Otwinowsky, W. Minor, DENZO and SCALEPACK. *Methods Enzymol*, **1997**, *276*, 307.

[189] G. M. Sheldrick, *Acta Crystallogr., Sect. A 46*, **1990**, 467.

[190] G. M. Sheldrick, SHELXTL-PLUS (VMS), Siemens Analytical X-Ray Instruments, Madison, WI, **1990**.

[191] G. M. Sheldrick, SHELXL-97, program for crystal structure refinement, University of Göttingen, Germany, **1993**.

[192] L. J. Farrugia, *J. Appl. Cryst.,* **1999***, 32, 837*. Windows programs for the solution, refinement and analysis of single crystal X-ray diffraction data. http://www.chem.gla.ac.uk/~louis/wingx.

[193] L. J. Farrugia, *J. Appl. Cryst.,* **1997**, *30*, 565.

[194] Persistence of Vision Raytracer (POV-Ray), Version 3.6, Persistence of Vision Raytracer Pty. Ltd., PO Box 407, Williamstown, Victoria 3016, Australia, **2005**.

[195] A. D. Becke, *J. Chem. Phys.,* **1993**, *98*, 5648.

[196] C. Lee, W. Yang, R.G. Parr, *Phys. Rev. B37*, **1998**, 785.

[197] J. S. Nowick, J. S. Chen, G. Noronha *J. Am. Chem. Soc.,* **1993**, *115*, 7636.

[198] T. J. Kistenmacher, M. Rossi, J. P. Caradonna, L. G. Marzilli *Adv. Mol. Relax. Interact. Processes,* **1979**, *15*, 119.

[199] G. B. Kauffmann, D. O. Cowan *Inorg. Synth.,* **1963**, *7*, 239.

[200] a) S. C. Dhara, *Indian. J. Chem.,* **1970**, *8*, 193. b) G. Raudaschl-Sieber,B.Lippert,J.D. Hoeschele, H. E. Howard-Lock, C. J. L. Lock, P. Pilon, *Inorg. Chim. Acta,* **1985**, *106*, 141.

[201] W. A. Cude, G. W. Watt *Inorg. Chem.,* **1968**, *7*, 335.

[202] O. Krizanovic, *Dissertation*, Universität Dortmund, **1991**.

[203] A. Schreiber, M. S. Lüth, A. Erxleben, E. C. Fusch, B. Lippert, *J. Am. Chem. Soc.*, **1996**, *118*, 4124.

[204] A. Iakovidis, N. Hadjiliadis, F. Dahan, J. P. Laussac, B. Lippert, *Inorg. Chim. Acta,* **1990**, *175*, 57.

[205] V. Aletras, N. Hadjiliadis, B. Lippert, *Polyhedron,* **1992**, *11*, 1259.

[206] A. Terzis, *Inorg. Chem.*, **1976**, *15*, 793.

List of abbreviations

Ligands and Chemicals

1-MeC	1-methylcytosine
1-MeUH	1-methyluracil in its neutral form
1-MeU$^-$	1-methyluracilate, deprotonated at N3
9-MeA	9-methyladenine
9-MeAH$^+$	9-methyladeninium, protonated at N1
9-EtA$^-$	9-ethyladenine, deprotonated at N1
9-EtGH	9-ethylguanine in its neutral form
1,9-DimeA	1,9-dimethyladenine (uncharged form; N6 forms an imino group)
1,9-DimeAH$^+$	1,9-dimethyladeninium (protonated at N6; N6 forms an amino group)
A (C, G, T, U)	general abbreviation for adenin- (cytosin-, guanin-, thymin-, uracyl-) derivates
cis/*trans*-DDP	*cis*/*trans*-diamminodichloroplatinum (II)
dien	diethylenetriamine
[(dien)Pt^{II}]	[(dien)Pt(H_2O)]$^{2+}$ or [(dien)Pt(D_2O)]$^{2+}$
DMSO-*d6*	deuterated dimethylsulfoxide
DNA	desoxyribonucleic acid
EDTA	Ethylendiaminetetraacetic acid – disodium salt
pzH	pyrazol
pyz	pyrazine
RNA	ribonucleic acid
TSP	sodium 3-trimethylsilyl-propanesulfonate

Spectroscopy

NMR	nuclear magnetic resonance
NOE	nuclear Overhauser effect

δ	NMR chemical shift in ppm
ppm	parts per million
IR	infrared

Common abbreviations

ca.	approximately
eq.	equivalent
et al.	and co-workers
h	hour
M	molar
pD	negative logarithms of the deuterium ion concentration
pH*	uncorrected pH meter reading in D_2O
pK_a	negative logarithms of the acidity constant
viz.	in other words
vs.	versus
s	singlet
brs	broad signal
d	doublet
m	multiplet

List of compounds

1 [(dien)Pt(9-MeA-*N1*)]$(NO_3)_2$

2 *cis*-[$(NH_3)_2$Pt(1-MeC-*N3*)(9-MeA-*N7*)]$(ClO_4)_2 \cdot H_2O$

3 *trans*-[$(NH_3)_2$Pt(9-MeA-*N7*)$_2$]$(ClO_4)_2 \cdot 2H_2O$

4 *cis*-[$(NH_3)_2$Pt(9-MeA-*N7*)$_2$]$(NO_3)_2 \cdot 2H_2O$

5 *cis*-[$(NH_3)_2$Pt(1-MeC-*N3*)(*N7*-9-MeA-*N1*)(dienPt)]$(ClO_4)_4$

6 *cis*-[{$(NH_3)_2$Pt(1-MeC-*N3*)}$_2$(9-MeA-*N1,N7)*]$(ClO_4)_4$

7 *trans*-[{$(NH_3)_2$Pt(1-MeC-*N3*)}$_2$(9-MeA-*N1,N7)*]$(ClO_4)_4$

8 *trans*-[$(NH_3)_2$ClPt(*N7*-9-MeA-*N1*)(dienPt)]$(ClO_4)_3$

9 *trans*-[$(NH_3)_2$Pt(*N7*-9-MeA)(*N7*-9-MeA-*N1*)(dienPt)]$^{4+}$

10 *trans*-[$(NH_3)_2$Pt{(*N7*-9-MeA-*N1*)(dienPt)}$_2$]$^{6+}$

11 *cis*-[$(NH_3)_2$Pt{(*N1*-9-MeA-*N7*)Pt$(NH_3)_3$}$_2$]$(NO_3)_6 \cdot 2H_2O$

12 *cis*-[$(NH_3)_2$Pt{(*N7*-9-MeA-*N1*)(dienPt)}$_2$]$(NO_3)_6$

13 *trans,trans,trans*-[$(NH_3)_2$Pt(*N7*-9-MeA-*N1*)(dienPt)(*N7*-9-EtA-*N1*){$(NH_3)_2$Pt(9-MeGH-*N7*)}]$(ClO_4)_3(NO_3)_3$

14 *trans*,*trans*,*trans*-{$(NH_3)_2$Pt(*N7*-9-MeA-*N1*)$_2$[$(NH_3)_2$Pt(9-EtGH-*N7*)]$_2$}$^{6+}$

15 *trans*-[{$(NH_3)_2$Pt(1-MeC-*N3*)}$_2$(9-MeA-*N7*,*N6*)]$(ClO_4)_3 \cdot 3.5H_2O$

16 [(9-MeA-*N7*)Pt$(NH_3)_3$]$Cl_2 \cdot 2H_2O$

17 *cis*-[$(NH_3)_2$Pt(*N1*-9-MeA-*N7*)(*N6*-9-MeA-*N7)*{Pt$(NH_3)_3$}$_2$]$^{5+}$

18 *cis*-[$(NH_3)_2$Pt(*N6*-9-MeA-*N7)*$_2${Pt$(NH_3)_3$}$_2$]$(NO_3)_4 \cdot 6H_2O$

19 [{(dien)Pd}$_3$(9-MeA-*N1*,*N7*,*N6*)]$Cl_{3.5}(PF_6)_{1.5} \cdot 3H_2O$

20 [Pt(1-MeC-*N3*)$_3$(9-MeA-*N7*)]$(NO_3)_2$

21 [Pt(1-MeC-*N3*)$_3$(OH)]$(ClO_4)_{0.5}(OH)_{0.5} \cdot 7H_2O$

22 *trans*-[$(NH_3)_2$Pt(1,9-DimeAH-*N7*)(1-MeC-*N3*)]$(NO_3)_3$

23 *trans*-[$(NH_3)_2$Pt(1,9-DimeAH-*N7*)(9-MeGH-*N7*)]$(NO_3)_3$

24 *trans*-[$(NH_3)_2$Pt(6,9-DimeA-*N7*)(1-MeC-*N3*)]$(NO_3)_2 \cdot H_2O$

25 *trans*-[$(NH_3)_2$Pt(6,9-DimeA-*N7*)(9-MeGH-*N7*)]$(NO_3)_2 \cdot 5H_2O$

26 *trans*-[$(NH_3)_2$Pt(1-MeC-*N3*)$_2$]$^{2+}$

27 *trans*-[$(NH_3)_2$Pt(1-MeC-*N3*)(9-MeA-*N7*)]$(ClO_4)_2$

28 *trans*-[$(NH_3)_2$Pt(pzH)Cl](NO_3)

29 *trans*,*trans*,*trans*-{$(NH_3)_2$Pt(*N1*-pz-*N2*)$_2$[$(NH_3)_2$Pt(1-MeC-*N3*)]$_2$}$^{6+}$

30 *trans*-$[(NH_3)_2Pt\{(pzH)Cl\}_2](NO_3)_2 \cdot H_2O$

31 *trans*,*trans*-$[(NH_3)_2Pt(pzH)_2Cl_2][(NH_3)_2Pt(pzH)_2](ClO_4)_4 \cdot H_2O$

32 *trans*-$[(NH_3)_2Pt\{(pzH)Cl\}_2](ClO_4)_2 \cdot H_2O$

33 *trans*-$[(NH_3)_2Pt(pzH)(9\text{-MeGH-}N7)](NO_3)_2$

34 *trans,trans*-$[(NH_3)_2Pt(9\text{-MeGH-}N7)(N1\text{-pz-}N2)(NH_3)_2Pt(1\text{-MeC-}N3)](NO_3)_3$

Tables of the pD dependences

1. pD dependences of the different compounds studied in this thesis

Table B-1: *Chemical shifts for compound **1** in D_2O in dependence of pD.*

pD	CH_3	H8
1.04	3.910	8.610
1.42	3.863	8.343
1.55	3.853	8.283
1.88	3.840	8.205
2.09	3.836	8.180
2.33	3.834	8.167
2.92	3.833	8.156
3.55	3.832	8.153
4.35	3.832	8.153
5.05	3.832	8.153
6.45	3.832	8.153
7.4	3.833	8.153
7.84	3.831	8.150
9.35	3.831	8.150
10.66	3.832	8.152
11.47	3.831	8.149
11.96	3.828	8.141
12.37	3.824	8.128
12.50	3.822	8.124
12.79	3.809	8.091
13.21	3.778	8.011

Table B-2: *Chemical shifts for compound **2** in D_2O in dependence of pD.*

pD	CH_3-A	CH_3-C	H6	H5	H2/8	H2/8
7.12	3.868	3.346	7.556	6.007	8.341	8.562
10.32	3.869	3.346	7.554	6.006	8.341	8.566
10.78	3.869	3.346	7.550	6.003	8.342	8.563
10.94	3.869	3.346	7.549	6.002	8.342	8.561
11.10	3.867	3.344	7.545	6.0015	8.337	

11.25	3.868	3.345	7.544	6.0015	8.339
11.56	3.867	3.345	7.534	5.993	8.339
11.7	3.867	3.344	7.526	5.987	8.336
11.94	3.866	3.338	7.503	5.967	8.338
12.15	3.865	3.326	7.464	5.942	8.335
12.22	3.865	3.318	7.432	5.919	8.336
12.47	3.863	3.294	7.351	5.865	8.333
12.52	3.862	3.295	7.356	5.871	8.331
12.7	3.858	3.267	7.263	5.807	8.327
12.78	3.857	3.256	7.228	5.785	8.324
12.92	3.856	3.227	7.125	5.718	8.320
13.02	3.852	3.231	7.062	5.675	8.315
13.11	3.855	3.221	7.098	5.701	8.316

Table B-3: *Chemical shifts for compound **3** in D_2O in dependence of pD.*

pD	CH_3
0.88	4.059
1.17	4.050
1.78	4.014
1.93	3.996
2.27	3.992
2.64	3.985
4.47	3.976
5.84	3.977
6.78	3.977
8.92	3.977
9.33	3.976
10.46	3.976
11.08	3.976
11.42	3.976
12.20	3.974
12.58	3.969
12.75	3.964
12.87	3.956
13.29	3.947

Table B-4: *Chemical shifts for compound* ***4*** *in D_2O in dependence of pD.*

pD	CH_3
0.15	3.909
0.55	3.907
0.66	3.906
0.96	3.900
1.17	3.900
1.66	3.876
2.05	3.852
2.43	3.829
2.81	3.815
3.06	3.814
3.2	3.813
3.4	3.813
4.15	3.812
4.47	3.812
4.75	3.813
6.2	3.813
8	3.812
10.9	3.813
11.54	3.812
11.82	3.812
12.56	3.809
12.7	3.810
13	3.808

Table B-5: *Chemical shifts for compound* ***5*** *in D_2O in dependence of pD.*

pD	CH_3-A	CH_3-C	H5	H6	H2/8
5.90	3.892	3.362	6.021	7.558	8.700
6.05	3.891	3.361	6.021	7.558	8.700
6.40	3.891	3.358	6.026	7.559	8.703
7.05	3.890	3.356	6.025	7.560	8.703
7.90	3.892	3.361	6.024	7.560	8.776
8.25	3.890	3.357	6.026	7.560	8.779
9.15	3.891	3.361	6.024	7.559	8.777
9.66	3.890	3.368	6.022	7.561	8.758
9.9	3.885	3.365	6.020	7.559	8.747

10.05	3.884	3.364	6.019	7.559	8.743
10.15	3.884	3.359	6.024	7.559	8.757
10.45	3.875	3.368	6.015	7.556	8.705
10.50	3.869	3.366	6.015	7.556	8.694
10.63	3.867	3.366	6.014	7.555	8.685
10.78	3.864	3.366	6.013	7.554	8.674
10.79	3.864	3.372	6.012	7.554	8.663
10.85	3.850	3.373	6.007	7.555	8.607
10.90	3.855	3.369	6.01	7.553	8.641
10.95	3.836	3.377			8.547
11.44	3.795	3.385	5.975	7.537	8.384
11.80	3.778	3.388	5.964	7.527	8.315
12.18	3.752	3.383	5.934	7.493	8.220
12.41	3.740	3.372	5.902	7.449	8.181
12.81	3.730	3.346	5.844	7.363	8.156
13.18	3.717	3.290	5.726	7.186	8.131

Table B-6: *Chemical shifts for compound* ***6*** *in D_2O in dependence of pD.*

pD	CH_3-A
3.57	3.874
3.73	3.878
4.77	3.875
5.84	3.878
6.60	3.877
7.84	3.879
9.02	3.876
10.09	3.876
10.64	3.859
11.03	3.842
11.28	3.825
11.41	3.816
11.48	3.814
11.69	3.799
11.77	3.793
11.93	3.766
11.95	3.760
12.20	3.754

12.45	3.740
12.50	3.735
12.66	3.732
12.98	3.714
13.22	3.700

Table B-7: *Chemical shifts for compound **7** in D_2O in dependence of pD.*

pD	CH_3-A
5.8	4.008
7.3	4.008
8.14	4.005
8.6	4.005
9.25	3.992
9.54	3.991
9.63	3.990
9.74	3.984
9.92	3.980
10.23	3.953
10.48	3.934
10.84	3.894
11.14	3.874
11.86	3.839
12.31	3.836
12.41	3.834

Table B-8: *Chemical shifts for compound **8** in D_2O in dependence of pD.*

pD	CH_3	H8
2.05	3.947	8.860
2.52	3.947	8.860
3.99	3.947	8.862
5.08	3.948	8.861
5.48	3.947	8.861
6.28	3.948	8.862
7.90	3.946	8.861
9.18	3.947	8.861
10.08	3.945	8.857

10.48	3.935	-
11.36	3.884	8.649
11.97	-	8.389
12.10	3.824	8.332
12.58	-	-
12.32	3.812	8.285
12.96	3.783	8.179
13.32	3.771	8.154

Table B-9: *Chemical shifts for compound* **9** *in D_2O in dependence of pD.*

pD	CH_3	CH_3
3.01	4.009	4.001
3.4	4.010	4.000
3.57	4.009	4.000
3.86	4.008	4.000
4.88	4.009	3.999
5.18	4.008	3.999
5.2	4.008	3.999
5.5	4.008	3.999
5.73	4.008	3.999
5.85	4.007	3.999
6.99	4.008	3.998
7.85	4.004	3.999
8.8	3.950	3.980
9.84	-	3.973
10.26	3.879	3.967
10.58	3.854	3.961
11.27	3.829	3.955
11.5	3.826	3.954
11.8	3.822	3.953
12.7	3.822	3.952
13.48	3.818	3.949

Table B-10: *Chemical shifts for compound **10** in D_2O in dependence of pD.*

pD	CH_3
3.32	4.023
3.88	4.023
5.5	4.022
6.49	4.022
7.07	4.024
7.65	4.019
7.96	4.007
8.30	4.001
8.44	3.994
9.17	3.970
9.42	3.951
9.67	3.939
10.13	3.920
10.60	3.908
10.68	3.903
10.80	3.893
11.33	3.878
11.61	3.871
12.32	3.861

Table B-11: *Chemical shifts for compound **11** in D_2O in dependence of pD.*

pD	H2/H2'	H8
5,97	9,005/9,056	8,784
6,22	9,006/9,051	8,778
6,71	9,008/9,051	8,782
7,09	9,005/9,046	8,785
7,21	9,006/9,047	8,780
7,51	9,011	8,778
7,64	9,010	8,777
7,75	9,009	8,775
7,92	9,006	8,773
8,03	8,994	8,769
8,21	8,977	8,759
8,68	8,936	8,728
8,95	8,894	8,699

9,4	8,808	8,638
9,69	8,755	8,599
9,84	8,743	
10,1	8,674	
10,55	8,632	
10,65	8,614	
11,1	8,498	
11,34	8,441	
12,14	8,318	
13	8,275	

Table B-12: *Chemical shifts for compound **12** in D_2O in dependence of pD.*

pD	H2	H8
5,63	8,722	
6,46	8,723	
6,98	8,731	8,802
7,3	8,737	8,801
7,85	8,733	8,801
8,16	8,725	8,780
8,34	8,706	8,758
8,53	8,701	8,747
9,02	8,672	
9,44	8,644	
9,52	8,620	
9,56	8,604	
9,84	8,572	
10,1	8,554	
10,43	8,443	
10,66	8,316	
11,12	8,247	
11,47	8,191	
12,23	8,142	
13,25	8,114	

Table B-13: *Chemical shifts for compound **13** in D_2O in dependence of pD.*

pD	CH_2(Et)	CH_3-A	CH_3-G	CH_3(Et)
2.38	4.504	4.049	3.806	1.618
3.78	4.507	4.050	3.809	1.613
4.26		4.049	3.805	1.620
4.46	4.504	4.049	3.806	1.619
4.80		4.050	3.806	1.620
5.07		4.049	3.806	1.620
5.64	4.505	4.048	3.807	1.612
6.25		4.048	3.806	1.619
6.59	4.505	4.049	3.806	1.618
6.72	4.498	4.046	3.804	1.615
6.80	4.498	4.047	3.805	1.617
7.09	4.503	4.046	3.805	1.612
7.19	4.502	4.046	3.805	1.617
7.27	4.502	4.046	3.804	1.612
7.46	4.500	4.045	3.803	1.612
7.52	4.501	4.045	3.804	1.612
7.71	4.499	4.044	3.802	1.614
7.81	4.497	4.043	3.801	1.613
7.99	4.492	4.040	3.799	1.609
8.13	4.488	4.038	3.798	1.608
8.20	4.489	4.038	3.798	1.609
8.37		4.028	3.793	1.598
8.53	4.465	4.018	3.791	1.595
8.67	4.438	3.999	3.787	1.582
8.75	4.444	4.003	3.787	1.585
8.94	4.428	3.986	3.785	1.575
9.16		3.978	3.785	1.571
9.27	4.402	3.967	3.783	1.563
9.77	4.372	3.940	3.783	1.549
10.55	4.355	3.924	3.781	1.539
10.73	4.353	3.922	3.781	1.539

Table B-14: *Chemical shifts for compound **14** in D_2O in dependence of pD.*

pD	CH_2(G)	CH_3(A)	CH_3(G)
3.01	4.239	4.087	1.502
3.50	4.240	4.087	1.502
4.70	4.240	4.087	1.502
5.05	4.241	4.088	1.504
5.50	4.240	4.088	1.504
6.13	4.238	4.083	1.503
6.64	4.234	4.078	1.502
6.85	4.230	4.068	1.502
7.13	4.215	4.031	1.497
7.52	4.203	4.006	1.493
7.65	4.201	4.001	1.493
7.85	4.194	3.990	1.489
8.02	4.187	3.980	1.486
8.35	4.175	3.969	1.481
8.73	4.169	3.958	1.476
8.94	4.165	3.953	1.473
9.10	4.165	3.949	1.471
9.20	4.158	3.945	1.469
9.47	4.154	3.941	1.467
10.02	4.147	3.933	1.462
10.13	4.147	3.933	1.461
10.80	4.144	3.930	1.460
11.45	4.143	3.929	1.458
11.70	4.142	3.929	1.459
12.18	4.143	3.928	1.458

Table B-15: *Chemical shifts for compound **15** in D_2O in dependence of pD.*

pD	H2
2.53	8.34
3.0	8.34
4.15	8.34
4.42	8.33
5.02	8.30
5.25	8.28
5.42	8.25

5.55	8.24
5.74	8.21
6.03	8.18
6.89	8.14
7.48	8.14
7.94	8.14

Table B-16: *Chemical shifts for compound* ***17*** *in D_2O in dependence of pD.*

pD	CH_3	CH_3	H8(A)	H2(A)
1.97	3.902	3.863	9.105	8.333
2.31	3.905	3.866	9.104	8.335
2.82	3.902	3.863	9.105	8.333
4.04	3.903	3.859	9.105	8.332
4.35	3.902	3.862	9.105	8.332
4.44	3.903	3.853	9.102	8.318
4.90	3.905	3.843	9.099	8.303
5.14	3.906	3.841	9.092	8.308
5.24	3.906	3.843	9.094	8.310
5.64	3.909	3.837	9.087	8.267
5.79	3.911	3.802	9.083	8.242
5.91	3.910	3.802	9.084	8.241
6.53	3.912	3.783	9.077	8.218
6.87	3.913	3.783	9.076	8.213
7.61	3.913	3.782	9.074	8.211
8.06	3.919	3.787	9.080	8.219
8.70	3.914	3.780	9.076	8.209
9.22	3.911	3.779	9.070	8.206
9.59	3.913	3.784	9.064	8.211
10.24	3.909	3.780	9.063	8.205
11.07	3.867	3.779	8.908	8.184
11.56	3.826	3.782	8.756	8.170
12.06	3.799	3.777	8.652	8.154
12.13	3.789	3.779	8.617	8.153
12.46	3.782	3.763	8.517	8.144
12.57	3.777	3.764	8.509	8.138
13.14	3.782	3.744	8.436	8.136
13.27	3.781	3.744	8.432	8.135

Table B-17: *Chemical shifts for compound **18** in D_2O in dependence of pD.*

pD	H8/2
2.92	8.36
4.00	8.35
5.10	8.32
5.61	8.30
6.12	8.26
6.60	8.22
7.20	8.18
7.80	8.14
8.74	8.12
10.53	8.12

Table B-18: *Chemical shifts for compound **20** in D_2O in dependence of pD.*

pD	CH_3(A)	CH_3(C1)	CH_3(C2)	H2(A)	H6(C2)	H6(C1)	H5(C2)	H5(C1)
3.30	3.850	3.428	3.336	8.272	7.517	7.568	5.930	6.002
5.88	3.844	3.425	3.331	8.260	7.505	7.562	5.921	5.999
6.40	3.847	3.429	3.337	8.262	7.516	7.568	5.930	6.004
7.54	3.846	3.427	3.335	8.261	7.515	7.566	5.928	6.002
7.60	3.846	3.428	3.336	8.262	7.516	7.567	5.929	6.003
8.28	3.846	3.428	3.336	8.262	7.517	7.568	5.929	6.003
8.97	3.846	3.428	3.336	8.261	7.516	7.567	5.929	6.003
9.82	3.847	3.429	3.336	8.263	7.517	7.568	5.930	6.004
10.32	3.847	3.428	3.336	8.264	7.517	7.569	5.930	6.004
10.67	3.851	3.432	3.340	8.266	7.519	7.572	5.932	6.007
10.72	3.850	3.432	3.339	8.266	7.519	7.571	5.932	6.007
10.92	3.850	3.432	3.339	8.266	7.517	7.571	5.931	6.006
11.17	3.842	3.423	3.330	8.257	7.507	7.561	5.922	5.996
11.20	3.850	3.431	3.338	8.266	7.515	7.570	5.929	6.005
11.45	3.846	3.428	3.336	8.263	7.517	7.568	5.929	6.004
11.55	3.842	3.423	3.328	8.257	7.500	7.559	5.917	5.995
12.30	3.843	3.416	3.315	8.259	7.455	7.546	5.885	5.98
12.75	3.837	3.400	3.287	8.253	7.379	7.515	5.830	5.957
12.86	3.836	3.397	3.280	8.250	7.360	7.507	5.816	5.951
13.08	3.833	3.386	3.263	8.248	7.314	7.488	5.782	5.934
13.38	3.823	3.366	3.229	8.237	7.226	7.447	5.717	5.899
13.52	3.821	3.359	3.217	8.235	7.193	7.433	5.693	5.887

13.61	3.819	3.354	3.207	8.234	7.164	7.420	5.672	5.876
13.72	3.815	3.340	3.186	8.231	7.103	7.385	5.627	5.850

Table B-19: *Chemical shifts for compound **21** in D_2O in dependence of pD.*

pD	CH_3(1)
2.79	3.423
5.14	3.422
5.48	3.420
5.96	3.418
6.24	3.415
7.0	3.411
7.9	3.409
9.95	3.409
10.37	3.409
12.1	3.408

Table B-20: *Chemical shifts for compound **22** in D_2O in dependence of pD.*

pD	H2	H8	H6	H5	CH_3-N9	CH_3-N1	CH_3-C
1.5	8.754	8.969	7.683	6.099	4.073	4.047	3.505
2.02	8.753	8.967	7.682	6.097	4.070	4.044	3.503
4.68	8.751	8.982	7.683	6.099	4.069	4.045	3.504
5.92	8.699	8.915	7.681	6.096	4.024		3.501
6.14	8.674	8.897	7.680	6.095	4.018	4.008	3.501
6.24	8.663	8.891	7.679	6.094	4.015	3.999	3.501
7.0	8.461	8.697	7.671	6.086	3.950	3.838	3.494
7.13	8.378	8.627	7.667	6.084	3.925	3.776	3.491
8.22	8.238	8.486	7.663	6.077	3.883		3.488
8.45	8.209	8.478	7.666	6.078	3.875	3.636	3.487
8.76	8.206	8.486	7.665	6.079	3.876	3.635	3.486
9.04	8.202	8.479	7.666	6.080	3.874	3.632	3.487
9.18	8.217	8.466	7.668	6.081	3.875	3.639	3.486
9.20	8.204	8.480	7.666	6.080	3.874	3.632	3.488
9.37	8.202	8.478	7.666	6.079	3.874	3.631	3.488
9.76	8.200	8.471	7.666	6.078	3.873	3.629	3.488
9.86	8.200	8.480	7.668	6.082	3.875	3.629	3.488
10.28	8.200	8.475	7.667	6.080	3.874	3.629	3.488

11.91	8.201	8.470	7.657	6.072	3.873	3.630	3.486
12.15	8.197	8.430	7.606	6.041			

Table B-21: *Chemical shifts for compound **23** in D_2O in dependence of pD.*

pD	CH_3-N9	CH_3-N1	CH_3-(G)	H2(A)	H8(A)	H8(G)
1.81	4.050	4.017	3.788	8.741	9.089	8.357
2.87	4.055		3.794	8.741	9.120	8.400
3.34	4.051	3.957	3.786	8.739		8.448
5.13	4.048		3.790			
6.07	4.046		3.790	8.727		8.410
6.14	4.020	3.980	3.785	8.653	9.001	8.356
7.28	3.980	3.943	3.786			
7.62	3.941	3.914	3.779			
7.85	3.913	3.899				
8.75	3.888	3.771	3.619	8.336	8.611	8.220
9.48	3.878	3.753	3.602	8.235	8.410	8.187
11.53	3.879	3.754	3.598	8.243	8.593	8.188
12.09	3.877	3.749	3.600			
12.83	3.878	3.749	3.598			

Table B-22: *Chemical shifts for compound **24** in D_2O in dependence of pD.*

pD	CH_3-C	CH_3-N9	CH_3-N6	H8	H2	H6	H5
0.61	3.524	4.043	3.551	8.916	8.640	7.681	6.095
0.76	3.524	4.042	3.548	8.901	8.638	7.681	6.092
0.92	3.525	4.042	3.547	8.911	8.638	7.683	6.095
1.12	3.525	4.039	3.541	8.896	8.634	7.685	6.095
1.28	3.526	4.036	3.534	8.891	8.628	7.687	6.097
1.46	3.521	4.029	3.525	8.867	8.614	7.688	6.096
1.55	3.510	4.024	3.526	8.829	8.591	7.688	6.097
1.68	3.496	4.018	3.526	8.829	8.591	7.689	6.097
1.86	3.472	4.005	3.526	8.790	8.567	7.688	6.097
2.14	3.435	3.986	3.525	8.726	8.530	7.689	6.097
2.43	3.436	3.984	3.521	8.740	8.524	7.677	6.091
2.50	3.433	3.983	3.521	8.726	8.521	7.677	6.092
2.56	3.426	3.980	3.521	8.722	8.514	7.678	6.093
2.60	3.383	3.960	3.525	8.634	8.479	7.688	6.096

3.03	3.378	3.955	3.520	8.643	8.463	7.675	6.092
3.20	3.373	3.953	3.520	8.637	8.457	7.675	6.093
3.28	3.367	3.949	3.520	8.626	8.451	7.674	6.092
3.40	3.352	3.945	3.524	8.599	8.445	7.686	6.097
3.73	3.350	3.941	3.520	8.602	8.433	7.674	6.093
6.47	3.339	3.935	3.519	8.574	8.423	7.674	6.091

Table B-23: *Chemical shifts for compound **26** in D_2O in dependence of pD.*

pD	CH_3	H5	H6
6.94	3.454	6.073	7.654
10.28	3.453	6.072	7.653
10.56	3.454	6.072	7.653
11.29	3.452	6.069	7.647
11.94	3.439	6.042	7.605
12.24	3.439	6.043	7.606
12.40	3.418	6.0015	7.538
12.62	3.405	5.973	7.494
12.66	3.406	5.976	7.498
12.69	3.420	6.004	7.543
13.05	3.361	5.885	7.355
13.07	3.372		7.459
13.1	3.362	5.887	7.358

Table B-24: *Chemical shifts for compound **27** in D_2O in dependence of pD.*

pD	CH_3-A	CH_3-C	H6	H5	H2/8
3.18	3.951	3.489	7.6805	6.0945	8.419
3.75	3.947	3.489	7.679	6.0945	8.408
6.90	3.946	3.489	7.680	6.095	8.403
8.04	3.946	3.489	7.679	6.095	8.402
10.91	3.945	3.487	7.675	6.090	8.403
11.0	3.945	3.487	7.675		8.404
11.34	3.945	3.482	7.656	6.082	8.402
11.54	3.945	3.479	7.651	6.078	8.402
12.1	3.941	3.441	7.531	6.0005	8.397
12.2	3.941	3.435	7.508	5.985	8.395
12.36	3.939	3.416	7.448	5.949	8.393
12.77	3.935	3.369	7.297	5.852	8.386

Table B-25: *Chemical shifts for compound **33** in D_2O in dependence of pD.*

pD	CH_3-G	H8	H6	H5
7.40	3.757	8.315	7.967	6.592
8.00	3.753	8.297	7.294	6.559
8.21	3.751	8.286	7.903	6.540
8.58	3.744	8.250	7.840	6.491
8.65	3.744	8.256	7.844	6.494
8.80	3.744	8.253	7.839	6.495
8.97	3.738	8.229	7.798	6.458
9.09	3.736	8.217	7.781	6.444
9.29	3.737	8.225	7.795	6.446
9.33	3.732	8.195	7.751	6.425
9.57	3.726	8.169	7.709	6.399
10.26	3.718	8.129	7.669	6.366
10.72	3.714	8.112	7.656	6.353
11.08	3.714	8.111	7.649	6.348
11.57	3.713	8.105	7.649	6.347
12.16	3.713	8.103	7.654	6.345
12.30	3.714	8.109	7.648	6.345
13.63	3.712	8.101	7.645	6.344

Table B-26: *Chemical shifts for compound **34** in D_2O in dependence of pD.*

pD	CH_3
2.23	3.783
5.97	3.783
6.35	3.783
6.84	3.783
7.14	3.783
7.60	3.781
7.90	3.782
8.45	3.779
8.85	3.772
9.05	3.771

2. pD dependences of 9-MeA in different solvents

Mixture of 20% Acetone / 80% D_2O

pD	H2	H8	CH_3
2.02	8.489	8.345	3.931
2.5	8.476	8.332	3.925
3.72	8.401	8.269	3.895
4.07	8.353	8.226	3.875
5.12	8.233	8.118	3.824
5.9	8.188	8.081	3.804
6.34	8.183	8.073	3.800
7.8	8.173	8.063	3.793
11.22	8.166	8.058	3.790

Mixture of 80% Acetone / 20% D_2O

pD	H2	H8	CH_3
1.63	8.564	8.445	3.978
2.21	8.549	8.433	3.973
2.65	8.538	8.421	3.969
3.13	8.502	8.388	3.954
3.76	8.383	8.278	3.910
4.58	8.262	8.160	3.863
5.09	8.254	8.156	3.861
7.34	8.245	8.147	3.859
8.81	8.244	8.145	3.857
13.31	8.252	8.158	3.861
14.45	8.247	8.152	3.859

Mixture of 80% Methanol / 20% D_2O

pD	H2	H8	CH_3
1.39	8.423	8.318	3.920
1.95	8.420	8.316	3.919
2.3	8.414	8.311	3.917
2.66	8.403	8.300	3.913
3.56	8.338	8.226	3.882
4.27	8.261	8.138	3.850

4.31	8.258	8.136	3.850
4.46	8.250	8.127	3.845
5.23	8.221	8.105	3.832
6.06	8.221	8.101	3.834
6.3	8.222	8.100	3.834
6.85	8.219	8.091	3.834
7.7	8.217	8.091	3.832
8.78	8.218	8.091	3.831
11.32	8.217	8.089	3.832
12.75	8.217	8.090	3.831
12.9	8.217	8.091	3.831

3. pD dpendences of compounds *cis*-$[L_2PtX(H_2O)]^{2+}$ and *trans*-$[L_2PtX(H_2O)]^{2+}$

Compound cis-$[(NH_3)_2Pt(1\text{-}MeC\text{-}N3)(H_2O)]^{2+}$

pD	CH_3	H5	H6
2.19	3.432	6.029	7.622
3.63	3.432	6.026	7.620
4.44	3.432	6.027	7.621
5.24	3.432	6.027	7.619
5.67	3.431	6.024	7.617
6.00	3.430	6.023	7.610
6.22	3.429	6.020	7.605
7.02	3.426	6.016	7.591
8.4	3.425	6.015	7.586
10.29	3.425	6.014	7.585
10.69	3.425	6.015	7.586
11.36	3.425	6.015	7.586
11.54	3.425	6.015	7.586
12.08	3.424	6.015	7.585
12.68	3.420	6.010	7.578
13.03	3.419	6.005	7.570
13.27	3.414	5.995	7.553
13.43	3.407	5.982	7.533
13.64	3.391	5.952	7.485
13.75	3.373	5.915	7.427

Compound trans-[$(NH_3)_2$Pt(1-MeC-N3)(H_2O)]$^{2+}$

pD	CH_3	H5	H6
2.10	3.427	5.989	7.587
2.83	3.426	5.987	7.584
3.92	3.428	5.990	7.588
5.16	3.425	5.992	7.582
5.22	3.424	5.991	7.582
5.60	3.422	5.992	7.576
5.78	3.416	5.993	7.559
6.32	3.421	5.993	7.572
6.69	3.414	5.993	7.557
6.85	3.415	5.994	7.557
7.02	3.413	5.993	7.554
7.83	3.413	5.994	7.553
9.68	3.413	5.995	7.554
9.92	3.413	5.995	7.554
10.19	3.413	5.994	7.552
10.48	3.413	5.995	7.554
10.84	3.413	5.993	7.552
12.34	3.411	5.991	7.548
12.78	3.405	5.985	7.539
13.21	3.390	5.963	7.507
13.48	3.383	5.944	7.478

Compound trans-[$(NH_3)_2$Pt(9-MeGH-N7)(H_2O)]$^{2+}$

pD	CH_3	H8
1.70	3.731	8.234
2.64	3.732	8.235
3.25	3.731	8.234
3.88	3.728	8.231
4.07	3.730	8.231
4.99	3.724	8.216
5.28	3.726	8.216
5.44	3.721	8.209
5.71	3.715	8.194
6.48	3.702	8.168
8.29	3.693	8.135
8.6	3.663	7.965

9.75	3.675	8.031
9.77	3.674	8.018
10.02	3.670	8.005
10.37	3.667	7.986
10.86	3.664	7.971
11.53	3.664	7.966
11.78	3.691	8.120
12.55	3.663	7.963
12.88	3.663	7.965

Compound cis-[{NH(CH$_3$)$_2$}$_2$Pt(9-MeGH-N7)(H$_2$O)]$^{2+}$

pD	CH_3-G	H8
3.26	3.803	8.415
3.28	3.764	8.266
4.16	3.796	8.407
5.10	3.798	8.405
5.40	3.804	8.405
5.60	3.791	8.384
5.87	3.799	8.378
6.14	3.791	8.359
6.18	3.762	8.264
6.23	3.786	8.341
6.68	3.792	8.333
6.88	3.778	8.295
7.37	3.777	8.295
7.74	3.775	8.286
8.05	3.774	8.283
8.77	3.771	8.242
9.46	3.762	8.190
9.47	3.752	8.174
10.68	3.746	8.106